Nuclear Organisation in Stem Cells

Annie E. Wiblin

Submitted for the Degree of PhD in
The University of Edinburgh

June 2006

Declaration

I declare that this thesis has been composed by me, and that all of the work is my own unless otherwise stated.

Annie Wiblin
June 2006

Acknowledgements

First and foremost, thanks go to Wendy for introducing me to these fascinating cells and teaching me that science is not just about lab work but about communicating ideas. Without her support and enthusiasm this thesis would not be here. To the Bickmore lab members past and present (Catherine, Celine, Clemence, Duncan, Elodie, Heidi, Inga, Liz, Jon, Nick, Sev, Shelagh, Steph and Sue) for cakes, cocktails and chromosome painting. Special mentions go to Inga-winga, for putting the 'Oooops' back into lab work and Shelagh for teaching me everything I ever wanted to know about FISH, and then some. To Wei Cui and her lab at Roslin, for meeting the constant demand for hES cells, along with the late John Clark, an inspiration to the stem cell field who is sadly missed.

Thanks to fellow Aberystwythian, Paul Perry, who resuscitated Granny for me on numerous occasions, not to mention what he can do with a pivoc. To Sandy, for just one or two last minute posters! To Ian Adams for moral guidance – or should that be misguidance; I'm still not in favour of reproductive cloning but thanks for the ovary. To Diana for working around my life in the hood and numerous tissue culture related miracles, as well as Nicola Reynolds who shared her Real-time PCR expertises and didn't laugh too loudly at mine. Many thanks go to Mary T, for her unsurpassed knowledge of all things orderable. To Andrew Caruthers and Douglas Heggie for bringing my 3D world into perspective and Lee Spraggon for helpful discussions on all things neuronal. I would also like to thank Bill Earnshaw, Robin Lovell-Badge and Thomas Jessell for the kind gifts of antibodies and Adrian Bird, Thomas Jenuwein, En Li and Austin Smith for the cell lines.

Wow, this is beginning to sound like an Oscar acceptance speech… thanks to Donncha and Alexey for their late night office banter and teaching me the Russian approach to

collaborating "Я довер вам, но проверяю", right Alexey! To the great and good of E3 for many happy memories, especially Fiona, Ewelina, Jeremy and Sonia who kept me smiling through numerous tissue culture disasters. To Heather, Pam and Laura on C3, and the students of the HGU for everything from antibodies to zebra making, you guys are all fantastic and I look forward to running into you again somewhere.

My thanks to Andy Childs, for instilling an air of normality into the otherwise chaotic world of West Maitland Street, although I will never be able to look at black leather gloves in the same light again, I will always smile when I hear Tony Christy (!). Thanks also to Mr Joel (from Gloucestershire) and Mr James for making Edinburgh a home to remember, as well as Hannah for her tolerant approach to houseguests. To the one and only pink Muppet, Miss Sally Burn, what can I say... from directors chairs to killer moths, I'm in need of a good therapist and I'm leaving the best one behind, stay happy.

In real world I'd like to thank everyone in the BJA and the EJA for taking me away from this madness, into the sanity of street parties in Svendborg and swamps in Ptuj, you guys know who you are, don't think I'm not grateful. Thanks also to the London crew (Abi G & Assia, Claire, Emily, Helen, Kath & John, and Sarah), for never missing a chance to party, not to mention Lou, Mark, Abi C & Christophe for their constant support. To friends in far flung places (Annette, Lis, Roz & Nick, Sian J, Sian K & Leon, Tim M, Vicky & Dave, and Tim W) e-mail makes the world seem smaller, thanks for keeping the faith. To Tim, for more than he would imagine, and last but by no means least to my family for their unwavering support, looks like I finally got a round tuit!

Abstract

The spatial arrangement of the human genome in the nucleus is thought to be important for regulating gene expression. Previous studies have shown that chromosomes adopt a radial organisation, whereby gene-rich chromosomes are situated towards the centre of the nucleus and gene-poor chromosomes are located closer to the nuclear periphery. Centromeres, telomeres and gene clusters also have distinct nuclear localisations in somatic cells. If nuclear organisation regulates gene expression, then it may have a role in gene silencing as a cell commits to differentiation. It is therefore important to determine the nuclear organisation of stem cells. Here I ask if the nuclear architecture of human and mouse embryonic stem (ES) cells is different from that of differentiated cells?

I have examined the position of chromosomes 18 (gene-poor) and 19 (gene-rich) and show that their radial nuclear organisation, seen in differentiated cells, is already established in human ES cells. However, I show that the position of centromeres is different in ES cells and differentiated cells. I have investigated the location of two gene dense regions, 11p15 and 6p21 (which contains the pluripotent gene *OCT4*) and the 12p13 region (containing *NANOG*), in differentiated and human ES cells. I show that although the position of gene dense regions is maintained through differentiation, specific genes involved in pluripotency change position either within the nucleus or relative to their chromosome territories. In parallel I have established data on nuclear reorganisation during differentiation of murine ES cells towards an ectodermal lineage. I show the relocalisation of chromosome territories and genes involved in neural development during differentiation, which is accompanied by substantial clustering of centromeric heterochromatin. Using mutant mouse ES cells I show that clustering still occurs in cells that lack DNA methylation, the DNA binding protein MeCP2 and the Suv39h histone methyltransferase. I conclude that although some of the basic principles of nuclear organisation are already established in ES cells, spatial reorganisation of the genome is evident during differentiation.

Contents

List of Figures

Chapter 1

Chapter 3

Chapter 4

Chapter 5

List of Tables

Chapter 1

Chapter 2

Chapter 3

Chapter 4

Chapter 5

Chapter 6

List of Abbreviations

ATRX – alpha-thalassemia retardation X-linked
β–me – β-mercaptoethanol
BAC – bacterial artificial chromosome
BDNF – brain derived neurotrophic factor
bFGF – basic fibroblastic growth factor
BMPs – bone morphogenetic protein
BrdU – bromodeoxyuridine
BSA – bovine serum albumin
ChIP – chromatin immunoprecipitation
CT - chromosome territory
DAPI – 4,6-diamidino-2-phenylindole
DIC – differential interface contrast
dig-dUTP – digoxigenin-11-dUTP
DMEM – Dulbecco's modified eagle medium
DMF – dimethylformamide
DMSO – dimethyl sulfoxide
Dnmt – DNA methyltransferase
dNTP – deoxynucleoside triphosphate
DTT – dithiothreitol
EBF – early B-cell factor
EBs – embryoid bodies
EC – embryonic carcinoma
ECL – enhanced chemiluminescence
EDTA – ethylenediamine tetra-acetic acid
EG – embryonic germ
EGTA – ethyleneglycol-*bis*(β-aminoethyl)-N,N,N',N'-tetraacetic acid
ES – embryonic stem
EtBr – ethidium bromide (2,7-diamino-10-ethly-9-phenyl-phenathridium bromide)
FCS – foetal calf serum
FISH – fluorescence *in situ* hybridisation
FITC – fluorescein isothiocyanate
g – relative centrifugal force
GAPDH – glyceraldehyde-3-phosphate dehydrogenase
GFAP – glial fibrillary acidic protein
GMEM – Glasgow modified eagle medium
HAT – histone acetyltransferase
HDAC – histone deacetylase
hES – human embryonic stem
HMT – histone methyltransferase
HP1 – heterochromatin-associated protein 1
HS – hypersensitive site
HSA – Homo sapiens autosome
ICF – immunodeficiency centromeric instability facial anomalies syndrome
ICM – inner cell mass
LCL – lymphoblast cell line
LCR – locus control region
LIF – leukaemia inhibitory factor

MAA – methanol:acetic acid
MBD – methyl-binding domain
MBP – methyl-binding protein
mES – mouse embryonic stem
MHC – major histocompatibility complex
NEAA – non-essential amino acids
NRSF – neuron restrictive silencing factor
OD – optical density
PBS – phosphate buffered saline
PcG – polycomb group
PCR – polymerase chain reaction
pFa – paraformaldehyde
PK – proteinase K
PML – promyelocytic leukaemia
PMSF - phenylmethylsulphonylfluoride
PVDF – polyvinylidene difluoride
rmp – revolutions per minute
RPMI – Roswell park memorial institute 1640 medium
RT – reverse transcriptase
RT-PCR – reverse transcription polymerase chain reaction
SAGE – serial analysis of gene expression
SCID – severe combined immunodeficient
SDS – sodium dodecylsulphate
SDS-PAGE – sodium dodecylsulphide polyacrylamide gel electrophoresis
SSC – saline sodium citrate
STAT – signal transducer and activator of transcription
TBE – tris-borate-EDTA
TBS – tris buffered saline
TBST – tris buffered saline and tween
TE – tris EDTA
TEMED – N,N,N',N'-tetramethylethylenediamine
TGF – transforming growth factor
TrxG – trithorax group
TSA – trichostatin A
TxRd – Texas Red
WNT – wingless type
X-Gal – 5-Bromo-4-chloro-3-indolyl-β-D-galactoside

Chapter 1: Introduction

Chapter 1

Introduction

It is now three years since completion of the human genome project and our understanding of the DNA code has greatly increased. However, this linear sequence tells us nothing about how the genome is arranged into chromosomes, or which parts of the DNA sequence are in close proximity to each other within the nucleus (Bridger and Bickmore, 1998). The spatial arrangement of the genome is thought to be important for regulating gene expression. Therefore, as one mapping project came to an end, others were already underway to locate the genome and its epigenetic modifications within the 3D nucleus (Murrell et al. 2005; and references therein).

In an embryonic stem (ES) cell the genome is thought of as plastic, being poised for both self-renewal and the generation of numerous lineages, however as a particular cell fate is determined the need to keep parts of the genome in an open state is lost (Szutorisz and Dillon, 2005). This is evident from studies of both histone modifications and non-histone proteins in ES cells (Bernstein et al., 2006a; Boyer et al., 2006). It has been suggested that during differentiation the spatial arrangement of the genome is reorganised, allowing active regions access to transcription factors and silent regions to be packaged away. In this chapter, I will summarise current theories on epigenetic regulation of the human genome and that of model organisms, with emphasis on the relevance of these mechanisms to early development.

1.1 Experimenting with pluripotency

Three cell types can differentiate into all three embryonic germ layers and are therefore pluripotent, embryonic carcinoma (EC) cells (Kleinsmith and Pierce, 1964; Martin and Evans, 1975), embryonic stem (ES) cells (Evans and Kaufman, 1981; Martin, 1981; Thomson et al., 1998) and embryonic germ (EG) cells (Matsui et al., 1992; Shamblott et al., 1998). EC cell lines are derived from teratocarcinomas, which are thought to originate from the epiblast (Hogan et al., 1994). These cells expand continuously in culture and when reintroduced into a developing embryo they participated in embryogenesis, contributing to various tissues of chimaeric foetuses and live born mice (Brinster, 1974; Mintz and Illmensee, 1975). However this was soon found to be the exception rather than the rule. EC cells are normally aneuploid, as a result of selection pressures during tumour growth; many lines lose their potency in culture, show weak differentiation and contribute poorly to chimeras producing embryonic tumours (Kahan and Ephrussi, 1970; Evans, 1972; Rossant and McBurney, 1982). Although these cells are not 'true' stem cells, because of their abnormal karyotype, this research led to the derivation of ES cells (sections 1.1.1 and 1.1.2). The third cell type, EG cells, are derived from primordial germ cells (Matsui et al., 1992; Shamblott et al., 1998). EG cells have very similar developmental capacities to ES cells, but differ in the expression of imprinted genes (reviewed by Zwaka and Thomson, 2005). However the culture of human EG (hEG) cells is still very challenging as the cells spontaneously differentiate in culture (Turnpenny et al., 2003), so for the purpose of this thesis I have used ES cells.

1.1.1 Mouse ES cells

In 1981, the first ES cells were derived from the inner cell mass (ICM) of mouse blastocysts (*figure* 1.1; Evans and Kaufman, 1981; Martin, 1981). Mouse ES (mES) cells can both self renew and give rise to teratocarcinomas containing mesodermal, endodermal, and ectodermal cell types (Evans and Kaufman, 1983). There is no G1

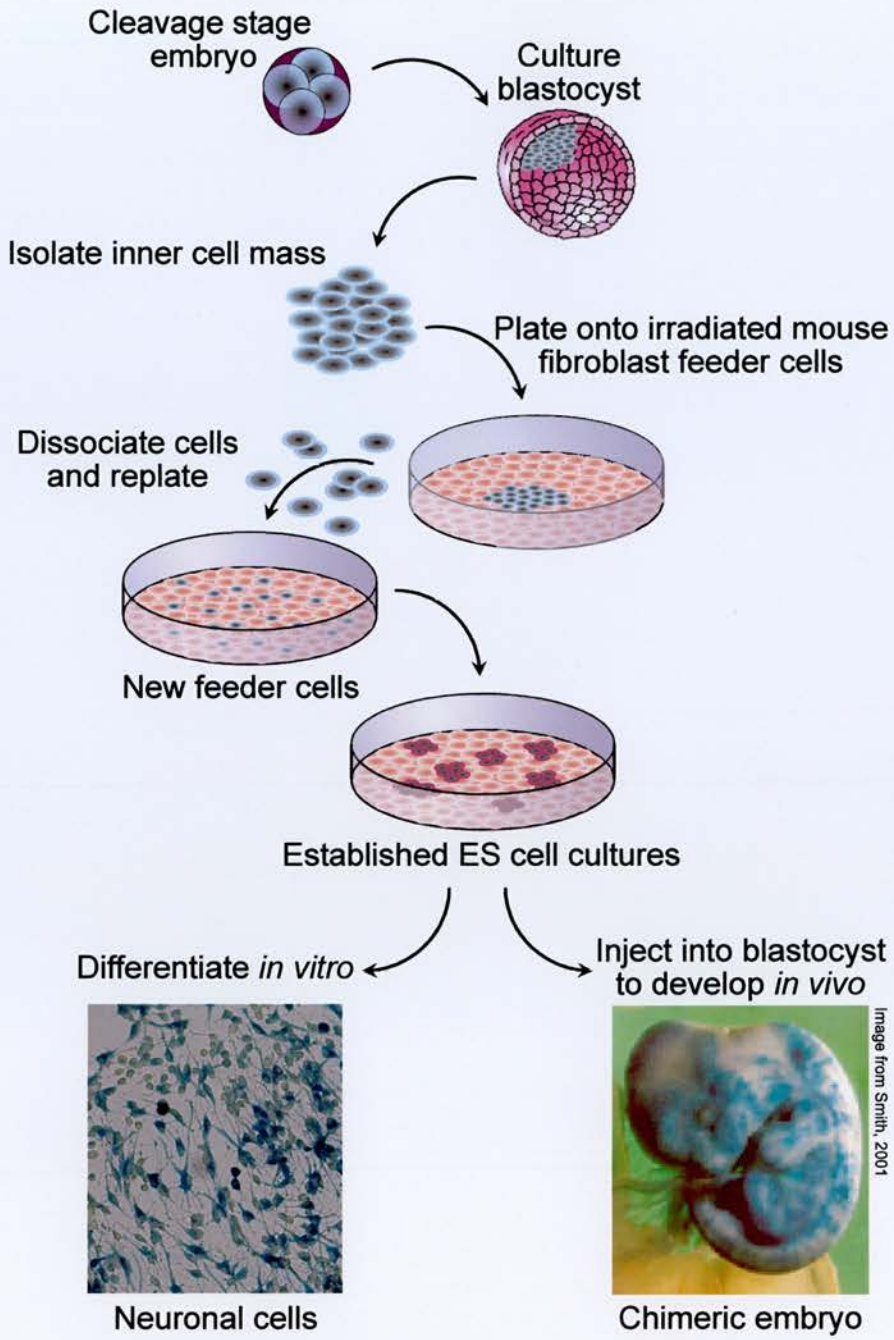

Fig. 1.1 The derivation of ES cells. Cleavage stage embryos are cultured until the blastocyst stage. The inner cell mass is then separated from the surrounding trophectoderm and plated onto a feeder layer of irradiated mouse embryonic fibroblasts. Following a period of attachment and expansion, the outgrowth is dissociated and replated onto another feeder layer. Colonies are then expanded and passaged to form cell lines. These cells can then be differentiated *in vitro*, or injected back into blastocysts and implanted to make chimeras *in vivo*. The chimeric embryo shown here was generated with ES cells containing the β-galactosidase gene. Therefore when stained for β-galactosidase (blue), the ES cell descendants are visible throughout the foetus.

checkpoint in their cell cycle which facilitates programmed cell death, preventing cells with damaged genomes from contributing to a developing embryo (Aladjem et al., 1998). In female ES cells both X chromosomes are active (Rastan and Robertson, 1985). However, even after extensive propagation in culture mES cells retain their capacity to enter embryogenesis, making chimeras with relative consistency, although earlier passage cells are more likely to be transmitted through the germ-line. They have been shown to contribute to all the fetal lineages plus the yolk sac mesoderm, allantois and amnion (Bradley et al., 1984). In keeping with their epiblast origin, mES cells contribute poorly to the primitive endoderm and never to the trophectoderm (*figure* 1.2A; Beddington and Robertson, 1989). This is why mES cell are considered to be pluripotent, whereas cells of the early embryo are totipotent. Unlike EC cells, mES cells maintain their diploid karyotype, therefore, if they colonise the germ cell lineage in a chimera, the cells are capable of proceeding through meiosis to produce mature gametes. Thus mES cells have proven very useful for engineering the mouse genome and for creating mutant mouse lines (reviewed by van der Weyden et al., 2002).

The first mES cells were cultured on mitotically inactivated fibroblast 'feeder' cells, which have since been replaced by preparations of defined media. Central to this change was the discovery that a cytokine, leukaemia inhibitory factor (LIF), produced by the feeders could sustain mES cell self-renewal in the presence of serum (Smith et al., 1988; Williams et al., 1988). LIF acts via the gp130 receptor to activate STAT3 in a JAK kinase mediated process (*figure* 1.2C; Yoshida et al., 1994; Niwa et al., 1998). Following the withdrawal of LIF (or feeders) mES cells start to differentiate spontaneously and the majority of stem cells are lost from the culture within a few days. Interestingly the STAT3 signalling pathway is not exclusive to mES cells and has been implicated in a number of differentiation pathways ranging from astrocyte precursors to myeloid cells (Rajan and McKay, 1998; Minami et al., 1996). Along with feeders, the necessity for serum in the media has also been replaced, following the discovery that bone morphogenetic proteins (BMPs) act in combination with LIF to sustain mES cell self-renewal (Ying et al., 2003).

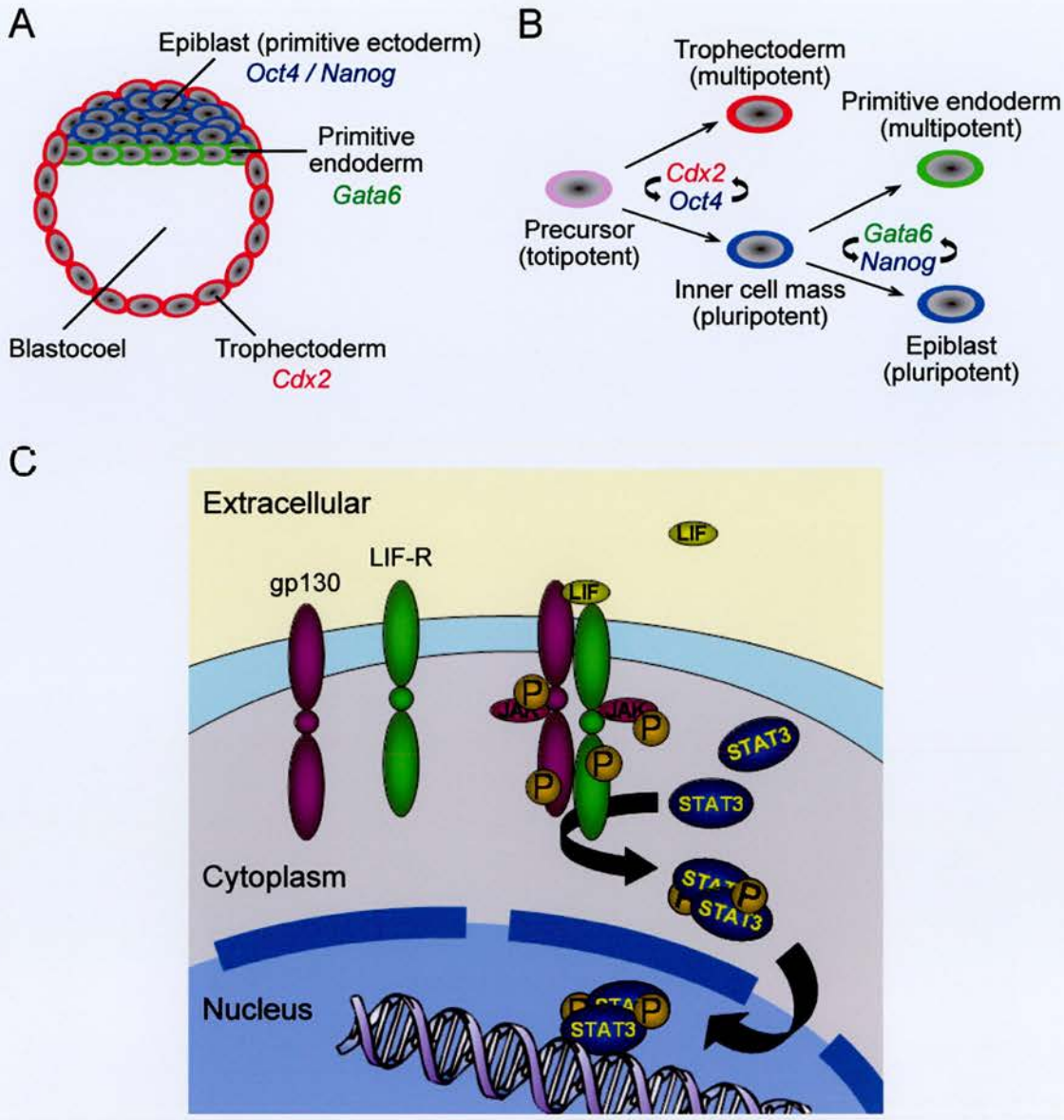

Fig. 1.2 Controlling early lineage selection. (A) Diagram of the late blastocyst stage, showing expression patterns for *Cdx2* (red), *Gata6* (green), *Oct4* and *Nanog* (blue). (B) Early lineage decisions are controlled by repression of *Cdx2* by Oct4 in the inner cell mass, and repression of *Oct4* by Cdx2 in the trophectoderm. Similarly within the inner cell mass, antagonism between *Nanog* and *Gata6* allows segregation of the epiblast and primitive endoderm (adapted from Ralston and Rossant, 2005). (C) Activation of the STAT3 transcription factor by LIF maintains pluripotency of mES cells *in vitro* and the blastocyst during diapause *in vivo*. LIF binds to a LIF receptor (LIF-R) - gp130 receptor heterodimer, which recruits the nonreceptor tyrosine kinase Janus (JAK) and becomes phosphorylated (P). STAT3 binds to the phosphotyrosine residues on the activated receptor where it undergoes phosphorylation and dimerization. STAT3 dimers can then translocate to the nucleus where they function as transcription factors (based on Boiani and Schöler, 2005).

Transcriptional profiling of mES cells in comparison with adult neuronal and haematopoietic stem cells, has identified between 1500 and 2300 genes enriched in the mES cell population. Approximately 250 of these genes are common to all three cell types, highlighting the possibility that a common genetic program exists for stem cells (Ivanova et al., 2002; Ramalho-Santos et al., 2002). Others, expressed only in the mES cell population are thought to have a role in maintaining pluripotency. Two of these genes will be analysed in this thesis. The first is the POU family transcription factor *Oct4* (Schöler et al., 1989; also known as *Oct3* or *Pou5f1*, Okamoto et al., 1990; Rosner et al., 1990), which is essential to establish the pluripotent identity of both nascent ICM cells *in vivo* and mES cells *in vitro* (Nichols et al., 1998; Niwa et al., 2000). Disruption of *Oct4* expression causes these cells to differentiate into trophoblasts, implicating this gene in the control of epiblast and trophectoderm lineages (Niwa et al., 2000). In trophectoderm the caudal-related transcription factor, *Cdx2*, is one of the genes needed to maintain cell fate and is thought to suppress the expression of ICM genes such as *Oct4* (Chawengsaksophak et al., 1997; Strumpf et al., 2005). Therefore current models suggest that *Oct4* and *Cdx2* have a role in controlling ICM and trophectoderm fates, whereby they negatively regulate each other reinforcing segregation of the two lineages (*figure* 1.2B; reviewed in Ralston and Rossant, 2005). Recently, *Oct4* has been shown to bind ~1000 sites across the genome, with over half of these located in gene coding regions (Boyer et al., 2005; Loh et al., 2006).

Expressed alongside *Oct4* in the ICM, is the other gene important for pluripotency to be analysed in this thesis, the variant homeodomain protein *Nanog* (Chambers et al., 2003; Mitsui et al., 2003). Both *Oct4* and *Nanog* are downregulated during differentiation towards the primitive endoderm (Palmieri et al., 1994; Chambers et al., 2003; Mitsui et al., 2003), but despite being coexpressed they are thought to act on different pathways, as loss of either gene does not affect the others expression in the blastocyst (Chambers and Smith, 2004). In the absence of *Nanog*, embryos can form trophectoderm and primitive endoderm lineages, but not ICM (Mitsui et al., 2003). Similarly, the loss of

Nanog from mES cells causes them to take on primitive endoderm characteristics (Mitsui et al., 2003). The same phenotype is seen when over expressing the Gata binding proteins, *Gata4* or *Gata6*, which control endoderm differentiation in mES cells (Fujikura et al., 2002). *Gata6* also has a *Nanog* binding site in its enhancer region and is upregulated in *Nanog* null cells (Mitsui et al., 2003). Together these observations suggest a role for *Nanog* in controlling the segregation of ICM and primitive endoderm lineages, possibly via repression of *Gata* genes (*figure* 1.2B).

Depending upon tissue culture conditions, mES cells can be differentiated into a variety of cell types representing all three germ layers (reviewed by Smith, 2001, Chambers and Smith, 2004). However to date, they have only been shown to generate trophoblast cells following genetic manipulation (Niwa et al., 2000, 2005), even when isolated from pre-blastocyst embryos (Tesar, 2005). The principle method of differentiating ES cells involves allowing them to aggregate in suspension leading to the formation of structures called embryoid bodies. This differentiation is thought to occur on a similar schedule to *in vivo* development (Keller et al., 1993; Wichterle et al., 2002), however the bodies lack the orientation and elaborate body plan of the early embryo (Doetschman et al., 1985). Other protocols have been developed to differentiate mES cells in monolayers enabling better observation, dissociation and access to the cultures (Nishikawa et al., 1998). It is possible to bias differentiation toward certain lineages by adding different concentrations of retinoic acid (Rohwedel et al., 1999; Okada et al., 2004) or growth factors (Okabe et al., 1996) however the resulting culture remains a heterogeneous mixture of cells. Various methods have been explored to achieve a more homogenous population and are discussed elsewhere (section 4.1).

1.1.2 Human ES cells

In 1998, the first human ES (hES) cells were derived from the ICM of the early blastocyst (Thomson et al., 1998). Although we cannot confirm their ES cell status via

germ line chimeras, hES lines have both the ability to self-renew and differentiate into all three embryonic germ layers when injected into severe combined immunodeficient (SCID) mice (*figure* 1.3A, Thomson et al., 1998). The hES cells resemble their murine counterparts in many ways, including the expression of common genes important for pluripotency i.e. *OCT4* (Reubinoff et al., 2000) and *NANOG* (Clark et al., 2004). However, there are many differences between mES and hES cells in their morphology, culture, gene expression, differentiation and regulation of self-renewal (Pera and Trounson, 2004; Ginis et al., 2004). In contrast to mES cells, hES cells can be differentiated into all three germ layers of the epiblast plus extraembryonic lineages, giving rise to trophectoderm spontaneously in culture and in the presence of BMP4 (*figure* 1.3B; Thomson et al., 1998; Xu et al., 2002). This suggests either hES cells are derived from an earlier cell type than mES cells, or that lineage allocation between human and mouse is different, for example, the human ICM may retain the potential to differentiate into trophectoderm (Ralston and Rossant, 2005). There is also a third possibility, that hES cells are more comparable to a different cell type all together, for example germ cells (Zwaka and Thomson, 2005).

The hES cells do not respond to gp130/LIF stimulation (Thomson et al., 1998; Reubinoff et al., 2000). Although at present the reasons behind this are unknown, several groups have attributed it to absence or low-level expression of components in the LIF pathway and poor activation of the STAT3 pathway in hES cells (Ginis et al., 2004; Richards et al., 2004; Sato et al., 2004). In mouse, there is a physiological significance for the role of LIF as it is required during diapause, a resting state induced in the blastocyst that allows one litter to finish suckling before a second litter can implant. There is no equivalent stage in human development (Nichols et al., 2001). Other pathways reported to function differently in hES cells include the BMP signalling pathway, which promotes differentiation and the fibroblast growth factor (FGF) pathway, which supports self-renewal (Amit et al., 2000; Xu et al., 2002). The BMP antagonist noggin has been shown to synergize with bFGF, repressing BMP signalling and sustaining self-renewal of hES cells without the need for feeders or conditioned

A

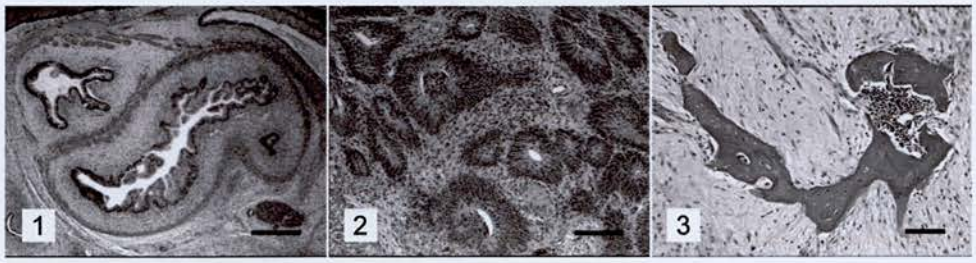

B

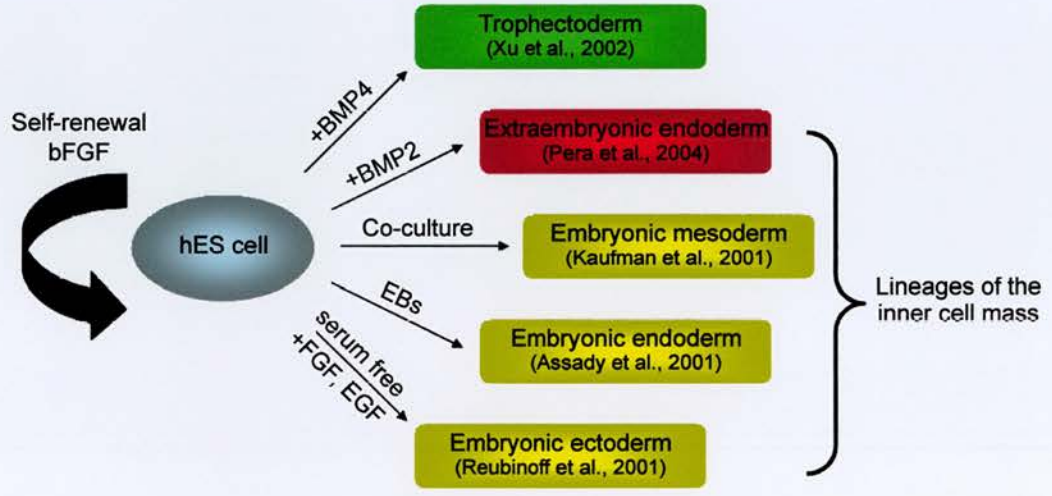

Fig. 1.3 Differentiation of hES cells. (A) Teratoma formation following the injection of hES cells into SCID-beige mice. (1) Gutlike structures, scale bar 400μm. (2) Rosettes of neural epithelium, scale bar 200μm (3) Bone, scale bar 100μm. (images from Thomson et al., 1998). (B) Schematic of hES cell differentiation *in vitro*. In spontaneously differentiating hES cell cultures, trophectoderm (green box) and four lineages of the inner cell mass (the extraembryonic endoderm (red box) and the three germ layers of the epiblast (yellow boxes)) have been identified. One of the first attempts to control each differentiation is referenced and the main culture condition used is written along the appropriate arrow.

medium (Xu et al., 2005a). Furthermore, at concentrations of 100ng/ml, bFGF alone can sustain cultures in unconditioned media with effectiveness comparable to conditioned media (Levenstein et al., 2006). This has enabled Ludwig et al., (2006) to derive hES cells feeder free, under defined conditions that include only protein components derived from recombinant sources or purified from human material. The new lines are therefore more directly applicable to clinical use than the original lines derived in the presence of animal products.

In comparisons between the human and mES cell transcriptomes, a group of nine genes have been identified that are common to both species and more or less specific to pluripotent cells (*table* 1.1). Unsurprisingly, as none of the pathways implemented in pluripotency are exclusive to ES cells, a further 100 to 200 of the genes identified are upregulated in the ES cells of both species, but are not specific to pluripotent cells (Sato et al., 2003; Wei et al., 2005). Perhaps more significantly these studies highlight a number of differences between the two species. In mES cells, genes involve in the LIF signalling pathway, gp130, and FGF4 are highly expressed, whereas in hES cells, FGF signalling, trophectoderm differentiation and inhibition the LIF pathway are prevalent (Ginis et al., 2004; Wei et al., 2005). The largest proportion of the hES cell transcriptome is made up of genes involved in signal transduction and regulation, which represent 17% of the genes enriched in pluripotent cells when compared to differentiated cells. These genes encode receptors and secreted inhibitors of the FGF, transforming growth factor (TGF)-β/BMP, Nodal and Wingless type (WNT) signalling pathways (Brandenberger et al., 2004; Sato et al., 2003); all of which have been implicated in the decision to self renew or differentiate made by hES cells and in some cases, mES cells (Sato et al., 2004; Vallier et al., 2005; Xu et al., 2005a). There is less variation between hES cell lines than between ES cells from different species, but there are still differences in their expression profiles. One analysis compared three different hES cell lines and showed that only 52% of the genes expressed were common to all three lines (Abeyta et al., 2004). Reports of differences between the hES cell lines are not restricted to gene expression and are also seen in growth rates and varying degrees of X-inactivation

(Cowan et al., 2004; Hoffman et al., 2005). This may reflect not only the different derivation and culture conditions of the cell lines, but also the different genetic backgrounds of the blastocysts from which the lines are derived.

Class of molecule	Name	Expressed in mES	Expressed in Hes
Surface Markers	SSEA-1	+	-
	SSEA-3	-	+
	SSEA-4	-	+
	TRA-1-60	-	+
	TRA-1-81	-	+
Transcription Factors	POU5F1/ OCT4*	+	+
	NANOG*	+	+
	SOX2	+	+
	FOXD3*	+	+[a]
	UTF1*	+	+
	REX1*	+	+
Growth Factors	GDF3*	+	+
	FGF2	-	+
	FGF4	+	-
	TDGF1 / CRIPTO*	+	+
Receptors	FGFR1 & 2	-	+
	LIFR	+	+[b]
	Gp130	+	+[b]
Other	STELLA / DPPA3*	+	+
	FLJ10713*	+	+

Table 1.1 A selective list of markers and genes expressed at high levels in pluripotent cells. Marker expression in mouse and hES cells, (+) denotes expression, (-) denotes the marker is not expressed; green boxes highlight differences between species. (a) denotes variable expression between cell lines, (b) denotes the gene is expressed only at low levels and (*) are genes expressed only in early embryos, germ cells, ES cells and few other cell types (adapted from Pera et al., 2000, 2004; Ginis et al., 2004).

Despite all of these differences, the main genes identified as controlling pluripotency in mouse are also thought to be important in hES cells. Downregulation of both *OCT4* and *NANOG* causes the up regulation of primitive endoderm factor *GATA6*, caudal-related transcription factor *CDX2* and other trophectoderm markers (Hay et al., 2004; Hyslop et al., 2005; Zaehres et al., 2005). Therefore as in mouse, *OCT4* and *NANOG* are required to suppress extraembryonic differentiation, although in humans both genes can repress trophectoderm and primitive endoderm lineages, perhaps indicative of being derived from an earlier lineage. In mES cells, an octamer-Sox2 binding complex regulates *Oct4*, the transcription factor *Sox2* (which is important for epiblast formation, Avilion et al., 2003) and *Nanog* (Catena et al., 2004; Kuroda et al., 2004b; Okumura-Nakanishi et al., 2005; Rodda et al., 2005). Recently, a screen by Boyer et al., (2005) found that OCT4, SOX2 and NANOG co-occupy a substantial portion of their target genes in hES cells, which are both activated and repressed. This screen confirmed that the autoregulatory loop described for mES cells is conserved in hES cells, but more importantly, it showed that NANOG is a component of this regulatory loop. However, as more target genes are identified stem cell research has moved into another field, epigenetics, to investigate modifications to the genome that enable self-renewal or differentiation to take place.

1.2 Primary chromatin structure

In eukaryotic cells, DNA is packaged along with histones and non-histone proteins as chromatin. This serves two major purposes: first it enables the ~2m of DNA to fit into a single nucleus, secondly, it facilitates the regulation of cellular processes such as transcription, DNA replication, cell division and differentiation. The basic sub-unit of chromatin is the nucleosome, in which 146bp of DNA are wrapped 1.7 times around an octamer of core histones (containing two molecules each of H2A, H2B, H3 and H4) sealed with a linker histone (Luger et al., 1997; Thomas, 1999). Each nucleosome is separated by 10-60bp of linker DNA, resulting in a chromatin fibre ~11nm in diameter (*figure* 1.4). During interphase, this 'beads-on-a-string' arrangement of nucleosomes

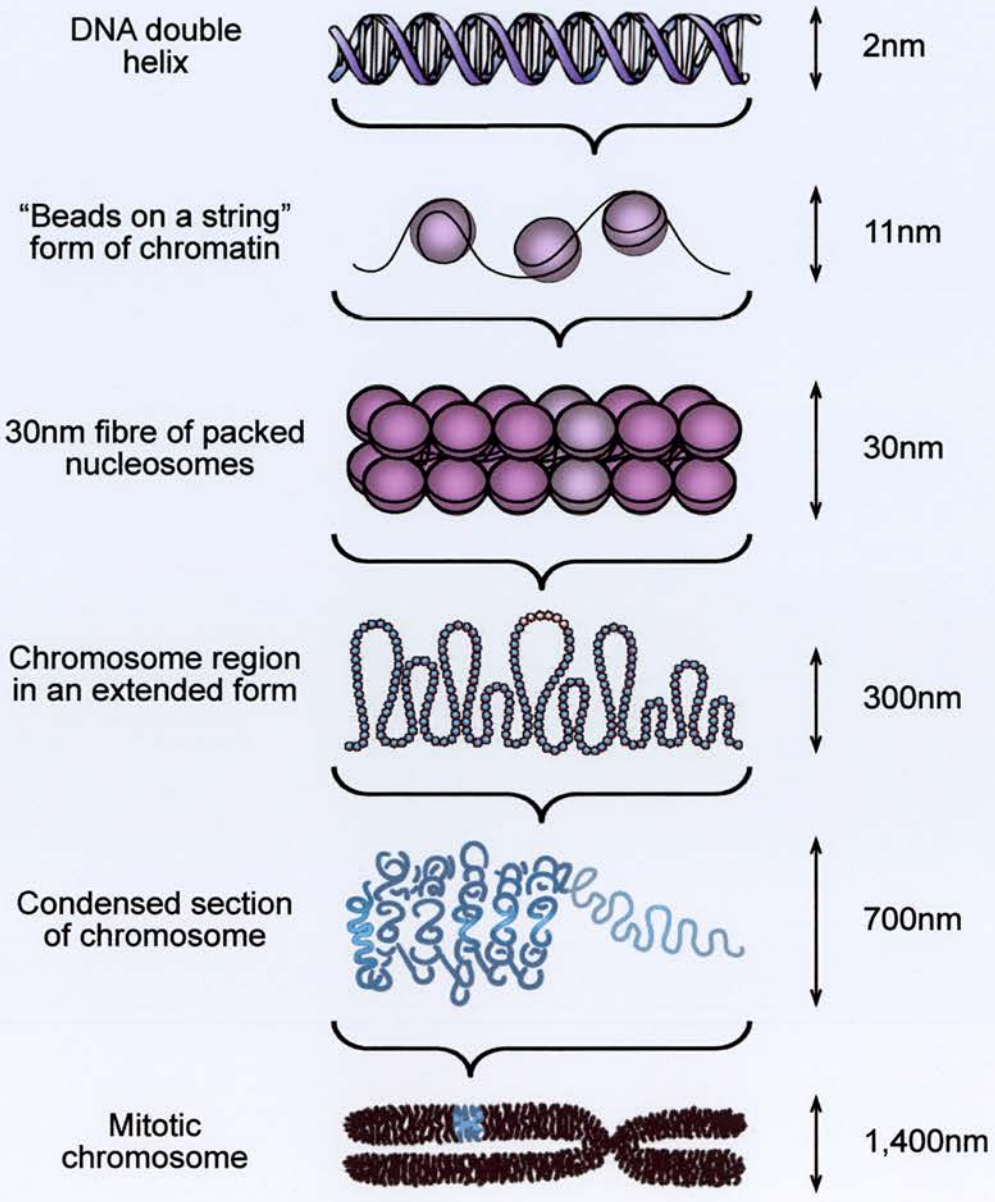

Fig. 1.4 Organisation of DNA within the chromatin template. DNA is arranged in nucleosomes, which consist of approximately 146bp of DNA wrapped around a histone octamer. Nucleosomes are connected to one another by short stretches of linker DNA. This string of nucleosomes folds into a chromatin fibre 30nm in diameter, which is further folded to form higher-order structures (Redrawn from Felsenfeld and Groudine, 2003).

compacts to form a 30nm chromatin fibre. It is uncertain precisely how this chromatin fibre condenses to form interphase chromosomes, or how changes in its conformation contribute to the control of gene expression.

1.2.1 Histone modifications

The C-terminal region of core histones contains a 'histone fold' domain, which is shared by many proteins and thought to be involved in histone:histone and histone:DNA interactions. The N-terminal regions extend outside of the nucleosome, enabling interactions with other proteins (Schroth et al., 1990). Histones are subject to post translational modifications such as lysine and arginine methylation, lysine acetylation, serine and threonine phosphorylation, lysine ubiquitination and sumoylation, and ADP-ribosylation (*figure* 1.5; Strahl and Allis, 2000; Zhang and Reinberg, 2001). In addition, modifications such as lysine methylation can exist in mono-, di- and tri-methylated forms leading to a further level of complexity. The discovery of enzymes that perform these modifications and chromatin-associated proteins that selectively bind to them, revealed that histone modifications significantly extend the potential of the genetic code. This led to the 'histone code' hypothesis which suggests that groups of particular histone modifications provide chromatin signals to control gene expression and chromatin condensation (Strahl and Allis, 2000; Fischle et al., 2003). However, so far there is no evidence to back up this hypothesis, therefore histone modifications might not 'code' for the same function every time.

1.2.1.1 Histone methylation and acetylation

Currently ~60 positions across the four core histones are known to be modified by methylation, acetylation, phosphorylation or ubiquitination. For clarity, I will concentrate on three, H3-K4, K9 and K27 that are relevant to this thesis and stem cell

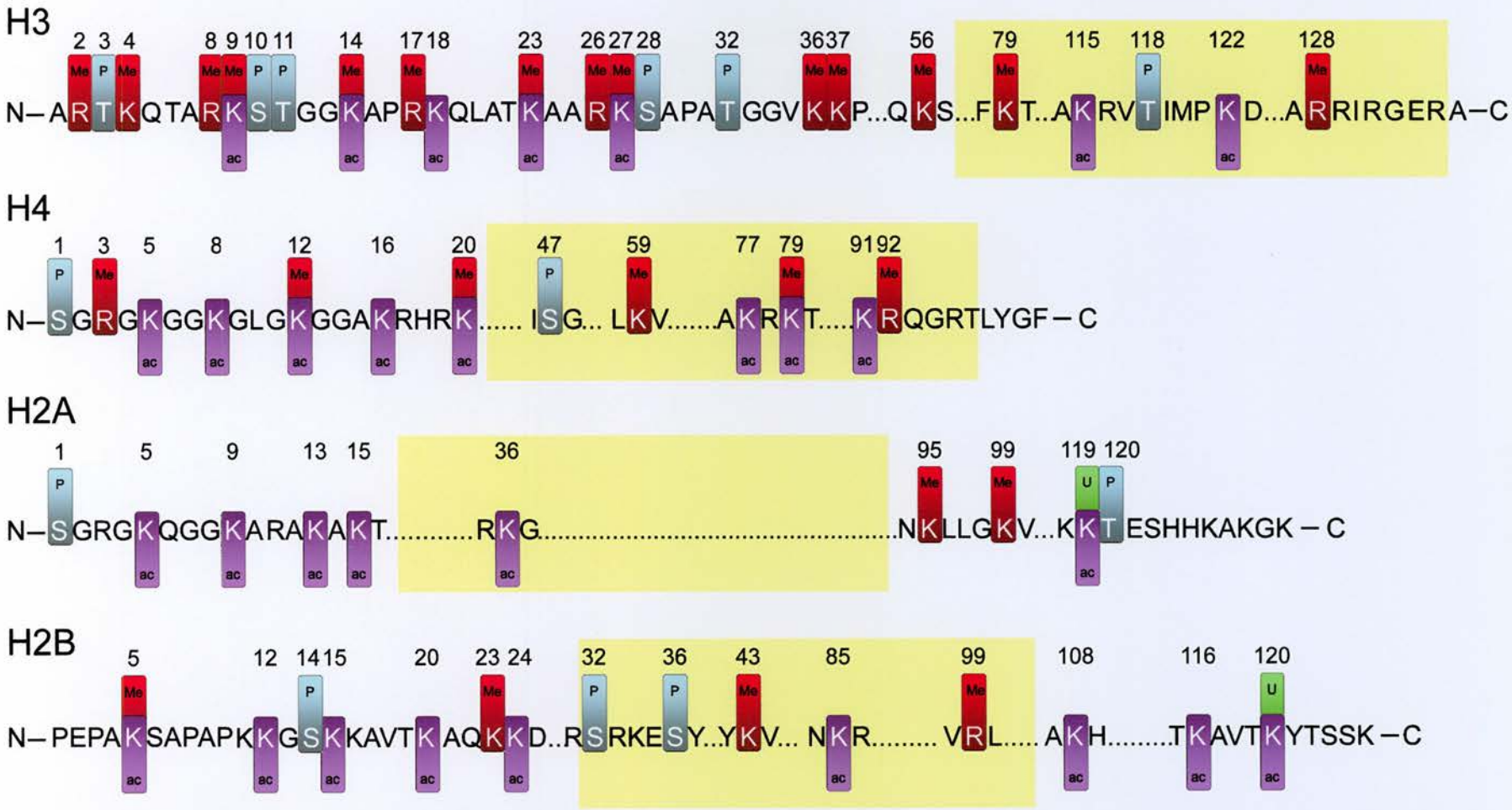

Fig. 1.5 Human histone modification map. Potential modification sites on the four core histones, phosphorylation (P) of serine or threonine (S/T) blue boxes, acetylation (Ac) of lysine (K) purple boxes, methylation (Me) of lysine or arginine (R) red boxes, ubiquitination (U) of lysine green boxes. Yellow rectangles mark the globular domains (adapted from www.abcam.com).

research. In general, H3-K9 acetylation and H3-K4 methylation are associated with active genes, whereas H3-K9 and K27 methylation are associated with gene silencing (Lachner et al., 2003). An example of this is the inactive X chromosome, which is hypoacetylated and lacks methylation of H3-K4, but shows both H3-K9 and K27 methylation (Heard et al., 2001; Plath et al., 2003). However, recently H3-K9 methylation has also been associated with active genes, where it is important for transcription elongation (Vakoc et al., 2005).

The different combinations of histone modifications result from targeting histone-modifying enzymes to specific loci. Histone acetyl-transferases (HATs) are responsible for the acetylation of lysine residues and histone methyl-transferases (HMTs) for the methylation of lysine and arginine residues. Within these two groups, different enzymes recognise specific residues. For example, the HMTs group is comprised of the SET domain family, which methylates lysine residues and the CARM1 / PRMT1 family, which methylate arginines (Chen et al., 1999; Stallcup, 2001). The SET domain family includes Suv39h1/2, Eset (Setdb1) and Eu-HMTase which methylate H3-K9 (Rea et al., 2000; Yang et al., 2002; Ogawa et al., 2002), G9a which methylates H3-K9 and K27 *in vitro* (Tachibana et al., 2001), SET7/9 which methylate H3-K4 (Wang et al., 2001a) and the polycomb complex Ezh2-Eed which methylates H3-K27 (Cao et al., 2002; Kuzmichev et al., 2002). These modifications are reversible. Histone deacetylases (HDACs) remove acetyl groups and newly discovered groups of histone demethylases remove methyl groups. These include PAD4, which indirectly demethylates arginine residues by converting them to citrulline (Cuthbert et al., 2004; Wang et al., 2004a), LSD1 which reverts mono or di-methyl H3-K4 back to an unmethylated state via an oxidation mechanism (Shi et al., 2004); and JmjC domain proteins such as JHDM1A which demethylates H3-K36, JHDM2A which demethylates mono or di-methyl H3-K9 (Tsukada et al., 2006; Yamane et al., 2006) and JHDM3A (also known as JMJD2A) which demethylates tri-methyl H3-K9 and H3-K36 (Whetstine et al., 2006; Klose et al., 2006).

The pattern of histone modifications is thought to affect the binding of non-histone proteins via "cross-talk" either between modifications on the same histone 'cis' or different histones 'trans' (Jenuwein and Allis, 2001; Fischle et al., 2003). For example, in cis the phosphorylation of H3-S10 inhibits HP1 binding to methylated H3-K9 (Rea et al., 2000). In trans, cross-talk is exemplified during p53 dependent transcriptional activation whereby methylation of H4-R3 by PRMT1 stimulates acetylation of H4-K5, K8, K12 and K16 by the HAT, CBP-p300, which in turn promotes the methylation of H3-R2, R17 and R26 by CARM1 (Wang et al., 2001b).

The recruitment of HATs and HDACs is important for differentiation of many lineages including ES cells, oligodendrocytes, astrocytes and neurons (Lee et al., 2004; Nakashima et al., 1999; Shen et al., 2005; Sun et al., 2001). In non-neuronal lineages HDACs associate with transcription factors such as the neuron-restrictive silencing factor (NRSF, also known as REST) and the corepressor CoREST, recruiting HMTs, HP1 and methyl-binding proteins to repress neuronal genes (section 1.2.3; Lunyak et al., 2002; Hsieh and Gage, 2005). Changes in histone modifications during differentiation have also been described for specific loci. For example, progressive modifications to the *Sox2* promoter accompany the differentiation of oligodendrocyte precursors via type 2-astocytes to neuronal stem cells. In the starting population of precursor cells, where *Sox2* is not expressed, the promoter is methylated at H3-K9 and unmethylated at H3-K4. When differentiated into type 2-astrocytes, which express *Sox2*, H3-K4 is methylated and H3-K9 present in both methylated and acetylated forms. Then when further differentiated into neuronal stem cells, which display even higher levels of *Sox2* expression, H3-K4 is methylated and H3-K9 acetylated but unmethylated (Kondo and Raff, 2004). This pattern of histone modifications has also been observed during the differentiation of astrocytes, thymocytes, muscle and haematopoietic lineages, where it is implicated in formation of secondary chromatin structure (section 1.3; Litt et al., 2001; Song and Ghosh, 2004; Su et al., 2004; Zhang et al., 2002).

Recently several groups have started to analyse these chromatin modifications on a global scale, using a combination of chromatin immunoprecipitation (ChIP), DNA microarray and serial analysis of gene expression (SAGE) techniques. Thousands of acetyl H3-K9, K14 and methyl H3-K4 binding sites have been located, which are highly conserved between human and mouse (Roh et al., 2004, 2005; Bernstein et al., 2005; Kim et al., 2005). The vast majority show a punctate pattern, typically occurring at sites of ~1-2kb from the promoters of active genes and regulatory elements. However, in areas of high gene density such as Hox clusters, broad regions of H3-K4 methylation have been found spanning multiple active genes. Recently these regions were shown to be H3-K4 methylated in cell types such as mES cells, where the genes are repressed (Bernstein et al., 2006a). Intriguingly, a previous study has shown that the λ5-*VpreB1* locus is marked by H3 acetylation and H3-K4 methylation at a discrete site in mES cells. These markers spread across the rest of the locus during differentiation, so that when the genes are fully active in pre-B cells an active chromatin domain is already established. This suggests that genes expressed at later stages in development might be set up for transcription, as early as the pluripotent cell stage (Szutorisz et al., 2005).

On a genome-wide scale patterns of active histone modifications (di-methyl H3-K4, K36, K79) generally correlate closely with each other and areas of hyperacetylation, whereas markers of gene silencing (di-methyl H3-K27, H4-K20 and tri-methyl H3-K9) associate with each other and areas of hypoacetylation (Miao and Natarajan, 2005). However, recently H3-K27 methylation has been associated with the active markers of H3-K4 methylation and H3-K9 acetylation in ES cells, where it prevents the early expression of lineage specific genes in areas of open chromatin, via polycomb protein mediated repression (section 1.3.3). This allows pluripotency to continue whilst chromatin is remodelled, enabling lineage specific genes to become poised for differentiation (Azuara et al., 2006; Bernstein et al., 2006a; Boyer et al., 2006; Lee et al., 2006). Approximately 50% of genes found to contain this H3-K27, -K4 methylation bivalent mark are binding sites of at least one of the transcription factors Oct4, Nanog or

Sox2. It has been suggested that this creates a chromatin state in which key lineage markers are repressed but yet transcriptionally poised.

1.2.2 DNA methylation

One of the mechanisms responsible for silencing chromatin is DNA methylation, where predominantly CpG dinucleotides are modified at cytosine bases by the addition of methyl groups. This cytosine methylation can be copied after replication, resulting in heritable alterations to the chromatin fibre. It is associated with X-inactivation (Panning and Jaenisch, 1996), genomic imprinting (Ng and Bird, 1999), cancer (Jones and Baylin, 2002; Esteller and Herman, 2002) and several mental retardation disorders including immunodeficiency centromeric instability facial anomalies syndrome (ICF), fragile X, Alpha-Thalassemia Retardation X-linked (ATRX) and Rett syndromes (Robertson and Wolffe, 2000). DNA methylation is thought to affect gene expression by either blocking the binding of transcription factors (Watt and Molloy, 1988) or attracting proteins that modify nucleosomes (Boyes and Bird, 1991; Hendrich and Bird, 1998). However, recently a further two ways it might regulate transcription have been suggested. First, the DNA methyltransferase (DNMT) enzymes themselves may be involved in gene repression in addition to their catalytic activities; and second, DNA methylation might affect transcriptional elongation as well as inhibiting transcriptional activation (reviewed by Klose and Bird, 2006).

DNA methylation of the mouse genome changes throughout development. During cleavage, a wave of demethylation strips the paternal genome of methylation within hours of fertilization; this is in contrast to the maternal genome, which is only passively demethylated during subsequent cleavage divisions (reviewed in Li, 2002). This process is conserved between mouse, pig and cow but not sheep or rabbit (Dean et al., 2001; Beaujean et al., 2004). However, studies analysing the DNA methylation pattern of human zygotes have provided opposing views on whether the paternal genome is ever

completely demethylated (Beaujean et al., 2004; Fulka et al., 2004; Xu et al., 2005b). Following implantation there is genome wide *de novo* methylation (Jaenisch, 1997), which accounts for the high levels of methylation seen in developing mouse embryos. These levels decrease in developing tissues (Ehrlich et al., 1982) and *de novo* methylation rarely occurs postgastrulation, although it is frequently seen in the development of cell lines *in vitro* (Jones et al., 1990; Kawai et al., 1994) and cancer cells (Rhee et al., 2002). Because hES cell lines are derived from the blastocyst stage, which is characterized by global epigenetic remodelling, it was thought that their DNA methylation status could be subject to variation. However, so far analysis of imprinted genes in hES cell lines has not revealed any aberrant changes in DNA methylation (Rugg-Gunn et al., 2005). In differentiated cells, ~80% of CpGs are methylated. The remaining CpGs are mainly present as CpG islands, which locate to the promoter regions of genes predominantly in early replicating R-bands; although, how these islands remain unmethylated is still not fully understood (Larsen et al., 1992; Craig and Bickmore, 1994).

1.2.2.1 DNA methyltransferases

Our current understanding of DNA methylation is mainly based on knockout mice for the DNMTs and the various DNA binding proteins (section 1.2.2.2). DNMTs are a family of enzymes responsible for catalysing the addition of methyl groups onto cytosine bases. The first of these genes to be studied, *Dnmt1*, is responsible for the methylation of hemi-methylated CpGs during DNA replication and therefore maintaining the pattern of DNA methylation (Bestor et al., 1988; Yoder et al., 1997). Deletion of this gene in mouse resulted in global demethylation and embryonic lethality, but had no effect on the viability of ES cells homozygous for the mutation (Li et al., 1992; Lei et al., 1996). The next two genes in the family, *Dnmt3a* and *Dnmt3b*, are also expressed in the developing mouse embryo and are responsible for the global *de novo* methylation of the genome after implantation (Okano et al., 1998, 1999). However, the

ability of Dnmt3a and 3b to maintain this methylation pattern has also been demonstrated, as in culture Dnmt3a/3b$^{-/-}$ cell lose their methylation (Chen et al., 2003a). Together with Dnmt3L, a protein that on its own has no methyltransferase activity, these proteins establish the methylation imprints in the female germ line (Bourc'his et al., 2001; Hata et al., 2002). *Dnmt3b* is of particular interest to nuclear organisation because mutations in this gene cause ICF syndrome, with patients showing destabilisation of centromeric heterochromatin (Xu et al., 1999). The last known protein in this family is Dnmt2, also has no detectable methyltransferase activity in mammals, and gives no apparent phenotype when knocked out in mice (Okano et al., 1998). However, in *Drosophila* this gene is expressed during oogenesis, where it may be responsible for the small amount of non-CpG methylation seen in the fly embryo (Lyko et al., 2000; Gowher et al., 2000).

When induced to differentiate Dnmt1$^{-/-}$ cells, which lack DNA methylation, apoptose (Panning and Jaenisch, 1996). Similarly, at very low levels of DNA methylation, Dnmt3a/3b$^{-/-}$ ES cells are unable to differentiate into myeloid, erythroid or cardiomyocyte colonies (Jackson et al., 2004). Even after 20 days of differentiation without LIF, Dnmt3a/3b$^{-/-}$ cells are not able to downregulated *Oct4* and large numbers of ES cell colonies can be recovered. Interesting, during the same differentiation with Dnmt1$^{-/-}$ ES cells *Oct4* is downregulated as normal, but is re-expressed at day 20 post-LIF withdrawal (Jackson et al., 2004). This re-expression can also be induced by treating differentiated ES cells with the inhibitor of DNA methylation 5-aza-2'deoxycytidine (Tsuji-Takayama et al., 2004).

Recently, attention has focused on the role of DNMTs during ectodermal differentiation. This work is based on experiments carried out by Teter et al., (1994) showing that several CpG sites in the astrocyte marker gene *GFAP* undergo a demethylation and remethylation process during embryonic development. It was later shown that one of these CpG sites, within the binding element of the signal transducer and activator of transcription (STAT) transcriptional activator, needed to be demethylated to allow

binding of STAT3 to the *GFAP* promoter, and subsequent *GFAP* expression (Takizawa et al., 2001). Even when strong glial inducing factors are present, the CNS progenitors are not capable of differentiating into glia with these binding sites methylated (Takizawa et al., 2001; Sauvagoet and Stiles, 2002). Most of the factors shown to influence glia are present in what is essential an astrogliogenic JAK-STAT pathway (Nakashima et al., 1999; Song and Ghosh, 2004; Sun et al., 2001; He et al., 2005), the activity of which, is suppressed during neuronal development and elevated upon a glial switch (He et al., 2005). In the CNS of Dnmt1$^{-/-}$ mice, the absence of methylation triggers precocious astrocyte differentiation (Fan et al., 2001). This confirms not only a role for DNA methylation in regulating the timing of astrocyte differentiation, but more importantly that for neuronal differentiation to occur the JAK-STAT pathway must be inhibited by DNA methylation (Fan et al., 2005). Further support for this theory comes from the Dnmt3a$^{-/-}$ knockout, which survives embryonic development but dies within a month of birth, coincident with a defect in terminal neuronal maturation (Okano et al., 1999). In contrast to the demethylation of genes involved in terminal differentiation, there is also the methylation of genes expressed earlier in development such as *Oct4*, which will be discussed later (section 1.2.3).

1.2.2.2 Methyl-CpG binding proteins

Methyl-CpG binding proteins (MBPs) are recruited to sites of DNA methylation along the chromatin fibre. Six MBPs have so far been identified, MeCP2, the methyl-CpG binding domain proteins MBD1-4, and the unrelated protein Kaiso. These proteins share a conserved MBD domain (with the exception of MBD3 and Kaiso) thought to mediate the effects of DNA methylation in mammalian cells (Hendrich and Bird, 1998). The first to be identified was MeCP2 (Lewis et al., 1992; Nan et al., 1997). This protein is ubiquitously expressed, although particularly high levels are seen in the brain. Mutations in MeCP2 are responsible for a neurological disorder in humans (Rett syndrome, Amir et al., 1999) and mice (Chen et al., 2001; Guy et al., 2001; Shahbazian et al., 2002), but

do not affect other cell types, therefore suggesting a structural role for MeCP2 in neurons (Brero et al., 2005). However, microarray analysis has identified only a few subtle differences in gene expression between the knockout and wild type mice (Tudor et al., 2002). This is due to the selectivity of the MeCP2 binding site, which means that MeCP2 does not compete with other MBPs for access to methyl-CpG nucleotides, but is restricted in its binding sites (Klose et al., 2005). So far only two known targets of MeCP2 have been associated with changes in chromatin organisation, the brain derived neurotrophic factor (BDNF) and the imprinted gene *Dlx5*. The depolarization of primary neurons induces expression of *BDNF*, which correlates with the dissociation of the MeCP2 histone deacetylase mSin3A repression complex from the *BDNF* promoter and a decrease in DNA methylation within the regulatory region of this gene (Chen et al., 2003b; Martinowich et al., 2003). Whereas the imprinted *Dlx5* locus and its adjacent non-imprinted *Dlx6* gene on chromosome 6, associate with MeCP2 to form a loop of silent chromatin characterised by methylated H3-K9 in wild types cells. This structure is absent in MeCP2 null mice, where *Dlx5* interacts with a more distant sequence to form an active chromatin loop, characterised by acetylated H3-K9 and K14 (Horike et al., 2005). Since a global de-repression of genes does not occur in MeCP2 null mice, the absence of MeCP2 may cause incomplete silencing of its target genes, rather than their full expression (Caballero and Hendrich, 2005). However, when coupled with changes in other MBPs or histone modifications the role of MeCP2 in regulating target genes will become more apparent.

Three of the other MBD proteins, (MBD1-3) also function as transcriptional repressors. MBD1 and MeCP2 are concentrated at centromeric heterochromatin where the DNA is highly methylated (Lewis et al., 1992; Ng et al., 2000). MBD1 knockout mice are viable, although their neuronal stem cells show reduced differentiation and genomic instability, which leads to decreased neurogenesis, impaired spatial learning and a reduction in long term potentiation in the brain (Zhao et al., 2003). MBD2 null mice show mild maternal behaviour deficits and lack the MeCP1 protein complex, comprising of MBD2 plus the nucleosome remodelling and histone deacetylation complex NuRD, which explains the

abnormal expression of some genes in MBD2$^{-/-}$ mice (Ng et al., 1999; Zhang et al., 1999; Hendrich et al., 2001). MBD3 is also a member of the NuRD complex, however the knockout for this gene was embryonic lethal with no normal embryos recovered after implantation (Zhang et al., 1999; Hendrich et al., 2001). Recently generation of Mbd3$^{-/-}$ ES cells, have shown that the cells are viable and can initiate differentiation but fail to commit to lineages, due to an inability to silence genes needed pre-implantation (Kaji et al., 2006).

1.2.3 Interactions between transcriptional repressors

Both MBPs and DNMTs can recruit or interact with HDACs and can therefore bind, remodel and deacetylate nucleosomes, thus connecting the processes of DNA methylation and histone modification (Nan et al., 1998; Feng and Zhang, 2001; Fuks et al., 2001). In both *Neurospora* and *Arabidopsis* HMT proteins are involved in the maintenance of DNA methylation (Tamaru and Selker, 2001; Jackson et al., 2002). However, in mammals the story is more complicated. It is known that heterochromatin-associated protein 1 (HP1), which binds to methylated H3-K9, interacts with MBPs, DNMTs and HMTs (Fujita et al., 2003; Fuks et al., 2003b; Lehnertz et al., 2003). This would suggest that as in *Neurospora* and *Arabidopsis* DNA methylation might depend on the methylation of H3-K9. However, the reverse can also occur, as MeCP2 associates with a HMT to increase the level of H3-K9 methylation at sites of DNA methylation (Fuks et al., 2003a). Therefore, MeCP2 can mediate a positive feedback loop to maintain H3-K9 methylation at silenced loci. In addition, Sarraf and Stancheva (2004) have shown that MBD1 also recruits a H3-K9 HMT, SETDB1, to form a complex that facilitates H3-K9 methylation during replication.

The inactivation of *Oct4* is thought to be mediated via trans-acting repressors, such as ARP-1, COUP-TF1 and GCNF, induced by the onset of differentiation (*figure* 1.6; Ben-Shushan et al., 1995; Gu et al., 2005). In undifferentiated cells the *Oct4* promoter is H3-

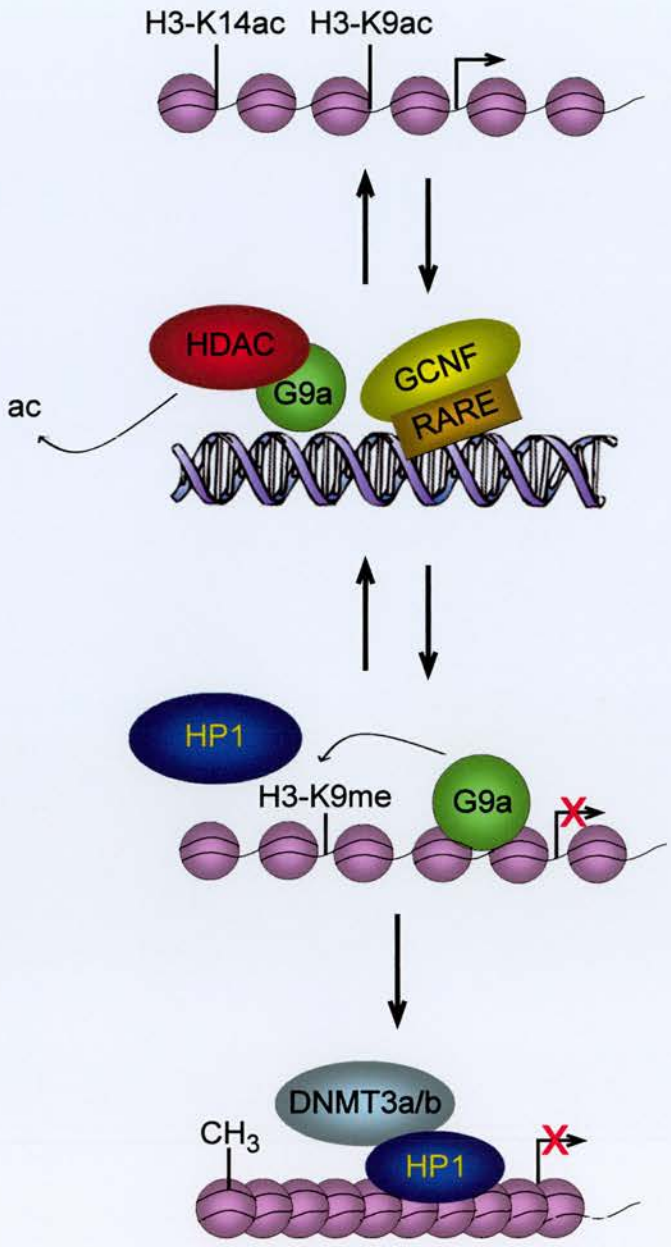

Fig. 1.6 Model for the transcriptional repression of *Oct4*. In ES cells, where the gene is expressed, the *Oct4* promoter region is acetylated at H3-K9 and K14. At the onset of differentiation transcriptional repressors (such as GCNF) bind to the RA receptor element (RARE). This brings about the binding of the histone methyltransferase (HMT) G9a, which recruits histone deacetylases (HDAC). Once deacetylated, H3-K9 can be methylated either by G9a or by another HMT. Methylated H3-K9 can then bind the chromodomain protein HP1. Together with G9a, HP1 recruits the DNA methyltransferases 3a and 3b (DNMT3a/b), which catalyse DNA methylation. Prior to DNA methylation Oct4 can be reactivated (double arrows), however following *de novo* methylation repression seems to be irreversible (adapted from Feldman et al., 2006).

K9, K14 acetylated and H3-K4 methylated. During differentiation, these markers of active chromatin are removed in parallel with a reduction in chromatin accessibility, as detected by DNaseI sensitivity (Feldman et al., 2006). Repression of *Oct4* is followed by increased H3-K9 methylation mediated by the SET-containing protein G9a or another HMT. HP1 can then bind the promoter, where it is required for subsequent *de novo* methylation by Dnmt3a/3b (Ben-Shushan et al., 1995; Gidekel and Bergman, 2002). Without this second layer of repression *Oct4* can switch back on (section 1.2.2.1.). In Dnmt3a/3b$^{-/-}$ ES cells, *Oct4* undergoes methylation of H3-K9, as well as the formation of heterochromatin through the binding of HP1 but without DNA methylation, the gene is not repressed. The process of H3-K9 methylation followed by HP1 binding also occurs at *Rex1* but not *Nanog*, *Sox2* or *Stella*, which suggests that only some of the embryonic genes use this silencing mechanism (Feldman et al., 2006).

1.3 Heterochromatin

1.3.1 Constitutive heterochromatin

Constitutive heterochromatin is generally comprised of tandem satellite repeats, and does not normally contain protein coding genes. These regions are marked by histone hypoacetylation, tri-methylation of H3-K9 and H4-K20, and DNA methylation (section 1.2.2; Kourmouli et al., 2004; Schotta et al., 2004). Facultative heterochromatin describes a previously permissive chromatin environment that is subject to transcriptional silencing, such as the inactive X chromosome. Although hallmarks of this chromatin state are not as well defined, they include hypoacetylation of H3 and H4 lysine residues, di-methylation of H3-K9 and tri-methylation of H3-K27. In contrast, euchromatin is associated with actively transcribed genes or regions of the genome that have the potential to become active, and is characterized by histone hyperacetylation, H3-K4 methylation and a lack of DNA methylation (Arney and Fisher, 2004).

In the current model of constitutive heterochromatin formation, Suv39h enzymes are first targeted to satellite repeats through interaction with the RNA interference (RNAi) machinery (Hall et al., 2002; Volpe et al., 2002; Maison et al., 2002). Tri-methylation of H3-K9 by Suv39h, then allows the binding of chromodomain containing proteins such as HP1 (Bannister et al., 2001; Lachner et al., 2001), which recruits more Suv39h and Suv4-20h enzymes, enabling the tri-methylation of neighbouring H3-K9 and H4-K20 residues (*figure* 1.7; Schotta et al., 2004). In mammals, the Suv39h-HP1 histone methylation system is necessary for both DNA methylation of pericentric heterochromatin by Dnmt3a and Dnmt3b (Lehnertz et al., 2003) and repression of euchromatic genes by the retinoblastoma protein (Nielsen et al., 2001). However in chicken erythrocytes, heterochromatin is formed in the absence of HP1 proteins (Gilbert et al., 2003), which suggests that this is not a universal mechanism.

1.3.2 The role of heterochromatin in gene silencing

Position effect variegation (PEV) is caused by the transcriptional repression of genes inserted within, or brought in close proximity to, heterochromatin. In *Drosophila*, this is illustrated by the insertion of a large (>1Mb) heterochromatic block into the coding region of the *brown* gene, known as the *brown* dominant (bw^D) allele. The bw^D allele associates in trans with similar repeat sequences in heterochromatin; however, through homologous pairing the normal allele is also recruited to these regions, where it to is silenced. Analysis of several rearrangements has shown that the amount of transcriptional silencing observed, correlates with the distance of the bw^D allele from the centromere, with both alleles localized close to centromeric heterochromatin in interphase nuclei (Csink and Henikoff, 1996; Dernburg et al., 1996). Relocalisation to regions of heterochromatin also occurs in mammals. For example in B-lymphocytes, some transcriptionally inactive genes associate with the DNA-binding protein, Ikaros, at centromeric heterochromatin (Brown et al., 1997, 1999). Furthermore, studies on immunoglobulin genes in B cells have found that one allele is often recruited to Ikaros

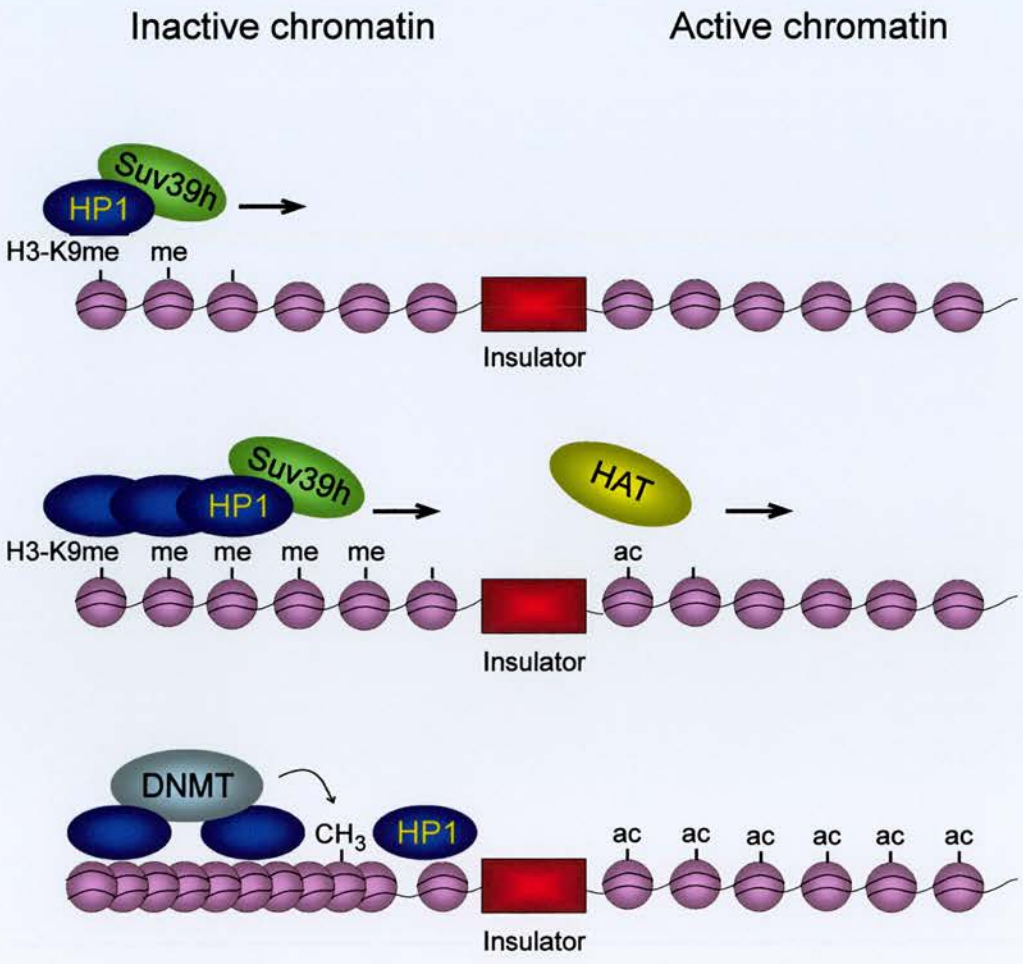

Fig. 1.7 The propagation of inactive and active chromatin states. Nucleosomes marked by H3-K9 methylation can bind HP1, which recruits HMTs such as Suv39h to methylate neighbouring nucleosomes at H3-K9. This way methylation is propagated along the chromatin fibre until it reaches an insulator element, which serves as a barrier to HMTs. HATs are also shown to acetylate nucleosomes by a similar mechanism. Nucleosomes bound by HP1 can associate with DNMTs, enabling DNA methylation and compaction of the chromatin fibre. The insulator therefore defines a boundary between areas of heterochromatin and euchromatin (adapted from Felsenfeld and Groudine, 2003).

containing heterochromatin domains, which has implications for the mono-allelic expression of these genes (Skok et al., 2001; Goldmit et al., 2005). However, analysis of a promoter mutation that interferes with Ikaros mediated silencing, has shown that silencing is not rescued by integration into heterochromatin. Therefore, it is Ikaros binding rather than centromere recruitment per se, which is responsible for influencing gene activity (Sabbattini et al., 2001).

Studies on the β-globin locus and derivative transgenes in erythroid cells have provided further evidence for an association between centromeric heterochromatin and gene expression. Francastel et al., (1999) showed that at genomic integration sites where stable expression does not require the presence of an enhancer, β-globin transgenes are located away from centromeric heterochromatin regardless of their transcriptional activity. However, at sites where an intact enhancer is required for stable expression, the active transgene is localised away from centromeric heterochromatin only when linked to a functional enhancer. Mutations in the enhancer not only affected its ability to suppress silencing but also result in the transgene locating to centromeric heterochromatin, even before the gene was silenced. Therefore, functional enhancers are required for both maintenance of transgene expression and localisation away from heterochromatin. A further study in erythroid cells showed that the β-globin locus is located away from pericentric heterochromatin when it displays an open chromatin structure, as assayed by nuclease sensitivity and histone hyperacetylation. In contrast, the same locus with a naturally occurring deletion in its LCR is recruited to heterochromatin, where it displays an inactive chromatin structure as revealed by nuclease insensitivity and histone hypoacetylation (Schübeler et al., 2000). Together these studies demonstrate the importance of enhancer elements or LCRs in preventing the relocalisation of active genes (or genes with a potential to become active) to centromeric heterochromatin.

The sequestering of genes into regions of heterochromatin is also important for differentiation, as recently shown by a study investigating the murine terminal

transferase gene, *Dntt*, during thymocyte maturation. Silencing of *Dntt* starts 2-6 hours into the differentiation programme with deacetylation of the promoter at H3-K9, which coincided with pericentromeric repositioning. H3-K4 methylation is lost within 4-12 hours, followed by H3-K9 methylation and bidirectional spreading of each event at a rate of 2kb/hour. Later on in the differentiation, when the thymocytes migrate into the spleen, CpG methylation is detected at the locus ensuring a more permanent state of repression. In transformed thymocytes, the inactivation of *Dntt* is reversible and occurs without repositioning or spreading of histone modifications (Su et al., 2004). This would suggest that for specific genes, relocation to heterochromatin is necessary to maintain transcriptional repression. A previous study into the silencing of a pre-B-cell specific λ5 transgene has shown that transcription factor dosage may be involved in relocalisation (Lundgren et al., 2000). Despite integration into pericentromeric heterochromatin and localisation next to centromeric heterochromatin, the λ5 transgene is expressed in pre-B-cells. The locus contains a DNaseI hypersensitive (HS) site located 3' of the gene, which when present excludes the transgene from centromeric heterochromatin. However when the HS site is deleted, the gene is embedded within centromeric heterochromatin. This affect is sensitive to the dosage of early B-cell factor (EBF), which binds to the λ5 promoter and is able to relocate the transgene outside of the heterochromatin complex in the absence of a HS site. Therefore, transcription factors, such as EBF can disrupt regions of heterochromatin to enable the expression of specific genes in a lineage dependent manner.

1.3.3 Polycomb proteins

The Polycomb group (PcG) proteins are negative regulators of transcription that were originally discovered in *Drosophila* (reviewed in Orlando, 2003; Valk-Lingbeek et al., 2004). In conjunction with their positively acting counterparts, the Trithorax group (TrxG), they maintain the transcription memory of several hundred genes during fly development, including the homeotic (Hox) genes. There are two distinct PcG proteins

complexes, polycomb repressive complex 2 (PRC2), is involved in the initiation of gene silencing and contains the H3-K27 HMTase Ezh2, and polycomb repressive complex 1 (PRC1), which is involved in the maintenance of gene repression. Similar to HP1 proteins the PCR1 protein Polycomb (Pc) contains a chromodomain capable of binding methylated H3-K27. It also contains H2A ubiquitination activity. PRC2 proteins bring about H3-K27 methylation on the inactive X chromosome, where they are thought to maintain gene silencing via the recruitment of PRC1 (Plath et al., 2003; Silva et al., 2003). However, it has been shown that the PRC2 protein Eed is not necessary for X chromosome inactivation in undifferentiated trophoblast stem (TS) cells, but is required to prevent reactivation upon differentiation (Kalantry et al., 2006).

PcG proteins have been implicated in the self-renewal of ES, neuronal, hematopoietic and cancer stem cells (reviewed in Valk-Lingbeek et al., 2004). For example, Ezh2 enhances the self renewal of hematopoietic stem cells (Kamminga et al., 2006; Iwama et al., 2004). The very early (gastrulation) phenotypes of mice mutant in components of the PRC2 complex points to the critical role of PRC2 in early development and differentiation. Until recently binding sites of PcG protein and their target genes in mammals were largely unknown. However, several recent large scale ChIP studies have identified numerous sites throughout the genome (Boyer et al., 2006; Lee et al., 2006).

Different homologs of the *Drosophila* Polycomb protein can bind either tri-methyl H3-K27, tri-methyl H3-K9 or both modifications in associations that are at least partially dependent upon the chromodomain binding to RNA (Bernstein et al., 2006b). Both of these histone modifications were previously associated with condensed heterochromatic regions of the genome. However, at genes not expressed by ES cells, tri-methyl H3-K27 has recently been found in areas of decondensed chromatin along with the active markers of H3-K4 methylation and H3-K9 acetylation (Azuara et al., 2006; Bernstein et al., 2006a). In both human and mES cells, PcG proteins have been shown to associate with over 200 repressed genes occupied by H3-K27 methylation, preventing the early expression of lineage specific genes (Boyer et al., 2006; Lee et al., 2006). This allows

pluripotency to continue whilst chromatin is remodelled, enabling genes expressed at later stages to become poised for differentiation. Interestingly, approximately 50% of genes containing this H3-K27, -K4 methylation domain are binding sites of at least one of the transcription factors Oct4, Nanog or Sox2. Therefore, suggesting that these domains in association with other non-histone proteins may prevent gene expression by blocking transcription factor binding in pluripotent stem cells (Boyer et al., 2005; Bernstein et al., 2006a). In another study Bracken et al., (2006), expanded on this theory by showing that for genes activated during neuronal differentiation, PcG proteins were displaced. However, for genes repressed during the differentiation, they found that these proteins were already associated, despite the genes being activity transcribed.

This model of lineage specific genes kept silent in region of open chromatin is supported by evidence from two other sources. The first is the global analysis of open and closed regions across the human genome, which revealed that regions of high gene density are present in an open state. This structure is not correlated with gene expression, since inactive genes are also found within the domains of open chromatin (Gilbert et al., 2004). Secondly, the genome-wide identification of DNaseI hypersensitive sites has identified a strong representation of both expressed and non-expressed genes, implying that a majority of genes reside within open chromatin domains, regardless of their transcriptional status (Sabo et al., 2004). In the future approaches such as DNaseI digestion linked with high-resolution microarrays will lead to a better understanding of the relationship between chromatin accessibility and gene expression profiles (Crawford et al., 2004; Weil et al., 2004).

1.4 Nuclear organisation

A cell nucleus is functionally compartmentalized (*figure* 1.8), and some areas, such as the nuclear periphery and regions surrounding centromeric heterochromatin, are associated with transcriptional repression, whereas others promote transcription, such as

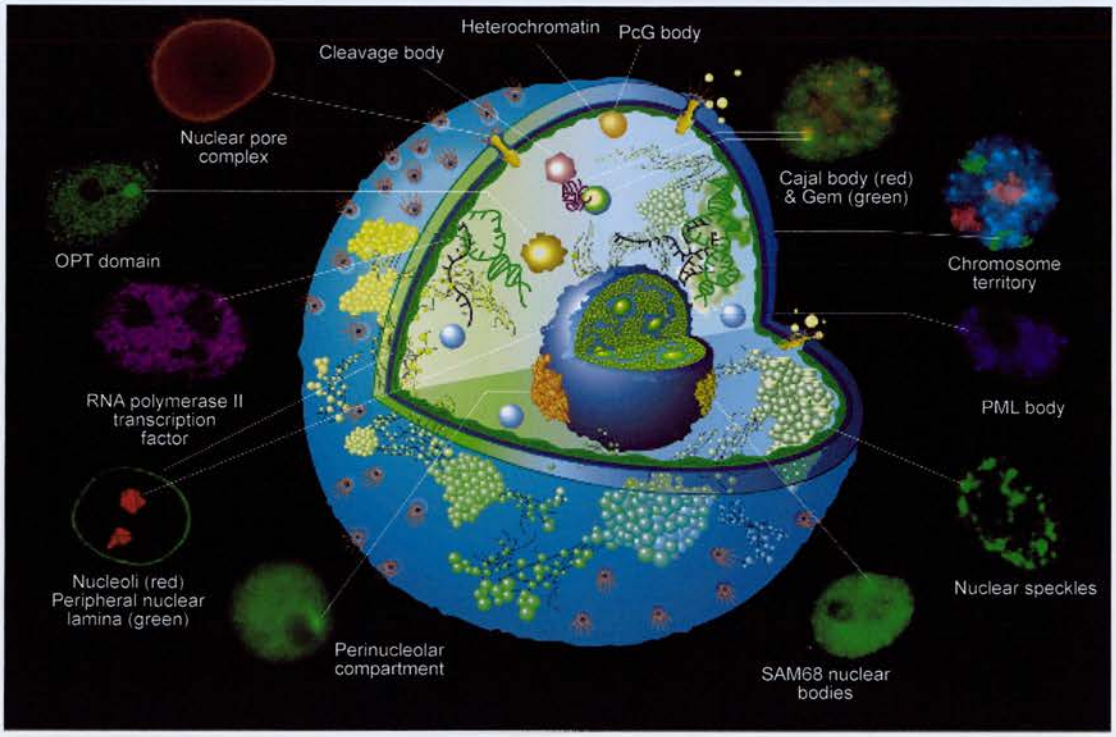

Fig. 1.8 Nuclear domains. Specialised domains or subnuclear organelles within the interphase nucleus, that can be observed by light microscopy (taken from Spector, 2001).

areas surrounding nuclear bodies or regions of high gene density (reviewed by van Driel et al., 2003; Kosak and Groudine, 2004). Therefore, it is not surprising that the spatial arrangement of a genome within this structure is thought to be important for gene expression. Chromosomes, centromeres and genes all have distinct localisations both in respect to the nucleus and each other, suggesting a functional relationship between the DNA sequence and its environment. Here I will outline current theories on how this relationship aids both the transcriptional plasticity of a stem cell and its progression through differentiation.

1.4.1 Chromosome territories

In the 1880s, Rabl and Boveri proposed that chromosomes retained their distribution throughout the cell cycle (Cremer et al., 1982). The 'Rabl' configuration suggests that nuclei are polarised and maintain their anaphase-telophase chromosome orientation during interphase. This gives rise to a nucleus with centromeres clustered towards one pole and telomeres located at the other. The Rabl configuration has been observed in numerous organisms, from plants (Abranches et al., 1998) to insects (Marshall et al., 1996), but it is not present in mammals. In *Drosophila*, the arrangement is particularly interesting, because it is seen in the embryo but not in the imaginal disks, suggesting that chromosome position can change during development (Csink and Henikoff, 1996).

The DNA from individual chromosomes is located in distinct regions of the nucleus, referred to as 'chromosome territories' (CTs), which can be visualised by fluorescent *in situ* hybridisation (FISH; Manuelidis, 1985). In humans, the first evidence that CTs have a preferred localisation came from work on the inactive X chromosome, which is positioned against the nuclear membrane, and the rDNA containing chromosomes 13, 14, 15, 21 and 22, which are clustered around the nucleolus (Manuelidis, 1990). Later analysis of *Homo sapiens* chromosomes 18 and 19 (HSA18 and 19) showed that CTs display a radial distribution related to gene density (Croft et al., 1999). HSA18 and 19

are similar sized chromosomes being 76 and 63 Mbp respectively, but HSA18 is gene poor with ~449 genes whereas HSA19 is gene-rich at ~1528 genes (http://www.ensembl.org/Homo_sapiens/). When visualised by FISH in a variety of differentiated cells, HSA18 is located towards the nuclear periphery and HSA19 is situated closer to the nuclear centre (Croft et al., 1999; Cremer et al., 2003). This radial organisation is applicable to all human chromosomes (Cremer et al., 2001; Boyle et al., 2001) conserved in higher primates (Tanabe et al., 2002) and chickens (Habermann et al., 2001; Stadler et al., 2004). Similarly, within a CT there is also evidence to suggest that gene-rich (R-bands, early replicating) are located towards the centre of the nucleus and gene-poor (G/C bands, late replicating) are towards the periphery (Sadoni et al., 1999). The evolutionary conservation of this chromosome distribution, would suggest that it has a functional relevance, but to date the precise nature of that function is still unknown. There are two main hypotheses: first, that it facilitates gene expression, and second, that it protects the genome by using gene-poor chromatin at the nuclear periphery as a sink for mutagens (Hsu, 1975), referred to as the 'bodyguard' hypothesis. However, a recent study into the affects of oxidation on radial organisation suggests that the nuclear periphery is unable to protect the interior from damage (Gazave et al., 2005).

The radial organisation of CTs is not without exceptions. In the flat nuclei of amniocytes and fibroblasts, gene-poor HSA18 is located nearer to the centre of the nucleus, rather than at the periphery as is characteristic of cells with more spherical nuclei (Cremer et al., 2001, 2003; Bolzer et al., 2005). Furthermore, in contrast to previous findings (Bridger et al., 2000), the Cremer lab has shown that in fibroblasts CTs are not arranged according to gene density. Instead, they propose a radial distribution dependent on chromosome size for these cells, whereby smaller chromosomes are positioned more centrally than larger ones (Sun et al., 2000; Cremer et al., 2001; Bolzer et al., 2005). HSA18 is also more centrally located in the nuclei of quiescent fibroblasts when compared to proliferating fibroblasts; although at present, it is unknown whether this change is due to cell cycle affects and/or further changes in the shape of the nucleus (Bridger et al., 2000; Bolzer et al., 2005).

Differences in chromosome position between various tissues and during differentiation were recently reported in the mouse, (Kim et al., 2004; Parada et al., 2004; Mayer et al., 2005) and the chicken (Stadler et al., 2004). In the mouse, chromosomes do not vary in terms of gene density or size as much as in humans, although in cell types such as lymphocytes, chromosome distribution has been related to gene density. However, in mES cells CT distribution showed a similar correlation with either gene density or chromosome size (Mayer et al., 2005). Significant changes in distribution were reported for the most gene dense chromosome in mouse, MMU11 (15.9 genes/Mbp), for example in mES cells this chromosome was more peripheral than in lymphocytes; although in both cell types it was still the most internal CT. In human cells, prior to this thesis, there were no reports of significant changes in the radial organisation of chromosomes during differentiation, only differences in chromosome associations (Kuroda et al., 2004a). The positions of HSA18 and 19 were shown to be already established in haematopoietic progenitor cells (Cremer et al., 2003) and similar findings were reported for HSA8 and 9 during myeloid differentiation of leukaemic promyelocytic cell lines (Skalnikova et al., 2000), suggesting that the radial distribution of CTs is established very early in development.

1.4.2 Centromere position

In addition to CTs, centromeres also display an organised distribution within the mammalian nucleus. This arrangement is cell-type specific, although it changes in response to cell cycle, physiological and differentiation state (Haaf and Schmid, 1991; Alcobia et al., 2000). In most differentiated cell types, the centromeres are located towards the nuclear periphery or around nucleoli (Carvalho et al., 2001; Weierich et al., 2003; Ochs and Press, 1992). It is currently unknown what determines this organisation, although the composition of chromosome arms is likely be an influencing factor. Carvalho et al., (2001) showed that centromeres surrounded by G-dark bands (gene-rich areas) were located at the nuclear periphery and centromeres with a lower content of G-

bands (gene-poor areas) tended to associate with the nucleolus, along with the rDNA containing chromosomes. This is consistent with the radial distribution of CTs (Boyle et al., 2001; Cremer et al., 2001; 2003), suggesting that centromere position is determined by the 'chromosome environment' as well as other currently unknown factors (Carvalho et al., 2001). However, recently another study has shown that even rDNA containing chromosomes associate with the nuclear periphery (Weierich et al., 2003).

Centromeres have a significantly different localisation in mES cells, when compared to fibroblasts, myoblasts, macrophages and lymphocytes (Mayer et al., 2005). Whereas lymphocytes display a more peripheral nuclear distribution of centromeres than mES cells the other cell types all showed a more internal localisation. This is surprising, as previous studies in mouse, rat and human, have shown that centromeres associate with the nuclear periphery following neuronal, muscle and haematopoietic differentiations (Manuelidis, 1985; Martou and de Boni, 2000; Chaly and Munro, 1996; Kim et al., 2004; Skalniková et al., 2000). During differentiation, centromeres are also known to cluster forming heterochromatic structures called chromocentres. These gene-poor regions of the nucleus are associated with markers of repression and have been implicated in gene silencing (Brown et al., 1997; Merkenschlager et al., 2004; Bártová et al., 2002). The combination of centromeres involved in the chromocentres is characteristic of each cell type and is therefore subject to change during differentiation (Alcobia et al., 2000; Alcobia et al., 2003).

In human and mouse, chromocentre clustering increases during neuronal, muscle, lymphoid and myeloid differentiation (Manuelidis, 1984; Brero et al., 2005; Terranova et al., 2005; Beil et al., 2002; Alcobia et al., 2003). However, in contrast to these studies, others have reported a decrease in the amount of clustering during mouse neuronal differentiation (Martou and de Boni, 2000; Meshorer et al., 2006). One explanation for these differences may be the differentiation status of the cell type. For example, Mayer at al., (2005) has shown that during differentiation of mES cells towards postmitotic macrophages the number of chromocentres decreases significantly. However, when they

compared mES cells to a precursor cell, such as a myoblast, the number of chromocentres is increased. Therefore, in specific lineages the number of chromocentres may first increase to facilitate the process of differentiation, before it decreases upon terminal differentiation to maintain a particular transcriptome. Another explanation could be the cell cycle, as clustering is less pronounced in the nuclei of cycling cells than terminally differentiated cells (Weierich et al., 2003). The distribution of centromeres has not been studied in hES cells. However, recently a study following the formation of chromocentres in relation to the establishment of transcriptional activity during early mouse development, has shown that chromocentres are established during zygotic genome activation. The process was reported to be complete by the blastocyst stage, with only subtle movements of pericentric heterochromatin associated with switches in replication timing and epigenetic markers that correlate with the onset of differential gene expression (Martin et al., 2006).

The nuclear periphery is enriched in hypoacetylated chromatin (Sadoni et al., 1999), although it is unclear whether histone acetylation has a direct role in nuclear organisation. In support of this theory Taddei et al., (2001) report that the histone deacetylase inhibitor Trichostatin A (TSA) reversibly disrupts HP1 binding at pericentric heterochromatin, which results in the relocalisation of centromeres towards the nuclear periphery. However, Gilchrist et al., (2004) have shown that TSA treatment does not alter centromere position and consistent with many other studies, that the majority of centromeres in differentiated cells are located at the nuclear periphery without drug treatment. In mouse, hypoacetylation occurs upon the induction of differentiation (Keohane et al., 1996), and therefore may have a role in enabling chromocentre formation. This theory has been tested by adding various HDAC inhibitors (TSA, Sodium butyrate and Valproic acid) to a muscle differentiation system (Terranova et al., 2005). However, adding these drugs within the first 24 hours, blocks the differentiation. Therefore, the inhibitors were added after 24 hours, when the changes in gene expression that allow myoblasts to differentiate into a myocytes have already occurred. The HDAC inhibitors interfere with tri-methylation of H3-K9 and

block centromere clustering, but no affect on gene expression is shown except for the delayed transcription of a myogenic regulatory factor. This differentiation was stopped after only 6 days. It would therefore be interesting to see if these cells could differentiate from myocytes to myotubes, or if centromere clustering and HDACs are required for terminal differentiation.

Terranova et al., (2005) also show that Cycloheximide (which inhibits transcription elongation) and 5-Azacytidine (which inhibits DNA methylation) has no affect on centromere clustering. This last result is interesting in light of another study, which reports that over expression of the MBP, MeCP2 induces centromere clustering (Brero et al., 2005). If cells that lack DNA methylation can still form chromocentres, then it would be unlikely that a MBP alone is responsible for their formation. In neurons, both H1 and the polycomb protein Eed are associated with chromocentres at the nucleolus (Akhmanova et al., 2000). The authors suggest that DNA replication and/or cell division might disrupt this association in progenitor cells, while it can proceed to completeness in terminally differentiated neurons, where neither of these processes takes place. However, the role of polycomb proteins in maintaining nuclear organisation has yet to be described.

1.4.3 Telomere position

Telomeres are the protein-DNA structures at the ends of eukaryotic chromosomes, essential for maintaining chromosome stability, positioning and complete replication (reviewed in Zalenskaya and Zalensky, 2002). Unlike centromeres, human telomeres are distributed throughout the nuclear interior (Molenaar et al., 2003; Weierich et al., 2003), whereas in mouse, half of the telomeres are associated with heterochromatic chromocentres at the periphery and the rest are distributed throughout the nucleus, as expected for telocentric chromosomes (Cerda et al., 1999; Weierich et al., 2003). Furthermore, the order of these domains, q-telomere, p-telomere and then centromere,

from the nuclear interior to the periphery, contributes to the polar organisation of human CTs (Ferguson and Ward, 1992; Amrichová et al., 2003) and to a lesser extent mouse CTs (Vourc'h et al., 1993). Telomere position has not been studied in other immortal cells, although Nagele et al., (2000) reported that telomeres cluster less frequently in cycling and immortal HeLa cells, then in non-cycling cells such as quiescent fibroblasts. They suggested that clustering might be important for stabilising chromosome positions in the interphase nucleus, however more recently these telomere associations have been shown to be transient in nature (Molenaar et al., 2003).

1.4.4 The nuclear periphery and gene expression

The position of a gene within the nucleus is thought to affect its transcription. For example in yeast, Andrulis et al., (1998) silenced a gene by tethering it to the nuclear periphery. However, the transcriptional activation of specific genes in yeast has also been shown to result in their relocation to the nuclear periphery, demonstrating that this change in position is not controlled by transcription alone (Casolari et al., 2004). In mammals, a direct link between nuclear position and transcription has yet to be demonstrated. However, some silent genes associated with the nuclear periphery have been shown to relocate to the nuclear interior when expressed (Kosak et al., 2002; Zink et al., 2004). This spatial arrangement is also consistent with the localisation of late replicating and gene-poor genomic regions at the nuclear periphery (Ferreira et al., 1997; Sadoni et al., 1999; Croft et al., 1999; Boyle et al., 2001). During differentiation of mES cells, both the *Hox* genes and the transcription factor *Mash1* (*Ascl1*) move towards the nuclear interior when activated (Chambeyron and Bickmore, 2004; Williams et al., 2006). In the case of *Mash1*, this relocalisation was shown to accompany a change in replication timing. *Mash1* is one of three genes found to be late replicating in mES cells by Perry et al., (2004). It is currently not known whether transcription of the other genes (*Neurod* and *Myf5*) is accompanied by relocation within the nucleus. Interestingly, Williams et al., (2006) showed that the position of *Mash1* is conserved in

undifferentiated mES cells lacking the Ezh2-Eed HMTase complex and several other chromatin silencing candidates (Suv39h1, Dnmt1, Dnmt3a and Dnmt3b). However, the position of a gene has yet to be followed during the differentiation of these cell types.

Not all genes change location in response to transcription. Some genes, such as the proteolipid protein (*PLP*) gene, are constantly located at the periphery, whereas others such as the immunoglobulin (Ig) genes show a conserved distribution throughout the nucleus, independent of both cell type and transcriptional activity (Nielsen et al., 2002; Bártová et al., 2002; Parreira et al., 1997). This is consistent with reports that sites of transcription are present throughout the nucleus (Verschure et al., 1999; Szentirmay and Sawadogo, 2000). Other loci such as CD4 only relocate to the nuclear interior in cells, which expressed the gene at high levels and not their precursors (Kim et al., 2004). This would suggest that although movement of a locus is not necessary for gene expression, the centre of the nucleus might confer some transcriptional advantage on gene-dense regions that require high levels of transcription.

1.4.5 Nuclear organisation and transcription

Instead of directly recruiting the transcriptional machinery, it has been suggested that genes move into preassembled transcription sites in the nucleus (Osborne et al., 2004). This would provide evidence for the model originally proposed by Cook, (2002), that the physical properties of chromatin and the sum of interacting proteins, such as polymerases, might determine the distribution of chromosomes and genes in a self-organizing manner. For example, whereas inactive genes on different chromosomes can colocalise in association with polycomb proteins (Bantignies et al., 2003) or centromeric heterochromatin (Brown et al., 1997, 1999; Su et al., 2004), active genes colocalise at sites of concentrated transcriptional components, such as RNA polymerase (Osborne et al., 2004), providing anchor points, which might determine the spatial organisation of the genome (Cook, 2002). A recent study has even documented colocalization of the

interferon (IFN)γ locus on mouse chromosome 10, with the Th2 cytokine gene cluster on chromosome 11, in the absence of transcription (Spilianakis et al., 2005). Interestingly, this association is only seen in cell types that have the potential to express the genes, and not in cells that will never express the genes. The interaction between chromosomes is also lost in favour of intrachromosomal associations upon gene activation. Therefore, physical associations between chromosomes may have implications for coordinating gene expression (Spilianakis et al., 2005). Unlike the cytokine genes, human α- and β-globin genes are frequently in spatial proximity when active (Brown et al., 2006). The human α-globin genes can extend outside of their CTs, irrespective of transcriptional status, but associate with each other and nuclear speckles in a transcription dependent manner. The same degree of proximity does not occur between human β-globin genes or between mouse globin genes, which are more constrained to their CTs (Brown et al., 2006). This suggests that spatial organisation of globin genes within the nucleus is controlled by both their expression and the genomic environment.

In a review, Gasser (2002) suggested a functional role for chromosome tethering in controlling the genetic plasticity of stem cells (*figure* 1.9). If anchorage in the cell nucleus controls gene expression, she perceived chromatin mobility as an indication of the active (or inactive) state of the nucleus. For example in large pluripotent nuclei, the chromatin may be fully dynamic. Integration of the lac operator at different positions in the human genome has shown that in general, chromatin associated with the nucleolus or the nuclear periphery is more restricted in its movement than that of chromatin associated with nucleoplasmic regions (Chubb et al., 2002). This motility may reflect the ability of the chromatin to either be transcribed or silenced, reminiscent of genes in an ES cell. As the cell differentiates and the transcription pattern of the nucleus is defined, the nuclei become smaller with less mobile chromatin. Recently this change in chromatin dynamics was reported to accompany the differentiation of mES cells towards a neuronal lineage (Meshorer et al., 2006).

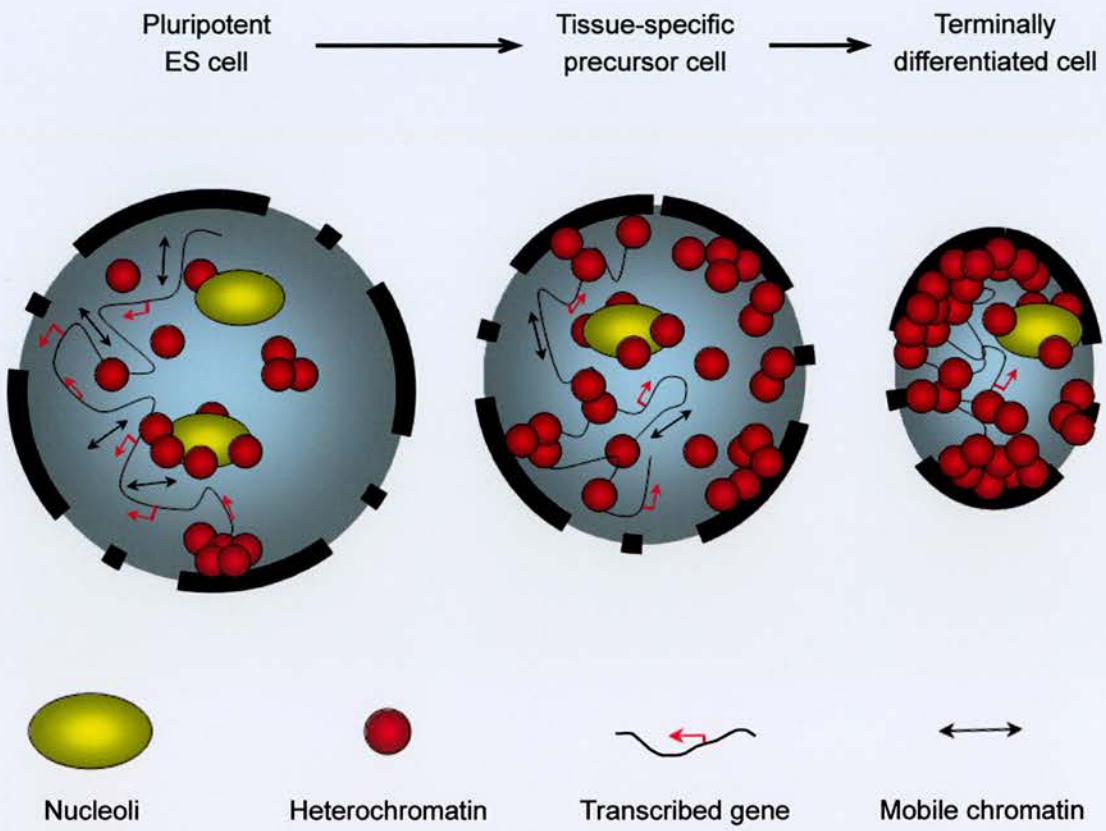

Fig. 1.9 Model for nuclear organisation during differentiation. This model predicts that progressive differentiation restricts both gene expression and chromatin mobility. For example in large pluripotent nuclei, the chromatin may be fully dynamic. This motility reflects the ability of the chromatin to either be transcribed or silenced, reminiscent of the genes in an ES cell. As the cell differentiates and the transcription pattern of the nucleus is defined, the nuclei become smaller with less mobile chromatin (adapted from Gasser, 2002).

1.4.6 Transcription and the chromosome territory

It was originally proposed that genes clustered together on chromosomes according to tissue specific expression or high transcription rates (Caron et al., 2001; Versteeg et al., 2003). However, more recently it has been shown that the most gene-dense regions of the genome contain genes, which are expressed in a wide range of tissues and cell types (Hurst et al., 2004; Lercher et al., 2002). Therefore, it is genes that are broadly expressed, rather than those that are highly expressed, which cluster together across the genome.

Early studies suggesting that transcription and RNA processing occurred in a compartment between the CTs, led to the interchromosome domain (ICD) model of nuclear organisation (*figure* 1.10; reviewed in Cremer and Cremer, 2001). Support for this model came from experiments showing that genes, but not non-coding regions, were positioned on the surface of CTs (Kurz et al., 1996). Furthermore, active genes on the X chromosomes were found to locate at the periphery of their CT, whereas a silent gene was located within the inactive X CTs interior (Dietzel et al., 1999). However, studies contradicting the ICD model have shown that transcription sites are found deep within CTs (Abranches et al., 1998; Verschure et al., 1999) and that both early and later replicating DNA, as well as C-G rich sequences are found throughout the CTs (Visser et al., 1998; Tajbakhsh et al., 2000). Together these observations led to the revised interchromatin compartment (IC) model (*figure* 1.10), which predicted that genes might also be transcribed from within CTs. Later, evidence confirming this prediction came from studying the WAGR locus at 11p13, which is active from within the chromosome 11 territory (Mahy et al., 2002a). Therefore, genes do not need to be at the surface of their CT or in the nuclear interior to be transcribed.

In addition to being on the surface or in the interior of a CT, some genes can also extend out from their CTs into the nucleus. Examples of this include the major histocompatibility complex (MHC) on 6p21 and the epidermal differentiation complex

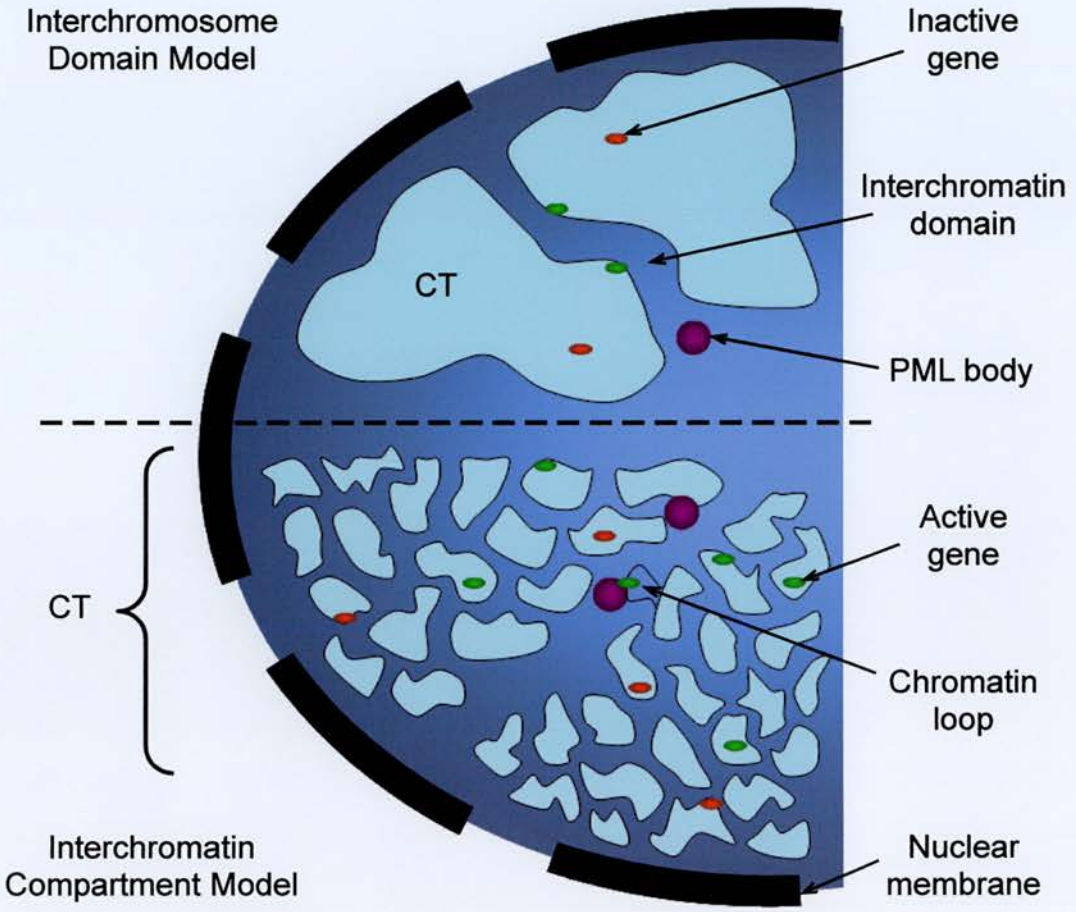

Fig. 1.10 A comparison of the interchromosome domain (ICD) model and the interchromatin compartment (IC) model. The ICD model, originally proposed that active genes would be located on the surface of CTs, where they could access transcription factors in the ICD, and inactive genes would be situated within the CT. However, evidence has now shown that transcription is not confined to the ICD, and takes place throughout the CT, leading to the proposed IC model.

(EDC) located at 1q21 (Volpi et al., 2000; Williams et al., 2002), which both loop out from their CTs in response to transcriptional activation. The genes within these clusters are not all structurally related, although they can be co-ordinately regulated. Therefore, it was unknown whether these gene-dense regions looped out of their CTs because of this specialized regulation, or if other regions of the genome also located outside of their CTs. This was addressed by analyses of 11p15.5, which is a gene-dense region that consists of functionally unrelated genes with different expression patterns (Mahy et al., 2002b). 11p15.5 was found outside of its CT in both lymphoblasts and fibroblasts, suggesting that local gene density and transcription, rather than the expression of individual genes are responsible for the nuclear organisation of these looped out regions.

The destination of these looped out regions is still unclear. It has been shown that proteins involved in transcription and RNA processing are present predominantly in the interchromatin space, inside and between CTs, and are largely excluded from domains of condensed chromatin (Verschure et al., 2002). Interestingly, the chromosome band 6p21 (which contains the MHC genes) was found to associate with the transcriptionally active OPT (Oct1/PTF/transcription) domains in nuclei of HeLa cells (Pombo et al., 1998). Therefore, even though fluorescence recovery after photobleaching (FRAP) experiments show that transcription factors are highly dynamic and are not excluded from CTs (Phair et al., 2004), perhaps these gene-dense regions need to decondense away from their CTs to gain access to large protein complexes or nuclear organelles that are restricted in their location, or to associate with regions of other CTs. Electron microscopy of BrdU labelled chromosomes has shown that chromatin from adjacent chromosomes may be in contact in limited regions (Visser et al., 2000). Recent evidence from Branco and Pombo (2006) has suggested that this overlap between CTs might be more significant than previously described. This would enable genes on adjacent chromosomes to associate with the same transcription site (section 1.4.5; Osborne et al., 2004; Brown et al., 2006). Although so far the distances measured between these genes (>400nm) imply that they are not sharing the same 'transcription factories', which are only 50nm in diameter, as detected by bromouridine triphosphate incorporation (Iborra,

2002). Gene-dense region have also been shown to colocalise with Promyelocytic leukemia (PML) bodies (Shiels et al., 2001; Wang et al., 2004b) and SC-35 domains (Shopland et al., 2003; Moen et al., 2004). However, disruption of PML bodies by RNAi does not have any significant consequences on the expression of genes associated with them, suggesting that although PML bodies are formed in transcriptionally activity regions, they are not necessary for transcription (Wang et al., 2004b).

It is also currently unclear if transcription happens prior to nuclear relocalisation or vice versa. The mammalian β-globin locus, for example, was reported to loop out of its CT prior to transcriptional activation (Ragoczy et al., 2003). However, during the differentiation of mES cells *in vitro* and mouse embryonic development *in vivo*, *Hox* genes are located outside their CT, accompanying their collinear pattern of expression (Chambeyron and Bickmore, 2004; Chambeyron et al., 2005). Prior to this movement, locus wide changes in chromatin structure (histone modifications and chromatin decondensation) may establish a transcriptionally poised state, but this alone is not enough for gene expression. Therefore, the nuclear reorganisation of *Hox* genes represents a transcriptionally active state and not a poised state. In light of recent advances in the stem cell field, it may also be important to note that polycomb group proteins are localised at the periphery of chromatin domains, and throughout the interchromatin space (Cmarko et al., 2003). This would provide a way in which neighbouring genes might be kept poised in amongst looped out regions of open chromatin.

1.4.7 PML bodies

First described by Szostecki et al., (1990) PML bodies (also known as nuclear domain 10 (ND10), PML oncogenic domains (PODs) and Kremer (Kr) bodies) are multi-protein domains. A mammalian nucleus contains 5-30 of these bodies, which vary in size from 0.3μm to 1.0μm in diameter (Melnick and Licht, 1999). They have been implicated in

many cellular processes including cell-cycle regulation, apoptosis, proteolysis, tumour suppression, DNA repair and transcription (reviewed by Dellaire and Bazett-Jones, 2004; Ching et al., 2005). There are currently three proposed models for PML body function. First, they may be aggregates of excess nuclear proteins, which can regulate nucleoplasmic levels by releasing proteins when they are needed. Second, these bodies might be sites of post-translational modification and protein degradation; and third, PML bodies may be sites of specific nuclear activities, for example transcriptional regulation (Ching et al., 2005). This last model is supported by the detection of nascent RNA around PML bodies (Boisvert et al., 2000) and their association with regions of high transcriptional activity (Shiels et al., 2001; Wang et al., 2004b). Prior to this thesis, their localisation within the nuclei of ES cells had not been described.

1.5 Proposed research

This thesis expands on previous work carried out in the Bickmore lab, which analysed the location of CTs and gene-dense regions of the genome in differentiated cells. It was thought that if nuclear organisation regulates gene expression, it would have a role in gene silencing as a cell commits to differentiation. Therefore, it is important to determine the nuclear organisation of a pluripotent stem cell. The initial aim was to locate CTs, centromeres and genes known to be important for pluripotency, within a hES cell nucleus. Prior to starting the project, no previous research had been published on this subject. Therefore, it was to provide the first description of nuclear organisation in a hES cell. In parallel, work on mES cells differentiated towards a neuroepithelial cell type, would allow any differences in nuclear organisation to be analysed throughout the early development of a lineage. This would enable questions about the role of chromatin modifying proteins in genome localisation to be addressed in knockout mES cells. Together both the human and the mES cell projects aim to identify whether spatial reorganisation is evident during differentiation, or if nuclear organisation is established prior the to ES cell stage.

Chapter 2: Materials and Methods

Chapter 2: Materials and Methods

All the reagents were analytical grade and obtained from Sigma or Roche, unless stated otherwise. General solutions were prepared by technical staff of the Human Genetics Unit (HGU), autoclaved and stored at the required temperature. Most nucleic acid manipulations were performed in 0.5ml or 1.5ml Eppendorf tubes. All centrifugations were carried out at room temperature, unless stated otherwise.

2.1 Mammalian cell culture

2.1.1 Cell counting

After harvesting, cells were resuspended in phosphate buffered saline (PBS) and counted using a haemocytometer (Weber Scientific International Ltd.). 10µl of cell suspension were pipetted onto the haemocytometer, which had a chamber 0.1mm in height with 4 etched grids of $1mm^2$. Therefore, the total volume defined by each grid was $1x10^{-4}$ ml, and the concentration of cells per ml was obtained by averaging the number of cells counted over 4 grids and multiplying by 10^4.

2.1.2 Freezing and thawing cells

Cell suspensions were frozen in cryotubes containing 0.5ml of freezing medium (10% DMSO (v/v) in foetal calf serum (FCS) (Globalpharm)), at a concentration of approximately 10^6 cells/ml and placed in -70°C for short term storage, or liquid N_2 for long term storage. To retrieve cells from liquid N_2, vials were thawed at 37°C in a water bath, after expelling excess nitrogen gas from the tube by loosening the cap. Cells were

diluted in 7ml culture medium and the medium changed after 24 hours incubation at 37°C.

2.1.3 Culture of transformed mammalian cell lines

All cells were incubated at 37°C with 5% CO_2 in tissue culture medium containing penicillin (10,000units/ml) and streptomycin (650μg/ml). Tissue culture solutions were pre-warmed to 37°C before use.

2.1.3.1 Suspension cells:

The FATO (46XY) human lymphoblast cell line (LCL) was grown as a suspension culture in Roswell Park Memorial Institute 1640 medium (RPMI, Invitrogen) supplemented with 10% FCS and 2mM glutamine (Invitrogen). Cells were split 1:3 – 1:5 in fresh medium every 2-3 days.

2.1.3.2 Monolayer cells:

Human HT1080 (male fibrosarcoma-derived; Chen et al., 1983) and RITVA (human primary fibroblasts carrying an aniridia-associated translocation, transformed with hTERT by C. Griffiths) cell lines were grown in high glucose Dulbecco's Modified Eagle Medium (DMEM, Invitrogen) supplemented with 10% FCS. Cells were grown to near confluence before splitting into fresh culture flasks (Costar). To passage cells, the medium was removed from flasks and monolayers rinsed once in PBS. Cells were then covered in a small volume of 10% Trypsin-EDTA/versene and incubated at 37°C for 5 minutes. Gentle agitation dislodged the cells, fresh medium was added and the cells pelleted at 400*g* for 5 minutes before being re-plated or fixed.

For immunofluorescence and 3D FISH (sections 2.6 and 2.8.4) cells were seeded directly onto sterile coverslips (processed through washes of 2M HCl, 100% ethanol,

dH_2O, 100% methanol and air dried in a sterile culture hood) in a 6-well plate (Greiner, Bio-one) or slides (washed in detergent, soaked for at least 1 hour in 100% ethanol with ~2 drops 8M HCl, stored in 100% methanol and flamed before use) in Quadriperm slide chambers (Vivascience, Satorius).

2.1.4 Primary human fibroblast culture

A 46XY primary fibroblast cell line (1HD), derived from foreskin tissue was obtained from J. Bridger, Brunel University. The cells were cultured in high glucose DMEM supplemented with 10% FCS. Cultures were grown to almost confluence and passaged using trypsin-EDTA/versene, as described above. Cells were seeded at concentrations of $1.5x10^5$ cells per slide and $5x10^5$ cells per $75cm^2$ tissue culture flask. Primary cell lines can be maintained in culture for a limited number of passages before they senesce.

2.1.5 Human embryonic stem cell culture

All hES cell culture was carried out under licence by W. Cui at the Roslin Institute. Human ES cell lines H1 (46XY), H7 and H9 (46XX) (Thomson et al., 1998) were grown as previously described (Xu et al., 2001), with minor modification. Briefly, the cells were cultured on Matrigel coated culture dishes with mouse embryonic fibroblast conditioned medium, supplemented with 8ng/ml basic fibroblast growth factor (bFGF). Cells were routinely split 1:3 with collagenase.

2.1.6 Mouse embryonic stem cell culture

The mES cell lines (*table* 2.1) were maintained in Glasgow Modified Eagle Medium (GMEM/BHK21, Invitrogen) supplemented with 10% FCS (v/v), 100mM sodium pyruvate, 1% non-essential amino acids (NEAA) (v/v), 2mM glutamine, 50μM β-mercaptoethanol (β-me), 100U/ml Leukaemia inhibitory factor (LIF) as described by Smith et al., (1988). The LIF was obtained from conditioned medium derived from

Cos-7 cells, transfected with a LIF expression construct. Mouse ES cells were maintained on gelatinised (0.1% gelatin/PBS) flasks. The flasks were coated 10 minutes before plating, excess gelatin was then removed and the cells seeded. The media was changed 24 hours later, and the cells passaged every 48 hours at 1:6.

Cell Line	Description	Source
OS25	40XY, *Oct4-HygTK*, *Sox2βgeo* into parental E14Tg2a. 129/Ola	A gift of A. Smith (Billon et al., 2002)
Suv39h double null	Suv39h1 and Suv39h2 targeted with *LacZ* and *neomycin*	A gift of T. Jenuwein (Peters et al., 2001)
Suv39h wt	WT ES cells from a C57BL6/129 background	A gift of T. Jenuwein
Dnmt3ab$^{-/-}$	Targeted disruption of Dnmt3a and 3b with IRES-*βgeo* in J1 ES cells	A gift of E. Li (Okano et al., 1999)
J1	WT ES cells from a 129S4/SvJae background	A gift of E. Li
MeCP2	MeCP2 targeted with *βgeo* in CGR8 cells	A gift of A. Bird (Tate et al., 1996)
CGR8	WT ES cells from a 129/ola background	A gift of A. Bird (Mountford et al., 1994)

Table 2.1 – mES cell lines used in this thesis.

2.1.7 Culture and disaggregation of embryoid bodies

To form embryoid bodies (EBs), OS25 cells at a density of $3x10^4$ cells/ml (in ES cell media –LIF) were cultured in 10μl hanging drops by pipetting onto 120 x 120mm square

dishes (greiner). After two days the EBs were resuspended in 15ml ES cell media –LIF on bacterial petri dishes and cultured further in suspension depending on the differentiation conditions (section 4.2). Every 48 hours, EBs were collected by sedimentation at the bottom of a 50ml falcon tube, the media changed and EBs moved to a fresh petri dish. To disaggregate EBs, they were first allowed to settle in 50ml falcon tubes, then the media was removed and the EBs washed once with PBS. The EBs were then incubated in a mixture of 1ml PBS, 1ml Dispase (2.4U/ml) and 20µl DNase I (7mg/ml) for 30 minutes at 37°C with gentle shaking, before being dissociated by gentle pipetting with a 5ml stripette. The dissociated cells were washed with 38ml of PBS and centrifuged at 300*g* for 4 minutes. The supernatant was removed and the pellet washed again in 20ml PBS, centrifuged at 300*g* for 4 minutes and resuspended in 10ml neuronal differentiation media (50/50 neurobasal media/DMEM-F12, B27 and N2 supplements). Cells were then plated onto gelatin coated coverslips or petri dishes as needed.

2.1.8 Cell culture drugs

Drugs were added to cell culture media at the specified concentrations for the appropriated time (*table* 2.2). Every 48 hours media was decanted from flasks and fresh media and drugs added.

2.1.9 Bromodeoxyuridine (BrdU) incorporation

BrdU is a thymidine analogue incorporated into DNA during S-phase, used to establish the percentage of cells in cell cycle. It was added to culture media at 10µM for 1 hour before slides were fixed in 4% paraformaldehyde (pFa). Slides were then processed with a 1 hour incubation using an anti-BrdU antibody as described in section 2.6.1.

Drug	Application	Concentration	Time
Colcemid	Mitotic spindle inhibitor used to arrest cells in metaphase.	0.1μg/ml	30 minutes
Hygromycin-B	An aminocyclitol antibiotic used to inhibit protein synthesis by interfering with translocation.	100μg/ml	7 Days for selection purposes
G418	An aminoglycoside antibiotic that blocks protein synthesis through interference with ribosomal functions.	100μg/ml	7 Days for selection purposes
Gancyclovir	The drug is phosphorylated by viral thymidine kinase, and incorporated into the DNA of replicating cells where it inhibits DNA polymerase. These cells are irreversibly arrested at the G2-M checkpoint and die.	2.5μM	7 Days for selection purposes

Table 2.2 - Drugs used in tissue culture.

2.2 Microbiology

2.2.1 Growth of E. coli bacterial strains

Competent DH5-α (Library Efficiency, Invitrogen) were used for all cloning procedures. Cultures were grown in Luria-Bertani (LB) medium with shaking or on L-agar plates at 37°C. Plasmids were stored in glycerol (15% glycerol/LB) at -70°C.

2.2.2 Bacterial transformations

Competent cells were incubated on ice with plasmid DNA for 30 minutes, then heat shocked at 42°C for 45 seconds. After addition of 400µl SOC medium (2% tryptone, 0.5% yeast extract, 10mM NaCl, 2.5mM KCl, 10mM $MgCl_2$, 10mM $MgSO_4$, 20mM glucose, Invitrogen), reactions were incubated at 37°C for 30 minutes before being plated on L-agar plates containing the appropriate antibiotic for selection (ampicillin at 50µg/ml or chloramphenicol at 170µg/ml). Transformation plates were then grown overnight at 37°C.

2.3 Preparation and analysis of nucleic acids

2.3.1 Isolation of plasmid DNA

Single bacterial colonies were picked and grown overnight in 3ml of LB medium at 37°C with shaking. Plasmid preparations were then harvested from these cultures using a miniprep kit (Qiagen). Briefly, bacteria were lysed under alkaline conditions. The lysate was then neutralised and passed through a silica-gel membrane that selectively absorbs DNA. The membrane was then washed before the plasmid DNA was eluted with dH_2O.

2.3.2 Isolation of bacterial artificial chromosome (BAC) clones

BAC stocks stored at -70°C in 15% glycerol were grown overnight in 3ml cultures containing chloramphenicol (170µg/ml), with shaking at 37°C. These were streaked out onto L-agar plates containing chloramphenicol to obtain single colonies; which were used to inoculate 3ml and then 200ml LB cultures, all grown overnight at 37°C. BAC DNA was isolated either by Qiagen prep (see section 2.3.1) for PCR or by maxi prep (without the Qiagen column step) to prepare FISH probes. Briefly, the colonies were pelleted and the bacteria lysed under alkaline conditions. The lysate was then neutralised

and the supernatant filtered through muslin. DNA was precipitated in cold isopropanol. This was centrifuged, and the pellet washed twice with 70% ethanol, air dried and resuspended in an appropriate amount of TE.

2.3.3 Purification of DNA

2.3.3.1 Phenol/chloroform extraction

An equal volume of buffered phenol/chloroform (50% buffered phenol pH>7.8/48% chloroform v/v, 2% isoamylalcohol v/v) was added to the DNA preparation and vortexed. This was centrifuged at ~12,000*g* for 15 minutes. The top aqueous layer was decanted into a fresh tube, avoiding any white precipitate present at the boundary between the two layers and an equal volume of chloroform added. Vortexing and centrifugation was repeated. Again, the top layer was decanted. Ethanol precipitation was then performed to concentrate the DNA (section 2.3.2.2).

2.3.3.2 Ethanol precipitation

DNA was precipitated by adding 0.1 volumes 3M sodium acetate, pH5.2 and 2 volumes 100% ice cold ethanol to the DNA sample. After vortexing, the sample was incubated at –20°C for 30 minutes and then centrifuged at 12,000*g* for 15 minutes at 4°C. The supernatant was discarded and the pellet washed in 70% ethanol (v/v with dH_2O). Centrifugation was repeated and the supernatant discarded. Once the pellet had dried at room temperature, it was resuspended in an appropriate volume of dH_2O.

2.3.4 DNA digestion and preparation

DNA was digested with restriction enzymes (New England Biolabs) in reaction buffer according to the manufacturers' instructions. Digestion products were then analysed by agarose gel electrophoresis.

2.3.5 Agarose gel electrophoresis

0.5-2% horizontal agarose ('HiPure' Low EEO agarose, BioGene UK) gels (w/v) in 1x Tris-borate-EDTA (TBE, 45Mm Tris-borate, 1mM EDTA pH8.3) were used with 1x TBE electrophoresis buffer to resolve DNA samples, PCR products and plasmid digestion products. 0.5-1% gels were used to resolve DNA molecules of 0.2 to 50Kb, to resolve smaller fragments of 0.05 to 5Kb 1.5-2% gels were used. Ethidium bromide (EtBr; 2,7-diamino-10-ethly-9-phenyl-phenathridium bromide), a DNA intercalating stain, was added to molten agarose to a final concentration of 0.2μg/ml before pouring the gel. One volume of 6x gel-loading buffer (15% Ficoll^{TM} 400 (Amersham Biosciences), 0.25% bromophenol blue, 0.25% xylene cyanol, all w/v in dH_2O) was added to five volumes of sample. DNA size markers ϕX174 DNA *HaeIII* digest (Promega) and λ DNA *HindIII* digest (Invitrogen) were diluted to 50ng/μl, with 500ng loaded on the gel to enable size determination and quantification of DNA fragments. Stained DNA was then visualised using UV light and photographed using Quantity One 4.4.1 (Bio-Rad) and a thermal printer (Mitsubishi).

2.3.6 Measuring quality and quantity of DNA

Quantification of DNA was either by comparison with a known quantity of DNA on an agarose gel (see section 2.3.4), or by measuring its absorbance in a spectrophotometer (Ultrospec 3000pro, Amersham Biosciences). For this DNA was diluted 1:100 in Tris EDTA (TE, 10mM Tris-HCl, 1mM EDTA, pH7) and transferred to a quartz cuvette. The optical density (OD) at 260nm (A_{260}) was then measured. An OD of one corresponds to

~50μg/ml of DNA. To determine the purity of nucleic acid, the A_{280} was also measured. Pure DNA has an A_{260}/A_{280} of 1.8 and values lower than this indicates contamination with proteins, RNA or phenol.

2.3.7 Polymerase chain reaction (PCR)

2.3.7.1 PCR reagents

dNTPs (Abgene) were purchased as 100mM stocks of each dNTP. Working stock concentrations of 10mM were prepared and used at a final concentration of 0.2mM. Primer3 (http://frodo.wi.mit.edu/) was used to design PCR primers between 17 and 25 nucleotides in length for which the [G+C]:[A+T] ratio was approximately equal, and which would not self anneal. Primers were purchased from Invitrogen as lyophilised desalted compounds and diluted to a stock concentration of 100μM with dH_2O. Working stock concentrations were prepared at 25μM and oligonucleotides were used at final concentrations of 0.5μM. Template DNA was at a concentration of 100ng/μl. Ampli*Taq*® DNA polymerase (5U/μl) was used at 0.5μl per 25μl reaction. 10x PCR buffer and 2.5mM $MgCl_2$, supplied with the polymerase, were used at 1:10 and 0.1mM respectively. Reaction mixes were made up to 25 or 50μl total volume with dH_2O.

2.3.7.2 PCR programs

PCRs were performed in 0.5ml centrifuge tubes or 96 well PCR plates in a DNA Engine Tetrad (MJ Research). The general PCR amplification program was as follows: -

1. An initial 10 minute DNA denaturation step at 95°C
2. 30 second denaturation step at 94°C
3. 30 second annealing step at *x* temperature (specific to the primers used)

4. 30 second elongation step at 72°C
5. Steps 2 to 4 were cycled 30 times
6. A final elongation step for 5 minutes at 72°C to complete the program

Primer sequences, product sizes and annealing temperatures used in PCRs are shown in *table* 2.3.

Gene	Species	Primer Sequence 5'-3'	Product Size (bp)	Annealing T (°C)
FLOT1	Human	CACAGTCTTCTCAACCCTTGC TGACATCCTTCCAGATGGTTC	385	58
OCT4	Human	GAGGGGTTGAGTAGTCCCTTC AGCTTCTCCTTCTCCAGCTTC	456	58
MICB	Human	GTTCGGGAATGGAGAAGTCA TCTAGCAGAATTGCGGGAAC	372	58
NANOG	Human	ACCTTCCAATGTGGAGCAAC GAATTTGGCTGGAACTGCAT	199	60
H2-Q1	Mouse	CCTTTCAGTTCTGTGGAGTCG CAGCTGAGGGTTTCTTCTTCC	392	58
Oct4	Mouse	CTTCAGACTTCGCCTTCTCAC GGTTCCACCTTCTCCAACTTC	355	58
Flot1	Mouse	TAGCTCTTGCTCCTCCTCTCC GAGGGCAGTCAGATTCATCAC	309	58
Nanog	Mouse	CCAGTGGAGTATCCCAGCAT GAAGTTATGGAGCGGAGCAG	237	60
Nestin	Mouse	AGCAGAACCAGCTGCTCAGT AGCTCTTCGGCAAGGTTGT	172	60
Olig2	Mouse	CTGGTGTCTAGTCGCCCATC AGGAGGTGCTGGAGGAAGAT	232	58
LacZ	Mouse	CCACGGAGAATCCGACGGGT CCTCCAGTACAGCGCGGCTG	361	60
Neo	Mouse	CCGGTGCCCTGAATGAACTG GCCCCTGATGCTCTTCGTCC	332	60
Zeo	Mouse	CCGACCGGCTCGGGTTCTCC TCGCGCAGGGCGAACTCCCG	258	60

Table 2.3 - Primer sequences, product sizes and annealing temperatures used in PCR. These primers were used to check the genomic sequences in BACs.

2.3.8 Real time PCR

Real time PCR was carried out using a QuantiTect™ SYBR® Green PCR kit (Qiagen) according to the manufactures' instructions. For each reaction 5µl of 2x QuantiTect SYBR Green PCR master mix were used together with 0.5µM of each primer in a final reaction volume of 10µl. The PCR amplification program was as follows: -

1. An initial 15 minute DNA denaturation step at 95°C
2. 15 second denaturation step at 95°C
3. 20 second annealing step at 60°C
4. 20 second elongation step at 72°C
5. Steps 2 to 4 were cycled 40 times
6. A melting curve was then taken from 55°C to 95°C
7. A final elongation step for 10 minutes at 72°C to complete the program

Primer sequences used in real time PCRs and their product sizes are shown in *table* 2.4.

Gene	Primer Sequence 5'-3'	Product Size (bp)
Oct4 Promoter	TGGAAGACACAGGCAGTAG CTCACCTAGGGACGGTTTCA	181
Oct4 Exon 1	GGATGGCATACTGTGGACCT AGTTGCTTTCCACTCGTGCT	105
Olig2 Exon 1	CTGCCTCCACCCAGCTATAA GAGGAGAACCTGGCTCTGG	98
Olig2 Exon 2	ATCTTCCTCCAGCACCTCCT GGGCTCAGTCATCTGCTTCT	82

Table 2.4 – Primer sequences used in real time PCRs and their product sizes.

Each reaction was performed in duplicate, on a PTC-200 Peltier Thermal Cycler coupled to a Chromo4 continuous fluorescence detector. Analysis was carried out using MJ OpticonMonitor^{TM} software version 3.1 (BIO-RAD).

2.3.9 RNA isolation and purification

Cells at $5x10^6$ cells/ml were lysed in 1ml TRI Reagent by repeat pipetting and then passed though a 21-gauge needle. After standing at room temperature for 5 minutes, 0.2 volumes of chloroform were added and mixed vigorously for 15 seconds before incubation at room temperature for a further 10 minutes. The homogenate was then centrifuged at 12,000*g* for 15 minutes at 4°C. The RNA in the upper aqueous phase was transferred to a fresh tube and mixed with 0.5ml isopropanol, per ml of TRI Reagent used. After 10 minutes at room temperature the RNA was pelleted by centrifuging at 12,000*g* for 10 minutes at 4°C, the supernatant removed and the pellet washed with 75% ethanol. The sample was vortexed and centrifuged at 7,500*g* for 5 minutes at 4°C before being allowed to air-dry for ~10 minutes and resuspended in an appropriate volume of dH_2O.

RNA was DNase treated (20µg RNA, 20U RNA inhibitor, 2U DNase I, 1X buffer) for one hour at 37°C. The RNA was then purified by adding one volume of phenol/chloroform, mixing and centrifuging for 10 minutes at 12,000*g*. The top aqueous layer was taken and one volume of chloroform added before centrifugation at 12,000*g* for 10 minutes. The upper aqueous layer was added to one volume of 5M ammonium acetate, two volumes of 100% ethanol and put at -20°C for ~30 minutes before centrifuging for a further 20 minutes at 12,000*g*. The pellet was then resuspended in an appropriate amount of DEPC treated H_2O and the RNA was quantified by measuring the A_{260} in a spectrophotometer. At A_{260} an OD of 1 corresponds to ~38µg/ml RNA. To determine the purity of the RNA the A_{280} was also measured. Pure RNA has an A_{260} /

A_{280} of approximately 1.8-2.0 and values lower then this indicate contamination. The RNA was then stored at -70°C.

2.3.10 cDNA synthesis

2μg RNA in 19μl dH_2O were added to 8μM of random hexamers (Amersham Biosciences) incubated at 70°C for 5 minutes, and then placed on ice. Added to this was 8μl of 5x first-strand buffer (250mM Tris-HCl, pH8.3, 375mM KCl, 15mM $MgCl_2$), 10mM dithiothreitol (DTT), 40U RNA inhibitor, 0.5mM dNTPs and 400U Superscript II reverse transcriptase (RT, Invitrogen™). RT was omitted from the negative RT control. Reactions were then incubated at 42°C for 1 hour in a total volume of 40μl, followed by 5 minutes at 80°C to inactivate the RT and complete first strand synthesis.

2.3.11 Reverse transcription polymerase chain reaction (RT PCR)

In each reaction 1μl RT was added to 2μl 10x PCR buffer II, 2.5mM $MgCl_2$, 0.2mM dNTPs, 1.25μM of each forward and reverse primer, and 1U Taq Gold polymerase in a total 20μl. Sequences for primers, sizes of the fragments generated, annealing temperatures and the numbers of cycles used are recorded in *table* 2.5. For RT PCR the program shown in section 2.3.6.2 was used with the exception of the GAPDH PCR, which requires an elongation step time of 20 seconds. The number of cycles used also varied between 25 and 35, depending on the abundance of the transcript. All PCR products were resolved on 1.5% agarose gels (section 2.3.5).

Gene	Primer Sequence 5'-3'	Product Size (bp)	Annealing T (°C)	Cycles
Oct 4	GGCGTTCTCTTTGGAAAGGTGTTC CTCGAACCACATCCTTCTCT	312	55	25
Sox 1	TTACTTCCCGCCAGCTCTTC TGATGCATTTTGGGGGTATCTCTC	373	62	30
Sox 2	CTGGTCATGGAGTTGTACTGCACG GGCAGCTACAGCATGATGCAGGAGC	130	58	30
Pax 2	CCAAAGTGGTGGACAAGATTGCC GGGATAGGAAGGACGCTCAAAGAC	545	61	30
Pax 5	CAGATGTAGTCCGCCAAAGGATAG ATGCCACTGATGGAGTATGAGGAGCC	451	61	30
Pax 6	GCTTCATCCGAGTCTTCTCCGTTAG CCATCTTTGCTTGGGAAATCCG	312	58	30
Nestin	TCCAGAAAGCCAAGAGAAGC GGAGTGTCGCTTAGAGGTGC	322	59	30
Otx 1	GCTGTTCGCAAAGACTCGCTAC ATGGCTCTGGCACTGATACGGATG	425	61	30
Otx 2	CCATGACCTATACTCAGGCTTCAGG GAAGCTCCATATCCCTGGGTGGAAAG	211	61	30
WT 1	CGCACATCCTGAATGCCTC GAGGCCCTACAGCAGTGACAA	228	57	30
Hoxb1	CCATATCCTCCGCCGCAG CGGACTGGTCAGAGGCATC	450	62	35
Olig2	CTGGTGTCTAGTCGCCCATC AGGAGGTGCTGGAGGAAGAT	232	58	30
GFAP	GAGTCCCTAGAGCGGCAAAT GTAGGTGGCGATCTCGATGT	189	59	30
Neurofilament 68Kd	GTTGGGAATAGGGCTCAATCT CCAGGAAGAGCAGACAGAGGT	302	59	30
Neurofilament 200Kd	CTTCTGTCACTCCTTCCGTCACCCG AGGACCGTCATCAGGCAGACATTGC	368	59	30
Nurr 1	TGAAGAGAGCGGAGAAGGAGATC TCTGGAGTTAAGAAATCGGAGCTG	255	61	30

Gene	Primer Sequence 5'-3'	Product Size (bp)	Annealing T (°C)	Cycles
MYF-5	AGGAAAAGAAGCCCTGAAGC GCAAAAAGAACAGGCAGAGG	151	58	30
T-Brachyury	TGCTGCCTGTGAGTCATAAC TCCAGGTGCTATATATTGCC	947	50	30/35
Indian Hedgehog	AAGGCCCACGTGCATTGCTCT GTCCGCAATGAAGAGCAGGTG	297	60	30
Alpha Fetoprotein	GCTCACACCAAAGCGTCAAC CCTGTGAACTCTGGTATCAG	410	60	30
Mvh	AGGAGCTTGCAGAGATGTTCAGCAGAC CAACTGGATTGGGAGCTTGTGAAGAAG	591	62	30
GAPDH	CTCAAGATTGTCAGCAATGCA CCTTCCACAATGCCAAAGTT	70	61	30
β–Actin	GGCCCAGAGCAAGAGAGGTATCC ACGCACGATTTCCCTCTCAGC	460	62	25

Table 2.5 - RT-PCR conditions. Mouse primer sequences, product size and PCR conditions used in RT-PCR.

2.4 Preparation and analysis of cellular proteins

2.4.1 Harvesting cellular proteins

Cells grown on flasks were washed twice with PBS, and lysed in equal volumes of PBS and 2x SDS (Sodium dodecylsulphate) protein loading buffer (125mM Tris pH6.8, 4% SDS w/v, 10% β-me v/v, 20% glycerol v/v, 0.1% bromophenol blue). Samples were scraped from the surface of flasks and boiled at 100°C for 5 minutes, before being stored at -20°C.

2.4.2 Resolution of proteins by SDS PAGE

Protein extracts were resolved by SDS polyacrylamide gel electrophoresis (SDS-PAGE). Samples were thawed on ice and sonicated at 5μA for 10 seconds (Soniprep 150) before loading 10 to 15μl onto the gel. Polyacrylamide minigels (12% acrylamide v/v, 0.39M Tris-HCl pH8.8, 0.1% SDS w/v, 0.1% ammonium persulphate w/v, 0.04% N,N,N',N'-tetramethylethylenediamine (TEMED) v/v in dH_2O) with stacking gels (5% acrylamide v/v, 0.13M Tris-HCl pH6.8, 0.1% SDS w/v, 0.1% ammonium persulphate w/v, 1% TEMED v/v in dH_2O) were poured using 30% acrylamide (29:1 acrylamide:bis-acrylamide v/v, Severn Biotech). Gels were resolved in electrophoresis tanks (Mighty Small, Hoefer) in Tris-glycine running buffer (25mM Tris base, 250mM glycine pH8.3, 0.1% SDS w/v) at 110V for 2 hours. 10μl of BenchMark™ pre-stained protein ladder (Invitrogen) were loaded to aid with analysis.

Following SDS-PAGE, the stacking gel was removed and the resolving gel was rinsed in transfer buffer (24mM Tris, 192mM glycine, 20% methanol v/v). The gel was then submerged in Coomassie Stain (0.25% Coomassie Brilliant Blue R-250 w/v, 45% methanol v/v, 45% dH_2O v/v, 10% glacial acetic acid v/v) for 1 hour with gentle agitation. The stain was discarded and gel was incubated overnight in destain (30% methanol v/v, 10% glacial acetic acid v/v in dH_2O) with gentle agitation.

2.4.3 Western blotting

After SDS-PAGE (section 2.4.2) protein samples were transferred to polyvinylidene difluoride (PVDF) membrane (Hybond-P, Amersham Pharmacia Biotech) by semi-dry transfer. Briefly, the stacking gels were removed and gels were washed in transfer buffer. The PVDF membrane was soaked in methanol for 10 seconds, rinsed twice in dH_2O and then equilibrated in transfer buffer. Transfer apparatus (W E B Company, Washington) was assembled in accordance with the manufacturers' instructions with the

gel and membrane sandwiched on each side by 3 pieces of 3MM filter paper (Whatman) equilibrated in transfer buffer. The apparatus was run at 20mA for 1 hour.

Membranes were blocked for 1 hour with agitation in 1x TBS (150mM NaCl, 10mM Tris-HCl pH7.5) with 4% milk protein (Marvel). Primary antibodies were diluted in 4% milk, 1x TBS and incubated with membranes overnight at 4°C with shaking (antibody dilutions are shown in *table* 2.6). Membranes were washed six times in 1x TBST (1x TBS, 0.05% Tween-20 v/v) and incubated with secondary antibodies (*table* 2.6) for at least 1 hour. After a further six washes membranes were detected by enhanced chemiluminescence (ECL) according to the manufacturer instructions (SuperSignal® West Pico Chemiluminescent Substrate, Pierce) and signals were exposed on Hyperfilm™ ECL (Amersham Biosciences).

Antibody	Species	Source	Concentration
GAPDH	Rabbit polyclonal	Abcam	1:2,000
Pan H3	Rabbit polyclonal	A. Verreault	1:30,000
H3-K9 di-methylated	Rabbit immunoaffinity purified	Upstate	1:2,000
H3-K9 tri-methylated	Rabbit polyclonal	T. Jenuwein	1:1,000
H3-K9 acetylated	Rabbit polyclonal	Upstate	1:1,000
H3-K4 methylated	Rabbit antiserum	Abcam	1:5,000
Serine 10 phosphorylation	Rabbit polyclonal	Upstate	1:1,000
Cyclin B1	Mouse monoclonal	Santa Cruz	1:1,000
Secondary Rabbit	Goat whole molecule	Sigma	1:10,000
Secondary Mouse	Goat FAB specific	Sigma	1:8,000

Table 2.6 - Antibody dilutions used for western blotting

2.5 Chromatin analysis

2.5.1 Chromatin immunoprecipitation (ChIP)

1% formaldehyde in culture medium was added to a confluent T75 cm^2 flask of cells, for 10 minutes at room temperature. The cells were rinsed in cold PBS and 5ml NBA (85mM KCL, 5.5% sucrose v/v, 10mM Tris pH7.5, 0.2mM EDTA, 0.5mM spermidine, 250μM PMSF) were added with 0.5% NP40 and 1μl protease inhibitor (1U/ml). Cells were harvested by scraping and placed on ice for 5 minutes. The flask was rinsed in 5ml NBA and this was added to the cells on ice. The nuclei were centrifuged at 250*g* for 3 minutes at 4°C. The supernatant was aspirated off and the nuclei resuspended in 100μl of NBA; this was then transferred into a centrifuge tube and placed on ice. 400μl of ChIP sonication buffer (1% SDS, 10mM EDTA, 50mM Tris-HCL pH8, 250uM PMSF) were added and the nuclei sonicated for 3x 15 seconds at 10u on ice. The sample was centrifuged for 3 minutes max speed at 4°C and the OD measured. A 150μg aliquot was frozen at -20°C to use as input chromatin. 30μg was purified through phenol/chloroform, chloroform and ethanol precipitation and run on a gel, and the remaining sample added to 100μl protein G agarose (previously washed twice with NBA) and 10μg Salmon sperm DNA. This was then incubated for 1 hour at 4°C with end-over-end rotation. The sample was centrifuged for 2 minutes at 3400*g* 4°C, and the supernatant diluted in TBS plus 0.5% TX-100 to give 150μg in 250μl for each IP. To each 250μl, the appropriate amount of antibody was added (*table* 2.7) and incubated at 4°C overnight with end-over-end rotation. One sample was incubated without antibody as a negative control.

Antibody	Species	Source	Concentration
Pan H3	Rabbit polyclonal	A. Verreault	12:1,000
H3-K4me_2	Rabbit antiserum	Abcam	20:1,000
H3-K9ac	Rabbit polyclonal	Upstate	20:1,000

Table 2.7 – Concentrations of antibodies used in ChIP.

100µl 50% protein G agarose and 100µg salmon sperm DNA were added to each tube and incubated at 4°C for 2 hours. Samples were then centrifuged at 3400*g* for 2 minutes, the supernatant removed and stored at -20°C. The pellet was taken though a series of washes: 1x TBS (100mM Tris pH8, 150mM NaCl, 0.5% TX-100), 1x TBS high salt (100mM Tris pH8, 500mM NaCl, 0.5% TX-100), 1x ChIP wash buffer (10mM Tris pH8, 500mM LiCl, 1% NP40, 1% deoxycholate (free acid)) and finally 1x TE pH8, all in 500µl for 5 minutes at room temperature with end-to-end rotation, centrifuging between washes for 2 minutes at 4700*g*. The pellet was resuspended in 100µl TE plus 5µl RNase A (10mg/ml) and incubated for 30 minutes at 37°C. The sample was then centrifuged for 2 minutes at 4700*g*, and eluted in 250µl freshly prepared ChIP elution buffer (1% SDS, 0.1M $NaHCO_3$), which was then incubated for 15 minutes at 37°C. The sample was centrifuged for a further 2 minutes, the supernatant stored, and 250µl of fresh ChIP elution buffer added to the pellet. This was incubated with end-to-end rotation at room temperature for 15 minutes, centrifuged again, and the supernatants pooled. NaCl was added to a final concentration of 200mM (to all samples including the input) and the samples incubated at 65°C for six hours to reverse the cross-links. The samples were incubated for 1 hour at 55°C with 20µg/ml Proteinase K (PK), then extracted with phenol/chloroform, and then chloroform, followed by ethanol precipitation overnight at –20°C. The pellet was resuspended in 20µl of dH_2O. This protocol was based on Christenson et al., (2001).

2.6 Immunohistochemistry

2.6.1 Immunofluorescence

For immunofluorescence, slides were prepared as in section 2.1.3.2. Cells grown in adherent monolayers were seeded directly onto slides, and cultured until the required confluency was reached. The media was removed, and the slides were washed twice

with PBS and fixed in 4% pFa/PBS (Boehringer) for 10 minutes. The fix was then quenched in 50mM NH_4Cl for 12 minutes, the slides washed twice in PBS and permeabilised in 0.1% Triton/PBS for 10 minutes. After a further two washes in PBS the slides were blocked for 20 minutes in 5% serum/PBS v/v under parafilm (the serum used to dilute antibodies should be from the same species in which secondary antibodies were raised). Primary antibodies diluted in 5% serum/PBS were then added to the slide and incubated under parafilm for a period of 1 hour to overnight in a moist chamber at room temperature. Concentrations of primary antibodies used are shown in *table* 2.8.

Antibody	Species	Source	Dilution Factor
CENP-C	Rabbit	Gift of W. Earnshaw	1:1,000
CREST (Cummings)	Human anti-sera	Gift of B. Sullivan	1:1,000
CREST (Campbell)	Human anti-sera	Gift of B. Sullivan	1:1,000
BrdU	Rat monoclonal	Harlan Seralab	1:100
5E10	Mouse monoclonal	Gift of P. De Jong	1:10
Ki67	Rabbit	DAKO	1:100
Fibrillarin	Mouse monoclonal	Gift of J. Aris	1:1,000
Nucleolin	Rabbit	Gift of B. McStay	1:250
SSEA-1	Mouse polyclonal	DSHB	1:200
β-gal	Rabbit polyclonal	Europa	1:2,000
Nestin	Mouse	DSHB	1:250
Oct4	Mouse	BD Bioscience	1:250
Sox1	Rabbit	Gift of R. Lovell-Badge	1:500
Olig2	Rabbit	Gift of T. Jessell	1:1,000
H3-K4me^2	Rabbit antiserum	Abcam	1:500
H3-K9me^2	Rabbit	Upstate	1:500
H3-K9ac	Rabbit polyclonal	Upstate	1:500

Table 2.8 - Primary antibodies used in immunofluorescence.

Slides were then washed three times in PBS. Species-specific fluorescein isothiocyanate (FITC) or Texas Red (TxRd) conjugated secondary antibodies (Jackson Labs, *table* 2.9) were diluted in 5% serum/PBS and applied in the same manner and incubated for at least one hour in moist chambers at 37°C. The slides were washed a further three times and mounted with 4,6-diamidino-2-phenylindole (DAPI) in Vectashield (Vector), at a concentration of 0.5μg/ml. Coverslips were sealed with rubber solution (Pang) and slides were stored in the dark at 4°C.

Antibody	Species	Dilution Factor
FITC anti-rabbit	Donkey	1:200
FITC anti-mouse	Donkey	1:150
FITC anti-human	Donkey/Goat	1:150
TxRd anti-human	Goat	1:100
TxRd anti-mouse	Donkey	1:100

Table 2.9 - Secondary antibodies used in immunofluorescence.

For suspension cultures and cells non-adherent to glass surfaces, the cells were first trypsinised and/or pelleted. The pellet was washed twice in PBS, and resuspended in 4% pFa for 10 minutes. The fix was then quenched in 50mM NH_4Cl for 12 minutes and the pellet washed a further two times with PBS. The cell suspension was diluted in PBS to a final concentration of $1x10^5$ cells/ml, and cytospun (Shandon, Cytospin3) in 500μl aliquots onto poly-L-lysine coated slides (BDH) at 11*g* for 5 minutes. The slides were then treated as for adherent cells.

2.7 Histochemical staining

2.7.1 Alkaline phosphatase staining

An alkaline phosphatase staining kit (Sigma, 86-R) was used to detect the differentiation state of mouse ES cells. The cells were grown on glass coverslips in 6-well plates. After rinsing the cells with PBS, 1ml of fix (for 98ml: 25ml citrate solution, 65ml acetone and 8ml of 37% formaldehyde) was added to each well for 30 seconds. The fix was replaced with dH_2O and the cells rinsed gently for 45 seconds. The dH_2O was then removed and ~400µl of freshly prepared stain was added to each well. Cells were incubated in the dark for 30 minutes at room temperature. Those cells that express alkaline phosphatase stain intensely pink. The stain was removed, the cells washed with dH_2O and mounted in an aqueous mountant (10g gelatin, 70g glycerine in 60ml dH_2O). The cells were then photographed under brightfield using x10 and x20 objectives.

2.7.2 X-Gal staining

The X-Gal staining solution was prepared by dissolving 250mg of 5-Bromo-4-chloro-3-indolyl-β-D-galactoside (X-Gal, Melford) in 5ml dimethylformamide (DMF) before adding the remainder of the buffer (5mM potassium ferricyanide ($K_3Fe(CN)_6$), 5mM potassium ferrocyanide ($K_4Fe(CN)_6$), 0.25mg/ml spermidine, 2mM $MgCl_2$ made up to 500ml with wash buffer (0.1M phosphate buffer (23:77 v/v 1M NaH_2PO_4:1M Na_2HPO_4), 2mM $MgCl_2$, 0.05% Bovine serum albumin (BSA)). The solution was stored at -20°C and filtered before use. Cells were rinsed twice in PBS before fixing for 15 minutes at 4°C in 0.5% glutaraldehyde, 2mM $MgCl_2$, 5mM EGTA made up in 0.1M phosphate buffer pH7.3. After washing twice in wash buffer, cells were stained in the dark at 37°C overnight for a maximum of 15 hours in X-Gal staining solution. The staining solution was then removed and the cells washed once with PBS before mounting in an aqueous mountant (10g gelatin, 70g glycerine in 60ml dH_2O). The cells were then photographed under brightfield using x10 and x20 objectives.

2.8 Fluorescence *in situ* hybridisation (FISH)

2.8.1 Preparation of nuclei for FISH

2.8.1.1 Harvesting and fixing cells in 3:1 methanol:acetic acid (MAA)

For 2D analysis, the cells were swollen after harvesting by suspension in 10ml hypotonic solution (75mM KCl), added drop-wise whilst continually agitating the tube (the concentration of cells in the hypotonic should be $<2x10^7$cells /ml). The cell suspension was left at room temperature for 10 minutes before centrifuging at 400g for 5 minutes. Cells were then fixed with 2ml of fresh 3:1 methanol:glacial acetic acid added drop-wise to the cells whilst the tube was agitated. A further 8ml of fix were added and the tube placed on ice for a minimum of 15 minutes or stored at -20°C overnight. Cells were fixed twice more and stored indefinitely at -20°C.

2.8.1.2 Preparation of three-dimensionally preserved nuclei

For 3D analysis, cells were grown on Superfrost plus microscope slides (BHD) prepared as in section 2.1.3.2 at a density of $1.5x10^5$ cells/slide in 5ml of media, to result in approximately 70% confluency after a further 16 hours in culture. Slides were washed three times for 5 minutes each in PBS and then permeabilised in CSK buffer (100mM NaCl, 300mM sucrose, 3mM $MgCl_2$, 10mM PIPES pH6.8, 0.5% Triton X100) for 5 minutes on ice. After washing in PBS, cells were fixed with 4% pFa/PBS for 10 minutes. Cells grown in suspension cultures or non-adherent to glass were fixed and cytospun onto slides as described in section 2.6.1. The slides were washed a further three times for 5 minutes in PBS before incubation in 20% glycerol (v/v, high grade)/PBS, either for 30 minutes at room temperature or at 4°C overnight.

Slides were dipped into liquid nitrogen until completely frozen, allowed to thaw at room temperature, then returned to 20% glycerol for ~three minutes before being frozen again.

This freeze thaw procedure was repeated four times, and on the fifth freezing the slides were either taken directly through the 3D FISH protocol (section 2.8.4) or stored indefinitely at -70°C.

2.8.2 Preparation of FISH probes

Probes were labelled using biotin-16-dUTP (biotin), digoxigenin-11-dUTP (dig-dUTP) or Alexa 488 incorporated into the DNA by PCR or nick translation. Following either method, unincorporated nucleotides were removed and efficiency of biotin or dig-dUTP labelling was assessed.

2.8.2.1 Preparation of labelled human chromosome paints by PCR

Human micro-dissected chromosome arms (gifts of Michael Bittner; Guan et al., 1996) were amplified on PTC-225 Peltier Thermal Cycler (MJ Research). Biotin or dig-dUTP was incorporated directly by PCR into chromosome paints by adding these analogues to the PCR reaction mix (used for HSA18p, 18q, 11p and 6p). For direct labelling of chromosome paints, 1µl of PCR template (from a second round of amplification of an original template stock) was added to a mixture of: 5µl each of 2mM dATP, dCTP, dGTP and 3µl of 0.5mM dTTP, 3µl of 1mM biotin or dig-dUTP, 400ng primer ($^{5'}$CCGACTCGAGNNNNNNATGTGG$^{3'}$), 3U Taq polymerase, 5µl $MgCl_2$ (25mM), 5µl PCR buffer (10x) and the volume made up to 50µl with dH_2O. Amplification conditions were four minutes at 94°C then 30 cycles of: 94°C for 30 seconds, 56°C for 30 seconds and 72°C initially for two minutes extending by three seconds per cycle. All chromosome PCR fragments were resolved on 2% agarose gels in TBE (section 2.3.4).

Alternatively, when the PCR products were too large (> ~500bp), cold PCR products were precipitated using ethanol and sodium acetate pH5.5 (section 2.3.2.2), then biotin or dig-labelled by nick translation (section 2.8.2.2) (used for HSA19p, HSA19q and BACs).

2.8.2.2 Nick translation

1-1.5μg of DNA were added to 4μl 10x nick translation salts (0.5M Tris-HCl pH7.5, 0.1M $MgSO_4$, 1mM DTT, 500μg/ml BSA), 4μl each of 2mM dATP, dGTP and dCTP, 2μl of 0.5mM dTTP and 4μl 1mM biotin or dig-dUTP. DNase I was freshly diluted to a concentration of 20U/ml in dH_2O at 4°C and 2μl added to the reaction mixture to give a final concentration of 1U/ml. After the addition of 1μl DNA polymerase I (Invitrogen, 10units/μl), dH_2O was added to make the total volume of reaction mixture 40μl. The reaction was mixed thoroughly and allowed to proceed at 16°C for 90 minutes. The reaction was stopped by placing at -20°C or immediately processed for removal of unincorporated label (section 2.8.2.3).

2.8.2.3 Removal of unincorporated label

Quick spin columns containing G50 Sephadex beads were used to remove any biotin or dig-dUTP that remained free in solution as per the manufacturer's instructions. Cleaned probes were eluted in ~60μl TE pH7.5.

2.8.2.4 Quantifying label incorporation

Gridded nitrocellulose membranes were prepared by soaking briefly in dH_2O followed by 20x SSC (3M NaCl, 0.3M tri-sodium citrate, pH7.4) for 10 minutes then allowing to air dry. Labelled DNA probes were diluted to $1x10^{-3}$ and $1x10^{-4}$ in TE (pH7.5) and 1μl of each was spotted twice onto a gridded membrane. After the spots had dried, a further 1μl was added to one of each dilution. On the same membrane 20, 10, 2 and 1pg of appropriately labelled lambda DNA standards were spotted. DNA was cross-linked onto the membrane by exposure to 30mJ of UV irradiation.

The membrane was immersed in buffer 1 (0.1M Tris-HCl pH7.5, 0.15M NaCl) for 5 minutes at room temperature, then in 3% BSA in buffer 1 for 45 minutes at 60°C. 10µl streptavidin-alkaline phosphatase (Boehringer) and/or anti-digoxigenin-alkaline phosphatase (Boehringer) were added to 10ml of buffer 1 and placed in a 50ml falcon tube with the membrane for 30 minutes with continuous agitation at room temperature. The membrane was washed twice for 15 minutes in buffer 1 then for 5 minutes in 0.1M Tris-HCl, pH9.5. The colour reaction was developed by incubation of the membrane, in a sealed polythene bag, with 5ml of 0.1M Tris-HCl pH9.5 and 2 drops from bottles 1-3 of the alkaline phosphatase substrate kit IV (Vector). The substrates in this colour reaction are 5-bromo-4-chloro-3-indolyl phosphate and nitroblue tetrazolium, which produce a blue reaction product. A complete colour reaction was observed within two hours and an estimate of the concentration of DNA labelled probe was made by comparison with the lambda standards.

2.8.3 FISH on two-dimensional MAA-fixed nuclei

2.8.3.1 Slide preparation

Glass slides were stored in a dilute solution of HCl in ethanol. Immediately prior to slide making, slides were dried and polished with muslin. Methanol:acetic acid (MAA) fixed cells (section 2.8.1.1) were removed from storage at -20°C, left to warm to room temperature for 30 minutes and centrifuged at 400g for 5 minutes. Fresh MAA fix was added until the cell suspension reached a 'milky' appearance. A single drop of cell suspension from a fine-tipped pastette was dropped onto a horizontal microscope slide from a height of ~30cm. The spread of cells on the slide was improved by coating the slide with a thin layer of moisture, usually by breathing. An air humidity of ~50% also aided spreading. Spreading was monitored by phase contrast microscopy. Slides were stored for two to six days prior to hybridisation. When fixed material had a high level of cytoplasm around the nuclei, slides were treated with pepsin prior to hybridisation (section 2.8.3.2).

2.8.3.2 Pepsin treatment

MAA nucleus preparations may not hybridise with a high efficiency after the 2D FISH protocol if they still have cytoplasm attached. To increase the efficiency of hybridisation, these slides were treated with pepsin. Slides were dehydrated in acetone for 5 minutes then air dried. RNase treatment was then carried out as in section 2.8.3.3. 43µl of 11M HCl were added to 50ml of dH_2O and pre-heated to 37°C, then 125µl of 2% pepsin were added and the slides incubated for three minutes before washing in PBS with 50mM $MgCl_2$. Slides were subsequently dehydrated through an ethanol series and hybridisation was carried out as described in section 2.8.3.3.

2.8.3.3 Hybridisation

Slides were mounted vertically in a metal rack and subsequent incubations carried out in 200ml glass troughs. Slides were first treated with 100µg/ml RNase A in 2x SSC for one hour at 37°C, washed briefly in 2x SSC and dehydrated through an ethanol series (two minutes each in 70%, 90% and 100% ethanol). The slides were left to air dry for 10 minutes before being heated in a 70°C oven for 5 minutes and immediately denatured in 70% formamide, 2x SSC pH7.5 at 70°C for 90 seconds, or 75 seconds for hES cells. After passing through 70% ethanol at 4°C and an ethanol series (as above), the slides were again air dried.

Probes were prepared at the same time as slides. Labelled DNA (section 2.8.2) (200ng human chromosome paint, 70ng BAC or plasmid per slide) suspended in TE, was precipitated with 5µg salmon sperm DNA and mouse or human Cot 1 DNA (Invitrogen) as a competitor (the amount of which varied from 5 to 50µg, depending on the potential repeat content of the probe). After the addition of 2 volumes of ethanol, probes were spun down under vacuum until they had precipitated, and re-suspended in 10µl hybridisation mix (50% deionised formamide v/v, 10% dextran sulphate v/v, and 1% Tween 20 v/v in 2x SSC). Commercial probes (Cambio) were usually provided in or

with hybridisation buffer and did not require addition of salmon sperm DNA or Cot 1 DNA. All probes were denatured at 70°C for 5 minutes and reannealed at 37°C for 15 minutes before spotting onto pre-cleaned coverslips. The denatured slides were carefully laid onto the appropriate coverslip and sealed with rubber solution (Tip Top) before placing in a metal tray in a 37°C water bath overnight.

2.8.3.4 Washing and detection

Slides were washed in glass racks in 200ml troughs. After removal of the rubber solution, they were immersed in 2x SSC at 45°C for three minutes, with gentle agitation to facilitate detachment of the coverslips. Slides were washed a further three times in the same buffer then four times for three minutes in 0.1x SSC at 60°C before transferring to 4x SSC/0.1% Tween 20. Detection was carried out in a moist chamber preheated to 37°C. Biotin was detected with sequential layers of fluorochrome-conjugated avidin (FITC or TxRd, Vector Laboratories), biotinylated anti-avidin (Vector Laboratories), and a further layer of fluorochrome-conjugated avidin. Digoxigenin labelled probes were detected with sequential layers of FITC- (BCL) or Rhodamine-conjugated anti-digoxigenin and FITC- or TR-conjugated anti-sheep antibodies (Vector Laboratories). Detection reagents were diluted in SSCM (4x SSC, 5% marvel dried skimmed milk w/v) to the appropriate concentration (*table* 2.10). After incubation with 40µl SSCM for 5 minutes at room temperature, 40µl of the appropriate detection layer were applied to the slide on a 22mm by 40mm coverslip. Slides were incubated in the moist chamber at 37°C for 45 minutes, followed by 3 washes of 2 minutes in 4x SSC/0.1% Tween 20 at 37°C.

All slides were mounted with 0.5µg/ml DAPI, in Vectashield (Vector). Coverslips were sealed with rubber solution (Pang) and slides were stored in the dark at 4°C.

Antibody or fluorochrome-conjugate	Species	Source	Stock concentration (mg/ml)	Dilution
Avidin-FITC	Goat	Vector	2.0	1:500
Avidin-TxRd	Goat	Vector	2.0	1:500
Biotinylated anti-avidin	Goat	Vector	0.5	1:100
Rhodamine-anti-digoxigenin	Sheep	Roche	0.2	1:20
TxRd-anti-sheep	Rabbit	Vector	0.5	1:100

Table 2.10 Antibodies and fluorochrome-conjugates used for FISH.

2.8.4 FISH on three-dimensionally preserved nuclei

This method was used to maintain the three-dimensional architecture of nuclei (Kurz et al., 1996; Croft et al., 1999) through the process of FISH. Cells were grown and fixed on slides as described in section 2.8.1.2. Slides were washed for 30 minutes at least twice with PBS then incubated in 2x SSC (300mM NaCl, 30mM tri-sodium citrate, pH7.4) containing 100μg/ml RNase A for 1 hour at 37°C. Following this, slides were returned briefly to PBS and then placed in 0.1M HCl in dH_2O for 7 minutes before being returned to PBS again. Slides were then denatured in 70% formamide, 2x SSC (pH7.0) for 3 minutes then 50% formamide, 2x SSC (pH7.0) for 1 minute, both at 78°C. Probes were applied immediately after the second formamide incubation. The probes were prepared, hybridised and detected as described in 2.8.3.3 and 2.8.3.4. When chromosome paints were used in conjunction with BAC probes, chromosome domains were always detected using FITC-conjugated secondary antibodies and BAC probes using TR-conjugated secondary antibodies (*table* 2.10).

2.8.5 ImmunoFISH

Cells were fixed as for 3D FISH (section 2.8.1.2) the slides were incubated in block (5% serum/PBS) for 20 minutes at room temperature and the primary antibody was added overnight as for immunofluorescence (section 2.6.1). Then the 3D FISH protocol was carried out (section2.8.4), the slides washed once in PBS and the secondary antibody for the immunofluorescence was added for one hour at room temperature. Slides were washes three times in PBS and mounted with DAPI in Vectashield (Vector), at a concentration of 1μg/ml for human and 0.5μg/ml for mouse. Coverslips were sealed with rubber solution (Pang) and slides were stored in the dark at 4°C.

2.8.6 PNA FISH

3D telomere FISH was carried out to the manufacturers' instructions using a PNA FISH kit (DAKO) on cells fixed in 3.7% formaldehyde.

2.9 Image capture and analysis

2.9.1 Capture and analysis of 2D images

Brightfield images of cells were taken using differential interface contrast (DIC) optics with a Photometrics CoolSnap HQ monochrome CCD camera (Roper Scientific, Arizona). IPLab Spectrum (Scanalytics Inc., VA) wrote the image capture scripts that controlled camera capture. After FISH or immunofluorescence, 2D slides were examined using a Zeiss Axioplan fluorescence microscope with a 100 Watt mercury bulb and triple band-pass filter (Chroma #83000), using x10, x20 and x40 objectives. Grey scale images for each fluorochrome were captured with a cooled CCD camera (Princeton Instruments Pentamax) and analysed using custom IPLab v3.6 scripts.

For 2D analysis 50 bin 2 images were collected of consecutive nuclei that fulfilled the following criteria: nuclei had to be intact and, when involving chromosome territories (CTs), contain two chromosome domains in which locus signals (if present) were visible; in addition, some analysis scripts required images of single nuclei not touching any other nuclei.

The radial distribution of CTs was determined using an erosion script, adapted from that previously described by Croft et al., (1999). Nuclei were segmented using a histogram of the image data. The valley between background and foreground peaks represented the nuclear periphery and the value at the bottom of this valley was set as the threshold value for segmenting nuclei. Mouse nuclei and human ES cell nuclei are particularly difficult to segment because of the wide variations in DAPI staining across the nucleus. The script then removed the background fluorescence by calculating the most frequent pixel value in the area outside the nucleus and subtracting this value across the whole image. The area and the sum of all pixels were measured for the segmented area. This was then eroded into five shells of equal area and the overlay transferred to both FITC and TxRd images. The fluorescence in each of the five shells was calculated for both FITC and TxRd images and normalised to the DAPI intensity.

Analysis of probe position relative to the surface of CTs was as previously described (Mahy et al., 2002a; Chambeyron and Bickmore, 2004). Briefly, the background was removed from the image, and the outline of the CT and the probe segmented. The distance between the centre of the CT and the probe was then calculated. A two tailed t-test was used to test the significance of this data.

2.9.2 Capture and analysis of 3D images

For 3D analysis, z-stacks of up to three colour images (DAPI, FITC and TxRd) were captured using an Axioplan microscope fitted with a 100 Watt mercury bulb, Ludl filter wheel, Chroma filter set #81000 and motorised stage, attached to a cooled CCD (Xillig

CCD camera) Kodak KAF 1401e sensor camera (Princeton Instruments). A script was devised (P. Perry) using IPLab software to capture bin 2 resolution images, the DAPI excitation filter was selected, as was a region of interest for capture. The number of optical slices to be collected, the *z* distance between each optical slice and the exposure times for each fluorochrome signal (from an automatic test capture in the plane of best focus) were also determined. The microscope focus motor then moves the stage downward for half the total depth of the focus series to the starting point for capture. To compensate for backlash in the focus mechanism, the stage was moved downwards a further 200μm, followed by an upward movement of the same distance. Image capture started, collecting the specified DAPI, FITC or TxRd images at each focal plane and placing each into a stack file, then moving the stage upwards the specified *z* distance before repeating the same capture sequence. After the final plane was captured, the stage returned to the original "best focus" focal plane. The stack files were then merged to provide a colour stack file that can be animated or projected. For each nucleus, 25-30 bin 2 image planes were captured at 0.25-0.5μm intervals in the z-plane, so as to include the whole nucleus in the image stack. The image stack was then deconvolved to remove excessive background fluorescence using Hazebuster (Vaytek, Inc) and analysed in IPLab.

CT positions in 3D were determined as previously described by Bridger et al., (2000). The distances between the centre of the CT and the nuclear periphery were measured in *x*, *y* and *z*-planes and expressed as proportions of the radius. The 3D analysis of centromeres, telomeres and PML bodies in the z-plane was performed using a custom IPLab script. Briefly, the script defines the outline of the DAPI nucleus in each frame of the z-stack, calculates the highest level of intensity for each fluorescent spot and locates which frame the spot is positioned in the z-plane. This was carried out for n=25 nuclei.

2.10 Statistical analysis

Differences in the radial position of CTs, the distances between BAC probes and centromere analysis were tested for statistical significance using a Mann-Whitney U test in Minitab 13 (Minitab Inc.). This is the nonparametric equivalent of a t-test, as it tests the hypothesis that two groups come from the same distribution without assuming that the data are normally distributed.

A two tailed T-test was used for BAC to CT analysis. This is a parametric test to determine whether the distributions of two normally distributed populations are significantly different. The other parametric test used in this thesis is one-way analysis of variance (ANOVA), which again tests whether two or more normally distributed data sets have the same mean.

Chapter 3: Nuclear Organisation in Human Embryonic Stem Cells

Chapter 3

Nuclear Organisation in Human Embryonic Stem Cells

3.1 Introduction

Within the nucleus of a differentiated cell, the human genome has a defined spatial organisation. In many differentiated cells, chromosome territories (CTs) adopt a radial organisation according to gene-density, with gene-rich chromosomes situated towards the centre of the nucleus and gene-poor chromosomes located closer to the nuclear periphery (Croft et al., 1999; Boyle et al., 2001; Cremer et al., 2001; Cremer et al., 2003). Alternatively, Bolzer et al., (2005) reported a size-related chromosome organisation, in the nuclei of fibroblasts and amniotic fluid cells. Individual genes and chromosome domains also occupy distinct locations, both within the nucleus and with respect to their CTs (Zink et al., 2004; Volpi et al., 2000; Williams et al., 2002; Mahy et al., 2002a). Non-coding regions such as centromeres are located near to the nuclear periphery or, for the acrocentric chromosomes containing rDNA genes (chromosomes 13, 14, 15, 21 and 22), cluster around the nucleolus (Manuelidis 1990; Carvalho et al., 2001; Weierich et al., 2003; Gilchrist et al., 2004), whereas telomeres have a more internal localisation (Weierich et al., 2003).

If spatial organisation of the genome reflects gene expression, as is believed for model organisms (Spector 2003), you would expect to see differences amongst cell types. In humans, there is a conserved radial organisation for all chromosomes with one noted exception. The gene-poor HSA18 is located nearer to the centre of the nucleus in the flat

ellipsoidal nuclei of amniocytes and fibroblast, rather than at the periphery as is characteristic of cells with spherical nuclei (Cremer et al., 2001, Cremer et al., 2003; Bolzer et al., 2005). The Misteli lab recently reported differences in chromosome positioning in the mouse, both between various tissues (Parada et al., 2004) and during T cell differentiation (Kim et al., 2004). However, there are no reports of significant changes in the radial organisation of chromosomes during differentiation of human cells, to date only differences in chromosome associations have been described (Kuroda et al., 2004a). Previous studies have focused on the spatial arrangement of chromosomes and centromeres in haemopoietic progenitor cells (Cremer et al., 2003) and $CD34^+$ stem cells from cord blood (Alcobia et al., 2003). It is therefore important to determine the nuclear organisation of uncommitted stem cells (Fisher and Merkenschlager, 2002).

In this chapter, I describe the nuclear organisation of hES cells in comparison to that of differentiated cell types. I show that already established in the nuclei of hES cells is the radial organisation of chromosomes related to gene density. However, I report differences in the location of chromosomes and genes with known roles in pluripotency and describe a more centralised distribution of centromeres within hES cell nuclei.

3.2 The radial organisation of HSA18 and 19 in hES cells

I started investigating the nuclear organisation of hES cells with FISH for HSA18 and 19. These were the first chromosomes used by Croft et al., (1999) to describe the radial organisation of CTs. HSA18 and 19 are a similar physical size being 76 and 63 Mbp respectively, although they have different gene densities and functional characteristics. HSA18 is gene-poor with ~449 genes while HSA19 is gene-rich at ~1528 genes (http://www.ensembl.org/Homo_sapiens/). When visualised by FISH in a variety of differentiated cells, HSA18 is located towards the nuclear periphery and HSA19 situated closer to the nuclear centre (Croft et al., 1999; Cremer 2003). This radial organisation is

applicable to all human chromosomes (Cremer et al., 2001; Boyle et al., 2001), conserved in higher primates (Tanabe et al., 2002) and chickens (Stadler et al., 2004).

I investigated the position of HSA18 and 19 first in 2D, on 3:1 methanol:acetic acid fixed nuclei from the Wisconsin hES cell lines, H1 (XY) and H9 (XX) (Thomson et al., 1998). Fixing the nuclei in this way flattens the nuclear morphology, but does not alter the organisation of the CTs and allows for large numbers of nuclei to be analysed (Croft et al., 1999). W. Cui of the Roslin Institute cultured the cells on matrigel coated culture dishes and described the cell populations using flow cytometry with the cell surface antigens SSEA4 and Tra-1-60 (*figure* 3.1). The H1 hES cells were 70% SSEA4 positive, 55% Tra-1-60 positive, confirming that the majority of the cells were undifferentiated (Draper et al., 2002; Carpenter et al., 2004). I prepared chromosome paints for HSA18 and 19, and carried out 2D FISH on both H1 and H9 hES cells. Fifty images of nuclei taken from each cell line were analysed through a 2D erosion script, previously described in Croft et al., (1999). Briefly, the script divides each nucleus into five shells of equal area and measures the amount of fluorescence in each of the segments. This was normalised to the amount of total DNA present in each shell (*figure* 3.2). In both hES cell lines, HSA19 was centrally localised in comparison to HSA18 ($p \leq 0.001$).

In many circumstances, 2D analysis is representative of the 3D nuclear organisation. However, when CTs are located in the centre of the nucleus by the erosion script this could be due to a peripheral localisation of the CT at the top of the nucleus flatted by the 2D fixation. Therefore, I carried out FISH on H1 hES cells fixed in 4% paraformaldehyde for 3D analysis. The nuclei were photographed at 0.25μm intervals through the *z*-plane and the distance measured from the centre of the CT to the edge of the nucleus in *x*, *y* and *z*-planes. 3D analysis confirmed the result previously described in 2D, showing that HSA19 was located near to the centre of the nucleus and HSA18 was towards the nuclear periphery (*figure* 3.3). HSA19 was significantly more central than HSA18 in both the *x* and *y* planes ($p \leq 0.001$), although they displayed similar

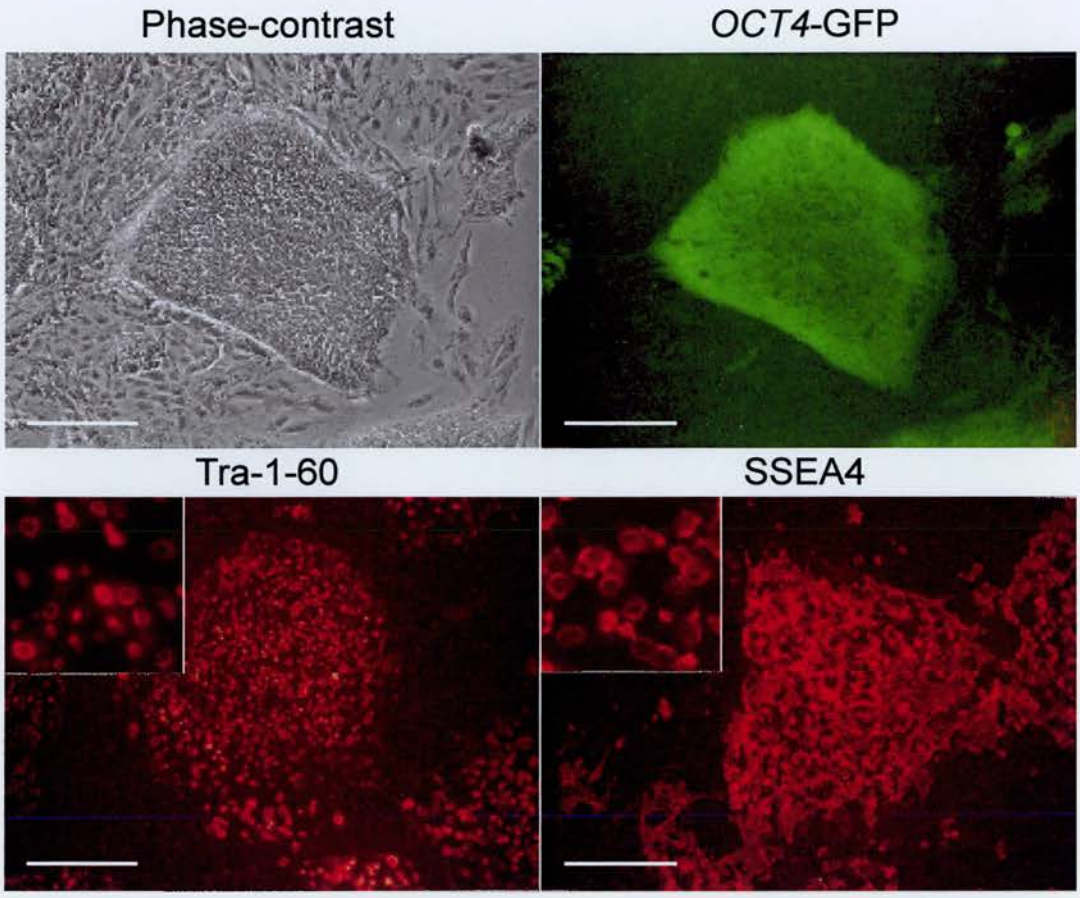

Fig. 3.1 Markers of pluripotency in hES cells. H9 hES cells with an *OCT4*-GFP transgene stained for cell surface antigens SSEA4 and Tra-1-60. Taken with a x4 objective, inserts x40 objective. Scale bars 20μm (images provided by W. Cui).

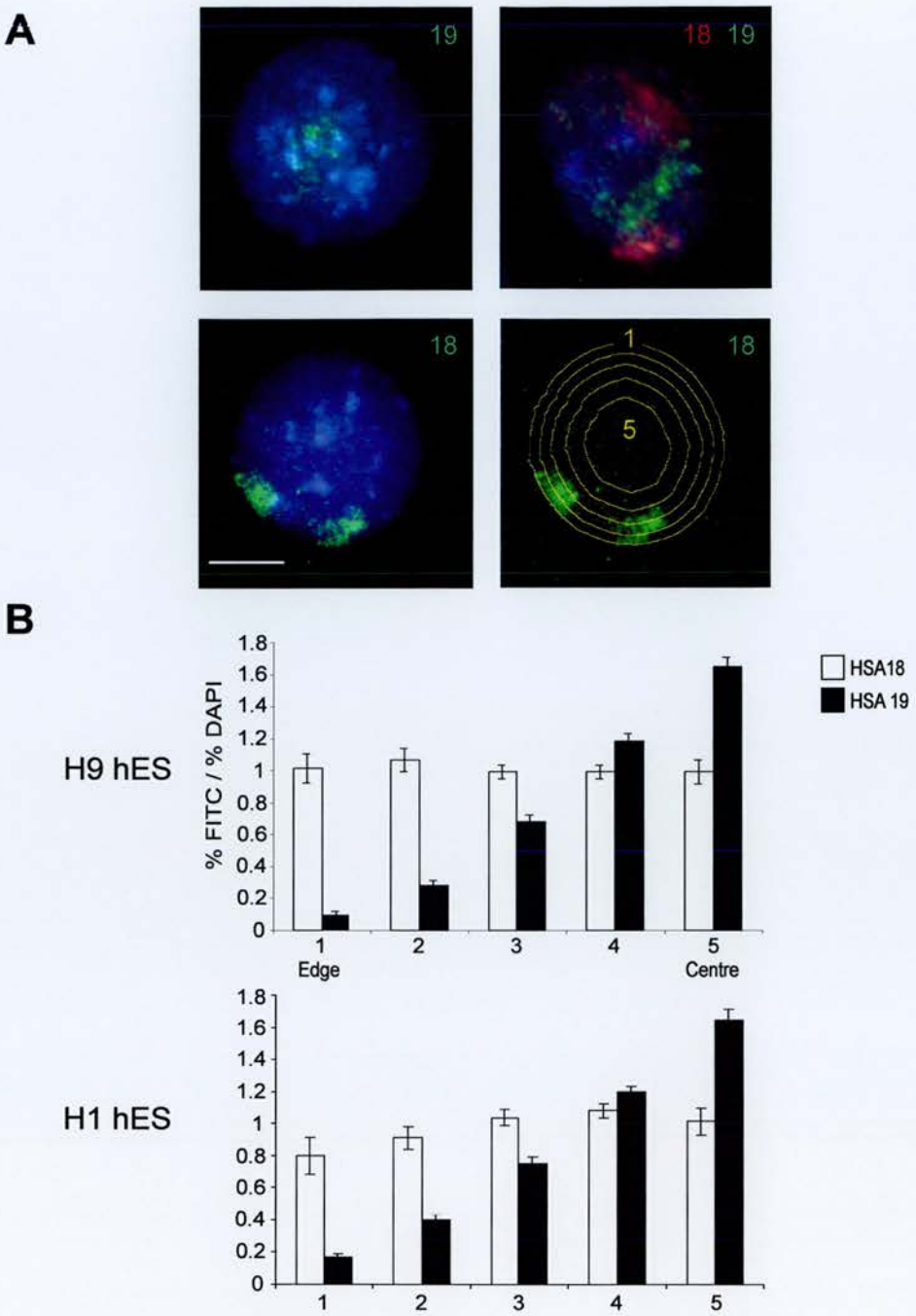

Fig. 3.2 The radial distribution of HSA18 and 19 in hES cells. (A) hES cell nuclei, counterstained with DAPI (blue) and hybridised with chromosome paints for HSA18, 19 or both. The bottom right hand image shows the nucleus divided into five shells of equal area by the erosion script. Green, biotin labelled paint detected with avidin-FITC. Red, dig-labelled paint detected with a TxRd anti-sheep. (B) Distribution of HSA18 and 19 hybridisation signals within the nucleus of H9 and H1 hES cells analysed by erosion of 2D images into five concentric shells from the edge (1) to the centre (5) of the nucleus. The mean (±s.e.m.) proportion of hybridisation signal, normalised to the amount of DAPI signal, is shown for each shell (n=50). Scale bar, 5μm.

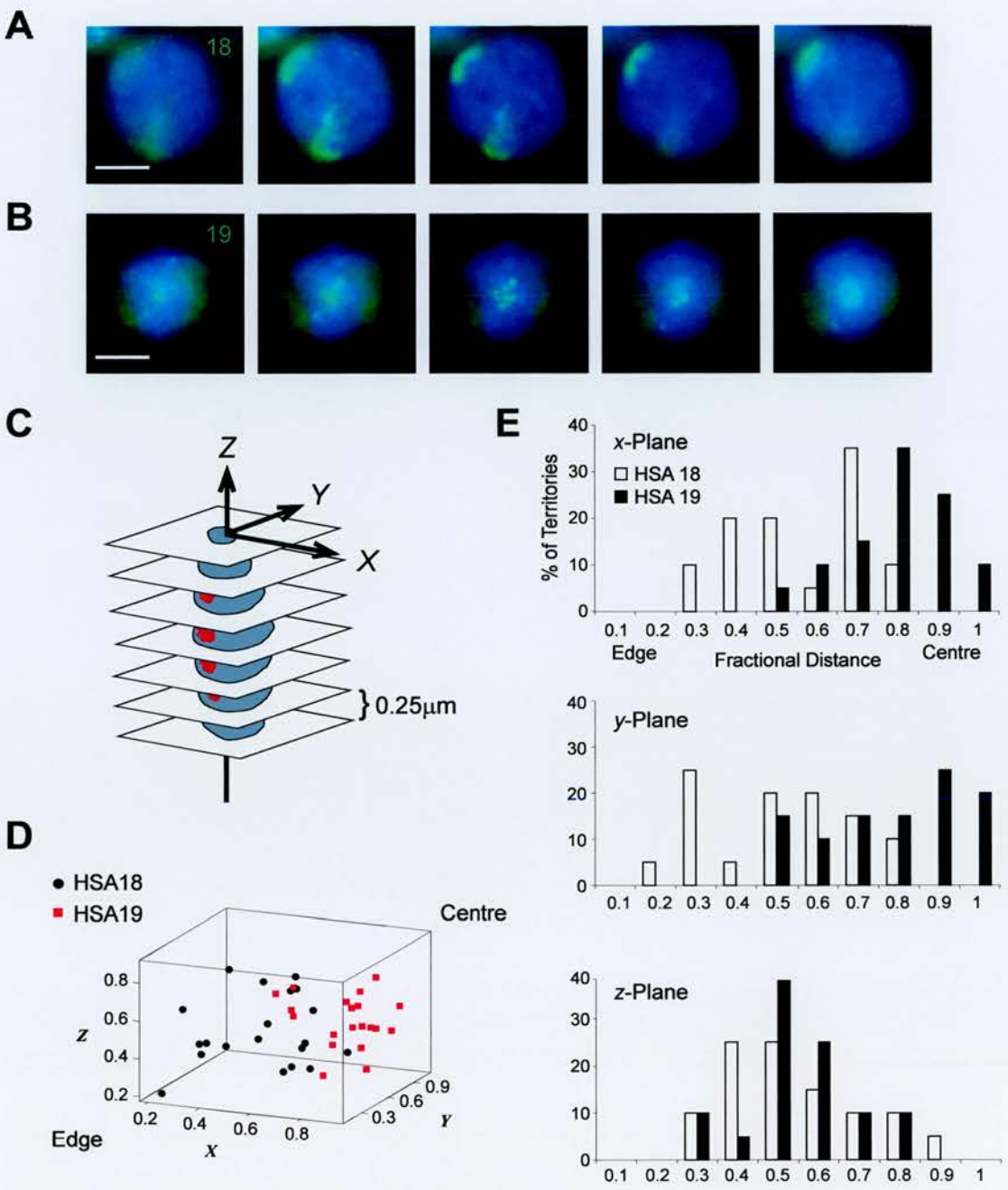

Fig. 3.3 The 3D localisation of HSA18 and 19 in hES cells. 3D FISH with biotin labelled paints for (A) HSA18 and (B) HSA19, detected with avidin-FITC (green). Images show single frames taken at 0.5μm intervals through the *z*-axis of H1 hES cell nuclei, counterstained with DAPI (blue). (C) Orientation of a cell nucleus within a z-stack. (D) Graph showing the distribution of the centres of HSA18 (black) and 19 (red) CTs, along the *x*, *y* and *z*-axis of 3D preserved H1 hES cell nuclei. The axis show the fractional distance between the nuclear periphery (0) and the centre of the nucleus (1) (*n*=20). (E) Analysis of HSA18 and 19 hybridisation signals within 3D-preserved H1 hES cell nuclei. Graphs are the distributions of the centres of HSA18 and 19 territories, along the fractional radius of each nucleus, in *x*, *y* and *z*-planes (*n*=20). Scale bar, 10μm.

distributions in the *z*-plane (p=0.68). I therefore conclude that a gene density related radial distribution of HSA18 and 19 CTs is present in hES cells.

3.3 Distribution of chromosomes 12p and 6p in hES cells

To investigate if there was a change in the position of CTs specific to hES cells, I analysed two CTs that contain genes important for pluripotency. *OCT4* (*Pou5F1*), a transcription factor essential for maintaining the undifferentiated state of hES cells (Matin et al., 2004), is located on HSA6p21.33 within the non-class I genes of the MHC class I region (*figure* 3.4A). *NANOG*, another transcription factor required to maintain the undifferentiated phenotype of ES cells (Zaehres et al., 2005) is located on HSA12p13.31, in a cluster of genes containing *GDF3* and *STELLA*, which are also down regulated upon differentiation (*figure* 3.4B; Clark et al., 2004). I carried out 2D FISH with chromosome paints for 6p or 12p together with BACs containing *OCT4* or *NANOG*, on hES cells and an LCL (*figure* 3.5A). Using the erosion script used in the analysis of HSA18 and 19 (*figure* 3.2), the radial positions of these CTs were established. In the LCL, 6p and 12p have distributions intermediate to those of HSA18 and 19, i.e. not at the nuclear periphery, or the nuclear centre, which is consistent with their gene density. A result confirmed by previous analysis in LCLs and fibroblasts (Boyle et al., 2001). In hES cells the localisation of HSA6p was analysed and found to be the same as in the LCL. However, HSA12p had a different localisation in the nuclei of hES cells and LCLs (*figure* 3.5B). In hES cells 12p occupied a significantly more central position, whereas in the LCL it was located closer to the nuclear periphery (shell 5, p=0.04).

A

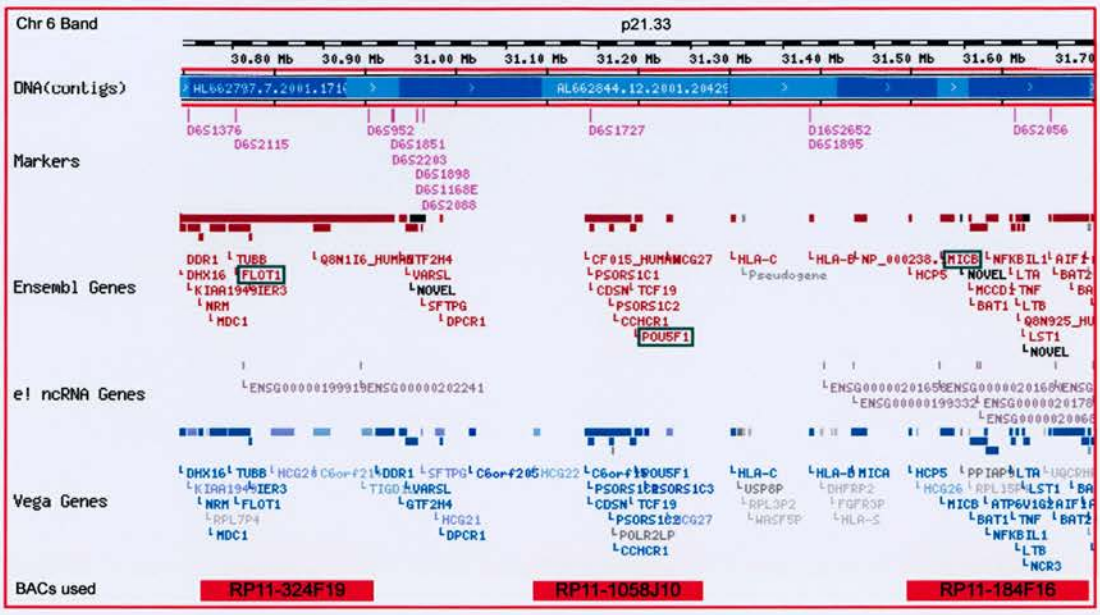

B

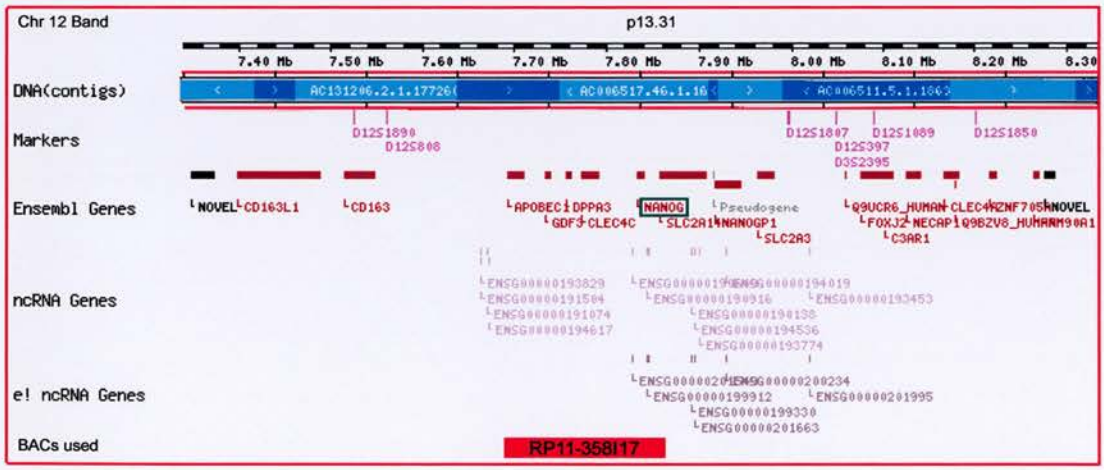

Fig. 3.4 The genomic regions surrounding *OCT4* and *NANOG* in humans. Green boxes show the positions of (A) *FLOT1*, *OCT4* (*POU5f1*) and *MICB* on HSA6, and (B) *NANOG* on HSA12. Red boxes show the positions of the BACs used. Images adapted from ensembl v37, Feb 2006.

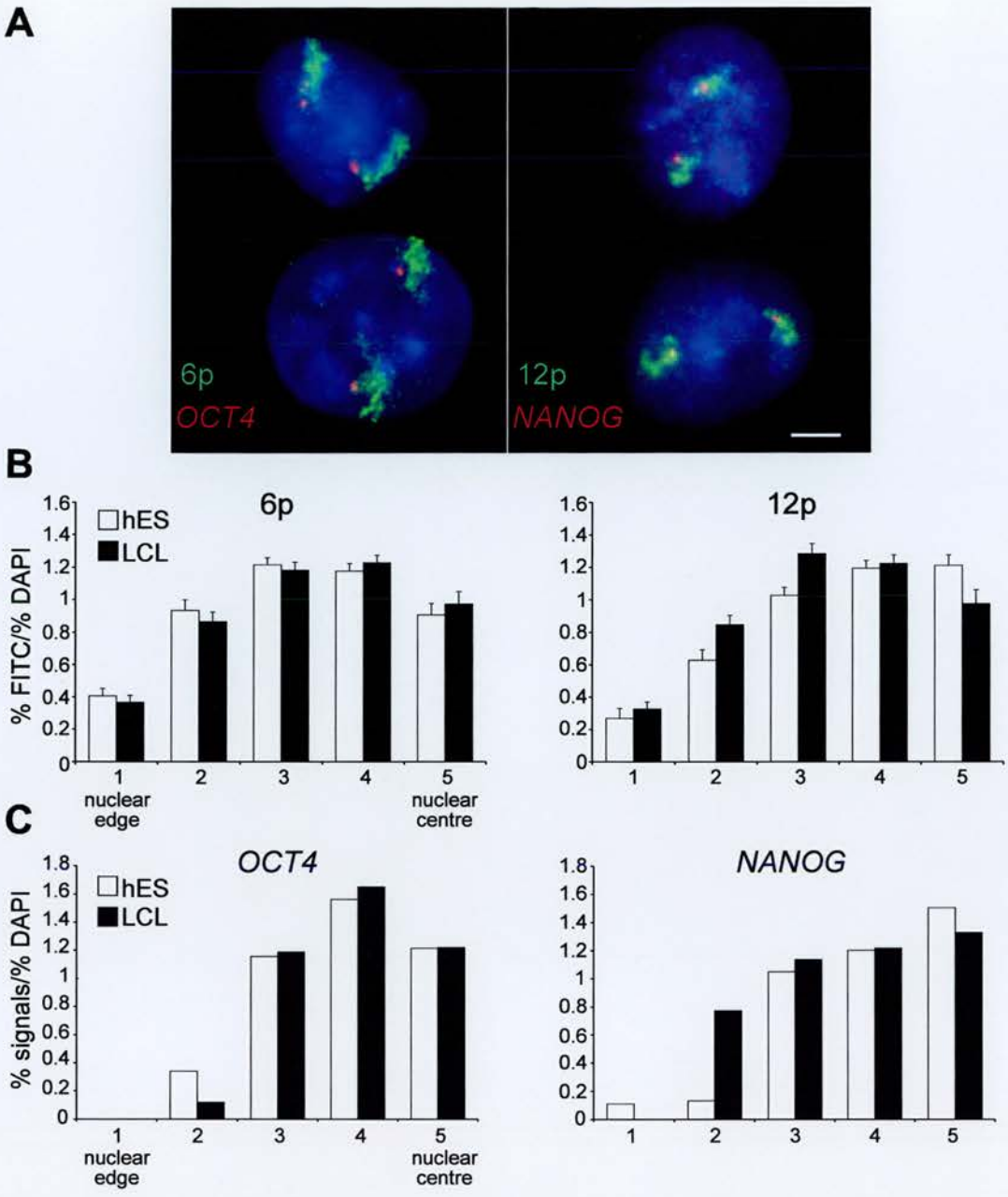

Fig. 3.5 Radial distribution of 6p, 12p, *OCT4* and *NANOG* in LCLs and hES cells. (A) 2D FISH with BAC probes containing either *OCT4* or *NANOG* (red), and chromosome paints for 6p or 12p (green), within interphase nuclei of hES counterstained with DAPI (blue). (B) Distribution of HSA6p or 12p hybridisation signals within the nucleus of LCLs and hES cells, by erosion of 2D images into five shells of equal area from the edge (1) to the centre (5) of the nucleus. The mean hybridisation signal normalised to the DAPI signal (± s.e.m.) is shown for each shell (n=50). (C) Distribution of signals from *OCT4* or *NANOG* containing BACs within the nucleus of LCLs and hES cells, by erosion of 2D images into five shells of equal area. The number of probe signals in each shell was counted and the proportion of probe normalised to the amount of DAPI signal, is shown for each shell (n=50). Scale bar, 5μm.

3.4 Gene position in the hES cell nucleus

If the position of a CT differs between undifferentiated and differentiated cells, then it is possible that the genes on these chromosomes will also change radial positions to follow their host chromosome. I investigated the position of both *OCT4* and *NANOG*, using the erosion script to segment the nuclei and manually counting the number of BAC signals in each shell (*figure* 3.5). Consistent with the CT HSA6p result, the position of *OCT4* in the nucleus did not change between the two differentiation states. However, the position of *NANOG* was more peripheral in the differentiated LCL compared to the hES cells.

This result agrees with the findings of Zink et al., (2004), who show that within the nucleus, the location of genes varies among cell types in a transcription dependent manner and that some genes move away from the nuclear periphery when they are active. In the mouse, Hox genes that are induced upon the differentiation of ES cells are also shown to move towards the nuclear interior (Chambeyron and Bickmore, 2004). However, in this case it was not accompanied by any change in radial position of their host chromosome (Bickmore et al., 2004). Instead, this relocalisation accompanied the movement of a gene out of its CT.

Similarly, alterations in the position of gene-dense regions of the genome, relative to their CTs occur in different somatic cell types (Volpi et al., 2000; Williams et al., 2002). This change in gene position relative to CT occurs during the differentiation of mES cells with RA (Chambeyron and Bickmore, 2004), but there is no previous study of the nuclear localisation of genes in hES cells. With this in mind, I began to look at the relationship between gene rich regions of the human genome and their host CTs. The telomeric end of HSA11p is one of the most gene-dense regions of the human genome. The genes are functionally unrelated and not co-ordinately expressed. However, this region loops out of its CT in lymphoblasts and fibroblasts (Mahy et al., 2002a). 11p13 contains genes such as *RCN*, a housekeeping gene, which is active from within the CT. In contrast, genes such as *IFITM3* (involved in early germ cell development) located at

the distal region of 11p (11p15.5) loop out of their CT. To investigate if this looping occurs in hES cells, I carried out 2D FISH with three cosmids containing the genes *RCN*, *INS* and *IFITM3* labelled in dig-dUTP, alongside a biotin labelled HSA11p chromosome paint (*figure* 3.6A). The script described previously by Mahy et al., (2002a) measured the distance between each cosmid and the edge of the 11p CT. The nuclear organisation of this region previously observed for somatic cells was also present in hES cells (*figure* 3.6B). The centromeric *RCN* loci, expressed in both LCLs (Mahy et al., 2002b) and hES cells (Ramalho-Santos et al., 2002) but located within the low gene density region 11p13 (32Mb), was within the 11p CT. In contrast the *INS* and *IFITM3* genes at the gene-dense telomeric end, 11p15.5 (positions 0.25-2.1 Mb, NCBI build 35, http://www.ensembl.org/Homo_sapiens), looped out of the CT in hES cells, even though this region does not contain genes with a known role in pluripotent cells. Distances relative to the edge of the CT are shown in *table* 3.1 on page 99.

I then investigated CT organisation for loci expressed specifically in pluripotent cells. Two regions significant to stem cell function were used, the MHC class I region on HSA6p which contains the non-class I gene *OCT4*, and the cluster of pluripotency genes on HSA12p containing the transcription factor *NANOG*. In the LCL, the class I genes of the MHC are constitutively expressed. Similarly, hES cells also express the MHC class I genes along with *OCT4* (Drukker et al., 2002; Draper et al., 2002; Carpenter et al., 2004). Chromosome paints for HSA6p and HSA12p labelled with biotin, and their corresponding BACs labelled with dig-dUTP, were hybridised to LCL and hES cell nuclei. Previous reports have shown the class I and class III regions of the MHC outside the HSA6p CT in lymphocytes (Volpi et al., 2000). I confirmed this using the two alleles either side of *OCT4*, *FLOT1* on the class I side and *MICB* on the centromeric side nearest the class III genes (*figure* 3.7A). These two genes located on average, outside the CT in hES cells and an LCL (*table* 3.1). However, in the LCL, *OCT4* relocated with respect to its CT in comparison to hES cells (*table* 3.1 and *figure* 3.7). When expressed in hES cells, *OCT4* was located on average outside of the 6p CT. In the LCL that does not express *OCT4*, the gene moved just inside the CT. This difference was small, but

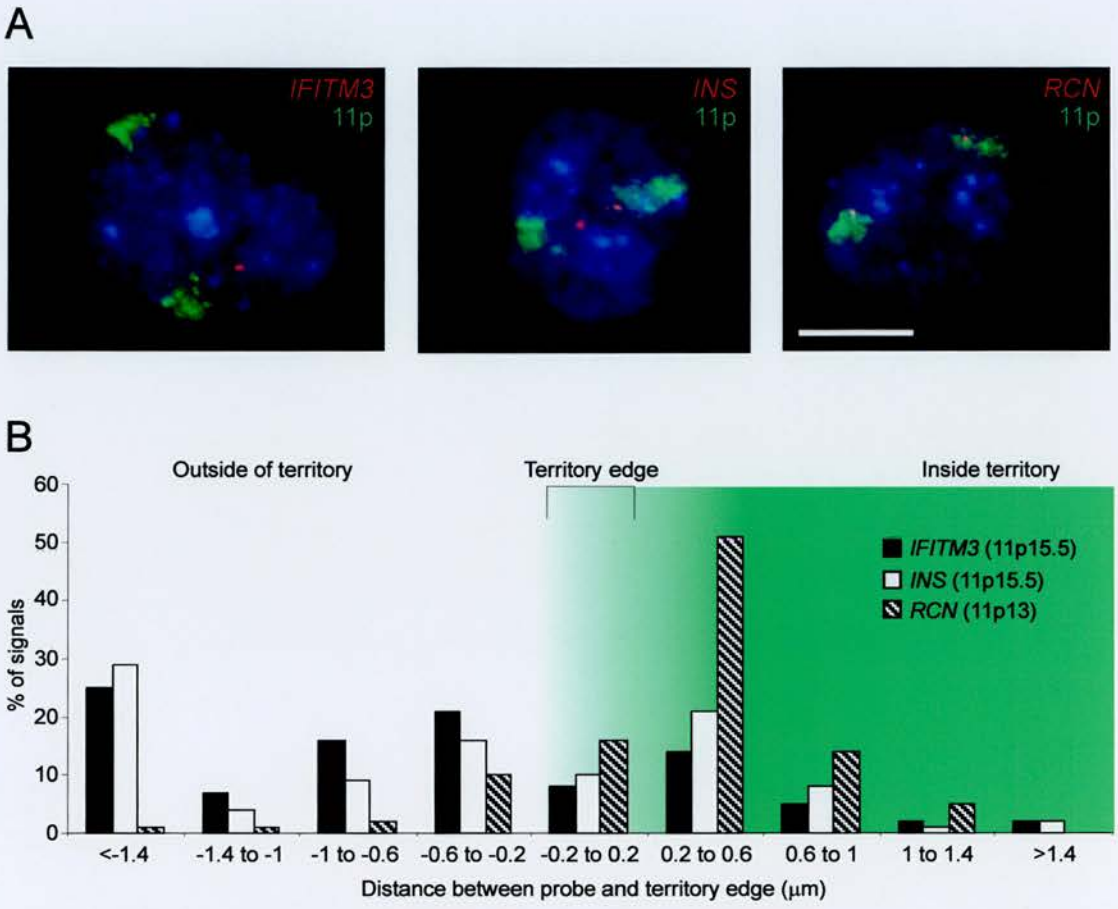

Fig. 3.6 Intrachromosome territory organisation of HSA11p in hES cells. (A) Interphase hybridisation of cosmid probes containing *IFITM3*, *INS* or *RCN* (red), and chromosome paint for HSA11p (green), within the nuclei of hES cells counterstained with DAPI (blue). (B) Histogram of the distribution of FISH signals from cosmids containing *IFITM3* (black), *INS* (white) or *RCN* (hatched), relative to the edge of the chromosome 11p CT, in the nuclei of hES cells. Negative distance indicates localisation outside the visible limits of the CT (n=100). Scale bar, 10μm.

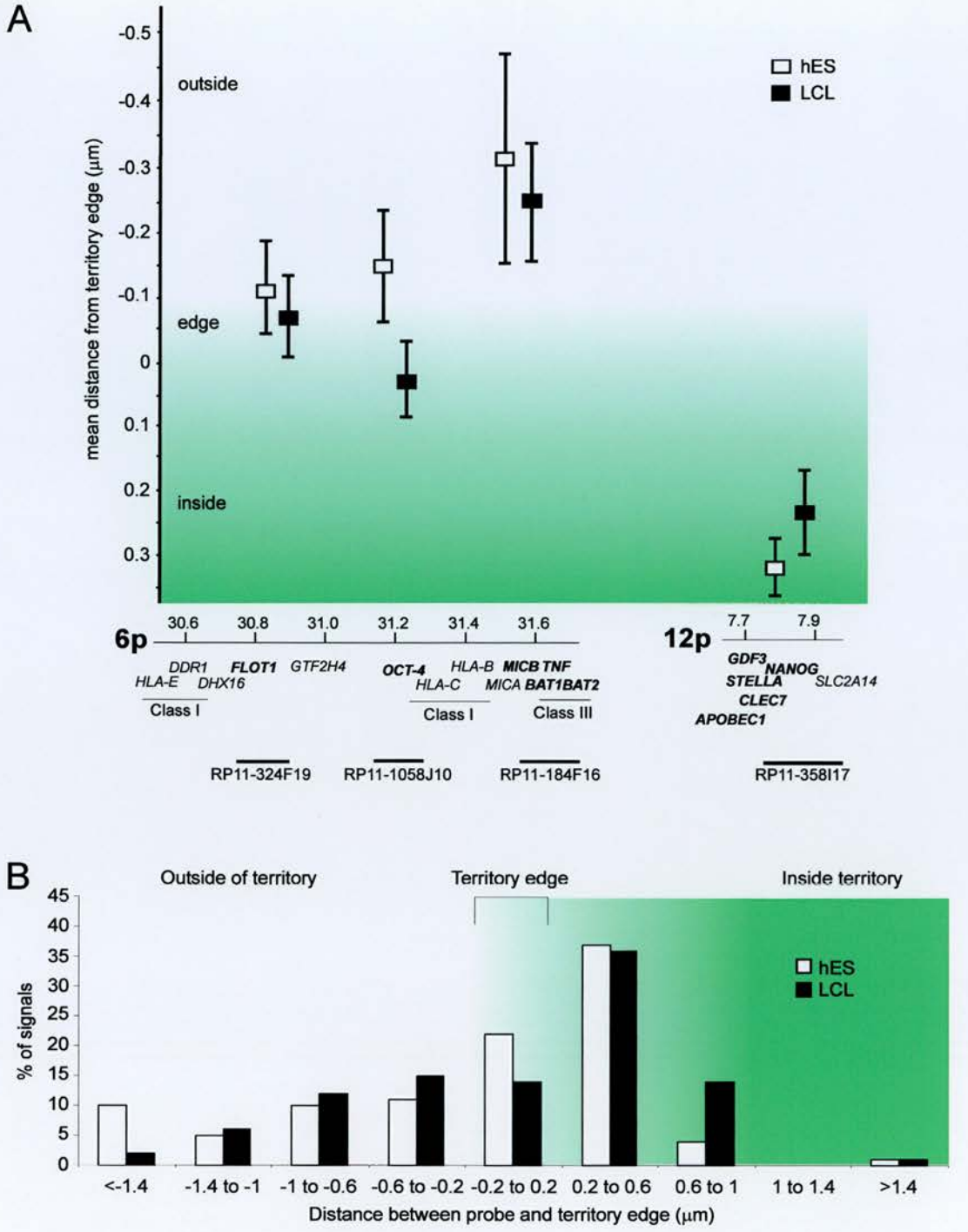

Fig. 3.7 Intrachromosome territory organisation of *NANOG* and *OCT4*. (A) Position relative to their CT, of *OCT4* and two flanking loci on HSA6p and *NANOG* on HSA12p, in the nuclei of hES and LCLs (*n*=100). Negative values indicate localisation outside the CT. Map of genomic regions around *OCT4* and *NANOG* (NCBI build 35) is shown below, with genes present in the BACs used, highlighted in bold. (B) Distribution of a BAC containing *OCT4* relative to the HSA6p CT, in nuclei from hES cells and LCLs. Negative distances indicate localisation outside of the CT (*n*=100).

statically significant (p=0.041). Closer inspection of the data (*figure* 3.7B) showed that the movement of *OCT4* into the 6p CT was not due to a change in the proportion of loci found far outside the CT (>0.2μm) which remained at 36% for both LCLs and hES cells. The change was in the number of loci found deep within the CT (>0.6μm), and in consequence the increased number of loci found at the edge of the CT. In contrast to *OCT4*, *NANOG* occupied a location just within the HSA12p territory in both hES cells and LCLs (p=0.12, *figure* 3.7A).

Locus	Cytogenetic position	Genomic position (Mb)	Probe name	Position relative to CT edge	
				LCL (μm)	hES (μm)
IFITM3	11p15.5	0.2	D11S483	-1.4±0.3	-0.70±1.13
INS	11p15.5	2.1	cINS/IGF2	-0.6±0.2	-0.55±0.15
RCN	11p13	32.0	cH11148	0.6±0.2	0.26±0.04
NANOG	12p13.31	7.8	RP11-358I17	0.23±0.06	0.32±0.04
FLOT1	6p21.33	30.8	RP11-324F19	-0.07±0.07	-0.11±0.08
OCT4	6p21.33	31.2	RP11-1058J10	0.03±0.06	-0.15±0.09
MICB	6p21.33	31.6	RP11-184F16	-0.25±0.09	-0.31±0.16

Table 3.1 Intra-CT position of loci in hES cells and LCLs. Cytogenetic and genomic positions (from NCBI build 35, http://www.ensembl.org/Homo_sapiens) of each locus, together with the name of the cosmid or BAC used in FISH. Mean (±s.e.m.) position, in μm, of loci relative to the edge of the CTs in hES and LCL nuclei. Negative values indicate the positions outside the visible limits of the CT. LCL data for 11p15.5 loci is taken from Mahy et al., (2002a).

The movement of loci with respect to their CTs has previously been associated with changes in condensation of the chromatin fibre (Chambeyron and Bickmore, 2004). To investigate this in the *OCT4* region, I carried out FISH with *OCT4* and the two flanking BAC clones in hES cells and the LCL (*figure* 3.8A). The interphase distance (*d*) was measure between *OCT4* and the *FLOT1* or *MICB* BACs. These distances always conformed to the distribution expected from the random walk model of chromatin

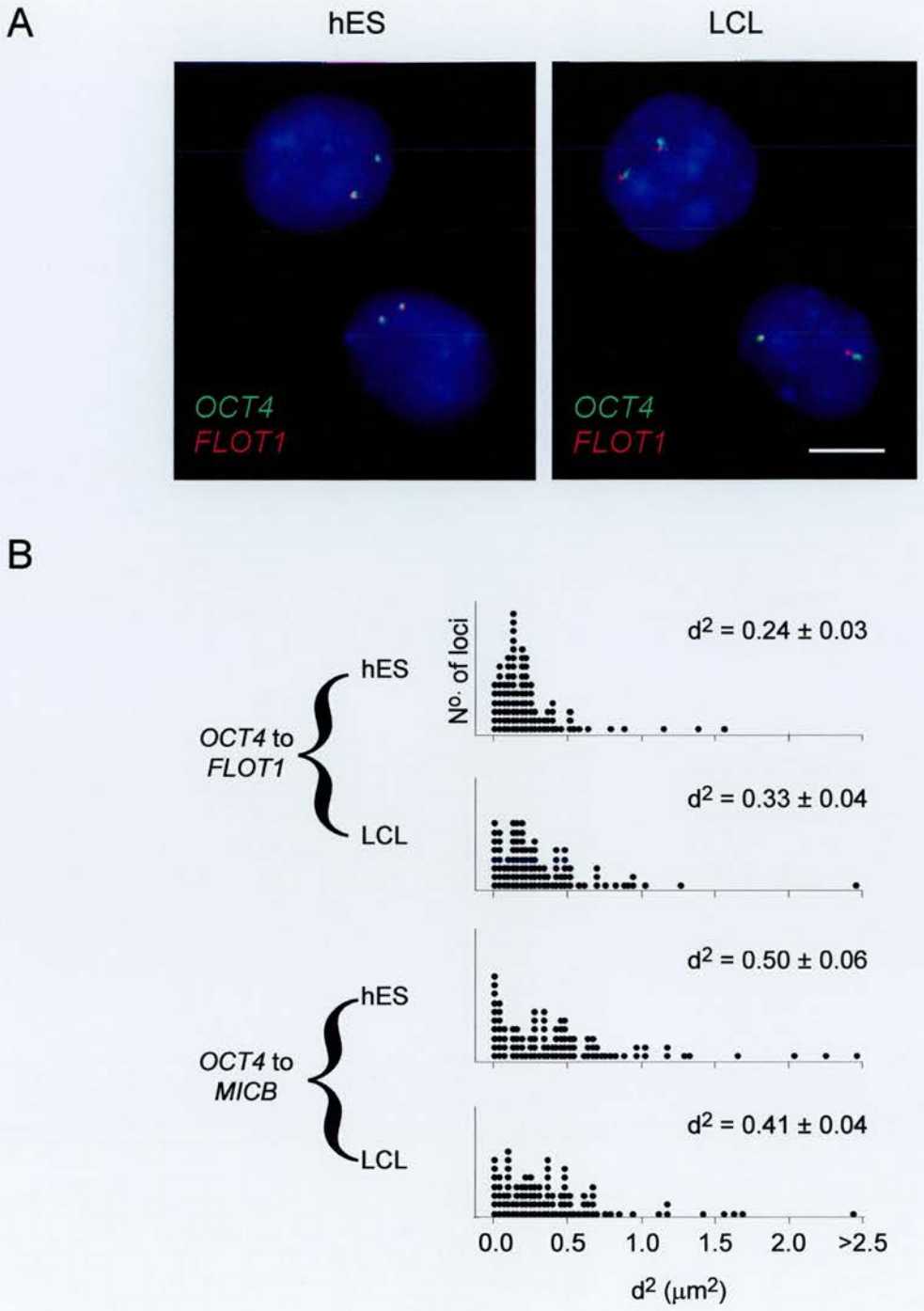

Fig. 3.8 Chromatin decondensation of the *OCT4* region in hES and differentiated cells. (A) 2D FISH with BAC probes containing *OCT4* (green) and *FLOT1* (red), within the interphase nuclei of H9 hES cells and a LCL, counterstained with DAPI (blue). (B) The distribution of squared interphase distances (d^2) in μm^2 measured between probes for *OCT4* and *FLOT1* or *MICB*, in the nuclei of hES cells and a LCL (n=100). Numbers show the mean d^2 value (±s.e.m). Scale bar, 10μm.

structure (s.d. = 0.52-0.6; median/mean ~1.0) (Sachs et al., 1995; Chambeyron and Bickmore, 2004). The mean-squared interphase distance ($<d^2>$) between *OCT4* and *MICB* BACs (genomic distance, 350kb) was not significantly different between hES cells and the LCL ($<d^2>$=0.5±0.06 and 0.41±0.04μm^2 respectively, p=0.41; *figure* 3.8B). However, there was a significant increase in the distance between *OCT4* and *FLOT1* (genomic distance, 400kb) in the LCL compared to hES cells ($<d^2>$=0.33±0.04 and 0.24±0.03μm^2 respectively, p=0.04). The large d^2 values measured around *OCT4* in both cell types is consistent with the gene being in an area of open chromatin, as apposed to a compact chromatin fibre (Gilbert et al., 2004). These results suggest a difference not only in the localisation of *OCT4* in respect to its CT but in the chromatin configuration of the *OCT4* region between undifferentiated and differentiated cell types.

3.5 Position of centromeres and PML bodies during differentiation

I have shown specific organisation of chromosomes and genes involved in maintaining pluripotency in hES cells. To investigate whether this defined organisation extends to the non-coding regions of the genome, I analysed the number and position of centromere clusters in hES cells. The position of centromeric heterochromatin in somatic cells has been associated with gene silencing in mouse (Brown et al., 1997). In both mouse and human cells, centromeres are generally located at the nuclear periphery or the nucleolus (Carvalho et al., 2001; Weierich et al., 2003). However, centromere position is specific to cell type and changes during the cell cycle, through differentiation or with cellular transformations (Beil et al., 2002, Shelby et al., 1996, Vourc'h et al., 1993, Manuelidis 1984). Centromeres also associate in lineage specific clusters known as chromocentres, which accompany transcriptional silencing. This centromere clustering increases during differentiation down lymphoid and myeloid lineages, accompanying the commitment of a cell to a lineage (Beil et al., 2002; Alcobia et al., 2003).

To study this clustering in human cells, I first visualised centromeres in primary fibroblasts by FISH with an alpha satellite repeat probe p82h (Mitchell et al., 1985), and by immunofluorescence with CREST anti serum (Cummings; Moroi et al., 1980) and an antibody to the centromeric protein CENP-C (Earnshaw and Rothfield, 1985). The CENP-C and CREST antisera detected the same number of centromeres, although the CREST serum identified more than one signal at the centromere of some chromosomes. This was due to the serum detecting the presence of other centromeric proteins, such as CENP-A (Gilbert personal communication). The FISH with p82h did not detect as many centromeres. Therefore, I continued the analysis with the CENP-C antibody (*figure* 3.9A). I compared the number of centromeres visualised in H7 hES cells (mean=34), with the number detected in proliferating primary fibroblasts (mean=38), ritva (hTERT transformed fibroblasts, mean=37), quiescent fibroblasts (serum starved for 7 days, mean=40) and a LCL (mean=36) (n=20). There was no significant difference in the extent of centromere clustering observed between the hES cells and any of the differentiated cell lines. Therefore, centromere clustering may be restricted to haematopoietic lineages in human cells.

I also investigated the number of promyelocytic leukaemia (PML) bodies in the nuclei of human cells by immunofluorescence with a 5E10 antibody, which recognises the PML protein (Stuurman et al., 1992; *figure* 3.9B). PML bodies have been implicated in many cell processes, from transcription regulation to apoptosis, DNA damage response and stress sensing (Dellaire and Bazett-Jones, 2004). The number of PML bodies changed significantly between cell types, with the average number in hES cells (11) lower than in LCLs (15), ritva (15), fibroblasts (27) or quiescent fibroblasts (27). A trend, which may indicate an increase in the presence of PML bodies towards the later stages of differentiation.

The position of PML bodies in the nucleus is not extensively studied, but transcriptionally active parts of the genome including the MHC on HSA6p, have been associated with them (Wang et al., 2004b). This link with transcriptionally active areas

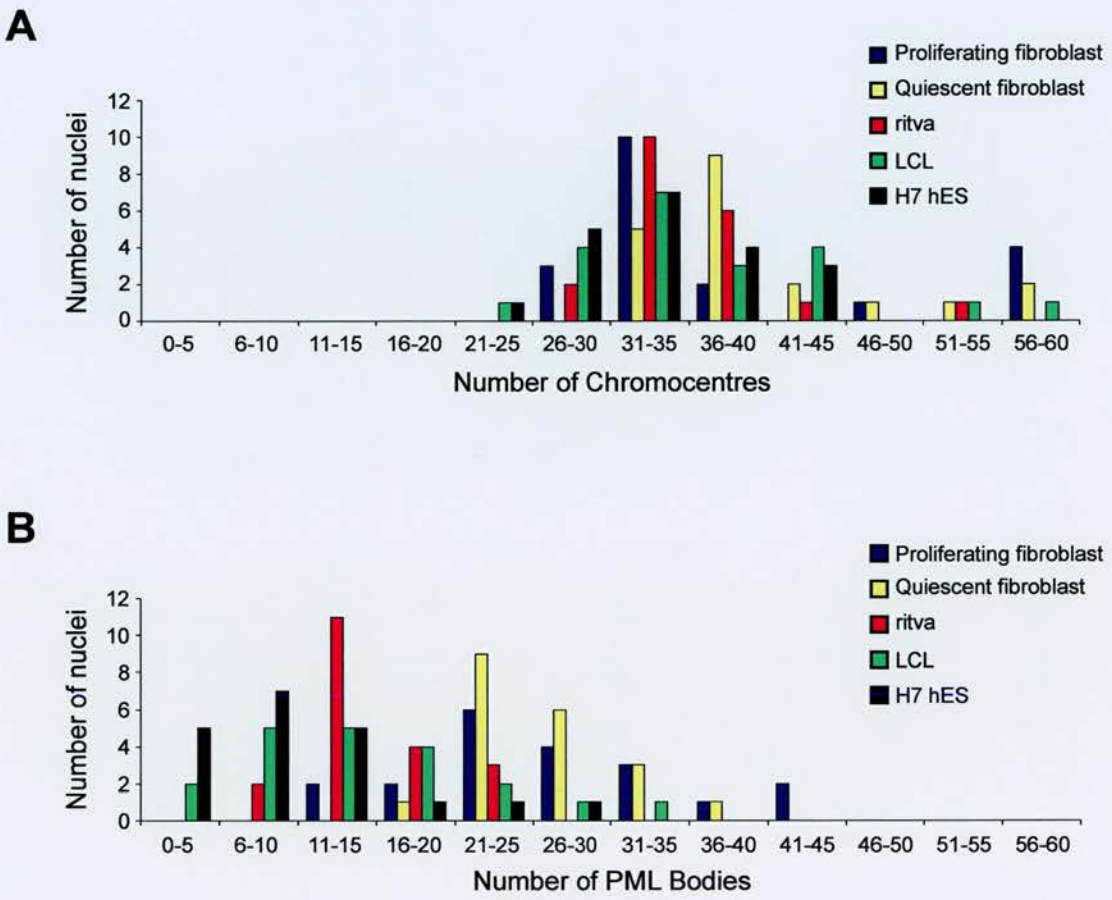

Fig. 3.9 Clustering of centromeres and PML bodies in human cells. (A) The number of chromocentres counted in proliferating primary fibroblasts, quiescent fibroblasts, ritva, a LCL and the H7 hES cell line, after immunofluorescence with a CENP-C antibody. (B) The number of PML bodies counted in proliferating primary fibroblasts, quiescent fibroblasts, ritva, a LCL and the H7 hES cell line, after immunofluorescence with a 5E10 antibody (*n*=20).

of the genome suggests that PML bodies would be present towards the centre of the nucleus, in contrast to the transcriptionally silent centromeric regions, which are known be located at the nuclear periphery. To confirm this, I localised the 3D position of centromeres (CENP-C) and PML bodies (5E10) by immunofluorescence in the nuclei of fibroblasts and H7 hES cells, relative to the nearest nuclear periphery (*figure* 3.10). This provided two obstacles in terms of analysis. Firstly, the nuclear periphery was difficult to define accurately. I visualise the nucleus with DAPI using a conventional fluorescence microscope, which gives a blurred edge to the nucleus as it comes in and out of focus. I could eliminate this to some extent by using a confocal microscope, and outlining the nucleus with an antibody to one of the nuclear membrane proteins, such as lamin A/C. However, in hES cells there is no expression of lamin A/C (Constantinescu et al., 2006). Lamins B1 and B2 are only dimly expressed and little known about the other nuclear membrane proteins. The second obstacle was that within a population of cells the nuclei are all different sizes, and here the two cell types for comparison are different morphologies. I attempted to overcome this problem by comparing each nucleus to a sphere of the same volume, and then plotting the distance between the object and the edge of the nucleus as a proportion of the volume (i.e. the cube root of (3 x volume/4π)).

Images taken at 0.25μm intervals throughout the *z*-axis of the nucleus (*figure* 3.3C) had the outline of the DAPI nucleus segmented from the background. Centromere and PML body positions were then calculated using the coordinates of the highest fluorescence intensity for each fluorescent spot in the *x*, *y* and *z* planes and the distance to the nearest nuclear edge was measured. This was then normalised to a sphere of the same volume as the nucleus and the distance between the fluorescent spot and the nearest nuclear edge plotted as a fraction of the radius. In fibroblasts, PML bodies and centromeres were localised to different parts of the nucleus. PML bodies were localised towards the centre of the nucleus, whereas centromeres had a more peripheral localisation. This showed the central localisation of the PML bodies in comparison to the centromeres relative to the nearest nuclear periphery, which is statistically significant by one-way ANOVA (0.5,

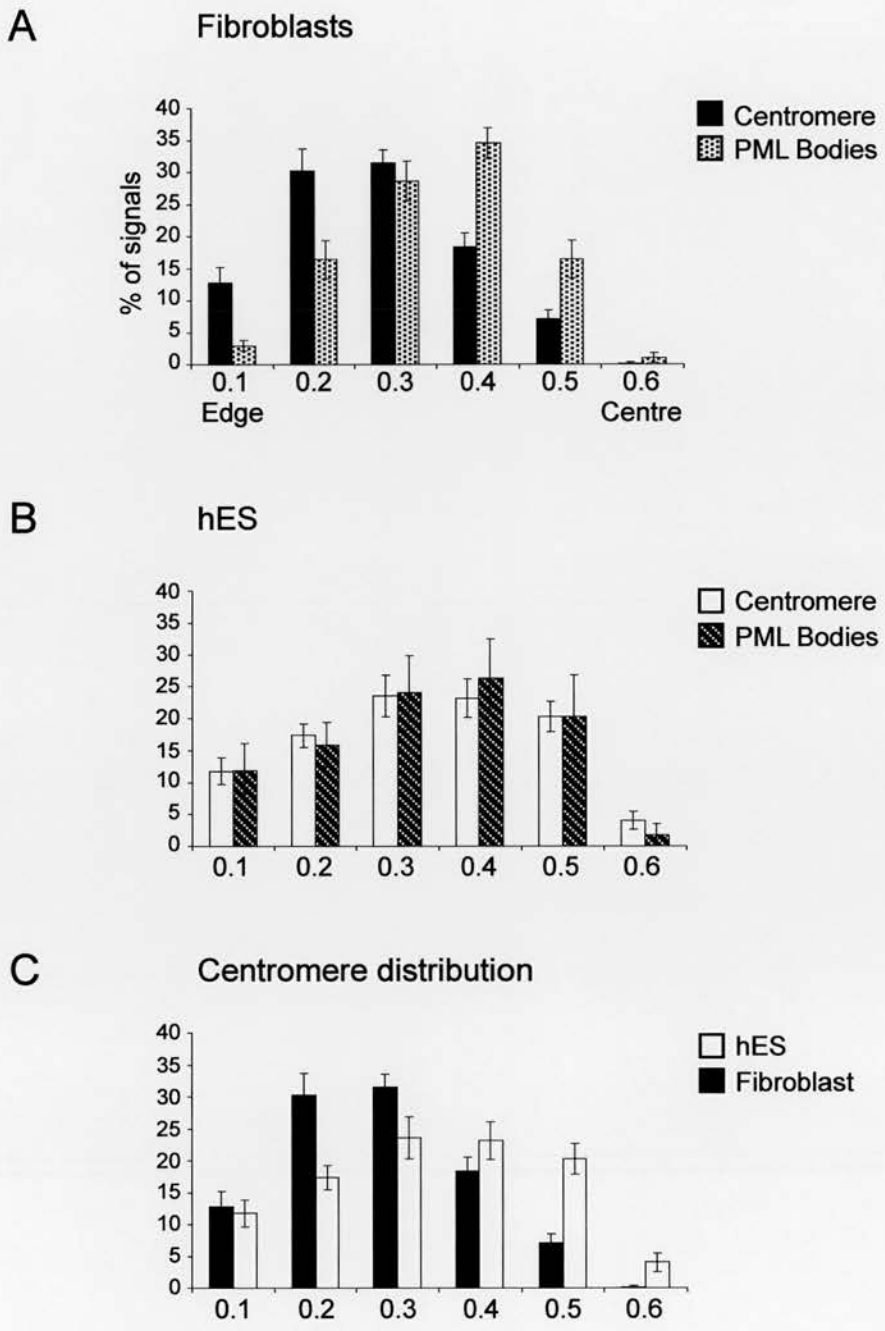

Fig. 3.10 Centromere and PML body distribution from the nearest edge of the nucleus. The mean distance (±s.e.m.) from centromeres (CENP-C) and PML bodies (5E10) to the nearest nuclear periphery, normalised to the volume of the nucleus in (A) fibroblasts and (B) H7 hES cells. (C) A comparison of the distribution of centromeres to the nearest nuclear edge, normalised to nuclear volume, in nuclei from fibroblasts and H7 hES cells (*n*=20).

$p<0.006$; *figure* 3.10A). In hES cells PML bodies were also distributed towards the nuclear centre (*figure* 3.10B), but in these cells the distribution of centromeres and PML bodies was the same as each other (0.5, $p=0.994$). A significantly more central localisation was observed for centromeres in hES cells than in fibroblasts (0.5, $p<0.001$; *figure* 3.10C). However, this method of normalising the data to nuclear volume, assumed that nuclear morphology was not important for spatial organisation.

The above analysis suggested that the location of centromeres in the nucleus is different in hES cells and fibroblasts. To investigate this further in a way that does not need a defined nuclear periphery, or that does not make any assumptions about the shape of the nucleus, the position of centromeres and PML bodies were analysed throughout the *z*-axis of nuclei. Images taken at 0.25μm intervals along the *z*-axis, had the DAPI nucleus segmented. The positions of centromeres and PML bodies were then calculated in the *z*-plane, using the coordinates of the highest fluorescence intensity for each fluorescent spot. I calculated the average distribution by dividing each nucleus into ten equal distances in the *z*-plane ($n=20$, *figure* 3.11). The position of PML bodies was investigated in proliferating fibroblasts, Ritva telomerase immortalised fibroblasts, quiescent fibroblasts, a LCL and H7 hES cell nuclei. Despite differences in abundance, in all these cell-lines PML bodies displayed a centralised localisation in the *z*-plane (*figure* 3.11).

Centromeres however, display a bi-modal distribution toward the nuclear periphery in primary fibroblasts and Ritva. So due to the flat nuclei of these cells, the graphs depict a peak of centromeres at the top surface of the nucleus, less centromeres in the middle and another peak at the bottom of the nucleus. Quiescent fibroblasts have a disrupted distribution, with less centromeres present towards the top of the nucleus, suggesting that centromere arrangement relates to cell cycle as was previously shown by Weimer et al., (1992). In hES cells and LCLs, centromeres have a normal distribution along the *z*-axis, which may reflect the position of the nucleolus and therefore the position of the centromeres from the acrocentric chromosomes (Manuelidis, 1990). To exclude any

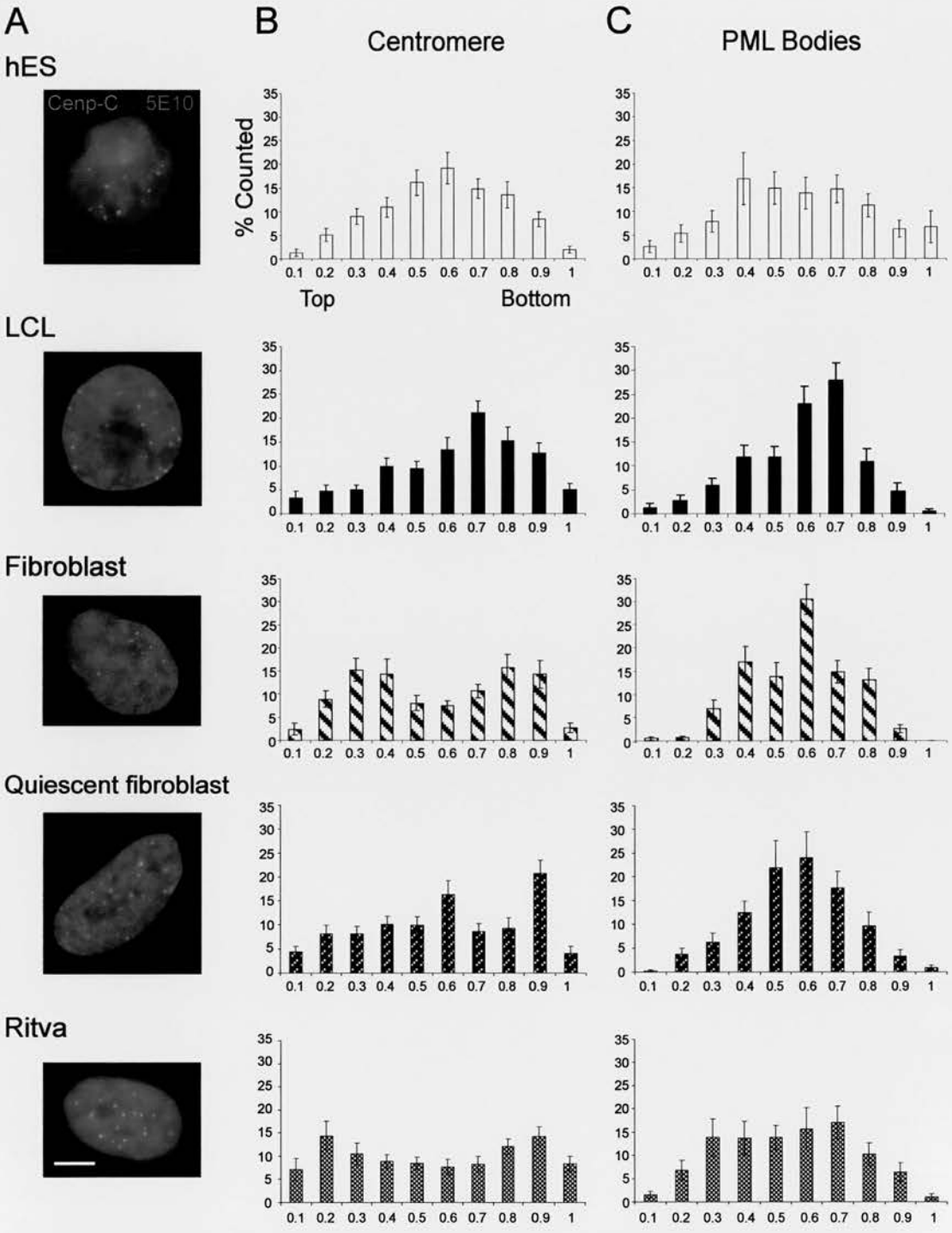

Fig. 3.11 Centromere and PML body localisation in human cells. (A) Localisation of centromeres (CENP-C, green), and PML bodies (5E10, red) in H7 hES, LCL, fibroblast, quiescent fibroblast and ritva cell nuclei counterstained with DAPI (blue). The mean (±s.e.m.) distribution of (B) centromeres and (C) PML bodies through the *z*-plane from top (0) to bottom (1) of nuclei from H7 hES, LCL, fibroblasts, quiescent fibroblasts and ritva cells (*n*=20). Scale bar, 5μm.

effects that cytospinning may have on these cell types, this experiment was repeated on proliferating fibroblasts that had been cytospun onto slides. In comparison to the proliferating fibroblasts grown on slides, no difference was observed in the position of centromeres relative to the nuclear periphery in the cytospun nuclei.

To investigate whether the increase of centromeres in the centre of the *z*-axis in hES cell nuclei was due to an increase of centromeres at the nucleolus, I stained fibroblast, LCL and hES cell nuclei with an antibody to the Ki67 antigen (pKi67) to detect the nucleoli (Verheijen et al., 1989), and CREST serum to identify the centromeres (*figure* 3.12A). The number of centromeres present at the nucleolus, nuclear periphery and not associated with either were counted (*figure* 3.12B). The number of centromeres present at the nucleolus of fibroblasts, a LCL and hES cells was similar ($p>0.39$). However, in fibroblasts ($p<0.001$) and LCLs ($p<0.04$) significantly more centromeres were present at the periphery of the nucleus than in hES cells. In comparison significantly more centromeres were found to be not associated with either the nucleolus or the nuclear periphery in hES cells ($p<0.004$). The normal distribution of centromeres observed in the *z*-plane of hES cells was not due to a change in number of centromeres at the nucleolus, but an increase in the numbers present in the nucleoplasm. A re-distribution of centromeres to the nuclear periphery during differentiation would be consistent with the nuclear periphery being associated with gene silencing as cells differentiate (Gasser, 2002; Kosak et al., 2002).

Lastly, I looked at the position of telomeres in human nuclei. In differentiated cells, telomeres are found distributed throughout the nucleoplasm (Weierich et al., 2003). Unlike somatic cells, hES cells and germ cells express telomerase, which stops telomere shortening and allows the cell to self-renew in culture (Thomson et al., 1998). I investigated the position of telomeres using a pan telomeric probe (Lansdorp et al., 1996), in the nuclei of primary fibroblasts, Ritva, hES cells, LCLs, HT1080 and HTC75-T19 cells with induced telomere fusions (van Steensel et al., 1998). These last cells had been transfected with a truncated form of the human telomeric binding protein TRF2

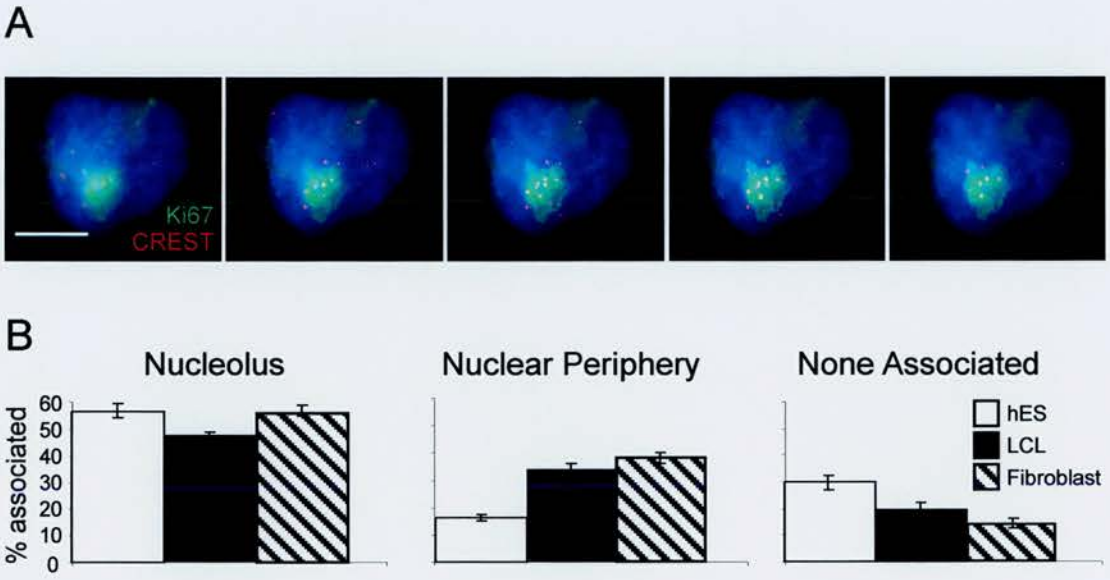

Fig. 3.12 Centromere localisation relative to the nucleolus. (A) Localisation of centromeres (CREST, red), and nucleoli (Ki67, green) in single frames, taken at 0.75μm intervals through the *z*-axis of H1 hES cell nuclei counterstained with DAPI (blue). (B) Mean proportion of centromeres per cell that are associated with the nucleolus (left), the nuclear periphery (middle), or neither of these nuclear compartments (right), in H1 hES cells (white), a LCL (black) and fibroblasts (hatched) (*n*=20). Scale bar, 10μm.

under G418 selection, which lacked both the N-terminal basic domain and the C-terminal Myb domain (ΔbasicΔmybTRF2), as well as tetracycline-controlled trans-activator under hygromycin selection. Therefore, the cells grow normally in the presence of doxycyclin and G418, but in the absence of doxycyclin, the expression of this dominant negative TRF2 protein induces telomere fusions within 4-5 days (van Steensel et al., 1998). There was a conserved telomere distribution across cell types grown on slides, with telomeres located in a skewed distribution towards the bottom of the nucleus (*figure* 3.13). Even in the transformed HTC75-T19 cells following induced telomere-telomere fusions, this distribution pattern was unchanged. The hES and LCLs that were cytospun onto slides show a near-normal distribution of telomeres, which may reflect the different nuclear morphology of these cells or the cytospinning.

3.6 Discussion

I have shown that some aspects of the radial organisation of CTs previously seen in differentiated cells are already established in hES cells. The gene-rich HSA19 is more centrally localised than gene-poor HSA18 in both 2D and 3D FISH (*figures* 3.2 and 3.3). HSA18 localises to the periphery in most cell types, including lymphocytes (Croft et al., 1999), keratinocytes and cancer cell lines (Cremer et al., 2003). However, HSA18 displays a more central localisation within the flat nuclei of amniotic fluid cells and quiescent fibroblasts (Bridger et al., 2000; Cremer et al., 2001). The nucleus of a hES (average height:length ratio=1.02±0.1) however, more closely resembles the shape of a spherical lymphocyte nucleus (ratio=1.00±0.1), than the shape of a flat fibroblast nucleus (ratio=0.25±0.4). Granulocyte-macrophage colony forming cells (GM-CFC) also display a radial organisation of CTs, and it has been suggested that haematopoietic stem cells have this arrangement as well (Cremer et al., 2003). I think that since this distribution of chromosomes is present in hES cells, it is likely that most cell types will have a radial organisation of CTs (with the exception of those, which have very flat nuclei).

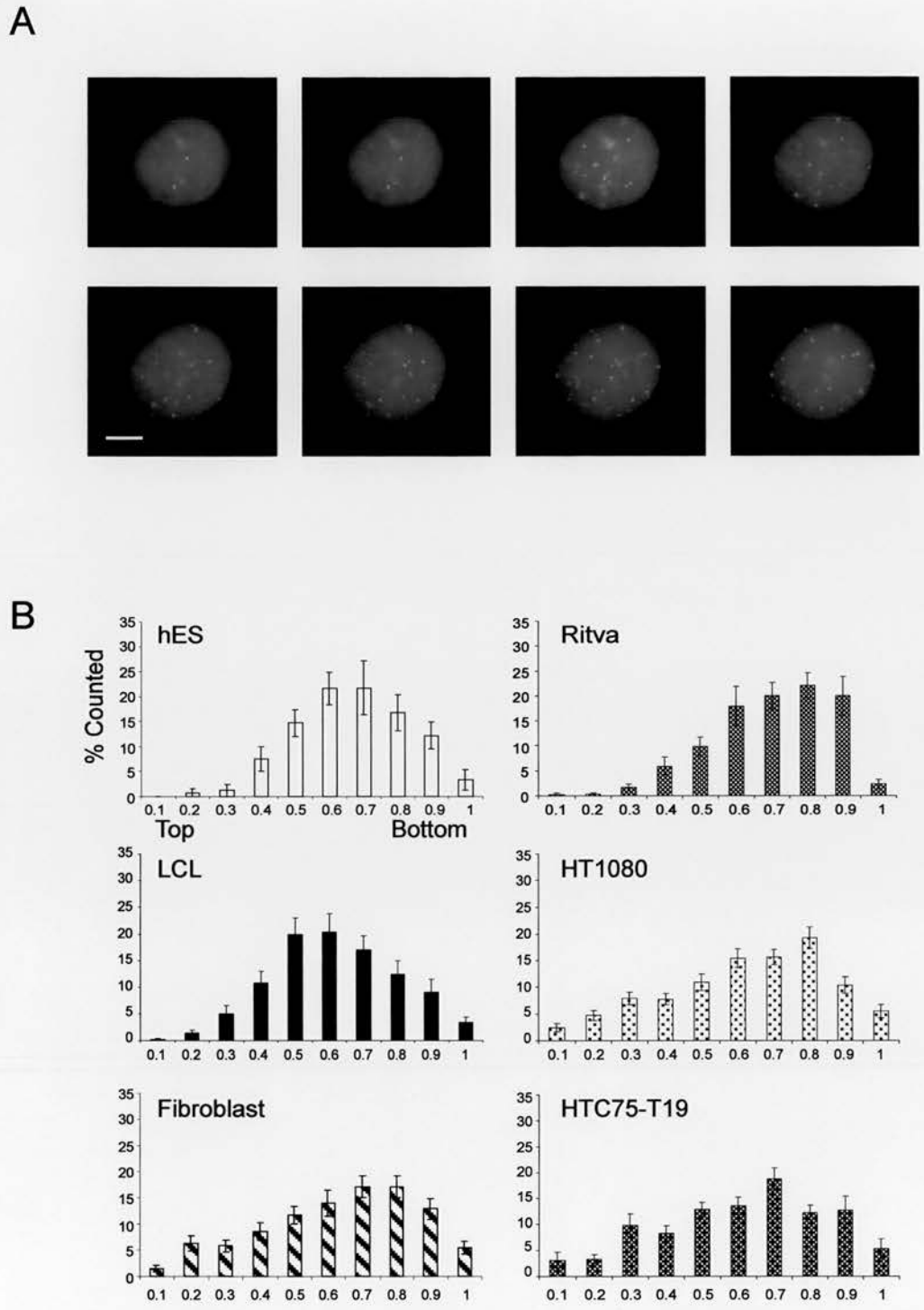

Fig. 3.13 Telomere localisation in human cells. (A) Localisation of telomeres (PNA probe, green) in single image frames, taken at 0.75μm intervals, through the *z*-axis of fibroblast cell nuclei counterstained with DAPI (blue). (B) Mean (±s.e.m.) distribution of telomeres through the *z*-plane from the top (0) to the bottom (1) of nuclei from H1 hES, LCL, fibroblast, Ritva, HT1080 and HTC75-T19 cell lines (*n*=20). Scale bar, 5μm.

Differences in the distribution of mouse chromosomes have been reported previously, both between different tissue types and during T cells differentiation (Parada et al., 2004; Kim et al., 2004), but only changes in chromosome associations have so far been identified in human cells (Kuroda et al., 2004a). I detected a more central localisation for HSA12p in hES cells. One of the chromosome abnormalities that occurs in hES cells is the recurrent gain of chromosome 12, including iso12p (Draper et al., 2004). It has been suggested that HSA12p is transcriptionally advantageous to pluripotent stem cells and increasing the number of chromosomes, therefore increases the amount of gene expression, which may help maintain the propagation of undifferentiated hES cells (Draper et al., 2004). In this experiment, not only HSA12p located towards the centre of the nucleus in hES cells, but also a BAC covering *NANOG* (*figure* 3.5). Although the significance of being located in the centre of the nucleus, is as yet unknown, the fact that the most gene dense chromosomes locate there (Boyle et al., 2001) suggests that it confers some transcriptional advantage.

In contrast, silenced genes are associated with the nuclear periphery in some differentiated cell types (Kosak et al., 2002; Zink et al., 2004). However, neither *NANOG* nor *OCT4* relocated to the nuclear periphery upon differentiation. It would be interesting to know if these pluripotent genes located to centromeric heterochromatin upon their silencing, or if genes involved in pluripotency are required to stay away from heterochromatin, either because of active genes in the surrounding region, or because their expression is required again at a later time point.

Alongside their organisation within the nucleus, I also explored the intra-CT organisation of these regions. The telomeric end of HSA11p has been shown to locate outside of its CT in differentiated cell types (Mahy et al., 2002a). This organisation was seen in hES cells, even though the region does not contain any genes with a known role in pluripotent cells (*figure* 3.6). Therefore, in both hES cells and differentiated cells

gene-dense regions may be organised in a similar manner, irrespective of gene expression.

There was no difference in the nuclear position of HSA6p and *OCT4* between hES cells and a differentiated cell type, with both the gene and the CT locating to an intermediate position in the nucleus (*figure* 3.5). However, *OCT4* was located just outside the 6p CT in hES cells, but inside the 6p CT in a LCL (*figure* 3.7). The flanking genes of the expressed class I regions were located outside 6p CT in both cell types consistent with previous results (Volpi et al., 2000). The local chromatin structure of the *OCT4* region is unknown in hES cells, but in mouse, there is increased DNA methylation and histone deacetylation of the *Oct4* promoter/enhancer in trophoblast cells compared to ES cells (Hattori et al., 2004). The data I present here would be consistent with a similar chromatin remodelling of the region around *OCT4* in hES cells, possibly contributing to its transcriptional regulation. Therefore, both *NANOG* and *OCT4* possess a distinctive nuclear organisation in hES cells, in comparison to LCLs. With *NANOG*, there is a movement of the whole CT out of the centre of the nucleus between hES cells and LCLs. Whereas *OCT4*, surrounded by active genes, moves back into the 6p CT during the differentiation of hES cells to LCLs.

I have also shown a difference in the distribution of centromeres between hES cells and differentiated cells, although I did not see any evidence for the clustering of centromeres previously reported in the literature, which may be specific to cell type. In differentiated cells, centromeres are located at the nuclear periphery and around the nucleolus (reviewed in Gilchrist et al., 2004). Centromeres in hES cells have a more internal distribution (*figure* 3.10 and 3.11), with less associated at the nuclear periphery (*figure* 3.12). It is not known what determines the nuclear distribution of centromeres. Levels of histone acetylation at centromeric heterochromatin are observed to alter the position of centromeres in human and mouse differentiated cells (Taddei et al., 2001), and histone hypoacetylation only occurs at satellite repeats upon differentiation in mES cells (Keohane et al., 1996), which if conserved between species would be consistent with my

data. This difference in centromere distribution in hES cells may reflect a change in the duration of the cell cycle. Alternatively, it could be influenced by mechanisms of gene silencing (Fisher and Merkenschlager, 2002). Changes in the nuclear positioning of centromeres have recently been correlated with the competency of mouse oocytes (Zuccotti et al., 2005). It would be interesting to see if other pluripotent cells such as EC and germ cells show the same internal centromere distribution as the hES cells, and determine whether this central distribution is necessary for their cellular plasticity.

The number of PML bodies present in the nucleus has been shown to vary between cell types. There is no difference between quiescent and proliferating fibroblasts, which suggests that these changes are not effects of the cell cycle. However, since PML bodies are linked to transcription, I am surprised to observe the least number in ES cells, which are thought to be more transcriptionally active than their differentiated counterparts (Keohane et al., 1996; Ramalho-Santos et al., 2002; Sato et al., 2003). This may reflect another role suggested for PML bodies as a nuclear storage site for excess proteins, which might not accumulate in the nucleus of hES cells, due to their active state. The distribution of PML bodies is central in both hES cells and differentiated cell types (*figure* 3.11). However, a broader distribution was observed in the nuclei of immortalised cells (i.e. the Ritva and hES cells). This is probably due to a decrease in the number of PML bodies present in the nucleus of these cells, but it is interesting to observe that the increase in number of PML bodies coincides with an increased localisation in the transcriptionally active centre of the nucleus.

Finally I looked at the distribution of telomeres in the nucleus of differentiated and hES cells (*figure* 3.13). Here the effects of nuclear morphology upon spatial arrangement are similar to that previously described for HSA18 and 19 CTs. In the flat-bottomed nuclei of fibroblasts and HT1080 cells grown on slides, telomeres have a skewed distribution toward the bottom of the nucleus. In contrast to this in LCLs and hES cells, grown as suspension cultures and colonies respectively, telomeres show a near normal

distribution, reflecting a more spherical shaped end to their nucleus. This illustrates the role of nuclear morphology in the spatial arrangement of the genome.

In summary, hES cells have a distinct nuclear architecture when compared to more differentiated cell types, especially in genomic regions involved in pluripotency. Areas of transcriptional silencing, such as the association of centromeric heterochromatin with the nuclear periphery seen in differentiated cells, are not established in the hES cell nucleus (Wiblin et al., 2005; Appendix 1). Determining how the genome is organised in hES cells, may help to identify the spatial rearrangements in the nuclei of differentiating cells that facilitate changes gene expression, and allow for a better understanding of pluripotency. In an attempt to understand the role of this organisation, I wanted to follow the spatial re-arrangement of the genome though differentiation of a specified lineage. However, when I began this work the field of hES cells differentiation was in its infancy. Five years after the first derivation, few protocols for the differentiation of hES cells into specific lineages were available, with reports of varying success rates. In comparison, it was possible to differentiate mES cells into many lineages (Smith, 2001). For this reason, I used mES cells in the remaining results chapters.

Chapter 4: Directed Differentiation of Mouse Embryonic Stem Cells

Chapter 4

Directed Differentiation of Mouse Embryonic Stem Cells

4.1 Introduction

First derived in 1981 (Evans and Kaufman, 1981; Martin 1981) mES cells can be maintained indefinitely *in vitro* by the presence of Leukaemia Inhibitory Factor (LIF) (Williams et al., 1988; Smith et al., 1988). Current understanding suggests that LIF acts through the gp130 receptor to activate STAT3 in a JAK kinase mediated process (Yoshida et al., 1994; Niwa et al., 1998). This is unlike hES cells, which neither require nor respond to gp130 stimulation (Reubinoff et al., 2000; Thomson et al., 1998). Following the removal of LIF it is possible to differentiate mES cells into almost all lineages, the only notable absence being trophectoderm, which has never been generated *in vitro* (Reviewed in Keller, 1995; Wobus, 2001; Smith, 2001).

ES cell differentiation is a good model in which to study early development. The expression of genes and proteins during the differentiation of mES cells *in vitro* closely resembles the pattern observed during mouse embryogenesis. Perhaps the best example of this is the differentiation of the haemopoietic system in embryoid bodies (EBs), where both the development of precursor cells and their response to growth factors parallels that found in the yolk sac and early fetal liver (Keller et al., 1993). Apart for their usefulness as a model system, mES also offer some advantages over using primary tissue. Populations of early precursor cells are difficult if not impossible to access *in*

vivo. An example of this is oligodendrocyte precursor cells (OPCs). Oligodendrocytes are post-mitotic cells responsible for myelinating axons in the CNS. Not only are the steps required in generating a mature oligodendrocyte under dispute but also the identity of the precursors cells involved (Noble et al., 2004). *In vivo* these OPC populations appear in the ventral neuroepithelium of the developing brain and spinal cord around E12.5. It is possible to purify these cells from the rat optic nerve (Raff et al., 1988; Barres et al., 1994) but not in large enough quantities to carry out conventional biochemical analyses. Furthermore, the progenitor cells that become OPCs cannot be isolated, which makes the oligodendrocyte lineage difficult to study in primary cells.

Protocols have been developed for the differentiation of mES cells into various neuronal and CNS lineages, such as neurons (Bain et al., 1995; Strubing et al., 1995), astrocytes (Fraichard et al., 1995) and oligodendrocytes (Brustle et al., 1999; Liu et al., 2000). However, the resulting cell populations are heterogeneous and although they share the expression patterns characteristic of a chosen lineage, other cells types including ES cells often persist within the cultures. To achieve a more homogeneous population many methods have been explored, including selective culture conditions (Rolletschek et al., 2001), co-culture with stromal cell lines (Kawasaki et al., 2000) and FACs sorting surface markers or GFP expressing cells from within a population (Ying et al., 2003). However, perhaps the most efficient way of restricting a population is by conferring drug resistance on a subset of the population. Previously mES cells have been genetically modified to allow for the selection of neuroepithelial cells following differentiation *in vitro* (Li et al., 1998; Billon et al., 2002). With the appropriate signalling molecules, seen to promote OPCs *in vivo*, these neuroepithelial cells produced OPCs and then oligodendrocytes in a similar time frame to their *in vivo* counterparts. In this chapter, I aim to outline the differentiation of mES cells to neural precursors that I will use in the remaining results chapter, with the OS25 cells adapted by Billon et al., (2002).

4.2 Directed differentiation of OS25 cells

The OS25 cell line was generated from the E14TG2a parental ES line by sequential gene targeting (Billon et al., 2002). A *hygromycin-thymidine kinase* (*hyg-tk*) fusion gene integrated into the *Oct4* (*Pou5f1*) locus by homologous recombination allows for the selection of undifferentiated (*Oct4*-expressing) cells with hygromycin before the onset of differentiation, and then negative selection with gancyclovir specifically eliminates any *Oct4* expressing cells remaining after differentiation. A *β-geo* cassette inserted into the *Sox2* locus, allows for positive selection with G418 to eliminate everything from the culture except for *Sox2* expressing ES cells and neural precursors (Li et al., 1998; Billon et al., 2002).

Prior to differentiation the cells were cultured in the presence of 100μg/ml hygromycin-β for seven days, to obtain a purer population of *Oct4* expressing cells. Differentiation was started by removing LIF from the culture media (*figure* 4.1). 6 x 10^5 cells/ml were plated for two days as hanging drops to form spherical embryoid bodies (EBs). This was different from the original protocol, where the mES cells formed EBs in suspension cultures (Billon et al., 2002). I have tried both methods and found that when left in suspension during the first two days of culture, EBs had a tendency to aggregate together forming irregular shaped bodies and long chains. The hanging drop method promoted more evenly sized EBs as the amount of cells starting each EB was constrained to the number of cells per drop. Therefore, the timing of EB development was more synchronous across a population formed by this method and it produced more spherical EBs, which did not aggregate during later stages of differentiation and prevented the formation of EB chains. I chose the EB method of differentiation as opposed to differentiation in a monolayer. Even though studies have shown specific cell types can be isolated from monolayers (Nishikawa et al., 1998), it is still uncertain to what extent multicellular interaction are needed in the development of specific lineages and in comparison to using EBs, lower cell numbers have been reported at the end of monolayer differentiations (reviewed in Höpfl et al., 2004).

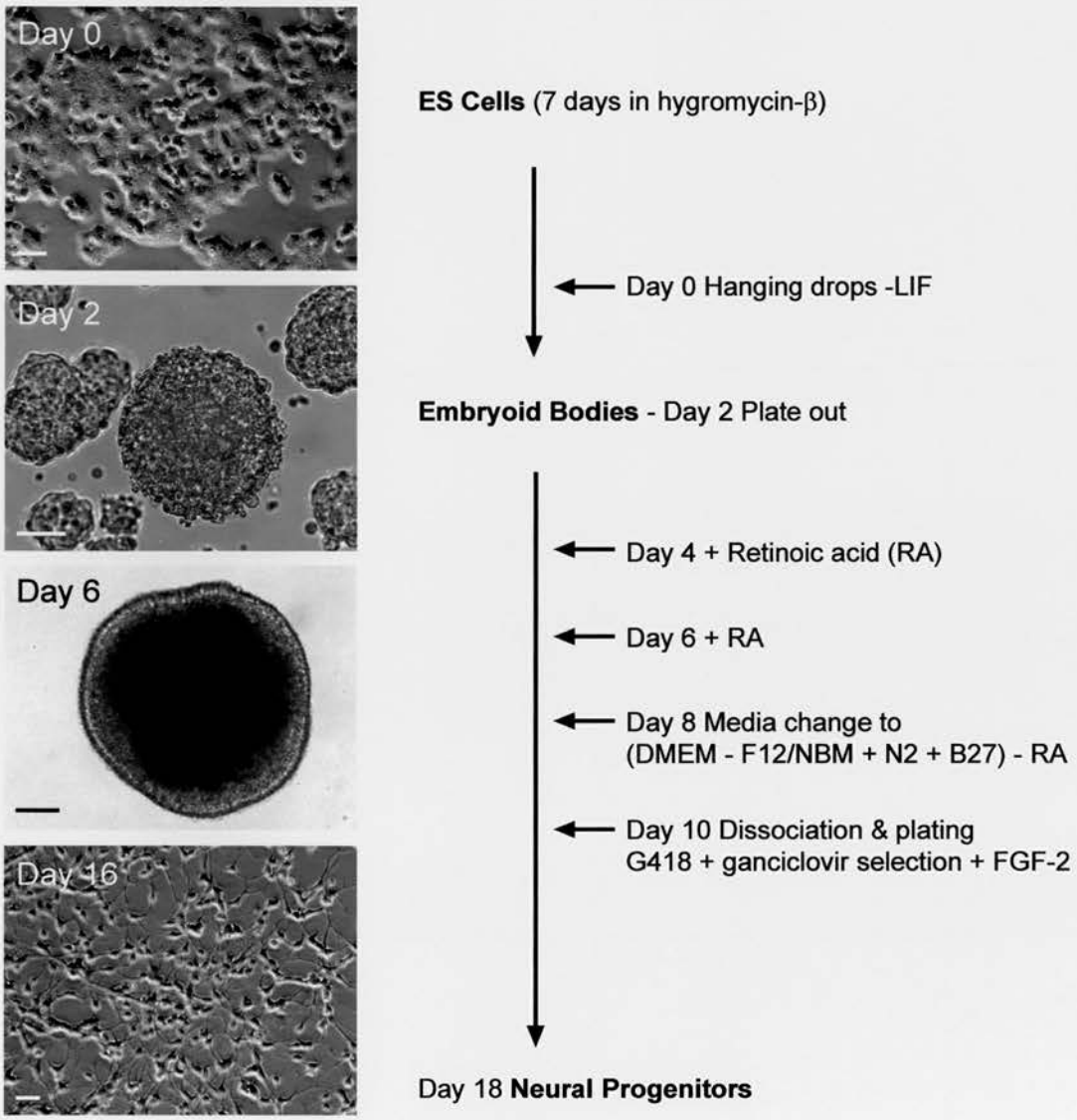

Fig. 4.1 Directed neural differentiation of mES cells. Retinoic acid induced differentiation of mouse OS25 cells (*Oct4-hyg-tk*, *Sox2βgeo*) into neural progenitors (protocol adapted from Billon et al., 2002). Images taken under phase contrast. Scale bar 50μm.

The hanging drops were knocked together and the EBs cultured in suspension for an additional two days, before retinoic acid (RA) was added at day 4 to push the differentiation further. RA functions as a ligand for nuclear receptors, which in turn transcriptionally regulates RA target genes, by binding to RA response elements (RAREs) within their promoters. The concentration of RA used affects neuronal cell identity (Okada et al., 2004). Here I used 10^{-6} M RA as in Billon et al., (2002) but have extended the time that cells were exposed to RA from two to four days, because RA induced genes were not expressed after only two days. After four days, the RA was removed and the media changed to a 50/50 mix of DMEM-F12 / Neurobasal media plus N2 and B27 supplements. Increasing the amount of DMEM-F12-N2 in the media lowers cell viability but promotes neuronal differentiation, whilst increasing the neurobasal media-B27 proportion improves cell viability, but reduces the efficiency of neuronal differentiation (Ying and Smith, 2003). EBs were left in this media for two days, to allow them to adjust to serum free conditions, before being dissociated and plated out as a monolayer. In another change from the protocol used by Billon et al., (2002) I found dissociating EBs in a mixture of 1ml PBS, 1ml dispase (2.4U/ml) and 20µl DNase I (7mg/ml) rather than trypsin, resulted in an increase in the number of viable cells (Taylor personal communication). At first, I plated cells on either gelatin or poly-L-lysine with laminin (*figure* 4.2A-B). However, whereas the majority of cells plated on gelatin appeared to have two main processes, those plated on poly-L-lysine were larger, flatter, multi processed cells with a much slower rate of growth. Due to this apparent change in cell morphology, from here onwards only gelatin was used. After dissociation on day 10, G418 was added to the media to select for *Sox2* expressing cells and gancyclovir was added to kill *Oct4* expressing cells. Alongside this drug selection, I added the growth factor FGF-2 (20ng/ml) to the culture to promote cell proliferation and thereafter the medium was changed every other day until the end of the differentiation on day 18.

Before and after differentiation the cells were stained with x-gal to determine how homogenous the cell population was and establish which passage numbers and cell

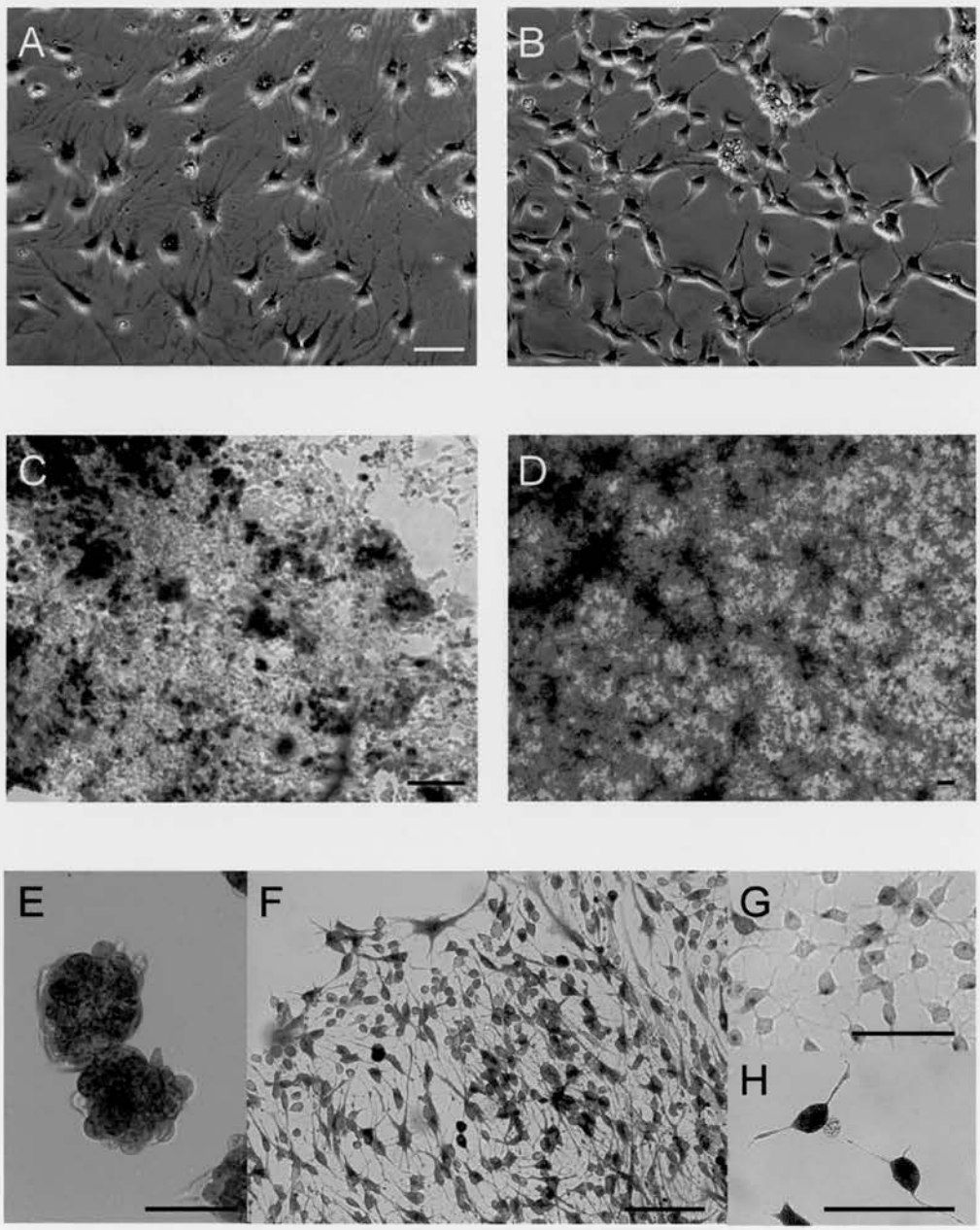

Fig. 4.2 Defining the conditions for neural differentiation of OS25 cells. OS25 cells after 18 days of differentiation plated on (A) poly-L-lysine plus laminin or (B) gelatin. Differentiation of (C) passage 60 and (D) passage 30 cells, stained on day 18 with x-gal (blue) for *Sox2βgeo* expression. X-gal staining for *Sox2βgeo* expression in (E) day 2 embryoid bodies and (F) day 18 neural precusors. Expression levels of *Sox2* varied across the day 18 population (G) and (H). Scale bars, 50μm.

densities resulted in the highest percentage of *Sox2* (β-*geo)* expressing cells. The *Sox2* transcription factor is an early marker of the nervous system and is expressed in neural stem cells isolated from embryos (Ferri et al., 2004). I found that it was expressed throughout my differentiation protocol (*figure* 4.2E-F; *figure* 4.6 and *table* 4.1). However, differences in the x-gal staining pattern were observed amongst the day 18 cell population (*figure* 4.2 G-H). Higher passage numbers (>50) produced less *Sox2* expressing cells at day 18 than lower passage numbers (<35) which was probably due to the cells acquiring defects, such as extra chromosomes, in tissue culture rather than passage number per se (*figure* 4.2 C-D). I observed similar differences in x-gal staining at day 18 between starting the differentiation with 7 x 10^6 cells, plated on 10cm bacterial dishes used by Billon et al., (2002) and 6 x 10^5 cells plated in hanging drops that I used. This was probably due to the effect of cell density on RA concentration (Okada et al., 2004).

4.3 Analysing markers of pluripotency during differentiation

To check for undifferentiated cells I looked for the presence of three markers of pluripotent cells, alkaline phosphatase, *Oct4* and the stage specific embryonic antigen 1 (SSEA1) in both day 0 and day 18 populations (*figure* 4.3). When stained for alkaline phosphatase undifferentiated cells, which express the gene, turn pink (Chiquoine 1954; Donovan et al., 1986; Matsui et al., 1992). Differentiated cells should not stain positive for alkaline phosphatase but I detected alkaline phosphatase expression in both the day 0 and day 18 populations (*figure* 4.3A). This could have been due to the presence of undifferentiated cells at day 18, but the morphology of these cells suggested otherwise. Therefore, there must be expression of alkaline phosphatase by the differentiated cells.

Oct4 expression is confined to the pluripotent cells of the developing embryo and their *in vitro* counterparts ES and EG cells (Smith, 2001). However, it has also been reported to be transiently expressed in the developing embryonic endoderm (Palmieri et al., 1994) and neurectoderm (Reim and Brand, 2002; Shimozaki et al., 2003) where it

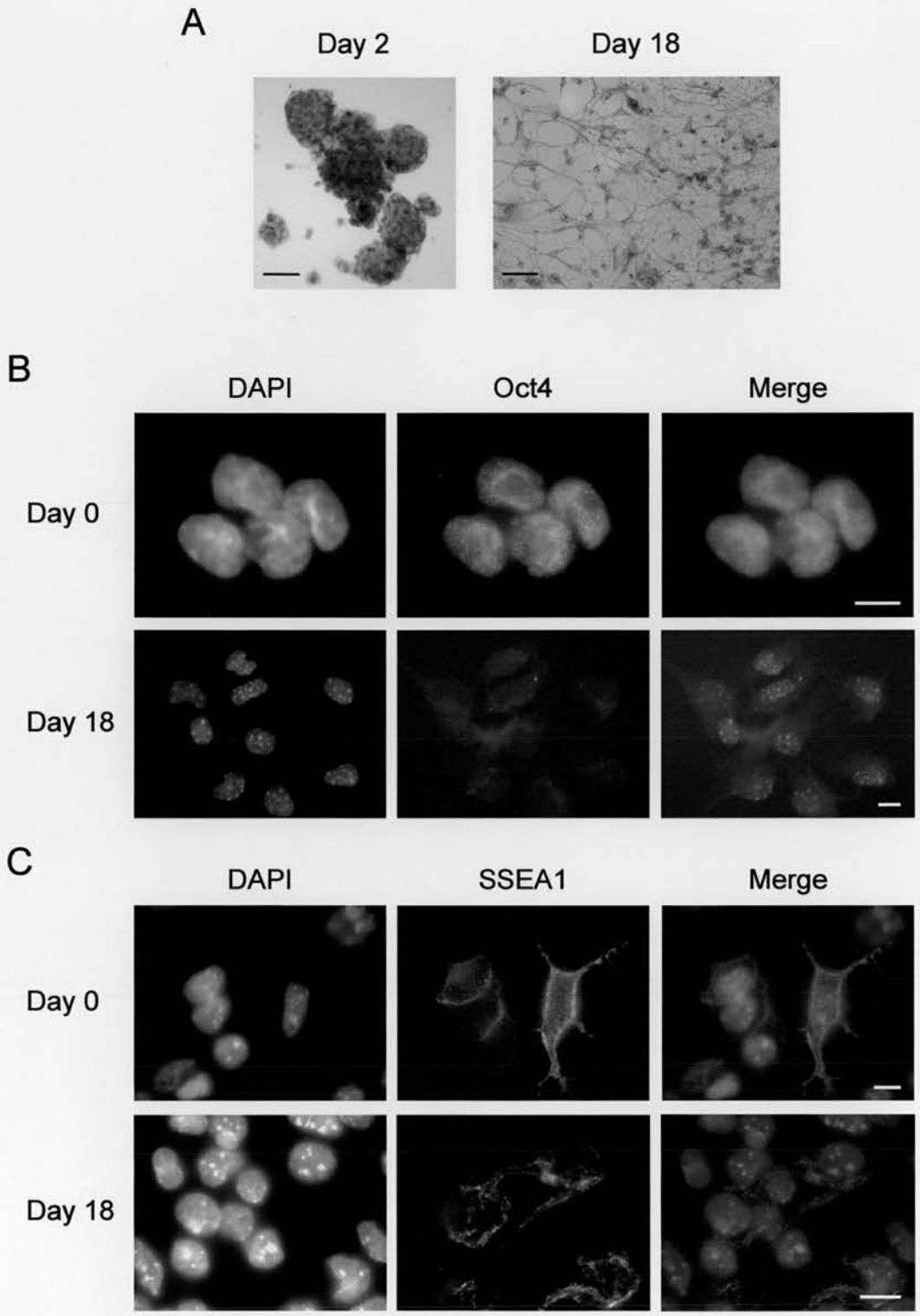

Fig. 4.3 Neural precursors express two markers of pluripotent mES cells. (A) Staining of day 2 embryoid bodies and day 18 differentiated OS25 cells with alkaline phosphatase (pink). Scale bars, 50μm. Immunofluorescence for (B) Oct4 and (C) SSEA1 (green) on day 0 and day 18 OS25 cells, nuclei counterstained with DAPI (blue). Scale bars, 10μm.

may have a role in specifying cell fate. Oct4 was detected in the nucleus of undifferentiated (day 0) cells (*figure* 4.3B), but no Oct4 protein (*figure* 4.3B) or mRNA (*figure* 4.6) was seen at day 18. Indeed I found that there was complete switch off of Oct4 by day 8 of differentiation (*figure* 4.6).

The final marker of mES cells I looked for was SSEA1, first identified at the eight cell stage of the blastomere (Solter and Knowles, 1978). This antigen is expressed by mES cells, but its expression has also been reported in the developing ectoderm (Fox et al, 1980). I observed expression of SSEA1 by immunofluorescence in both day 0 and day 18 populations (*figure* 4.3C). This is consistent with the recent findings of Conti et al., (2005) who also noted SSEA1 staining in neural precursors. However, it is in disagreement with the findings of Billon et al., (2002), who observed the loss of SSEA1 during differentiation of OS25 cells with drug selection. This variation in the expression of markers could be due to alterations in the differentiation protocol between labs.

4.4 Expression of germ layer markers during differentiation

To ascertain whether I was successfully differentiating cells restricted to the ectodermal lineage, I analysed the expression of ectoderm, mesoderm and endoderm lineage marker genes by RT-PCR (*figure* 4.4). For the ectoderm, I chose to analyse *Pax6* an important transcription factor for neurogenesis that is expressed in sub populations of neural progenitors (Ericson et al., 1997) and the intermediate filament protein *Nestin* which is expressed by progenitor cells in the CNS (Lendahl et al., 1990). *Pax6* expression was detected in the culture from day 0 but it increased 4 days after the addition of RA (day 8 of differentiation). *Nestin* was not expressed by mES cells (*figure* 4.5A) but was induced following the removal of LIF from the culture (*figure* 4.4B). Both *Pax6* and *nestin* were still expressed in cultures at day 18. The presence of Nestin protein in the cell processes of cells at day 18 was confirmed by immunofluorescence (*figure* 4.5A).

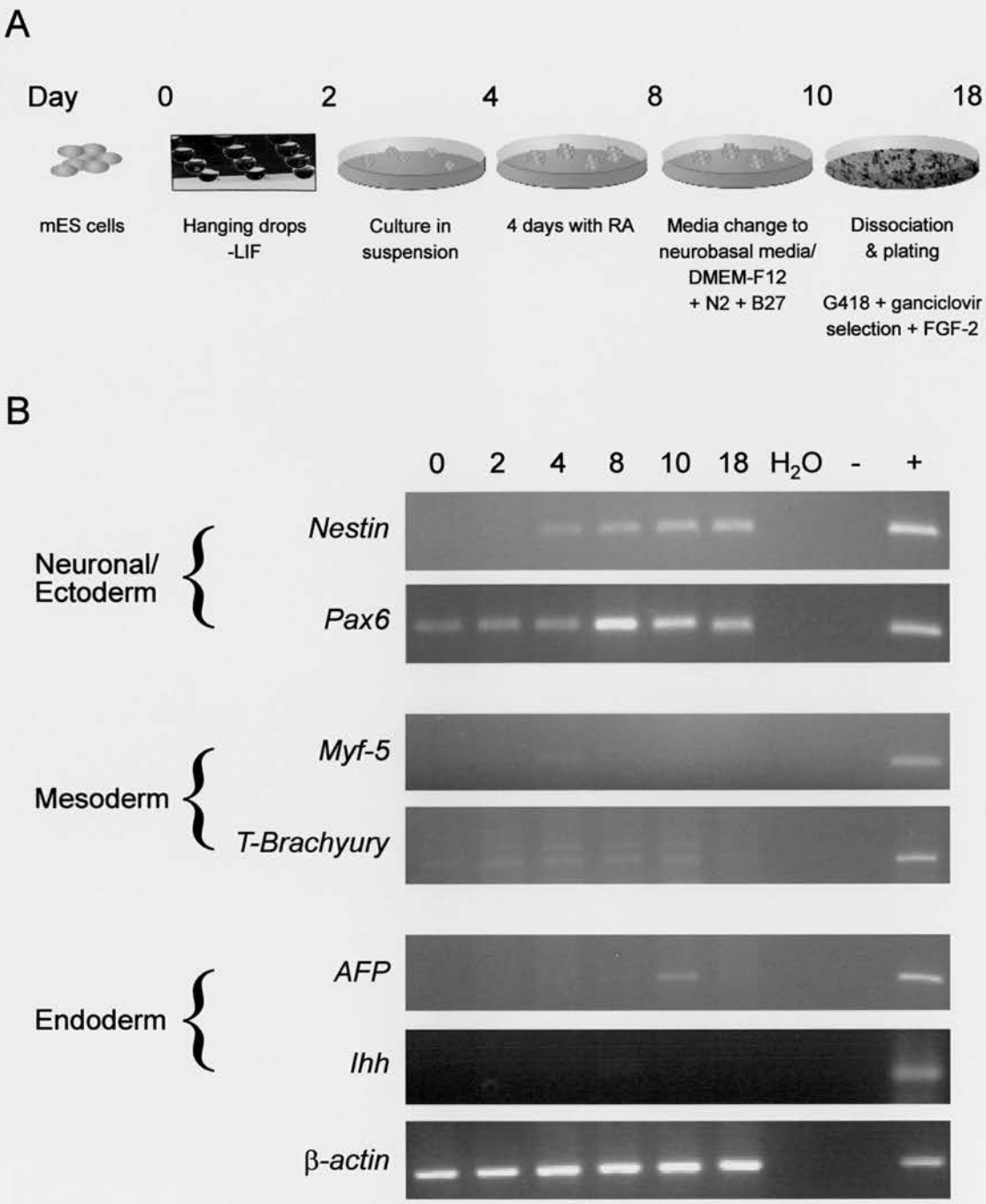

Fig. 4.4 Expression of ectoderm markers during differentiation of OS25 cells with RA. (A) RNA was collected at six time points during the differentiation. (B) RT-PCR analysis of ectoderm, mesoderm and endoderm markers during differentiation of OS25 cells. Lanes are numbered corresponding to the day of differentiation or no template (H_2O), no reverse transcriptase (-) and positive control (+). RNA from E9.5 dpc embryos was used as a positive control, with the exception of *Ihh* where RNA from a mouse ovary was used. To control for the levels of cDNA, RT-PCR for β-*actin* was carried out.

The markers chosen for the mesoderm lineages were *T-Brachyury* a marker of early mesoderm development and *Myf5* a regulator of myogenesis (Keller et al., 1993; Rohwedel et al., 1998). Expression of these genes was not detected in undifferentiated cells, or at any time point during differentiation. Similarly the endoderm markers *Alpha-Fetoprotein* (*AFP*), which is the fetal counterpart of serum albumin (Keller et al., 1993) and *Indian Hedgehog* (*Ihh*) a marker of the visceral endoderm, which has been suggested to have a role in embryonic ectoderm differentiation (Maye et al., 2000) were not expressed in the day 18 population (*figure* 4.4B). I therefore conclude that my differentiation protocol is restricting cells to the ectoderm germ layer, from which neural progenitors are derived.

4.5 Defining the population of neural progenitors

To further characterise the population of differentiated ectodermal cells, immunofluorescence for markers associated with neural differentiation *Nestin*, *Sox1* and *Olig2* was carried out on both mES cells and differentiated day 18 cells (*figure* 4.5). RT-PCR had previously shown that *Nestin* was not expressed by the mES cells, but was expressed in the day 18 population (*figure* 4.4B). This result was confirmed by immunofluorescence with a *Nestin* antibody (*figure* 4.5A and *table* 4.1). *Nestin* is not specific to neural progenitors and is present in somatic and pancreatic cells (Selander and Edlund, 2002). However, it is unlikely that cells other than neural precursors are the source of *Nestin* expression here, due to the absence of mesoderm markers *Myf5* and *T-Brachyury* from the culture (*figure* 4.4B).

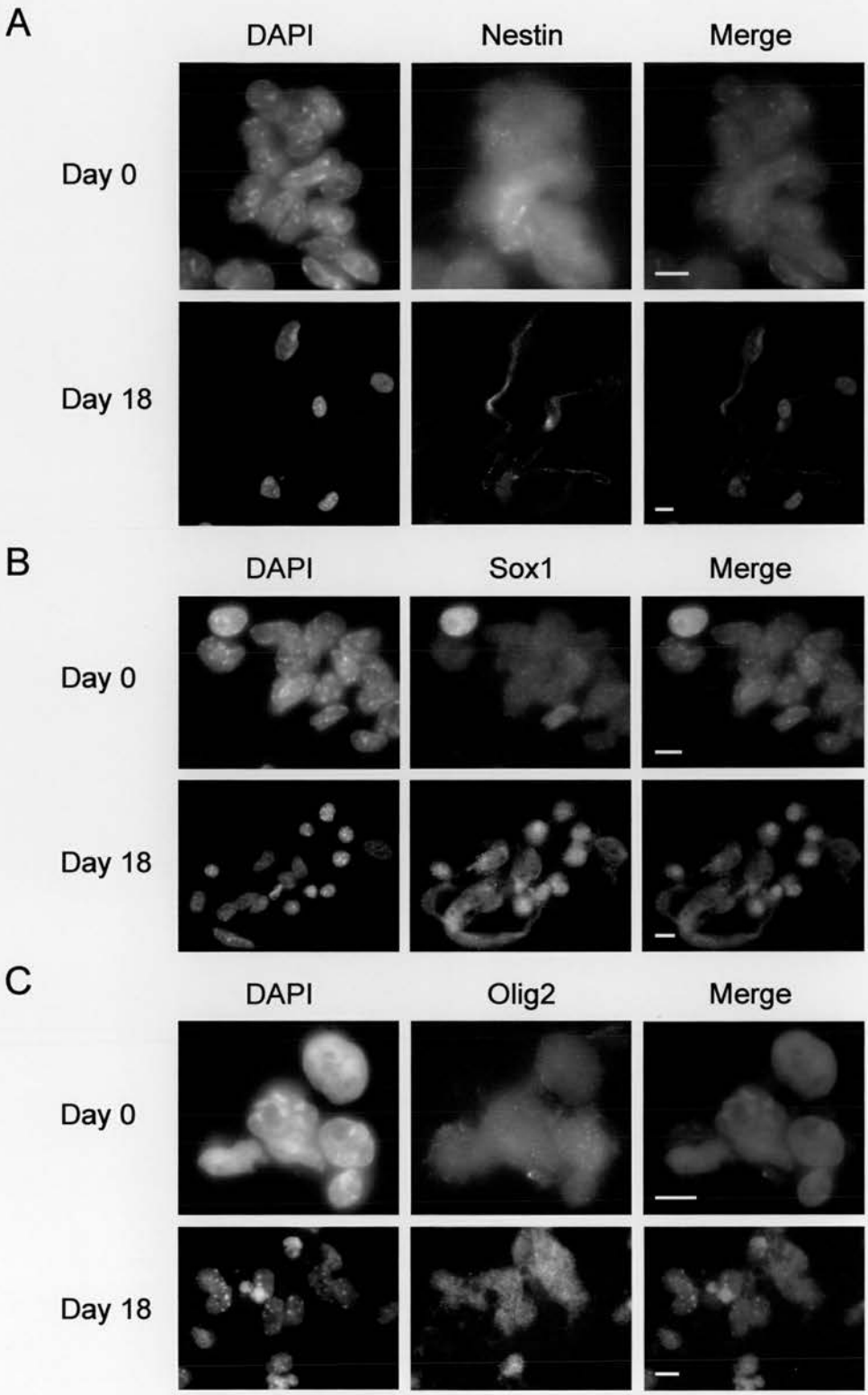

Fig. 4.5 Immunofluorescence for markers associated with neural differentiation. Immunofluorescence on day 0 and day 18 OS25 cells for (A) Nestin (red), (B) Sox1 (green), and (C) Olig2 (red), nuclei all counterstained with DAPI (blue). Scale bars, 10μm.

Marker	Day 0	Day 18
β-*galactosidase*	>90%	94%
Sox1	4%	88%
Nestin	2%	90%
Olig2	0%	15%

Table 4.1 Expression of neuroepithelial markers within the ES cell population and following drug selection on day 18.

The second marker I looked for was the SRY-related transcription factor *Sox1*, which is confined to the neuroepithelium of the neural plate and dividing neural progenitors in the early mouse embryo (Pevny et al., 1998). Similar to the pattern of *Nestin* expression, by immunofluorescence *Sox1* (antibody gift of Robin Lovell-Badge) was observed predominantly in the day 18 population, although a few *Sox1* positive cells were present in amongst the ES cell population at day 0 (*figure* 4.5B and *table* 4.1). However, *Sox1* is one of the earliest known markers of neuroectoderm in the mouse embryo (Wood and Episkopou, 1999) so it is unsurprising that this gene was active amongst cells spontaneously differentiating in culture. RT-PCR showed that *Sox1* was upregulated by day 8 of the differentiation (*figure* 4.6). Progressive differentiation into neurons and glia is accompanied by downregulation of *Sox1* (Pevny et al., 1998). I did not observe a decrease in the overall level of *Sox1* mRNA expression towards the end of the differentiation, perhaps suggesting that my differentiation was not proceeding as far as neurons and glial cells (*figure* 4.6). However, by immunofluorescence two different *Sox1* expressing cell types could be seen within the day 18 population. The small round nuclei of the early precursor cells were distinctive by the increased level of Sox1 protein in the nucleus, whereas towards the end of the differentiation, cells with oval shaped nuclei, which have less expression in the nucleus but more *Sox1* down their cell processes were also present (*figure* 4.5B). The final marker I looked at by immunofluorescence was the basic helix-loop-helix (bHLH) transcription factor *Olig2* (antibody gift of Thomas Jessell). In both *Drosophila* and *Xenopus,* bHLH transcription

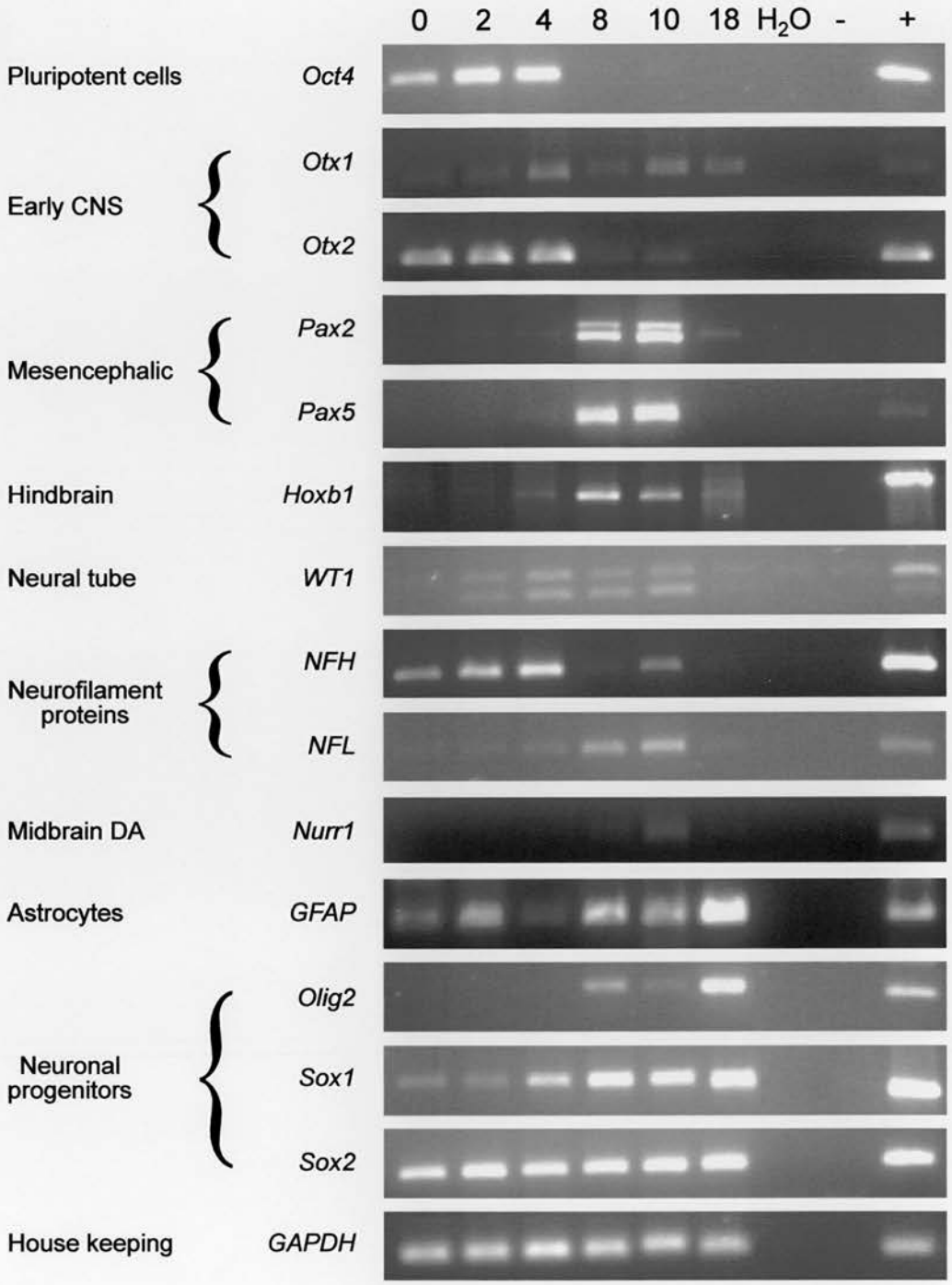

Fig. 4.6 Differentiated OS25 cells express genes characteristic of CNS and neuronal fates. RT-PCR analysis of neuronal and CNS genes on RNA collected from days 0, 2, 4, 8, 10 and 18 of the differentiation or no template H_2O, no reverse transcriptase (-) and RNA from mES cells, E9.5 dpc embryos or adult mouse brain as a positive control (+). The house keeping gene, *GAPDH* is shown as a loading control.

factors are responsible for neural determination. However, due to the late onset and restricted pattern of their gene expression in the mouse, people have in the past precluded them from a role in neural determination (Pevny et al., 1998). More recently, it has been shown that *Olig2* is necessary for both development of oligodendrocytes and motor neurons (Mizuguchi et al., 2001; Novitch et al., 2001; Lu et al., 2002) but block astrocyte differentiation (Gabay et al., 2003; Setoguchi and Kondo, 2004). *Olig2* was not present in the ES cells population, or before day 8 of differentiation but ~15% of the population expressed the gene at day 18 (*figure* 4.5C and 4.6). The presence of these three markers confirmed that by day 18 the majority of *Sox2* expressing cells were neural progenitors. I then used RT-PCR to investigate which neuronal and CNS lineages were present within the population (*figure* 4.6 and 4.7).

The *Otx* homeobox genes (*Otx1* and *Otx2*) are widely expressed in the developing neurectoderm (Simeone, 1998). *Otx2* is expressed throughout the developing epiblast before becoming restricted to the anterior neuroectoderm, where it is required for development of the forebrain and midbrain. More constrained in its expression, the paralog *Otx1* is expressed in the neurectoderm of the dorsal telencephalon. Interactions between these two genes are thought to specify midbrain and hindbrain development (Acampora and Simeone, 1999). Here *Otx2* was expressed in day 0 ES cells but switched off after the addition of RA to the culture, whereas *Otx1* was present at low levels throughout the differentiation, similar to the findings of Lee et al., (2000). The Pax genes (*Pax2* and *Pax5*) perhaps better known for their roles in mesoderm development (in particular the control of commitment to the B-cell lineage), are also involved in the development of the dopaminergic and serotonergic neurons of the midbrain and hindbrain (Stoykova and Gruss, 1994; Rowitch and McMahon, 1995). Both genes were expressed following the addition of RA to the cultures at day 8, although others reported expression of these genes after 10 days in cultures without RA (Lee et al., 2000). Expression of both *Pax2* and *Pax5* was no longer seen after drug selection to remove non-*Sox2* expressing cells. Similarly, *Hoxb1* a homeobox gene expressed in the hindbrain was expressed on day eight following four days with RA, but

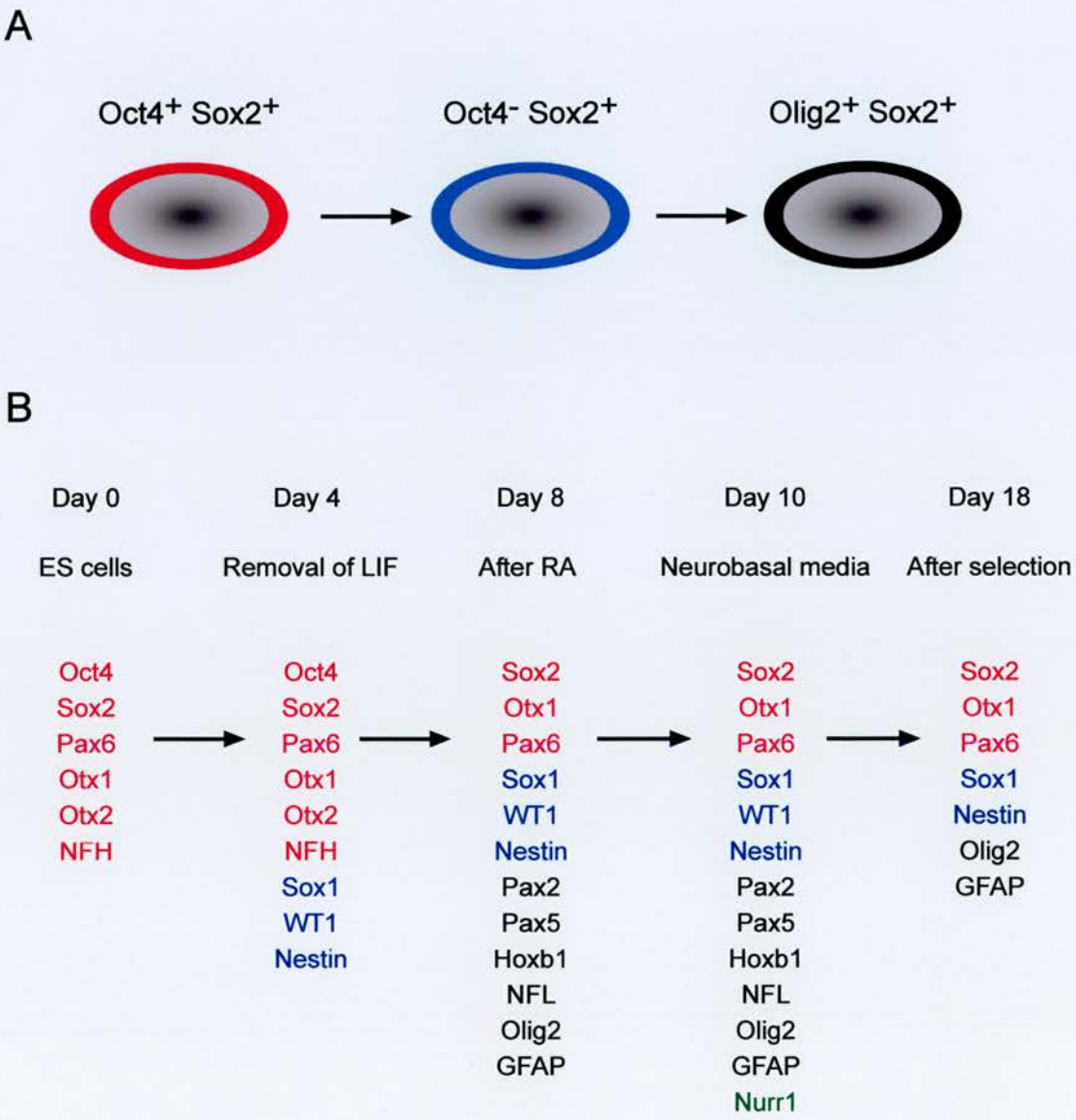

Fig. 4.7 Changes in gene expression observed through OS25 cell differentiation. (A) Proposed pathway for one of the cell types present in the differentiating population. (B) The genes shown are expressed in the mES cell population (red), after the removal of LIF (blue), after the addition of RA (black) or after the media change to Neurobasal media (green).

not in the *Sox2* expressing cells at day 18. However, previous studies using Noggin to inhibit BMP signalling have shown that Hox genes are activated in a RA dependant manor (Okada et al., 2004).

The expression of the Wilms' tumour suppressor gene (*WT1*) has previously been reported during the differentiation of glial cells from EC and ES cells (Scharnhorst et al., 1997; Spraggon personal communication). Here expression of *WT1* was apparent following the removal of LIF and before the expression of *Pax2* in the culture. This is unlike mesoderm differentiation where *Pax2* is thought to be responsible for inducing the expression of *WT1*. The primers for *WT1* give two bands corresponding to the absence or presence of alternative splice variant of exon 5. The 68kD and 200kD neurofilament proteins *NFL* and *NFH* respectively are two of the three neuron-specific proteins, which play a role in regenerating myelinated axons (Rohwedel et al., 1998). *NFL* was present from day 8 as has been described previously by Rohwedel et al., (1998), however expression of *NFH* was observed in the ES cells population and down regulated with the addition of RA which disagrees with the published expression pattern where this form is only expressed towards the end of neuronal differentiation. Finally, I looked at two genes with very specific expression patterns. The glial fibrillary acidic protein (*GFAP*) is a specific marker for astrocytes (Reeves et al., 1989), which was seen to increase in expression towards the end of the differentiation. In contrast, cells expressing nuclear receptor related-1 (*Nurr1*) which is specific for dopaminergic neurons (Rolletschek, 2001; Lee, 2000), were seen briefly when the culture was moved to neurobasal media, but killed by selection for *Sox2* progenitor cells with G418. The housekeeping gene *GAPDH* was used as a cDNA loading control.

4.6 Discussion

I have shown that the differentiation of OS25 cells following drug selection gives a nearly homogenous population of *Sox2* expressing neural precursor cells. However,

GFAP expression would suggest that glial lineages are also present within this population (*figure* 4.7). A number of culture conditions affected the percentage of *Sox2* expressing cells. Changing the substrate that cells were plated onto from poly-L-lysine and laminin to gelatin (*figure* 4.2A-B) had an effect on the cell morphology, which has been described for other mES cell lines during neuronal differentiation (Conti et al., 2005). Increasing the cell density or passage number (*figure* 4.2C-D) reduced the number of *Sox2* expressing cells within the day 18 population. The main difference between this protocol and those used by other labs is in the addition of growth factors.

Previously FGF-2 has been shown to expand cultures with transient retention of neuronal differentiation potential (Li et al., 1998; Okabe et al., 1996). However, continuous culture with FGF-2 restricts this to a glial fate (Brustle et al., 1999), which is also seen in the culture of primary foetal progenitors, and is suggested to resemble the *in vivo* progression during formation of the nervous system (Conti et al., 2005). A similar role in the maintaining a pluripotent state has recently been described for FGF-2 in the culture of hES cells (Xu et al., 2005a). Although the pathway by which this growth factor acts is still unknown, parallels can be drawn between its use in maintaining the potential of both neural stem cells and hES cells. Protocols for the development of terminally differentiated neuronal and oligodendrocyte lineages have shown that cells will only terminally differentiate following the withdrawal of FGF-2 from the culture (Gritti et al., 1995; Okabe et al., 1996). Recently a protocol to maintain the neuronal progenitor cells generated from mES cells in culture, has reported that neuronal stem cells die upon dissociation and passaging in the presence of FGF alone (Conti et al., 2005). It is now known that to maintain the presence of neural precursors in culture indefinitely, both FGF and EGF need to be added to the media.

The use of drug selection during this differentiation, limits the end population to the *Sox2* expressing cells of the neuroepithelium. Although this population was specific for *Sox2*, different cell types were still present within the culture (*figure* 4.2E-H). Using both RT-PCR (*figure* 4.6) and immunofluorescence (*figure* 4.3B), I have shown that

Oct4 was not expressed at day 18 and therefore mES cells were no longer present within the population. Alkaline phosphatase was expressed by the differentiated cells, although to use its full name "tissue non specific alkaline phosphatase" perhaps this was not surprising (*figure* 4.3A). Similarly, SSEA1 was also expressed in the differentiating culture (*figure* 4.3C), however the presence of this antigen in both the developing ectoderm (Fox et al., 1980) and neuronal stem cells (Conti et al., 2005) would suggest that this is not only a marker associated with pluripotent mES cells, but also the self-renewing cells of the developing ectoderm. Likewise, in human cells although SSEA1 is not expressed by the pluripotent hES cells, it is expressed by their differentiated derivatives, notably putative ectoderm (Henderson et al., 2002).

I have shown that markers of mesoderm and endoderm were not present in the culture at day 18 (*figure* 4.4B). This was in part due to the addition of RA, known promote neural differentiation but also to suppress mesodermal gene expression (Bain et al., 1996). Different concentrations of RA produce different neuronal cell types. Here the 10^{-6} M used is indicative of hindbrain and spinal cord development as opposed to forebrain or midbrain development (Okada et al., 2004), which was confirmed by both immunofluorescence and RT-PCR analysis.

In the mES cells population, the early CNS genes *Otx1* and *Otx2* were expressed alongside the transcription factors *Oct4*, *Sox2*, *Pax6* and the neurofilament protein *NFH*, which is not normally expressed until toward the end of differentiation (*figure* 4.6, Rohwedel et al., 1998). Following the removal of LIF none of the genes detected so far were silenced, but three more genes, *Sox1*, *WT1* and *Nestin* were expressed. I have shown by immunofluorescence (*figure* 4.5B) that a few *Sox1* positive cells are present in the day 0 population, although *Sox1* was predominantly expressed at day 18. In the developing chick spinal cord, Sox genes inhibit neuronal differentiation (Bylund et al., 2003); until genes such as *Neurogenin-2* are expressed, which promote differentiation by suppressing Sox gene expression. After the addition of RA to the culture for four days, *Oct4*, *Otx2* and *NFH* expression was no longer detected in the culture. However, the

mesencephalic genes *Pax2* and *Pax5* together with *Hoxb1*, the neuron specific protein *NFL*, the astrocyte marker *GFAP* and the transcription factor *Olig2* were now expressed. *Olig2* is regulated by the expression of *Pax6* and *Nkx6* (Novitch et al., 2001 and 2003), which coincides with the RT-PCR analysis as *Pax6* increased in expression towards day 8 when *Olig2* was first expressed in the culture (*figures* 4.4 and 4.6).

A change to neurobasal media brought with it expression of the midbrain dopaminergic neuron specific marker *Nurr1*. However, following seven days in drug selection only seven of the genes detected here were still expressed, the neuroepithelial genes, *Sox1* and *Sox2*, the markers of neural progenitors *Pax6*, *Nestin*, *Olig2*, the astrocyte specific marker *GFAP* and low levels of the early CNS marker *Otx1*. Upon terminal differentiation, *Nestin* would be downregulated and replaced by expression of neurofilament proteins (Dahlstrand et al., 1992), but while the Sox genes are expressed, the cells will not undergo terminal differentiation. For this reason in day 18 cultures, *Nestin* was still present and genes active later in differentiation such as *NFH* and *Otx2* were not expressed, unlike protocols without drug selection (Rohwedel et al., 1998; Lee et al., 2000). In comparison to protocols that use either the OS25 cells or their parental clonal line, which only has *Sox2* under selection, a similar percentage of the cells were found to be positive for *Sox1* or *Nestin* at the end of the differentiation (Li et al., 1998; Billon et al., 2002; Perry et al., 2004).

Drug selection for *Sox2* allowed a population of neural progenitors to be isolated, but due to the absence of EGF in the media these cells were not able to proliferate and as markers of more terminal differentiation repressed the *Sox2* gene, the cells died and the population size was greatly reduced. This differentiation could be improved by the addition of EGF alongside FGF-2 to allow for the expansion of the self-renewing neural precursors (Conti et al., 2005). Further refining the specificity of the end population could be achieved, if this protocol was applied to one of the cell lines where *Sox1* or *Olig2* are under selection (Ying et al., 2003; Xian et al., 2003; Gabay et al., 2003). This

would define a more specific population, although it would also decrease the cell number making biochemical analysis difficult.

The cells produced by the differentiation protocol described here are used in the next chapter, to investigate aspects of nuclear architecture previously shown for human cells in chapter 3, this time following the differences in spatial organisation down defined early neural lineages.

Chapter 5: Nuclear Reorganisation of Mouse ES Cells and ES Cell-Derived Neural Precursors

Chapter 5

Nuclear Reorganisation of Mouse ES Cells and Mouse ES Cell-Derived Neural Precursors

5.1 Introduction

Organisation of the mouse genome into chromosomes differs from that in humans and many other mammals. Differences in chromosome size and gene density are smaller between mouse chromosomes than between human chromosomes. Disregarding the Y-chromosome, the size of human chromosomes vary about fivefold (47-246 Mbp) whereas the size of mouse chromosomes only differs about threefold (61-195 Mbp). Gene density also varies about sixfold (3.9-23.3 gene/Mbp) between human chromosomes, whereas mouse chromosomes vary approximately twofold (7.4-15.6 gene/Mbp) based on NCBI mouse build 34, May 2005 and human build 35, June 2004. The position of centromeres is also different between mouse and human genomes. In humans, centromeres are mainly located toward the centre of the chromosome (metacentric), although some are located nearer to one end of the chromosome (acrocentric), whereas in mouse, centromeres are located towards the telomeres (telocentric).

Previous studies have described the spatial arrangement of the mouse genome within the nucleus of many cell types, including during ectoderm development, using neurons and oligodendrocytes (Manuelidis 1985; Martou and De Boni 2000; Nielsen et al., 2002). These studies show changes in nuclear organisation as cells undergo terminal differentiation. However, when I started this work, there was no published research on the reorganisation of the genome in mES cells as they acquire a particular cell fate.

Therefore, in this chapter I have used mES cells, differentiated towards a neuroepithelial lineage using the protocol that I described in chapter 4, to analyse the changes in nuclear organisation that occur early in differentiation. Briefly, this enables *Oct4*$^{+}$, *Sox2*$^{+}$ mES cells to be compared with an *Oct4*$^{-}$, *Sox2*$^{+}$ cell population the majority of which expressed the markers of neural precursors *Sox1* and *Nestin* at day 18.

5.2 Distribution of chromosome territories changes during the differentiation of mES cells

I started investigating the nuclear organisation of mES cells by 2D FISH with biotin labelled chromosome paints for *Mus musculus* chromosome (MMU) 3, 6, 16 and 17 (*figure* 5.1A and B). MMU6 and 17 contain the pluripotency genes *Nanog* and *Oct4* respectively, whereas MMU3 and 16 contain the genes *Nestin* and *Olig2*, which are important in neural progenitors (*figure* 5.2). I compared the distributions of these four CTs in 3:1 methanol:acetic acid fixed nuclei from undifferentiated mES cells, with their distributions in cell nuclei fixed after 18 days of differentiation towards an ectodermal lineage (chapter 4). Fifty images of nuclei, taken at each time point were analysed through a 2D erosion script, described previously (section 3.2, and *figure* 5.1C). In the differentiated population both MMU17 and 3 were more centrally localised in comparison to their distributions in mES cells (shell 5; $p=0.005$ and $p=0.033$, respectively). Whilst MMU6 did not move into the centre of the nucleus, but moved significantly away from the nuclear periphery during the differentiation (shell 1; $p=<0.001$) the distribution of MMU16 significantly increased at the nuclear periphery (shell 1; $p=0.003$). There is no previous study of CT arrangement during the differentiation of mES cells, although recently two papers from the Misteli Lab have reported similar findings for more terminally differentiated cells. The first analysed CTs in mouse primary tissue and concluded that the distribution of CTs was tissue-specific (Parada et al., 2004). The second followed the position of MMU6 during T-cell differentiation and described a similar distribution for MMU6 in T-cell precursors as I

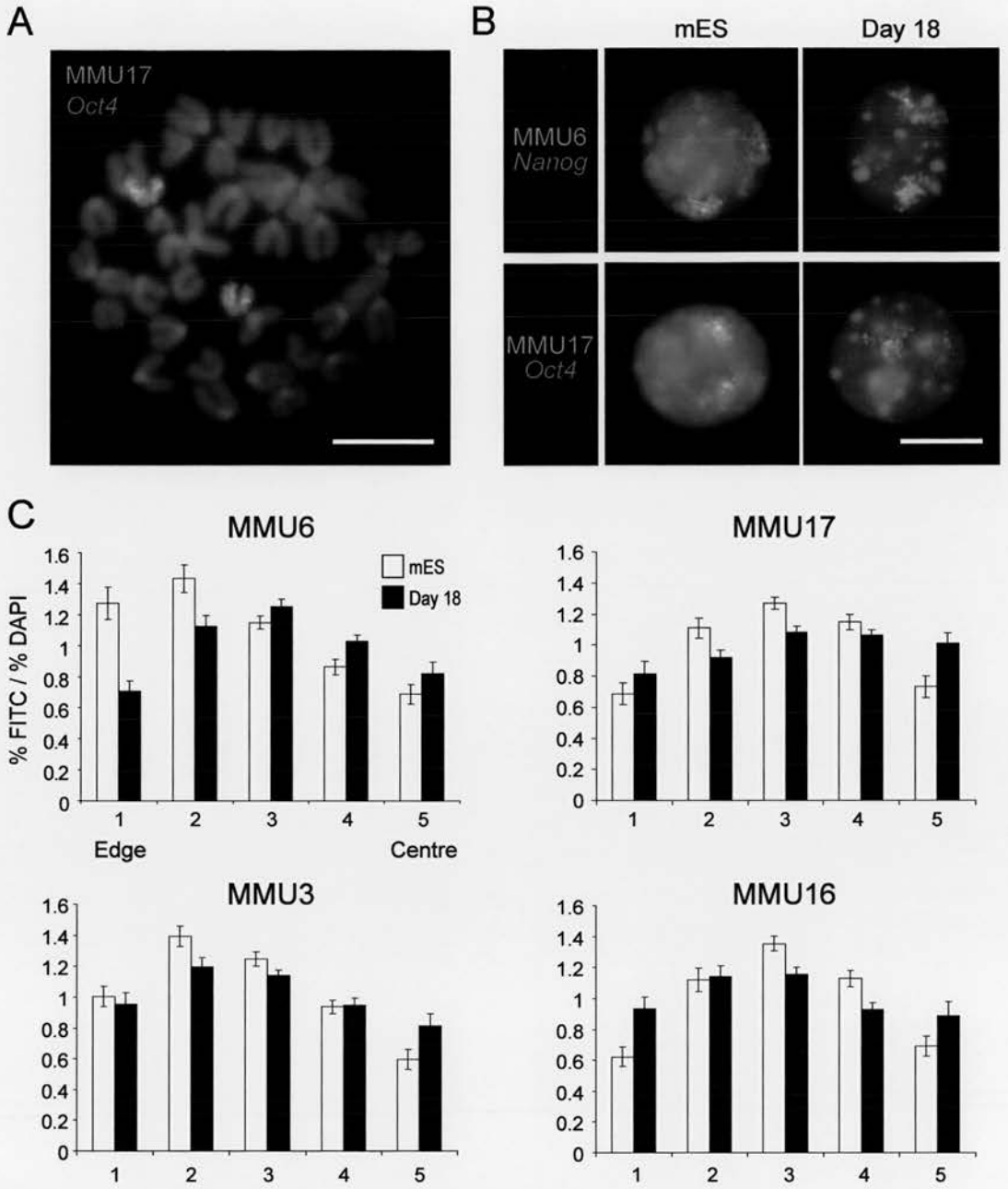

Fig. 5.1 The distribution of MMU3, 6, 16 and 17 territories in mES and differentiated day 18 cells. (A) 2D FISH with a BAC probe containing *Oct4* (red) and a MMU17 paint (green) on a metaphase spread, DNA counterstained with DAPI (blue). (B) mES or differentiated day 18 nuclei hybridised with BAC probes containing either *Nanog* or *Oct4* (red) and chromosome paints for 6 and 17 (green), counterstained with DAPI (blue). (C) Distribution of chromosome paint hybridisation signals within the nucleus of mES (white) and day 18 differentiated cells (black) analysed by erosion of 2D images into five concentric shells from the edge (1) to the centre (5) of the nucleus. The mean (±s.e.m) proportion of hybridisation signal, normalised to the amount of DAPI signal, is shown for each shell (n=50). Scale bar, 10μm.

A

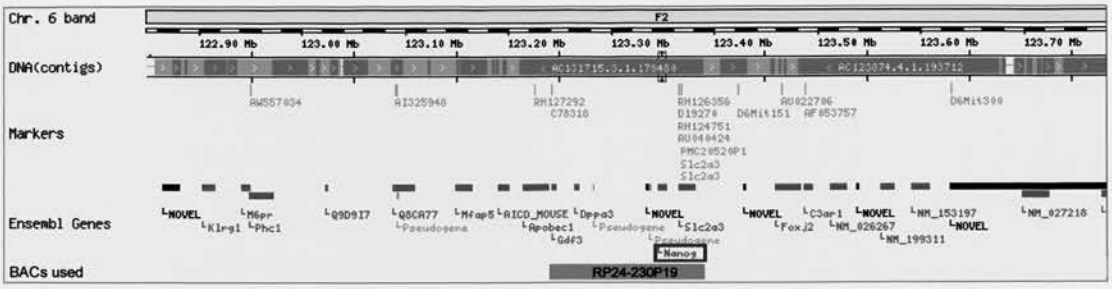

B

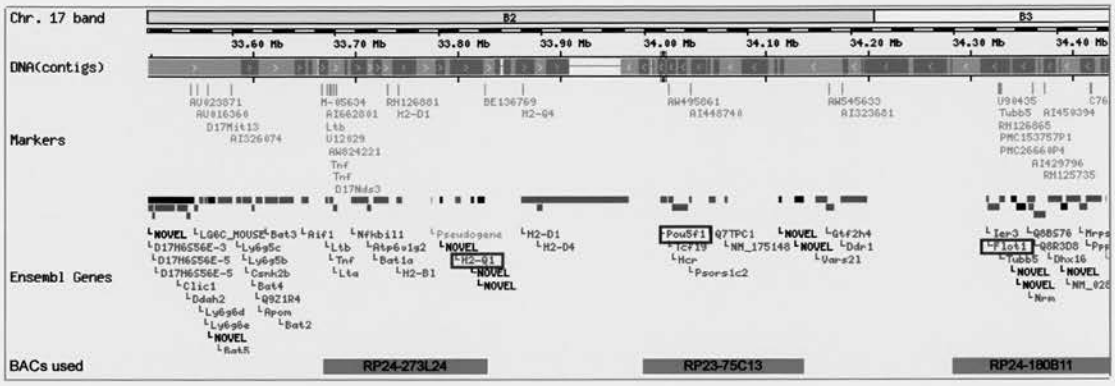

C

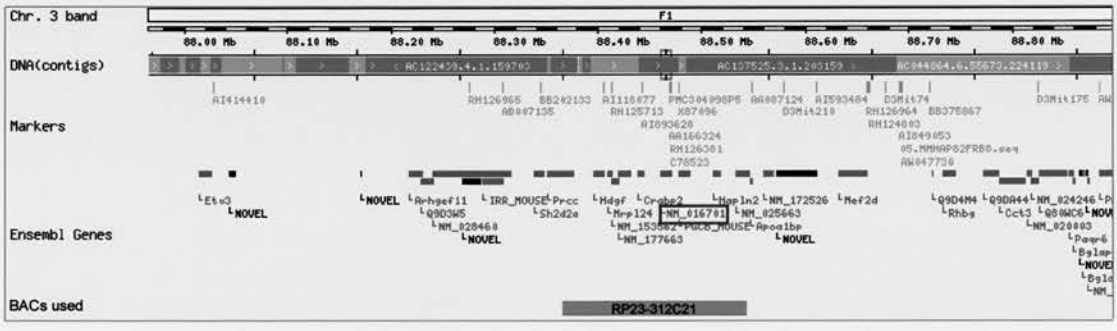

D

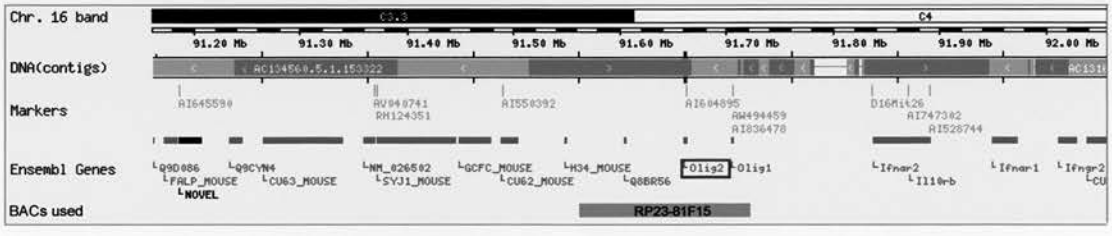

Fig. 5.2 The genomic regions surrounding *Nanog*, *Oct4*, *Nestin* and *Olig2* in the mouse. Green boxes show the positions of (A) *Nanog* on MMU6, (B) *H2-Q1*, *Oct4* (Pou5f1) and *Flot1* on MMU17, (C) *Nestin* (NM_016701) on MMU3 and (D) *Olig2* on MMU16. Red boxes show the positions of the BACs used. Images adapted from ensembl v31, May 2005.

have shown for the day 18 population of neural precursors (Kim et al., 2004). However, Kim et al., (2004) also showed that the distribution of MMU6 changes again as the T-cell precursors undergo terminal differentiation.

In a study of CT arrangement in mouse cells, Mayer et al., (2005) suggested that the position of CTs in mES cells correlated equally with chromosome size and gene density. I have previously shown that radial organisation of CTs in hES cells is dependant on gene density (section 3.2). To investigate whether this was true of mouse CTs, I divided the proportion of signal/DAPI in the first shell of the erosion script by the proportion of signal/DAPI in the fifth shell of the erosion script (*table* 5.1).

MMU	Size (Mbp)	Gene Density	Genes/Mbp	mES (shell 1/shell 5)	Day 18 (shell 1/shell 5)
3	159	1311	8.25	1.69	1.17
16	97	838	8.64	0.90	1.05
6	150	1454	9.69	1.85	0.86
17	93	1227	13.19	0.94	0.81

Table 5.1 Nuclear position of MMU in mES and differentiated cells. Chromosome size and gene density (from NCBI build 34, http://www.ensemble.org/Mus_Musculus) and the proportion of hybridisation signal in shell 1 divided by the proportion in shell 5 for the MMU used.

If the chromosomes had a radial distribution arranged according to gene density, they would be arranged 3, 16, 6 and 17 from the nuclear periphery to the centre of the nucleus. This distribution was observed in the differentiated day 18 cell population, but not in the mES cell nuclei. In the undifferentiated cells, the distribution has some similarity to chromosome size. Mayer et al., (2005) have suggested that MMU16 and 17

should not be included in the radial analysis, because they may contain nucleolar organising regions that are tethered to the nucleoli and thus spatial distribution of these CTs would be biased. However, since these CTs would be under the same constraints in both cell populations, I assume the fact that they may be tethered to another body such as the nucleolus, only increases the significance of this spatial reorganisation. I therefore conclude that the distribution of CTs in mouse nuclei changed during differentiation of mES cells towards ectodermal lineages, and that a radial organisation according to gene density was acquired during the differentiation.

5.3 The position of genes within the interphase nucleus changes as mES cells differentiate

If CT position changes during the differentiation of mES cells, then the radial position of specific gene loci on these chromosomes may also change to follow that of their host chromosome. This is of particular interest since several genes have been reported to relocalise away from the nuclear periphery when activated (Zink et al., 2004; Williams et al., 2006). I investigated the position of *Oct4*, *Nanog*, *Nestin* and *Olig2* within the nuclei of mES cells and cells differentiated for 18 days, by 2D FISH with dig labelled BACs for each gene. I used the 2D erosion script to segment the nuclei and manually counted the number of BAC signals in each shell (*figure* 5.3A). Consistent with the CT result for MMU17, *Oct4* was more centrally located in the nuclei of differentiated cells when compared with mES cells, which express the gene (*figure* 5.3B; *table* 5.2). The genes surrounding *Oct4* in the MHC complex may be influencing this unexpected nuclear relocalisation of *Oct4*. Unlike hES cells, mES do not express the MHC class 1 genes (Tian et al., 1997), but as the cells differentiate these genes are switched on and have previously been shown to loop out of the HSA6 territory in differentiated cells (Volpi et al., 2000). The position of *Nanog* also followed its MMU6 CT and moved away from the nuclear periphery in differentiated cells, which do not express the gene. However, unlike *Oct4* the genes surrounding *Nanog* are not active in the differentiated

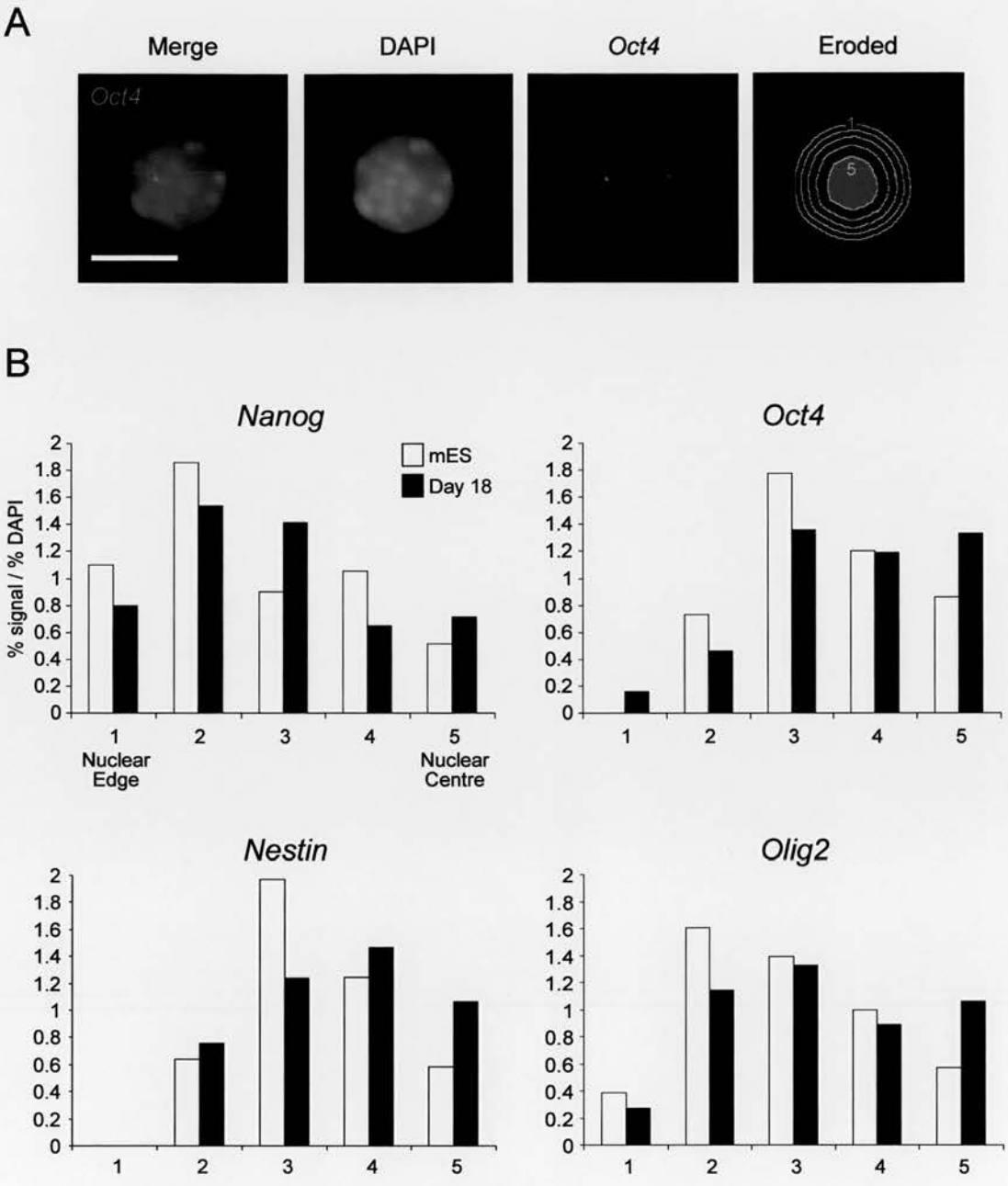

Fig. 5.3 The position of pluripotent and neural genes in mouse nuclei. (A) 2D FISH with a BAC probe containing *Oct4* (red) on a mES cell nucleus, counterstained with DAPI (blue). The last image shows the nucleus divided into five shells of equal area by the erosion script. (B) Distribution of signals from *Nanog*, *Oct4*, *Nestin* and *Olig2* containing BACs within the nucleus of mES and differentiated day 18 cells, by erosion of 2D images into five shells of equal area. The number of probe signals in each shell was counted and the proportion of probe normalised to the amount of DAPI signal, is shown for each shell (n=50). Scale bar, 10μm.

population (Clark et al., 2004). For the genes activated during differentiation, *Nestin* on MMU3 moved with its CT towards a more central nuclear position in the differentiated cell population, whereas *Olig2* on MMU16 was the only gene not to follow the distribution pattern of its host CT. There, as the distribution of the CT significantly increased at the nuclear periphery, the proportion of the *Olig2* signal increased in the centre of the nucleus. This predicts that there should be a re-localisation of *Olig2* relative to its CT during the differentiation of mES cells (see section 5.4).

Gene	Cell type	Gene expression	Radial gene position	Radial CT position
Oct4	mES cells	Yes	Equidistant	Equidistant
	Mouse differentiated cells	No	Towards centre	Towards centre
Nanog	mES cells	Yes	Towards periphery	Towards periphery
	Mouse differentiated cells	No	Towards periphery	Equidistant
Nestin	mES cells	No	Equidistant	Towards periphery
	Mouse differentiated cells	Yes	Towards centre	Towards centre
Olig2	mES cells	No	Towards periphery	Equidistant
	Mouse differentiated cells	Yes	Towards centre	Towards periphery

Table 5.2 The radial position of four loci in pluripotent and differentiated cells. The radial position of the four genes and their respective CTs analysed in mES and differentiated day 18 cells.

These results disagree with the findings of Zink et al., (2004) who showed that the position of genes within human nuclei varied among cell types in a transcription dependent manner, as only two of the genes analysed here moved in the predicted direction. Williams et al., (2006) recently described the relocation of the neuronal gene

Mash1 away from the nuclear periphery, during the differentiation of mES towards a neuronal lineage. They showed that this movement only occurs in cell types that express the gene. I conclude that the radial position of some genes within the nucleus change during differentiation, in a transcription dependent manner. This is dependent not only on the activity of the gene in question, but also on the expression patterns of adjacent genes as seen for *Oct4*. The results suggest that the repression of the pluripotent genes, *Oct4* and *Nanog*, occurs by a mechanism independent of nuclear organisation.

5.4 The position of genes relative to their CTs change during mES cell differentiation

In mouse, *Hox* genes induced upon the differentiation of ES cells with RA have also been shown to relocate towards the nuclear interior (Chambeyron and Bickmore, 2004). Although in this case, the movement did not accompany changes in the position of their host CT, rather the relocation of the genes outside their CT (Bickmore et al., 2004). Therefore, I analysed the nuclear position of *Oct4*, *Nanog*, *Nestin* and *Olig2* relative to their CTs in mES cells and cells differentiated towards an ectodermal lineage. BACs containing the genes labelled with dig-dUTP and the corresponding commercial chromosome paints for MMU17, 6, 3 and 16 labelled with biotin, were hybridised to 3:1 methanol:acetic acid fixed mES and differentiated cell nuclei. Unlike hES cells (section 3.4) where NANOG remained in the HSA12p CT but the whole CT moved, *Nanog* was found significantly closer to the edge of its CT in mES cells than in differentiated cells, where the gene is not expressed ($p=0.016$, *figure* 5.4A; *table* 5.3). The other pluripotent gene analysed, *Oct4*, was seen to move significantly nearer to the edge of its CT in the differentiated cell population, which do not express the gene than in undifferentiated cells ($p=<0.001$, *figure* 5.4B and C). However, as described above, the genes surrounding *Oct4* in the MHC class 1 region are not active in mES cells (Tian et al., 1997) and switch on during the differentiation. I conclude that this region moving out of its CT is likely to be due to the activation of class I genes. However, when I compared

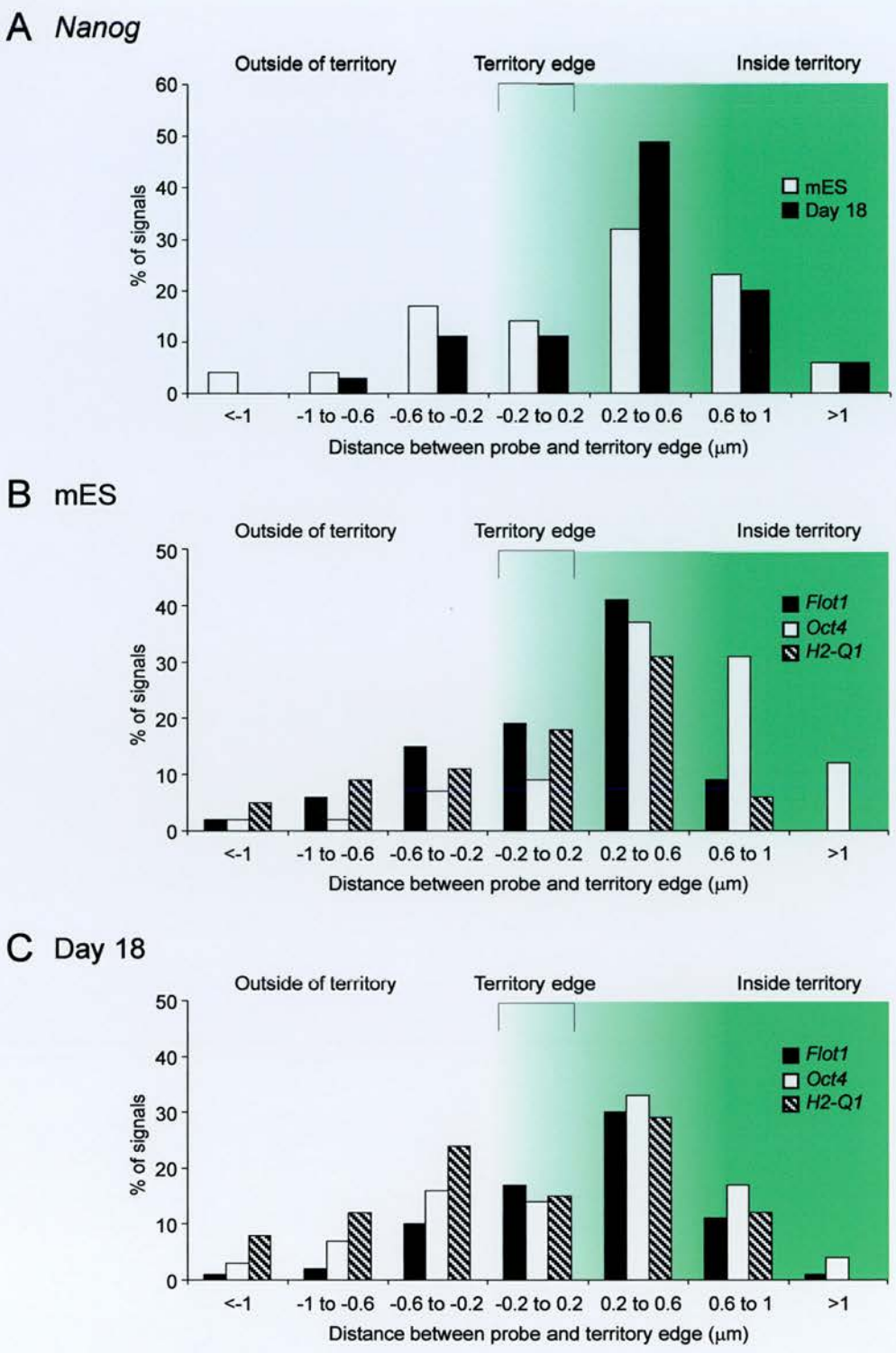

Fig. 5.4 Intrachromosome territory organisation of *Nanog* and *Oct4* in mouse nuclei. (A) Distribution of a BAC containing *Nanog* relative to the MMU6 CT, in nuclei from mES and differentiated day 18 cells. Negative distances indicate localisation outside of the CT (n=100). Distribution of *Oct4* and two flanking loci on MMU17 in the nuclei of (B) mES and (C) differentiated day 18 cells. Negative distances indicate localisation outside of the CT (n=100).

the distributions of two alleles either side of *Oct4*, (*Flot1* on the class 1 side and *H2-Q1* on the centromeric side nearest the class III genes), in mES and differentiated cell populations, neither of these genes significantly changed their positions relative to the MMU17 CT (*H2-Q1* p=0.318; *Flot1* p=0.074). This result was unexpected, but might be explained by the bi-modal distribution of *H2-Q1* in the day 18 population, which is not reflected by the statistics. Further analysis of the genes flanking *Oct4* is needed to determine whether the class III genes are responsible for the movement of the *Oct4* locus.

Locus	Cytogenetic position	Genomic position (Mb)	Probe name	Position relative to CT edge	
				mES (μm)	Day 18 (μm)
Nanog	6.F2	123.3	RP24-230P19	0.17±0.07	0.38±0.06
H2-Q1	17.B2	33.8	RP24-273L24	-0.03±0.06	-0.12±0.06
Oct4	17.B2	34.0	RP23-75C13	0.44±0.05	0.13±0.06
Flot1	17.B3	34.3	RP24-180B11	0.09±0.05	0.22±0.05
Nestin	3.F1	88.4	RP23-312C21	0.15±0.10	0.12±0.07
Olig2	16.C4	91.6	RP23-81F15	0.40±0.04	0.20±0.07

Table 5.3 Intra-CT position of loci in mES and differentiated day 18 cells. Cytogenetic and genomic positions (from NCBI build 35, http://www.ensembl.org/Mus_musculus) of each locus, together with the name of the BAC used in FISH. Mean (±s.e.m.) position, in μm, of loci relative to the edge of the CTs in mES and differentiated day 18 cell nuclei. Negative values indicate the positions outside the visible limits of the CT.

I then investigated CT organisation of the two loci activated in neural precursor cells, *Nestin* and *Olig2* (*figure* 5.5). *Nestin* which is expressed by 90% of the differentiated population (*figure* 4.5A; section 4.3), does not significantly change its position relative to the MMU3 CT during differentiation (p=0.813, *figure* 5.5C). A high proportion of

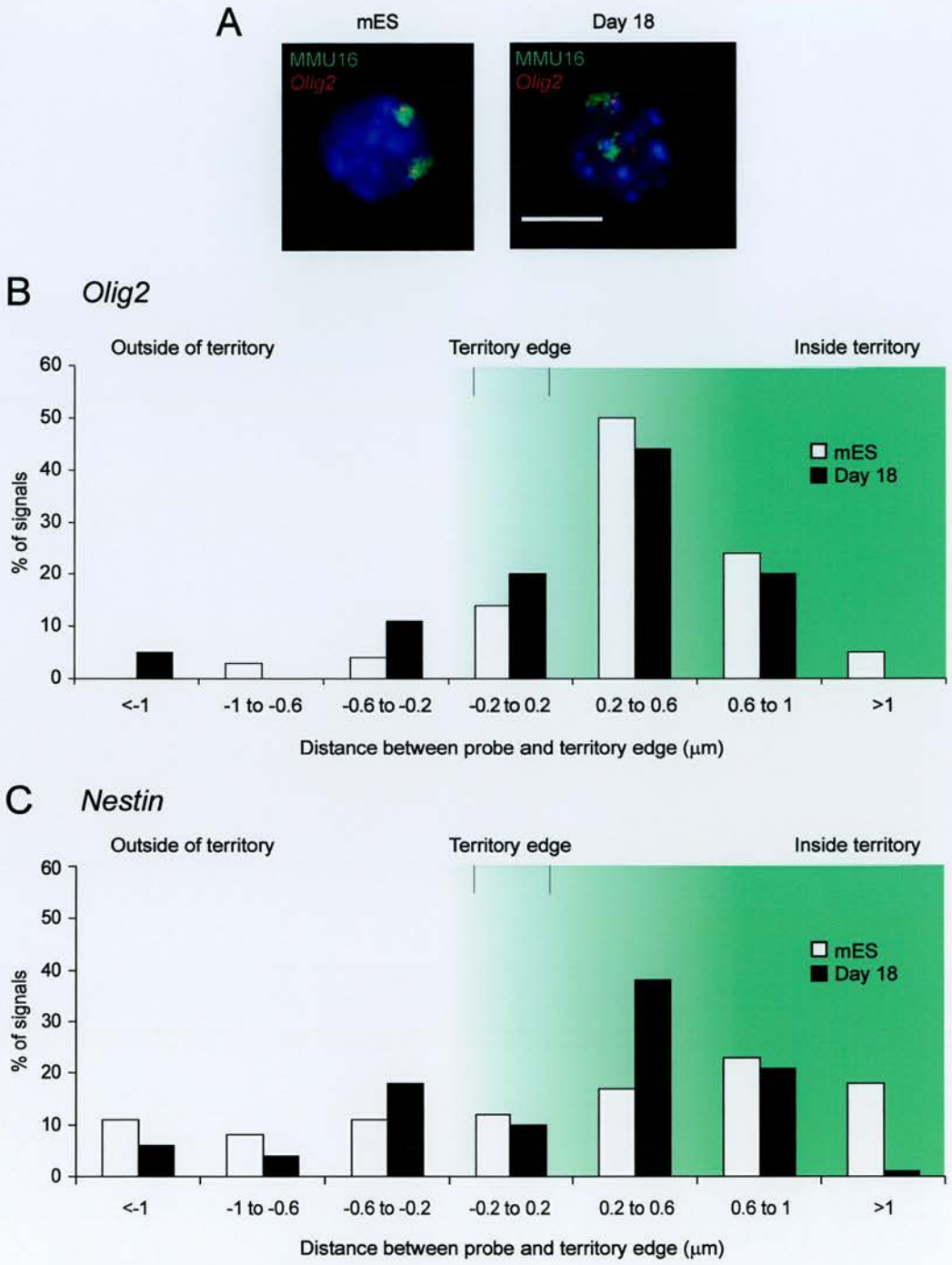

Fig. 5.5 Intrachromosome territory organisation of *Olig2* and *Nestin* in mouse nuclei. (A) Hybridisation of a BAC probe containing *Olig2* (red), and MMU16 paint (green), within the nuclei of mES and day 18 differentiated cells counterstained with DAPI (blue). Histograms of the distribution of FISH signals from BACs containing (B) *Olig2* and (C) *Nestin*, relative to the edge of MMU16 and 3 CTs respectively, in the nuclei of mES cells (white) and day 18 differentiated cells (black). Negative distances indicates localisation outside the visible limits of the CT (n=100). Scale bar, 10μm.

Nestin loci are found outside of the CT even in the mES cell population where the gene is not expressed. As *Nestin* is expressed within the first 24 hours of mES cell differentiation (Meshorer et al., 2006), this gene might have moved out of its CT prior to expression. Alternatively, out of the four genes analysed here, it is noteworthy that *Nestin* is embedded in a local region of high gene density. Therefore, it is possible that its immediate surroundings are dictating the genes position relative to its CT. Expression of *Olig2* was not detected in mES cells by either RT-PCR or immunofluorescence, however ~15% of the differentiated population expressed the gene, as determined by immunofluorescence for the Olig2 protein (*figure* 4.5C; section 4.3). The position of *Olig2* changed significantly relative to its CT during the differentiation (p=0.013). This is due to an increase in the percentage of loci found well (>0.2μm) outside the CT, from 7% in mES cells to 16% in differentiated cells and a reduction in the number of loci found deep within the CT (>0.6μm) from 29% in mES cells to 20% in differentiated cells. This change in position likely reflects the increased proportion of *Olig2* expressing cells in the differentiated population.

5.5 Chromatin decondensation of the *Oct4* region in mouse

The movement of loci relative to the surface of CTs is generally accompanied by cytologically detectable changes in chromatin condensation (Chambeyron and Bickmore, 2004). To investigate this further I carried out FISH with *Oct4* and two flanking BAC clones, containing *Flot1* and *H2-Q1*, in mES and differentiated cells (*figure* 5.6A). The interphase distance (*d*) was measured between *Oct4* and *Flot1* or *H2-Q1* BACs (*figure* 5.6B). The distribution of these distances, always conformed to that expected from the random walk model of chromatin structure (s.d. = 0.52-0.6; median/mean ~1.0) (Sachs et al., 1995; Chambeyron and Bickmore, 2004). The mean-squared interphase distance ($<d^2>$) between *Oct4* and *Flot1* (genomic distance, 120kb) was not significantly different between mES cells and the differentiated population ($<d^2>$=0.36±0.03 and 0.42±0.05 μm^2 respectively, p=0.861). However, there was a

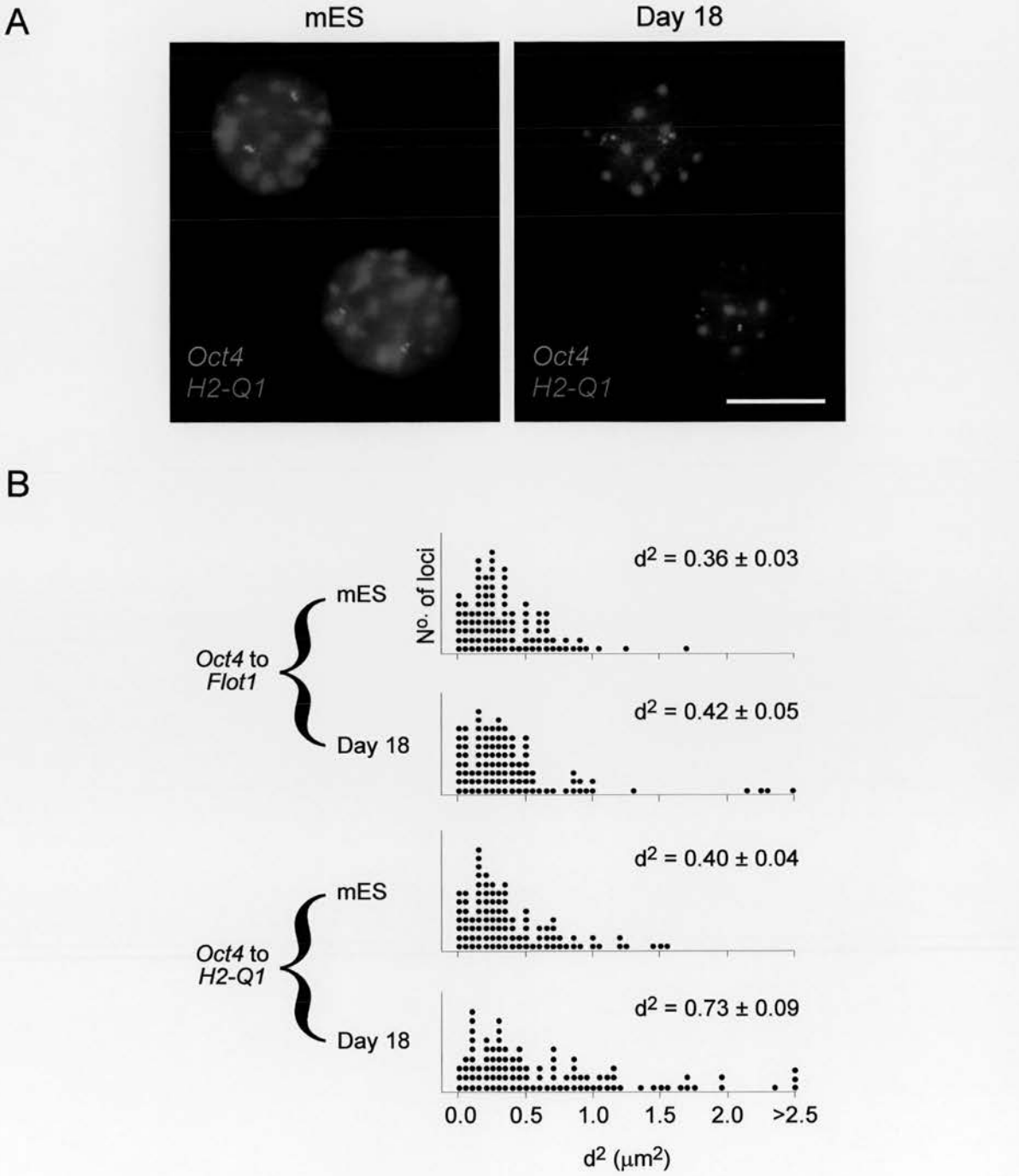

Fig. 5.6 Chromatin decondensation of the *Oct4* region in mES and differentiated cells. (A) 2D FISH with BAC probes containing *Oct4* (green) and *H2-Q1* (red), within the nuclei of mES and differentiated day 18 cells, counterstained with DAPI (blue). (B) The distribution of squared interphase distances (d^2) in μm^2 measured between probes for *Oct4* and *Flot1* or *H2-Q1*, in the nuclei of mES and differentiated day 18 cells (*n*=100). Numbers show the mean d^2 value (±s.e.m). Scale bar, 10μm.

significant increase between *Oct4* and *H2-Q1* (genomic distance, 140kb) in the differentiated population when compared to the mES cells ($<d^2>$=0.73±0.09 and 0.40±0.04 μm^2 respectively, p=0.002). Therefore, there is decondensation upon differentiation, but not as I had expected because the distance between *H2-Q1* and *Oct4* is greater than between *Oct4* and *Flot1*. This probably reflects high-level expression of the class III genes. The large d^2 values measured around *Oct4* in both cell populations are consistent with the presence of an open chromatin fibre (Gilbert et al., 2004). In conclusion, not only does *Oct4* change its location within the nucleus during differentiation, but as previously shown for hES cells (section 3.4) there are differences in the condensation of the chromatin fibre between mES and differentiated cells.

5.6 Gene association with centromeric heterochromatin

The position of genes relative to centromeric heterochromatin in somatic cells has been associated with gene silencing (Brown et al., 1997). To determine whether pluripotent genes associate with centromeric heterochromatin when they are repressed during differentiation, I carried out 2D FISH on mES and differentiated day 18 cells with dig-dUTP labelled BACs containing the genes *Oct4* or *Nanog* (*figure* 5.7A). I then counted the percentage of nuclei where both, one or neither of the gene loci associated with the bright heterochromatic foci in the DAPI stained nuclei. For both genes, the percentage of loci found to associate with the heterochromatic foci was similar in mES and differentiated cells (*figure* 5.7B). I therefore concluded that the association of these two genes with centromeric heterochromatin was not responsible for their silencing in mES cell differentiation. This is in agreement with recent data for the neuronal gene, *Mash1*, during mES cell differentiation, which also showed that gene repression was not due to association with heterochromatin (Williams et al., 2006).

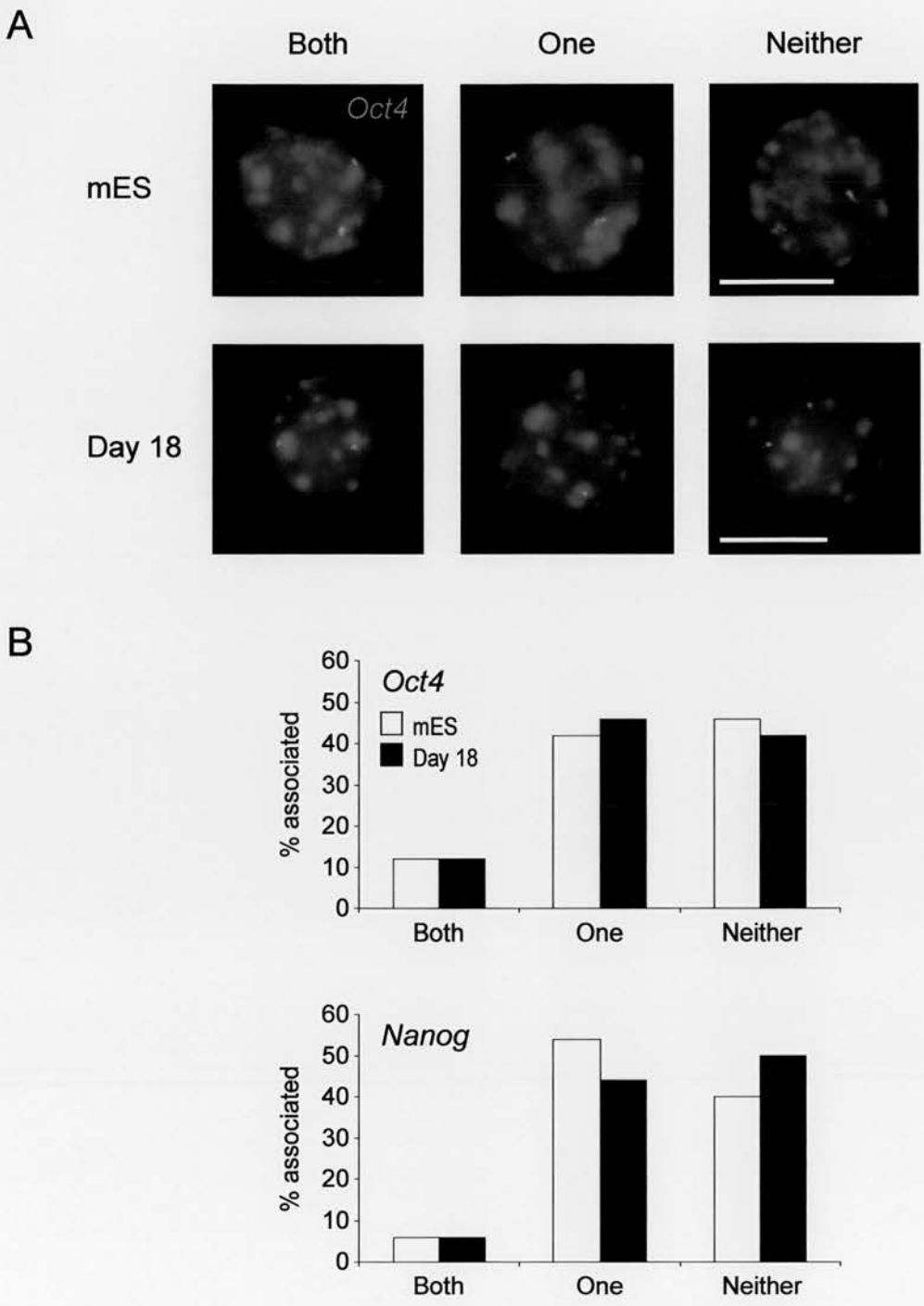

Fig. 5.7 The percentage of *Oct4* loci associated with heterochromatic foci in the DAPI. (A) 2D FISH with a BAC containing the gene *Oct4* (green) on OS25 mES and differentiated day 18 cells, nuclei counterstained with DAPI (blue). (B) The percentage of nuclei in mES (white bars) or differentiated day 18 cells (black bars) that have both BAC signals associated with DAPI foci (Both), only one of the signals associated (One), or neither of the signals associated (Neither) for BACs containing either *Oct4* or *Nanog* genes (*n*=50). Scale bar, 10μm.

5.7 Histone modifications in mES cells

During differentiation, the mouse genome is progressively silenced as cell fate becomes more restricted, as is evident from microarray data (Ramalho-Santos et al., 2002; Sato et al., 2003). This is accompanied by the acquisition of histone modifications associated with gene activation and gene silencing (reviewed in section 1.2.1). To investigate changes in the global levels of histone modifications between mES and differentiated day 19 cells, I carried out western blots on protein extracts from both populations (*figure* 5.8). These were quantified using Advanced Image Data Analyser (AIDA) software to measure the intensity of the bands, expressed as the Quantum Level per mm^2 (QL/mm^2), relative to a GAPDH loading control. Whereas the level of H3-K9me_2, a marker of gene silencing, increased during the differentiation the levels of H3-K9ac and H3-K4me_2, which are associated with gene expression, decreased in agreement with the progressive silencing of the genome during differentiation. This result was confirmed by previous analysis during the differentiation of both mES cells following LIF withdrawal (Lee et al., 2004) and adult neural stem cells induced to differentiate towards neurons, oligodendrocytes or astrocytes (Hsieh et al., 2004).

The distribution of these histone modifications within the nuclei of mES and differentiated cells was then analysed by immunofluorescence. H3-K4me_2 was visualised throughout the interphase nuclei of mES cells, differentiated cell populations and on metaphase chromosomes (*figure* 5.9). However, the histone modification was not present on blocks of heterochromatin, or at the nuclear periphery in the differentiated population. This corresponds with the distribution of H3-K4me_2 throughout the genome, as the vast majority of sites show a punctate pattern, typically occurring at sites of ~1-2kb from the promoters of active genes and regulatory elements (Roh et al., 2004; Bernstein et al., 2005). Similar to H3-K4me_2, H3-K9ac staining was apparent throughout the nuclear interior in both mES and differentiated cells, however the nuclear rim was devoid of staining in the day 19 population and this modification was not detected on metaphase chromosomes (*figure* 5.10A and B). It is likely that H3-K9ac is present on

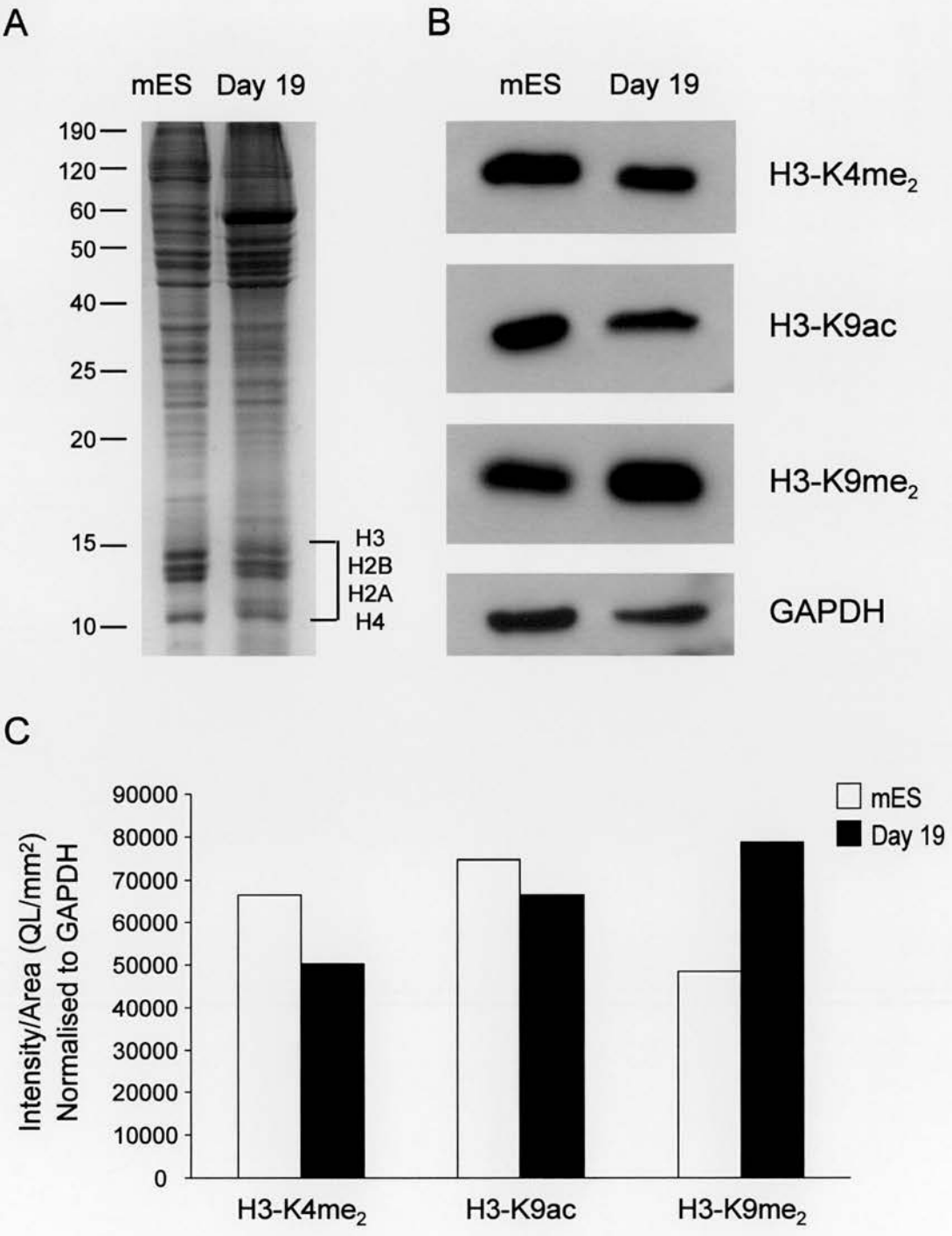

Fig. 5.8 Changes in the levels of histone modifications between mES and differentiated day 19 cells. (A) Total protein extracts harvested from mES and differentiated day 19 cells stained with coomassie blue as a protein loading control. (B) Western blots for the histone modifications H3-K4me$_2$, H3-K9ac and H3-K9me$_2$, with the housekeeping protein GAPDH used as a loading control. (C) Quantification of the western blots using AIDA software to measure the intensity (quantum level, QL) / area (mm^2) normalised to GAPDH.

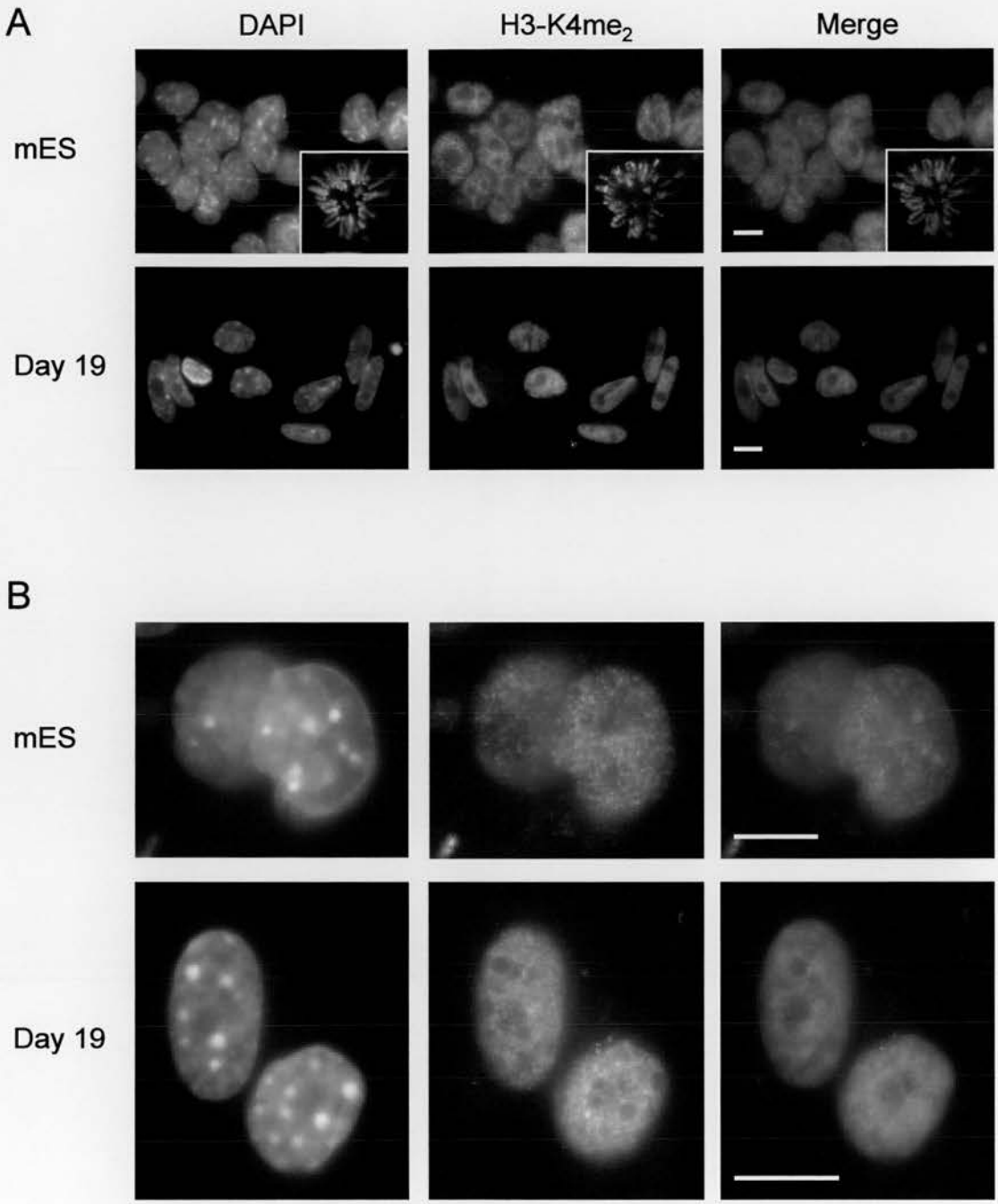

Fig. 5.9 Immunofluorescence for H3-K4me$_2$ in mES and differentiated cells. (A) mES and differentiated day 19 nuclei stained with an antibody for H3-K4me$_2$ detected using FITC (green), counterstained with DAPI (blue). Inserts show H3-K4me$_2$ on metaphase chromosomes. (B) Enlarged view of the staining pattern, showing absence of H3-K4me$_2$ at heterochromatin. Scale bars, 10μm.

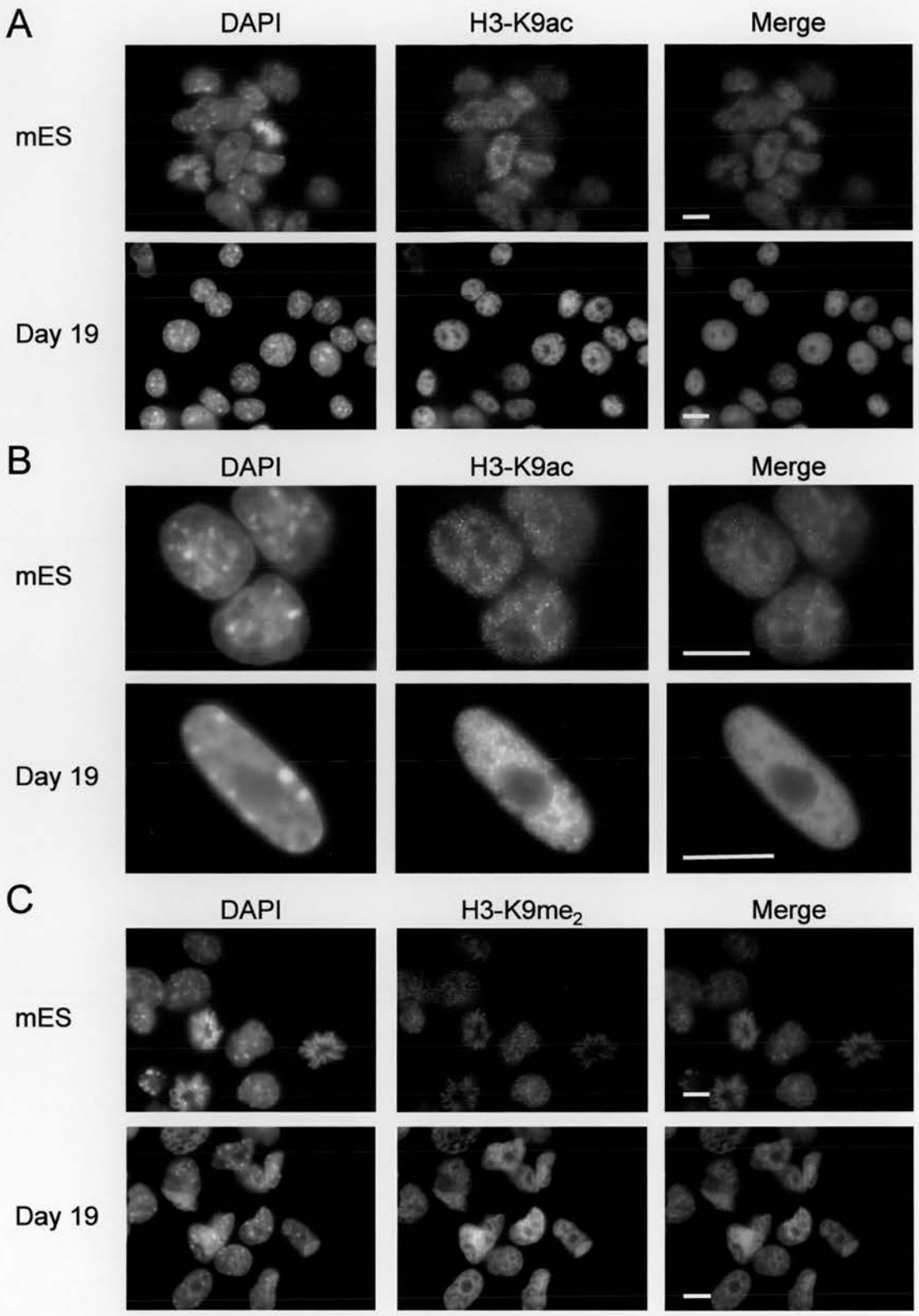

Fig. 5.10 Changes in the levels of histone modifications at H3-K9 detected by immunofluorescence. mES and differentiated day 19 nuclei stained with antibodies for (A and B) H3-K9ac and (C) H3-K9me$_2$ detected using FITC (green), counterstained with DAPI (blue). Scale bars, 10μm.

these metaphase chromosomes, but not detectable by immunofluorescence, which could be distinguished by using a microarray. This pattern of H3-K9ac staining was previously reported for human fibroblasts and HT1080 fibrosarcoma cells (Gilchrist et al., 2004). The level of H3-K9me$_2$ detected by immunofluorescence was substantially decreased in the mES cell population (*figure* 5.10C), consistent with the result obtained by western blotting. In mES cells, this modification appeared as distinct foci scattered across interphase nuclei and along the metaphase chromosomes. However, H3-K9me$_2$ was abundant throughout the nucleus of the differentiated cells including the nuclear periphery, which again enforces the role of the nuclear periphery in gene silencing.

To investigate the presence of these modifications at specific gene loci, I carried out ChIP with anti H3-K4me$_2$ and H3-K9ac antibodies and looked for the presence of the *Oct4* promoter and *Olig2* exon 1 sequences by Real-Time PCR (Schoorlemmer et al., 1994; Xian et al., 2005; *figure* 5.11). Both of these modifications were present at the *Oct4* promoter in mES cells, which express the gene, but not in the differentiated population where the gene is silenced. Hyperacetylation of the *Oct4* promoter region in mES cells has been reported previously, therefore confirming this result (Hattori et al., 2004; Kimura et al., 2004). At *Olig2* exon 1, H3-K4me$_2$ was present in both the mES cell population, which do not express the gene and the differentiated population, where the gene was expressed. However, H3-K9ac was only detected at *Olig2* exon 1 in the differentiated cells where the gene is expressed. Therefore, H3-K4me$_2$ and possibly H3-K9ac of exon1 precede *Olig2* activation. Both H3-K9ac and H3-K27me$_3$ were shown to precede transcriptional activation of the *Mash1* locus during neuronal differentiation (Williams et al., 2006) and interestingly, H3-K27me$_3$ is present at the *Olig2* locus in mES cells (Azuara et al., 2006). This would suggest that *Olig2* might be kept poised for transcription in mES cells, via protein associating with these histone modifications (Azuara et al., 2006; Boyer et al., 2006).

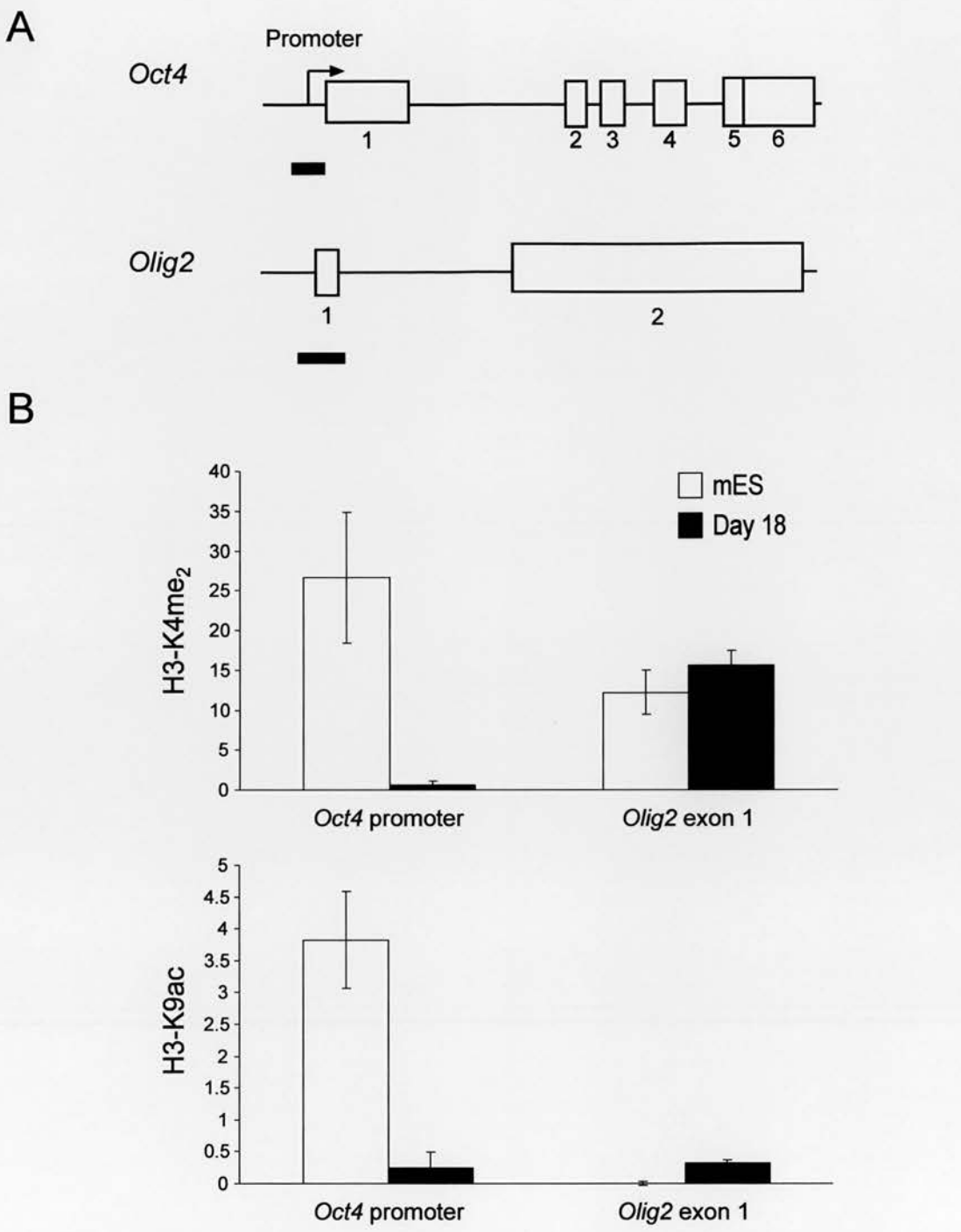

Fig. 5.11 Histone H3 modifications at *Oct4* and *Olig2*. (A) Maps of *Oct4* and *Olig2* showing the regions analysed by ChIP. Open bars represent the exons and the black bars underneath indicate the PCR products detected by ChIP. (B) Quantification of ChIP by real-time PCR. The graphs show the mean levels of product amplified from samples after ChIP with antibodies for H3-K4me$_2$ and H3-K9ac (after subtraction of mock IP levels). The analysis was carried out on chromatin prepared from undifferentiated ES cells (open bars) and cells after 18 days of differentiation (filled bars).

5.8 Centromere localisation in OS25 cells

I have previously shown differences in the location of centromeric heterochromatin between hES cells and differentiated cell-lines (section 3.5). To determine if this was also true of mES cells, I carried out 3D FISH with a mouse minor satellite (R198, Kipling et al., 1994) on 4% PFa fixed nuclei from mES and differentiated cells (*figure* 5.12A). I then took a series of images through the *z*-plane of each nucleus, and used the script (described in section 3.2) to determine which plane each centromere was located in, by using the point of greatest signal intensity. Unlike hES cells, centromeres were distributed randomly throughout the *z*-plane of both mES and differentiated cell populations (*figure* 5.12B). In a recent study, Mayer et al., (2005) found mES cells to have a significantly different distribution of centromeres in comparison to fibroblasts, lymphocytes, myoblasts, myotubes and macrophages. The images of centromere position before and after ectoderm differentiation appeared to show a more peripheral distribution of centromeres in the differentiated population. In mouse, repositioning of centromeres to the nuclear periphery has been described during myogenesis and is well documented for differentiated cells such as lymphocytes (Chaly and Munro, 1996, Vourc'h et al., 1993; Weierich et al., 2003).

To compare the proportion of centromeres at the nuclear periphery in mES and differentiated cells, I carried out an immunoFISH with an antibody to the nucleolar protein fibrillarin and a mouse minor satellite probe (R198) (*figure* 5.13C). Fibrillarin localises in the dense fibrillar centres of the nucleolus, so unlike the protein nucleolin, it does not highlight the nucleolus in its entirety (*figure* 5.13A). However, unlike fibrillarin the antibody to nucleolin did not survive the 3D FISH protocol. The number of centromeres found to associate with the nuclear periphery, nucleolus and neither of these compartments were then counted (*figure* 5.13D). The number of centromeres located at the nucleolus or not associated with either of the compartments did not change during the differentiation of mES cells ($p=0.608$ and $p=0.304$, respectively). However, the number of centromeres found at the periphery significantly increased in the population

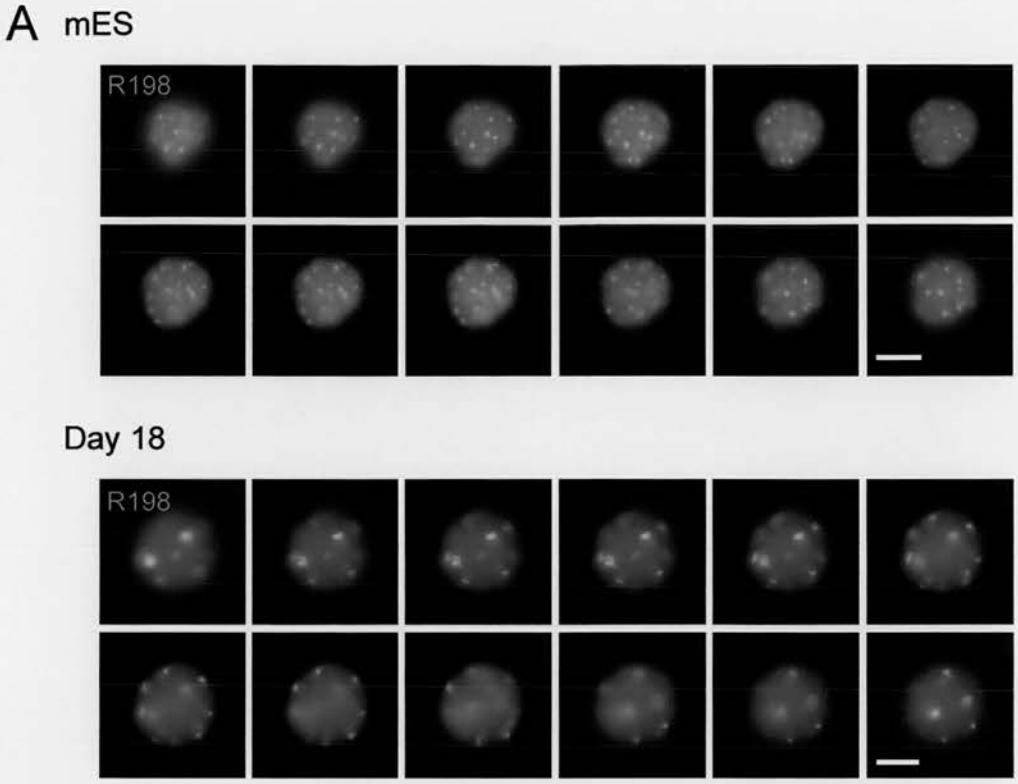

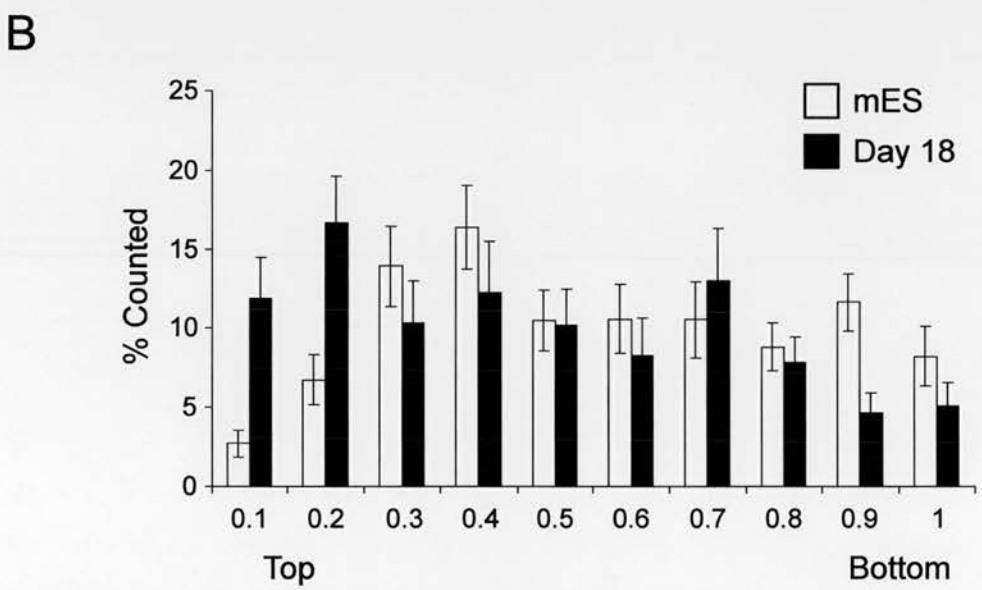

Fig. 5.12 Centromere localisation in mouse cells. (A) Localisation of minor satellite (R198 probe, green) in single image frames, taken at 0.5μm intervals, through the *z*-axis of mouse OS25 cell nuclei before and after 18 days of differentiation, nuclei counterstained with DAPI (blue). (B) The mean (±s.e.m.) distribution of minor satellite through the *z*-plane from top (0) to bottom (1) of nuclei from mES (white) and differentiated cells (black) (*n*=25). Scale bar, 5μm.

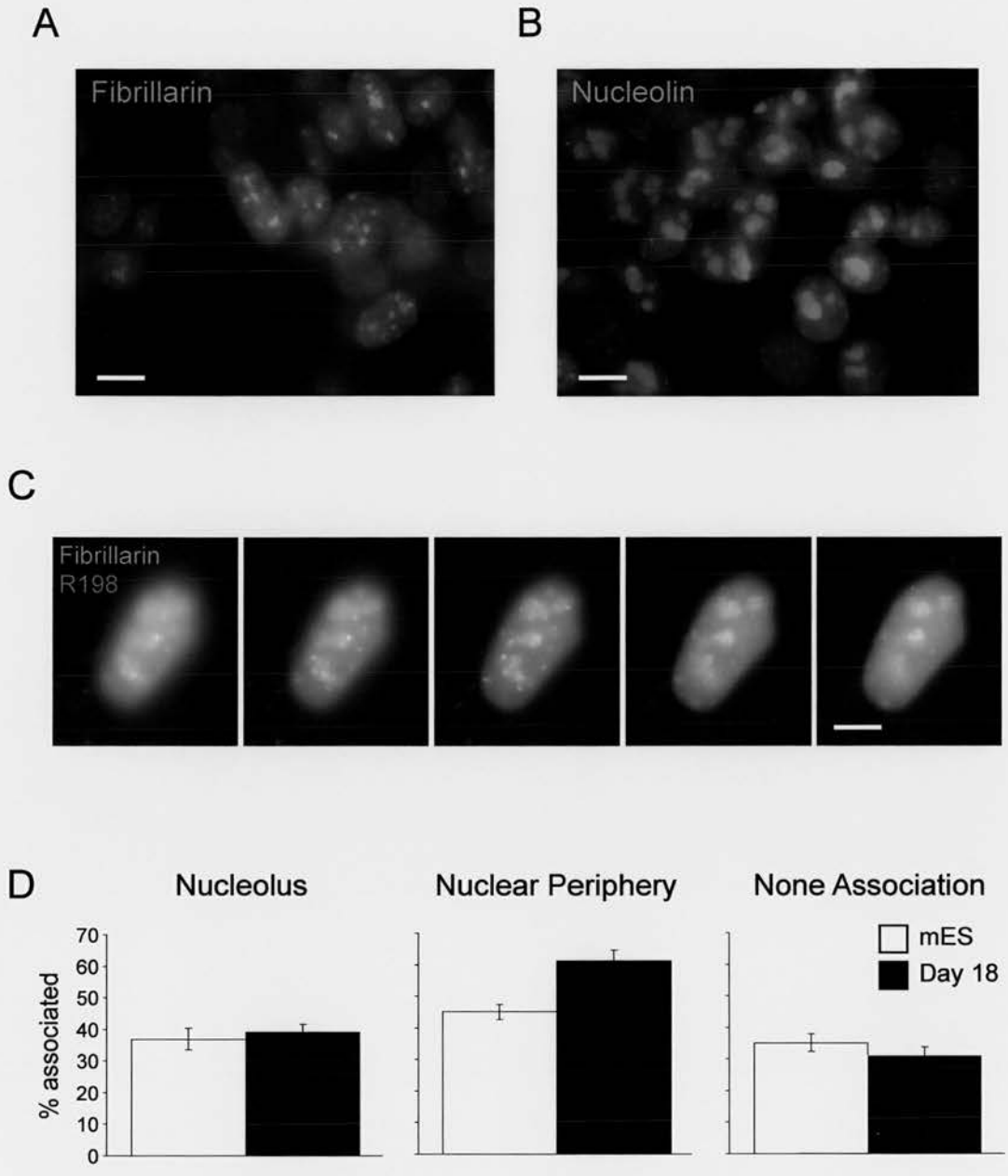

Fig. 5.13 Centromere localisation relative to the nucleolus in mouse cells. Immunofluorescence with antibodies to (A) fibrillarin and (B) nucleolin to locate the nucleolus in mES cells. (C) ImmunoFISH to locate centromeres (R198 probe, red) and nucleoli (fibrillarin, green) in single frames, taken at 0.75μm intervals through the *z*-axis of OS25 cell nucleus after 18 days of differentiation, counterstained with DAPI (blue). (D) Mean proportion (±s.e.m.) of centromeres per cell that are associated with the nucleolus (left), the nuclear periphery (middle), or neither of these nuclear compartments (right), in mES cells (white) and after 18 days of differentiation (black) (*n*=25) Scale bar, 5μm.

of differentiated cells (p=0.001), this would be consistent with the general move of CTs (i.e. chromosome arms) to the centre of the nucleus upon differentiation, as something has to take their place at the nuclear periphery. Mayer et al., (2005) used a similar approach to look at centromere position in mES cells and found 58% of centromeres at the nucleolus, 64% at the periphery and 6% in neither of these areas. This differs from the 37% of centromeres I found at the nucleolus of mES cells, 45% at periphery and 35% in neither of the areas, although Mayer et al., do not describe how they defined the nucleolus in their study. Therefore, these differences could be explained by how the two studies determine where the boundaries of nucleolar and nuclear periphery compartments are placed. This would also account for the decreased number of centromeres at the nucleolus in differentiated cells seen by Mayer et al., (2005) that I have not observed during the differentiation of ectodermal cells. However, both studies show an increase in the number of centromeres present at the nuclear periphery in differentiated cells. This is in agreement with the many reports of centromeres being located at, or moving to, the periphery in terminally differentiating murine cells (Vourc'h et al., 1993; Martou and De Boni, 2000), and during the differentiation of hES cells (section 3.5).

A property of centromeric heterochromatin that was very apparent from the DAPI stained nuclei of mES differentiating toward the ectodermal lineages, was its ability to cluster forming chromocentres (Hsu et al., 1971). I investigated this further by fixing cells at six time points during the differentiation and carried out 3D FISH on these cells using a mouse minor satellite probe. I then proceeded to count the visible probe signals (representing the minor satellite) and the bright spots of heterochromatin in the DAPI (representing the major satellite) (*figure* 5.14A and B). The average number of minor satellite signals visualised in the mES cells was 36.3, but by day 2 the number of signals visible was significantly lower at 30.6 (p=0.025). Similarly, by using the DAPI staining as a guide the number of distinct heterochromatic bright spots also significantly clustered between 20.5 at day 0 and 17.7 at day 2 (p=0.034). This clustering of both minor and major satellite continued throughout the differentiation until at day 18 there

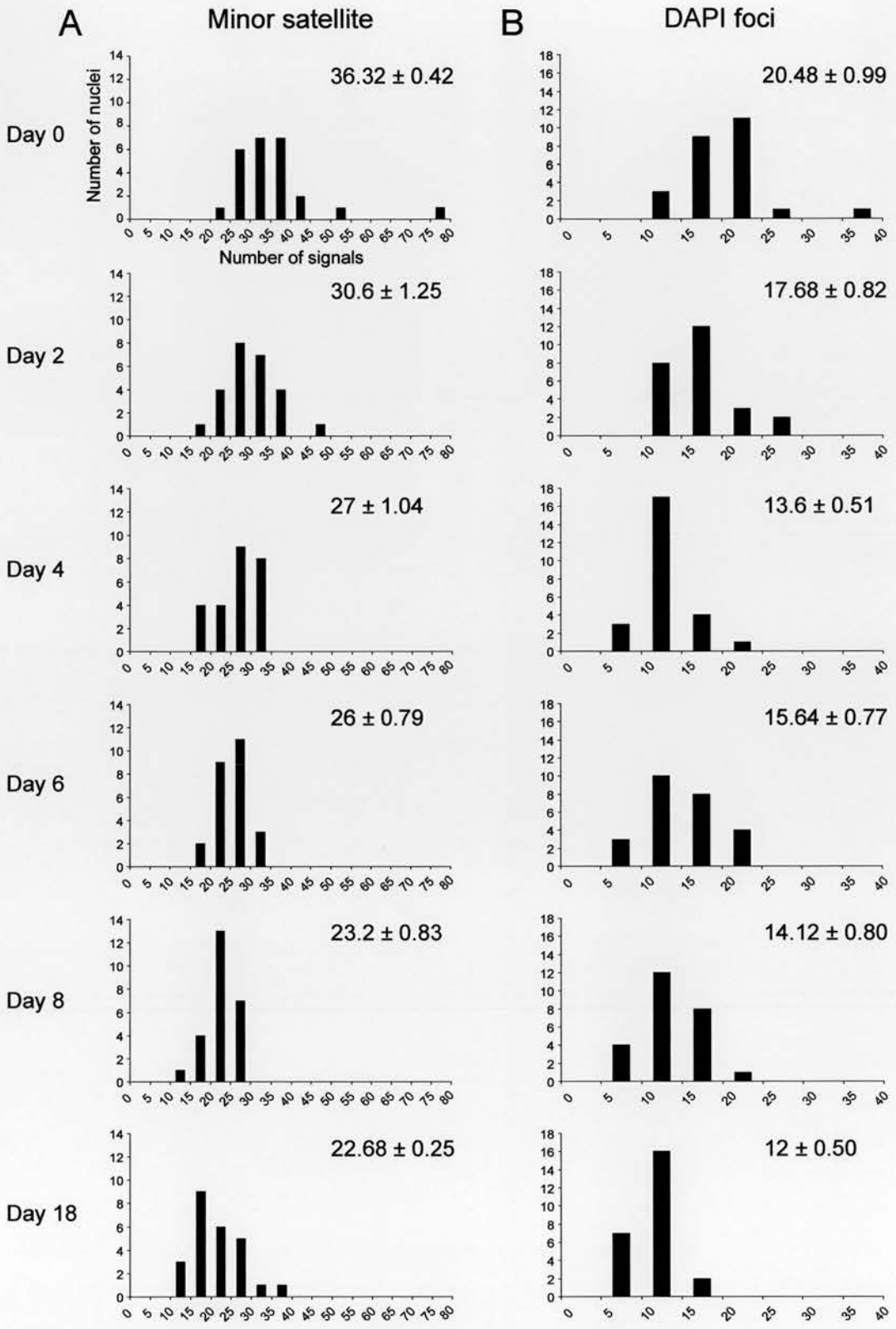

Fig. 5.14 Centromere clustering during the differentiation of OS25 cells. 3D FISH was carried out on cells fixed at six time points throughout the differentiation and the number of signals from (A) R198, a mouse minor satellite probe and (B) DAPI foci were counted. Numbers show averages ±s.e.m. (*n*=25).

were 22.7 minor satellite signals (37% decrease) and 12 major satellite signals (41% decrease). Previously chromocentres have been shown to cluster in murine neuronal cells (Manuelidis et al., 1984) Sertoli cells (Haaf et al., 1990) and during myogenesis (Brero et al., 2005; Terranova et al., 2005). In contrast to all of those studies, in a recent paper Meshorer et al., (2006) generated neuronal precursors from mES cells and report that the number of heterochromatic foci increased during differentiation. The number of foci they reported for neuronal progenitors was similar to the number seen in the differentiated day 18 cell population, but I have never seen heterochromatic foci cluster to that extent in an undifferentiated ES cell.

To confirm the clustering of centromeric heterochromatin during ectodermal differentiation, telomere FISH was carried out using both mES and differentiated cells (*figure* 5.15). The result was as expected, with the half of the telomeres that are adjacent to centromeres forming clusters, as previously described for 3T3 cells and bone marrow cells (Cerda et al., 1999). Cerda et al., (1999) amongst others have speculated that the Rabl distribution, seen in plants is present in some murine cell types. Although I have not seen the classic Rabl distribution, with centromeres clustered at one pole and telomeres at the other, I have seen the clustering of all but two centromeres towards one side of the nucleus on numerous occasions (*figure* 5.16). This distribution was seen in 60% of the OS25 cells 4 days into the differentiation and could be related to cell cycle.

5.9 Reorganisation of centromeric heterochromatin in knockout ES cells

Whether centromeres are clustering or un-clustering during differentiation, the question remains as to what is responsible for the movement of centromeric heterochromatin. There are three epigenetic hallmarks of centromeric heterochromatin, a high level of H3-K9me$_3$, deacetylated histone H4 and DNA methylation (reviewed in Richards and Elgin, 2002), which are known to change during differentiation (O'Neill and Turner, 1995; Martens et al., 2005). To investigate whether these epigenetic modifications may be

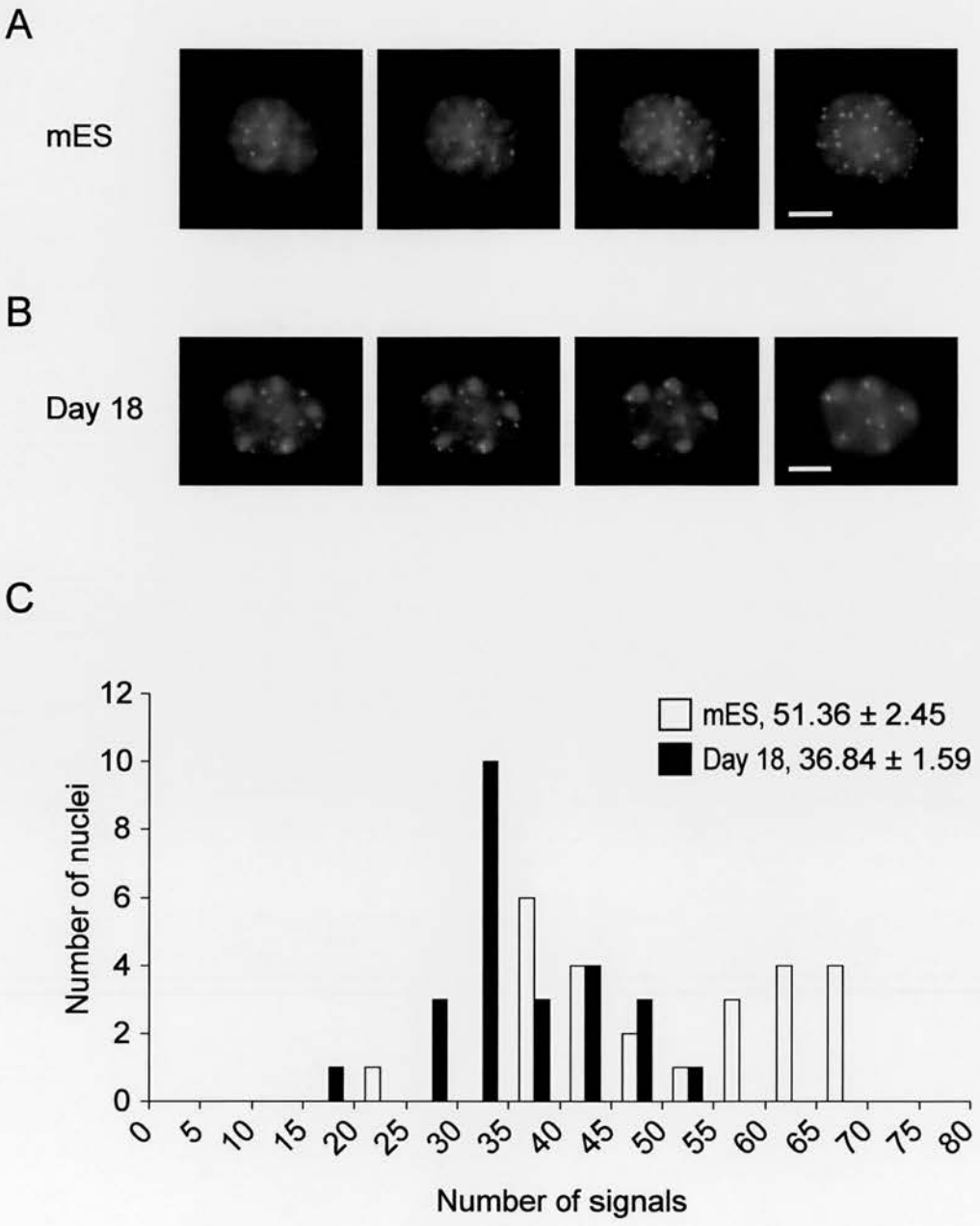

Fig. 5.15 Telomere FISH on undifferentiated and differentiated OS25 cells. Localisation of telomeres (PNA probe, green) in single frames, taken at 0.75μm intervals, through the *z*-axis of (A) undifferentiated and (B) differentiated for 18 days, OS25 cell nuclei counterstained with DAPI (blue). (C) The number of signals counted after telomere FISH on mES and differentiated day 18 cells (*n*=25). Numbers show the mean (±s.e.m.). Scale bar, 5μm.

A

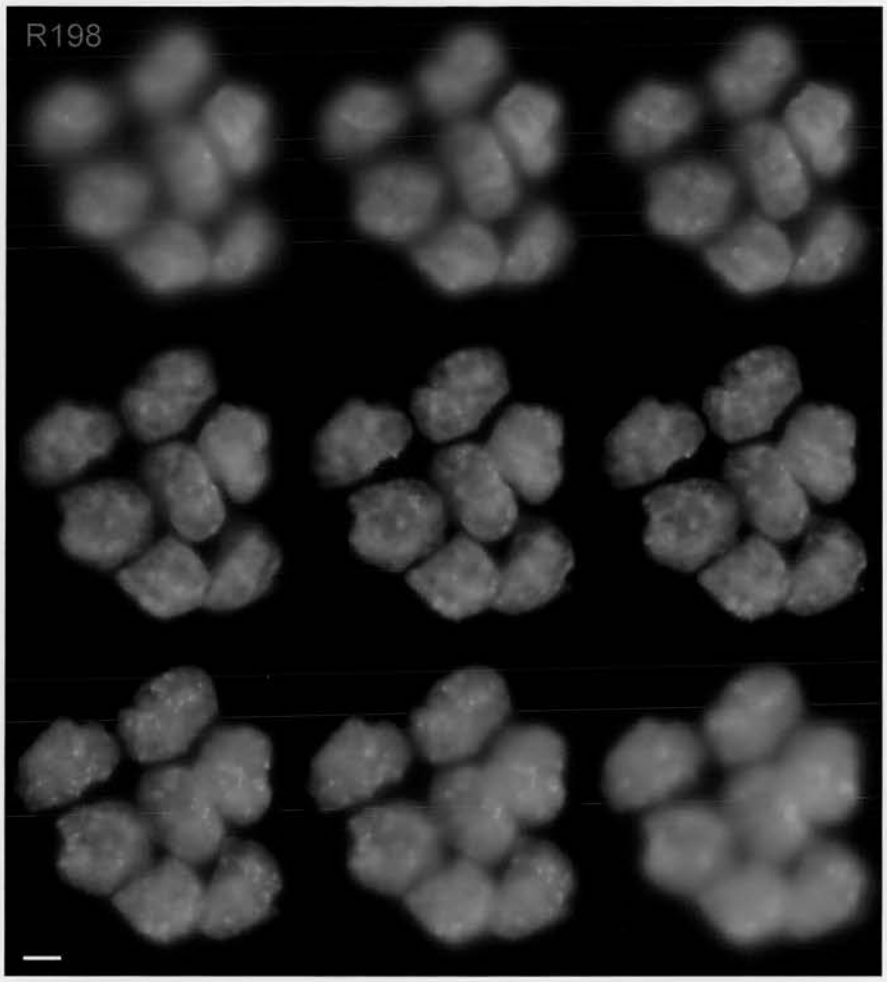

B

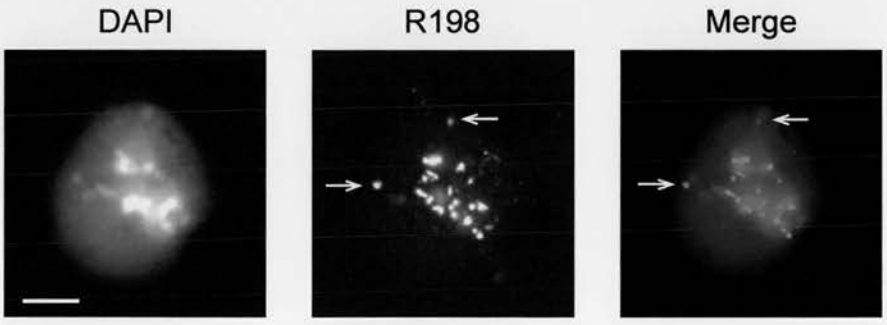

Fig. 5.16 Centromere localisation in OS25 cells after 4 days of differentiation. Centromeres were localised following 3D FISH with a minor satellite probe (R198, red). (A) Single frames taken at 0.5μm intervals, through the *z*-axis of OS25 cell nuclei after 4 days of differentiation. (B) A single nucleus, representing the centromere distribution observed in the majority of cells, at day 4 of differentiation. Arrows mark two centromeres that do not associate with the main group. Nuclei counterstained with DAPI (blue). Scale bars, 5μm.

responsible for the nuclear reorganisation and clustering of centromeric heterochromatin during the differentiation of mES cells, I examined this aspect of nuclear organisation in cells with null mutations in the enzymes responsible.

I started by asking whether H3-K9me$_3$ was involved in centromere clustering. Suv39h1 and Suv39h2 histone methyltransferase (HMTase) catalyse H3-K9me$_3$ at pericentric heterochromatin (Peters et al., 2001). Suv39h also creates a binding site for the heterochromatin protein 1 (HP1; Lachner et al., 2001). When both of these HMTase were knocked out, the phenotype was embryonic lethal as only 33% of the expected number of mice were born, fibroblasts derived from E12.5 foetuses showed chromosomal instability and the few mice that were viable showed an increased incidence of tumours (Peters et al., 2001). However, the double null mES cells are viable and can be differentiated. I differentiated the double knockout mES cells for Suv39h1 and Suv39h2 made by Peters et al., (2001) and the wild type parental (WT41) cell line towards an ectodermal lineage using the protocol described in section 4.2, however this time no drug selection was used (*figure* 5.17C and D). RT-PCR performed on RNA samples taken during the differentiation of both the knockout and wild type mES cells, showed that *Oct4* switched off and the neural precursor gene *Sox1* switched on during the differentiation of Suv39h$^{-/-}$ cells (*figure* 5.17A and B). Cells were taken at five time points throughout the differentiation, fixed in 4% PFa for 3D FISH with a mouse minor satellite (R198) (*figure* 5.18A) and the number of signals from minor satellite (R198) and major satellite (DAPI foci) were counted (*figure* 5.18B and C). Centromere clustering was evident during the differentiation of both the Suv39h$^{-/-}$ and WT41 cells, as previously seen in the OS25 cell line. Due to the cells not being under drug selection, the starting population was slightly more heterogeneous. This was reflected in the number of minor satellite signals counted at day 0, being 30.2 for Suv39h$^{-/-}$ and 31.0 for WT41, in comparison with 36.3 for OS25 cells under positive selection for *Oct4* expression with hygromycin. However, the number of chromocentres present at day 2 of Suv39h$^{-/-}$ differentiation was similar to the OS25 cell differentiation, being 30.6 for minor satellite and 18.8 for DAPI foci in the Suv39h$^{-/-}$ cells and 30.6 for minor satellite

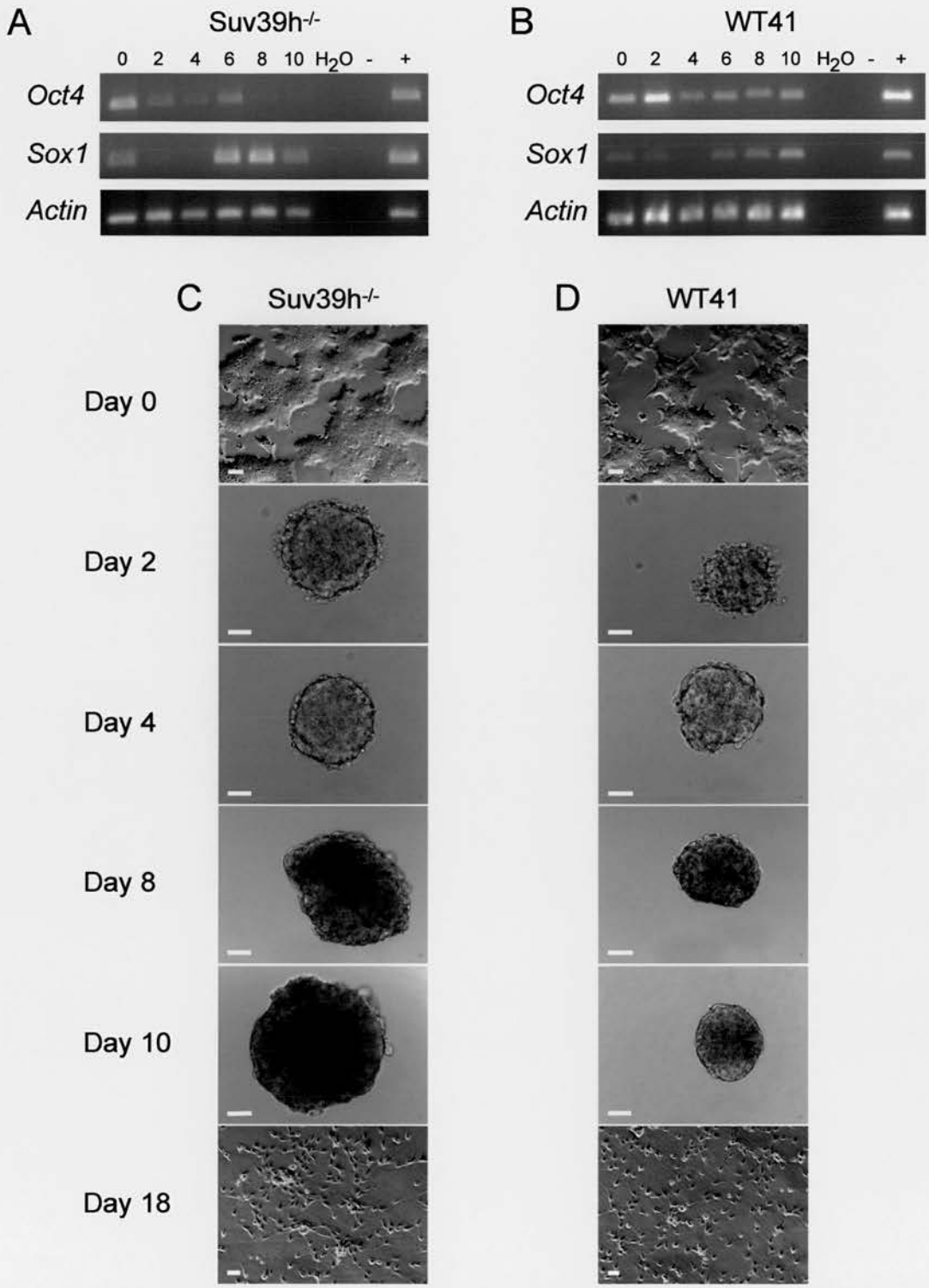

Fig. 5.17 Differentiation of Suv39h$^{-/-}$ and WT41 cells. RT-PCR analysis for *Oct4*, *Sox1* and *Actin* expression during the differentiation of (A) Suv39h$^{-/-}$ and (B) WT41 cells. Lanes are numbered corresponding to the day of differentiation or no template (H_2O), no reverse transcriptase (-) and positive control (+). Brightfield images taken under phase contrast during the differentiation of (C) Suv39h$^{-/-}$ and (D) WT41 cells. Scale bars, 50μm.

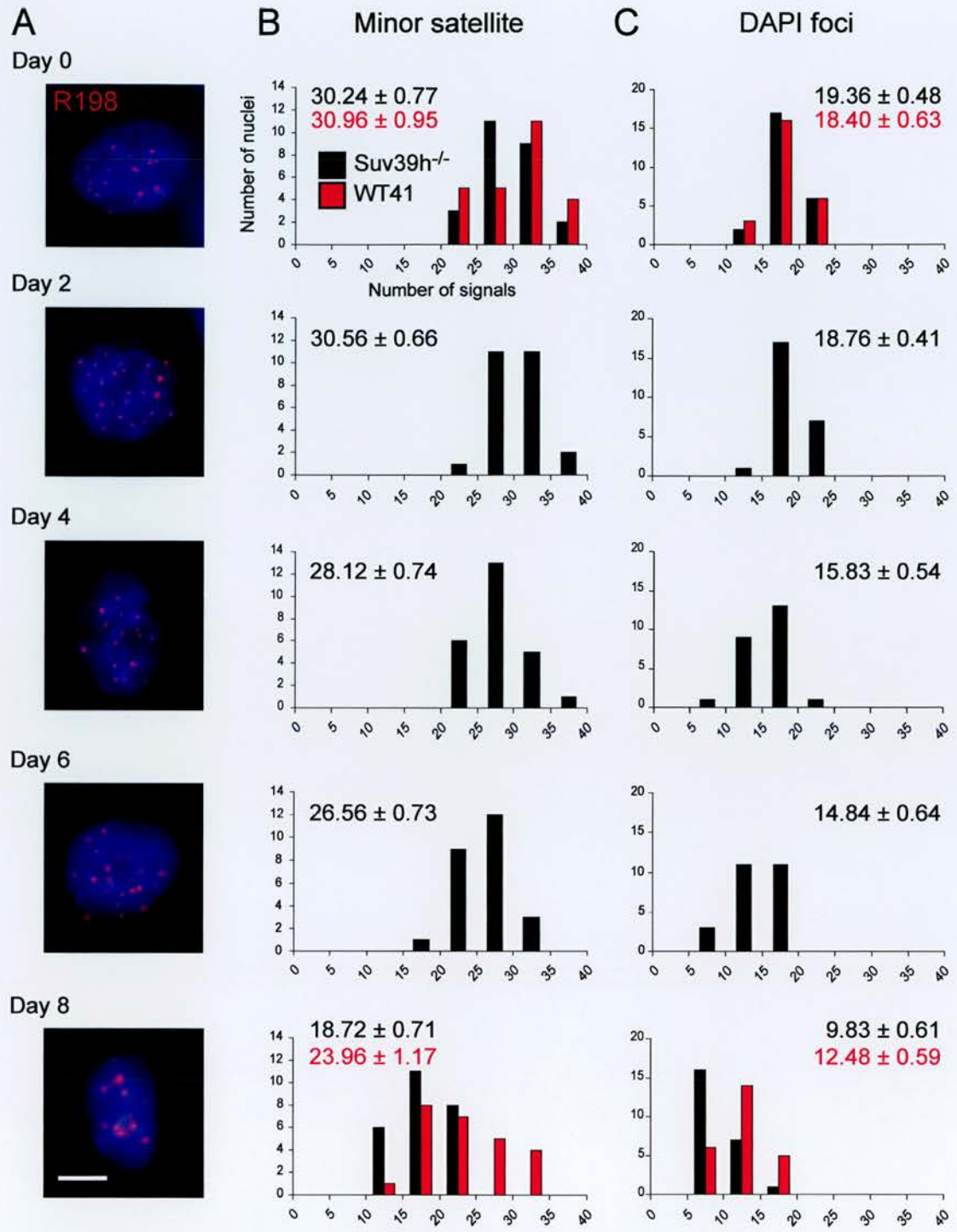

Fig. 5.18 Centromere clustering during the differentiation of Suv39h$^{-/-}$ and WT41 cells. (A) 3D FISH with a mouse minor satellite probe (R198, red) was carried out on cells fixed at five time points during the differentiation of Suv39h$^{-/-}$ cells, nuclei counterstained with DAPI (blue). The signals from (B) minor satellite (R198) and (C) DAPI foci were counted for Suv39h$^{-/-}$ (black bars) and WT41 cells (red bars), numbers show the mean (±s.e.m.) (n=25). Scale bar, 5μm.

and 17.7 for DAPI foci in OS25 cells. There was a significant decrease in the number of DAPI foci by day 4 and minor satellite signals by day 6 ($p=<0.001$). This suggests that after the initial clustering following the removal of LIF (seen in the OS25 cell population), the second wave of clustering accompanies the change in gene expression following RA treatment of the cells. I conclude therefore that trimethylation of H3-K9 at major and minor satellites, is not required for centromere clustering. This is in agreement with Brero et al., (2005), who have also shown centromeres to cluster during the differentiation of $Suv39h^{-/-}$ cells.

Recently it has been disputed as to whether histone deacetylases (HDACs) are important for centromere clustering (Gilchrist et al., 2004; Terranova et al., 2005). However, one of the proteins responsible for the recruitment of HDACs to centromeric heterochromatin, the methyl CpG-binding protein MeCP2 (Jones et al., 1998; Nan et al., 1998), has also been implicated in large-scale chromatin reorganisation during terminal differentiation (Brero et al., 2005). Expression of MeCP2 is known to increase during neuronal differentiation in humans (LaSalle et al., 2001), rats (Jung et al., 2003) and mice (Cohen et al., 2003) and is concentrated at pericentric heterochromatin (Lewis et al., 1992). To investigate whether MeCP2 was essential for centromere clustering, I have taken both the MeCP2 knockout and their wild type (CGR8) mES cells (Tate et al., 1996) through the ectodermal differentiation protocol described previously (section 4.2; *figure* 5.19C and D). The genotypes of the cell types used in this experiment were checked by PCR for the presence of the LacZ and Neomycin inserts in the knockout cells (*figure* 5.21B).

The MeCP2 knockout and wild type cells both appeared to differentiate normally until day 18 when clumps of what appeared to be undifferentiated cells materialized in the MeCP2 knockout cultures. RT-PCR showed that in wild type (CGR8) cells, *Oct4* switched off after 4 days, although only a very low level of *Sox1* expression was seen in the day 18 population (*figure* 5.19B). The knockout mES cells also switched off *Oct4* by day 8 of differentiation in the absence of MeCP2, but expression of *Oct4* was evident in

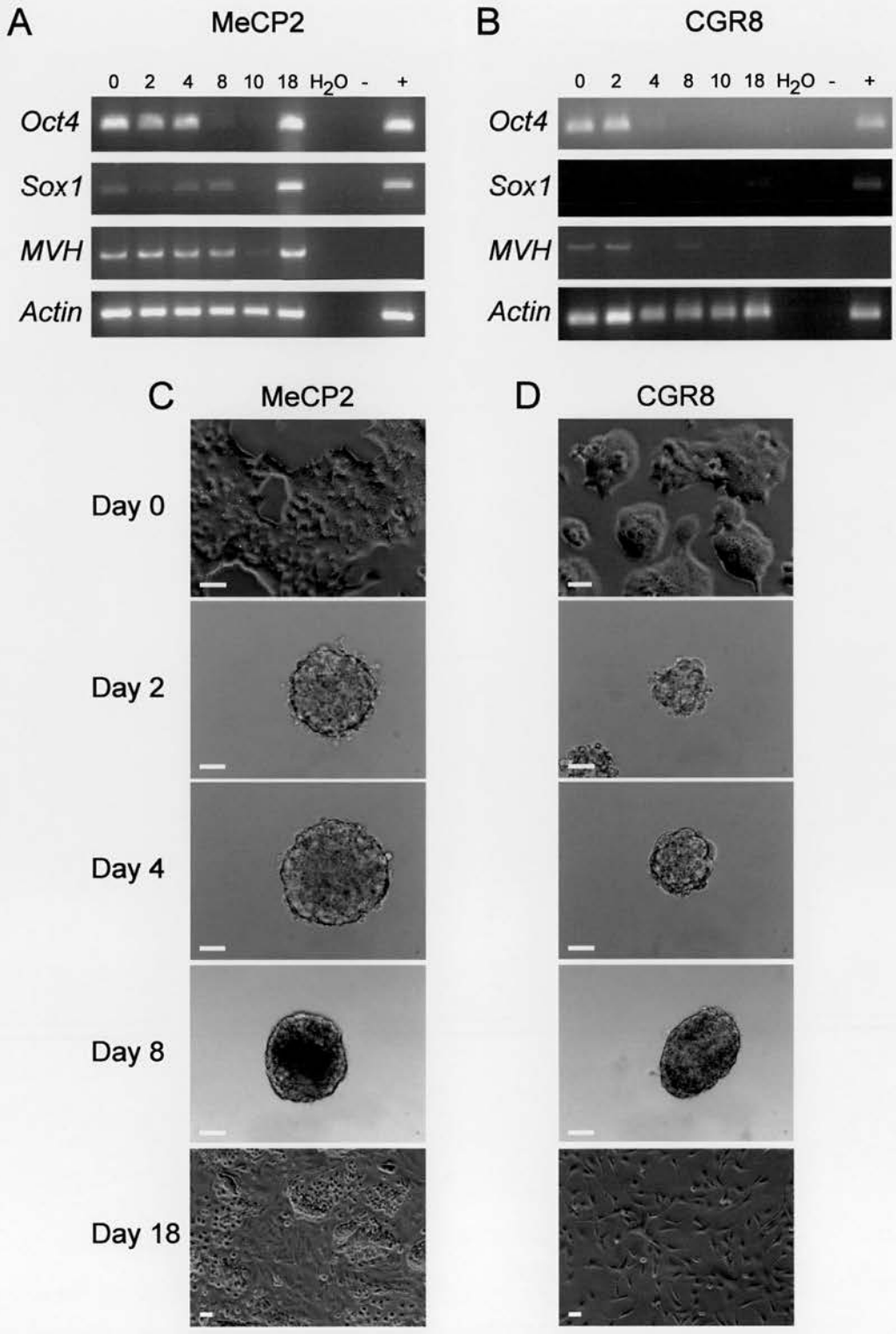

Fig. 5.19 Differentiation of MeCP2 and CGR8 cells. RT-PCR analysis for *Oct4*, *Sox1*, *MVH* and *Actin* expression during the differentiation of (A) MeCP2 and (B) CGR8 cells. Lanes are numbered corresponding to the day of differentiation or no template (H_2O), no reverse transcriptase (-) and positive control (+). Brightfield images taken under phase contrast during the differentiation of (C) MeCP2 and (D) CGR8 cells. Scale bars, 50μm.

the culture again at day 18, alongside the expression of the neural gene *Sox1* (*figure* 5.19A). One of the other cells types reported to express *Oct4*, are germ cells (Pesce and Scholer, 2000). To check the *Oct4* expressing cells in the differentiated MeCP2 population were not germ cells, I looked for the expression of *mouse vasa homolog* (*Mvh*), which some people believe is only expressed by germ cells (Fujiwara et al., 1994). However, by RT-PCR this gene was expressed not only in the day 18 population of MeCP2 cells, but also in the undifferentiated day 0 populations of both MeCP2 and CGR8 cells (*figure* 5.19A and B). The result in undifferentiated cells has since been repeated by immunofluorescence and western blot (Bolcun-Filas personal communication). If *Mvh* is only expressed by germ cells, this would mean I started the differentiation with germ cells present in the cultures, a concept that has been discussed recently (Zwaka and Thomson, 2005). However, until a clear distinction can be made between germ cells and ES cells, I cannot further identify the population of cells seen in the MeCP2 differentiation at day 18. These cells should be removed from future experiments by selective culture conditions, such as NS-A media plus N2 that does not support the propagation of ES cells and thereby eliminates them from the culture (Conti et al., 2005).

To analyse the centromere clustering in the day 18 populations the cells were replated onto glass coverslips and during this process, the clumps of strange undifferentiated cells were lost from the MeCP2 population. This was due either to the cells not sticking to the glass surface of the coverslip, or cell death following the dissociation of the cells from their clumps. The differentiated cells that adhered to the coverslips were fixed in 4% PFa for 3D FISH and hybridised to the R198 probe (*figure* 5.20A). In both knockout and wild type populations, the clustering of centromeric heterochromatin occurred in parallel during differentiation (*figure* 5.20B and C). The MeCP2 cells went from an average of 31.6 minor satellite signals at day 0 to 28.1 signals at day 6 ($p=0.009$), whereas the major satellite (DAPI foci) averaged 19 on day 0, 19.2 at day 6 ($p=0.742$) and 14 by day 10 ($p=<0.001$). By day 18 the average minor satellite signal had decreased by 32% in both MeCP2 and CGR8 cells, whereas the average number of DAPI foci had decreased

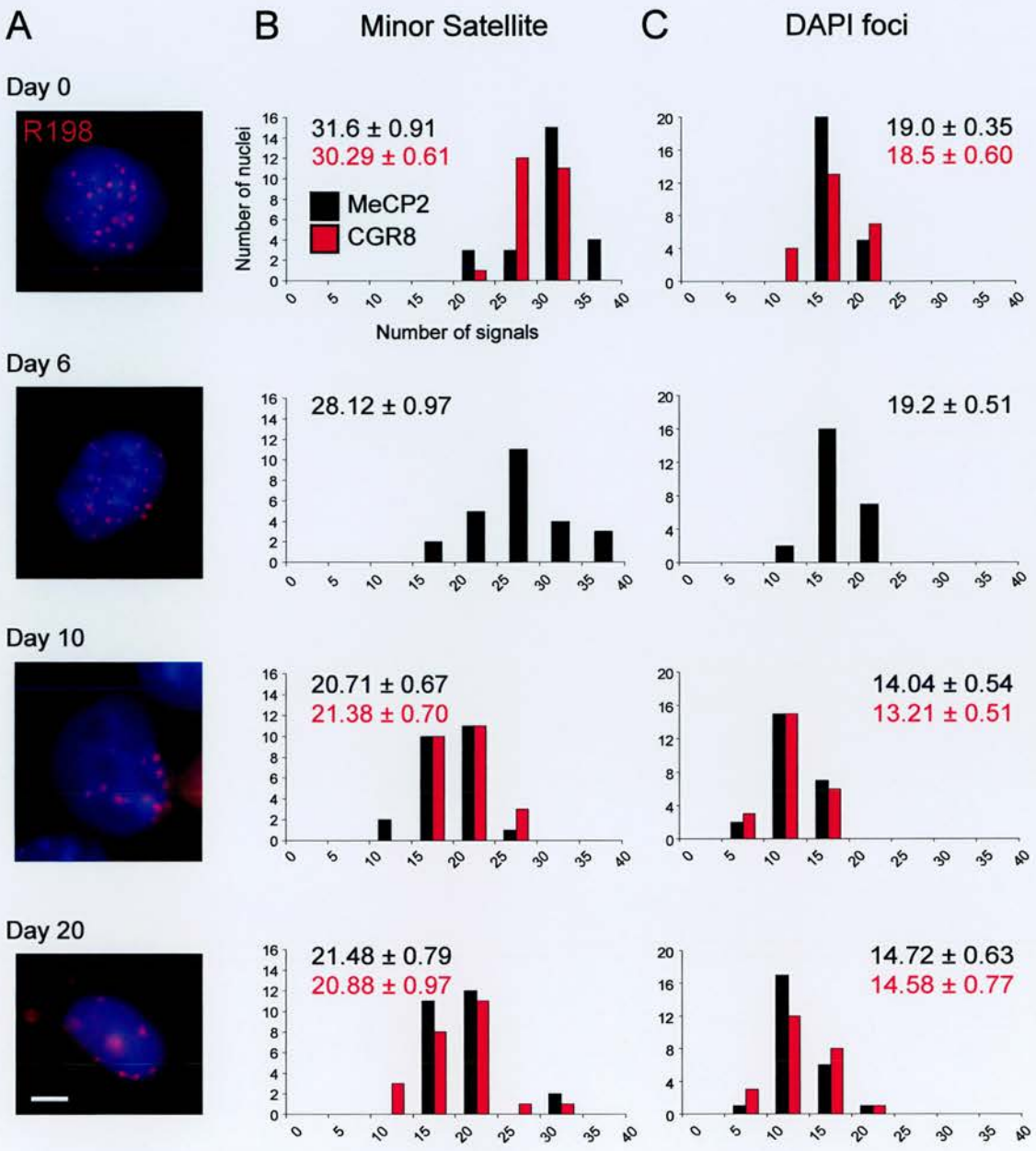

Fig. 5.20 Centromere clustering during the differentiation of MeCP2 and CGR8 cells. (A) 3D FISH with a mouse minor satellite probe (R198, red) was carried out on cells fixed at four time points during the differentiation of MeCP2 cells, nuclei counterstained with DAPI (blue). The signals from (B) minor satellite (R198) and (C) DAPI foci were counted for MeCP2 (black bars) and CGR8 cells (red bars), numbers show the mean (±s.e.m.) (*n*=25). Scale bar, 5μm.

by 22.6% in MeCP2 cells and 21.1% in CGR8 cells. Therefore, I conclude that although the absence of MeCP2 may affect the cells ability to differentiate, it does not effect the clustering of centromeres during differentiation. Brero et al., (2005) also showed that centromeres clustered in muscle tissue of MeCP2 knockout mice. However, they conclude that this clustering was due the functional redundancy of MeCP2 and other MBD proteins.

If this were the case, I wanted to know what would happen to centromere clustering if these proteins were unable to bind the chromatin fibre. MBD proteins only bind methylated DNA, so I analysed centromere clustering in a cell line that had reduced levels of DNA methylation. The methyltransferases Dnmt3a and Dnmt3b are responsible for establishing DNA methylation *de novo* (Okano et al., 1999). *Dnmt3a* and *Dnmt3b* are both constitutively expressed in ES cells and early embryos, however in the ectoderm; *Dnmt3a* is expressed by neural precursors, postmitotic CNS neurons and oligodendrocytes, whereas *Dnmt3b* is only expressed during a small window between E10.5 and 13.5 in the ventricular zone of the CNS (Feng et al., 2005). The double knockout of *Dnmt3a* and *Dnmt3b* ($Dnmt3^{-/-}$) is embryonic lethal in the mouse, and mutations in human DNMT3B cause ICF (immunodeficiency, centromere instability, facial anomaly) syndrome (Okano et al., 1999). This disease is characterised by an aberrant chromatin structure at pericentric heterochromatin (Xu et al., 1999). Despite the fact that these cells still have Dnmt1, amount of DNA methylation in $Dnmt3^{-/-}$ mES cells eventually declines in culture to negligible levels (Chen et al., 2003a).

Here, I have used the double knockout cell line for $Dnmt3^{-/-}$ cells, and their wild type (J1) cells (Okano et al., 1999). To check the methylation status of the cell lines I digested DNA from both cell types with MspI and HpaII. MspI cuts DNA regardless of its methylation status, whereas its isoschizomer HpaII is blocked by CpG methylation. This confirmed that the $Dnmt3^{-/-}$ cells have decreased levels of DNA methylation in comparison to the J1 cells (*figure* 5.21A). However, to double check the cell types used, I also confirmed the presence of the LacZ and Neomycin inserts in the knockout cell line

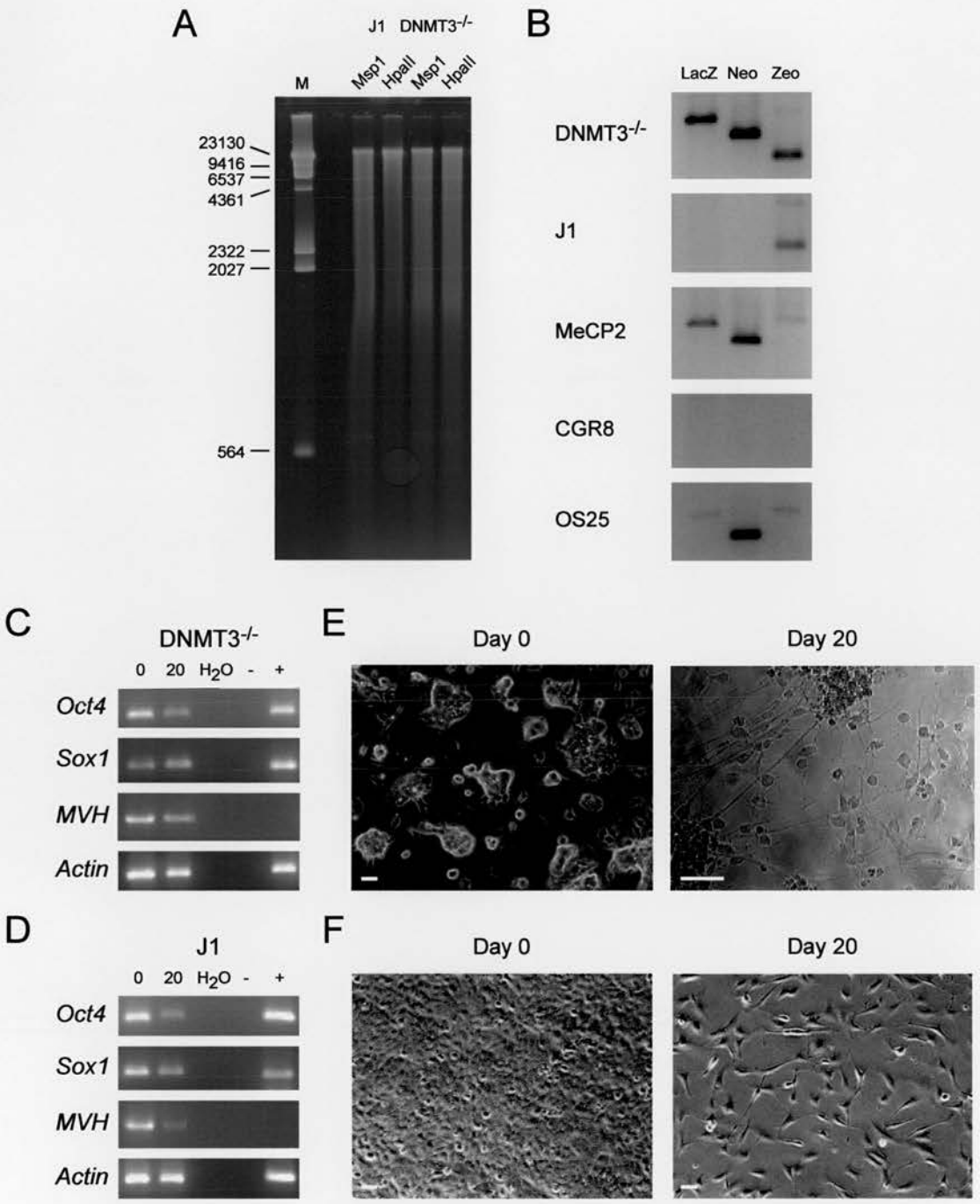

Fig. 5.21 Differentiation of DNMT3$^{-/-}$ and J1 cells. (A) Digests with Msp1 and HpaII to show the DNA methylation status of DNMT3$^{-/-}$ and the wild type (J1) cells. (B) Cell lines were also checked by PCR for LacZ, Neomycin (Neo) and Zeocin (Zeo). RT-PCR analysis for *Oct4*, *Sox1*, *MVH* and *Actin* expression before and after the differentiation of (C) DNMT3$^{-/-}$ and (D) J1 cells. Lanes are numbered corresponding to the day of differentiation or no template (H_2O), no reverse transcriptase (-) and positive control (+). Brightfield images taken under phase contrast before and after the differentiation of (E) DNMT3$^{-/-}$ and (F) J1 cells. Scale bar, 50μm.

by PCR (*figure* 5.21B). The cells were then differentiated towards ectodermal lineages following the protocol described previously (section 4.2; *figure* 5.21E and F). Whereas the wild type J1 cells differentiated as expected into numerous cell lineages, the Dnmt3$^{-/-}$ cells were restricted in their fate. Morphologically the day 20 Dnmt3$^{-/-}$ cell population consisted of cells that looked like clumps of undifferentiated mES cells and others that might be radial glia. RT-PCR analysis of this population showed that the pluripotent gene *Oct4* was expressed alongside the neural gene *Sox1* in the differentiated cells (*figure* 5.21C). However, *Sox1* expression was also seen in the undifferentiated population, which means either cells were spontaneously differentiating in the mES cell population or that *Sox1* is not repressed in Dnmt3$^{-/-}$ mES cells. Both populations were also found to express *Mvh*. However, no conclusions could be made from these PCRs because the wild type population also expressed *Oct4*, *Sox1* and *Mvh* at both time points (*figure* 5.21D). This was mainly due to the density at which the wild type J1 cells proliferated, which was substantially faster than the other cell lines I have used and as such, the concentration of cells to RA and growth factors needs to be optimised before future differentiations. Despite this the cells from both Dnmt3$^{-/-}$ and J1 differentiations were fixed in 4% PFa for 3D FISH and hybridised to the R198 probe (*figure* 5.22A). As previously seen for the MeCP2 cells, the clumps of supposed undifferentiated cells in the cultures, did not survive the 3D FISH protocol. The differentiated cells from both populations, which adhered to the glass coverslips, were clearly differentiated cells by the uniform oval shape of their nuclei and large heterochromatic foci. In Dnmt3$^{-/-}$ cells, both minor satellite and DAPI foci (major satellite) clustered by day 8 (*figure* 5.22B and C). Minor satellite averaged 31.5 signals on day 0 to 25.2 signals on day 8 ($p=0.009$) and major satellite averaged 18.5 signals on day 0 to 14.4 signals on day 8 ($p=<0.001$). By day 20 the average number of minor satellite signals had dropped by 35.9% in Dnmt3$^{-/-}$ cells and 34.7% in the J1 cells, whereas the number of DAPI foci analysed had decrease by 25.9% in Dnmt3$^{-/-}$ cells and 16.4% in the J1 cells. Therefore, I conclude that DNA methylation is not necessary for the clustering of centromeric heterochromatin. This conflicts with the paper from Brero et al., (2005), which suggests that DNA methylation is necessary to promote clustering of centromeres.

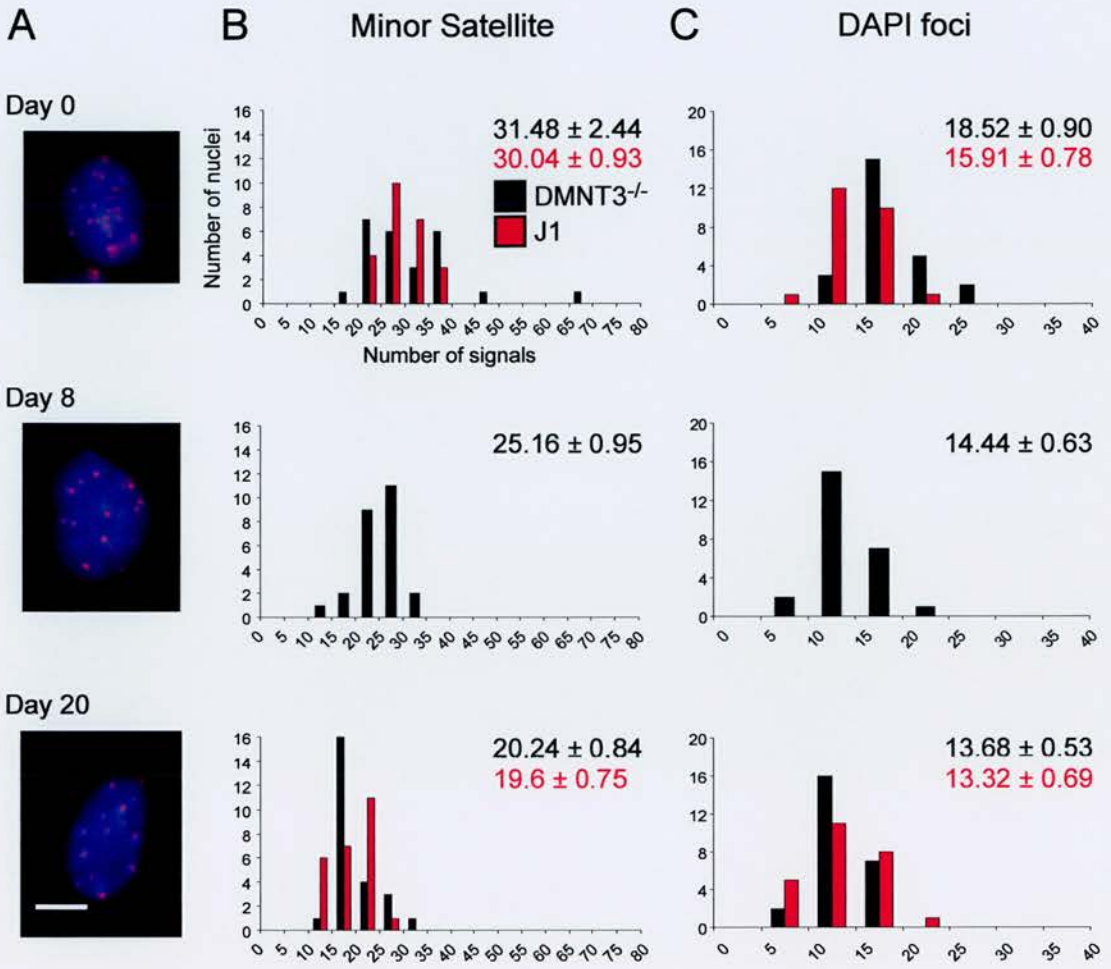

Fig. 5.22 Centromere clustering during the differentiation of DNMT3$^{-/-}$ and J1 cells. (A) 3D FISH with a mouse minor satellite probe (R198, red) was carried out on cells fixed at three time points during the differentiation of DNMT3$^{-/-}$ cells, nuclei counterstained with DAPI (blue). The signals from (B) minor satellite (R198) and (C) DAPI foci were counted for DNMT3$^{-/-}$ (black bars) and J1 cells (red bars), numbers show the mean (±s.e.m.) (*n*=25). Scale bar, 5μm.

5.10 Discussion

I have shown that the position of four CTs within mouse nuclei, changes during differentiation (*figure* 5.1). One of these the CTs for MMU6 contains the region surrounding the pluripotent gene *Nanog*. In humans, this region is part of HSA12p, the CT shown to occupy a more peripheral position in the nuclei of differentiated cells in comparison to hES cells. However in mouse, MMU6 moved away from the nuclear periphery during differentiation. This result has been reported previously, during the differentiation of T-cell precursors (Kim et al., 2004), suggesting that perhaps the location of this CT in murine precursor cells may confer some transcriptional advantage upon the chromosome. The global gene expression on MMU6 is known to vary with cell type. One study showed that more genes are highly expressed on this chromosome in mES cells than in differentiated cell types, however only 346 genes were analysed, 8 of which were identified as being highly expressed on MMU6 (Tanaka et al., 2002; Thomson personal communication). Therefore, it is possible that more genes on MMU6 are expressed in neural progenitor cells, in comparison to mES cells, which would explain the position of this CT in the differentiated day 18 cell population. Following the differentiation of mES cells towards ectodermal lineages, the four CTs analysed were arranged within the nucleus according to gene density. This distribution has previously been shown for human nuclei (Croft et al., 1999; Boyle et al., 2001) primates (Tanabe et al., 2002) and chickens (Stadler et al., 2004), therefore its presence in murine cells would further imply a functional significance to the arrangement.

The position of genes within the nucleus was also found to change during differentiation, although this seemed to be dependent on transcriptional activity of both the gene and its surrounding region (*figure* 5.3). Previous studies into gene position within the nucleus have shown both genes moving away from the nuclear periphery when expressed (Zink et al., 2004; Williams et al., 2006) and no gene movement following activation (Nielson et al., 2002; Parreira et al., 1997). The genes studied here all followed the position of their CTs with one exception, the neural precursor gene

Olig2. This gene looped out of its CT and towards the centre of the nucleus in differentiated cells. If this relocalisation of *Olig2* is dependant of gene expression, then the proportion of loci in the nuclear centre should increase if a purer population of *Olig2* positive cells could be obtained. In my system only 15% of the day 18 population expressed *Olig2*. A recent report indicated that the percentage of *Olig2* expressing cells could be increased to 33% by adding sonic hedgehog to the culture (Xian et al., 2005). Alternatively, GFP under the control of the *Olig2* promoter could be used to FACs sort an *Olig2* positive population for analysis. The distribution of both *Olig2* and *Nanog* loci relative to their CTs was consistent with their expression (*figure* 5.4A and 5.5B). However, *Nestin* was looped outside of its CT in mES cells, which do not express the gene (*figure* 5.5C). This might be explained by expression of the gene-dense region surrounding *Nestin* in mES cells. However, it also poses the question; do genes move outside of their CT prior to transcription? Ragoczy et al., (2003) has suggested that looping out of CT represents a poised state, prior to gene expression. Whilst Chambeyron and Bickmore, (2004) have shown that movement of the *Hox* locus outside of its CT, represents a transcriptionally active state.

In both hES cells and lymphocytes, *OCT4* was located in the centre of the nucleus (*figure* 3.5) whereas in mouse *Oct4* moves towards the centre of the nucleus during differentiation (*figure* 5.3B). This is likely due to differences in the expression of the region surrounding *Oct4*. The relocation also accompanies the movement of *Oct4* towards the edge of its CT in the differentiated cells, which is opposite to the result observed for hES cells (*figure* 5.4B and C). Again, this was attributed to the late expression of the class 1 MHC genes in mouse; however, the mean position of two loci adjacent to *Oct4*, *H2-Q1* and *Flot1* did not change relative to the MMU17 CT. Therefore further investigation is need to find out whether other genes flanking *Oct4* change position relative to their CT, or if the almost bi-modal distribution of *H2-Q1* represents different cell types, and expression pattern of these genes within the differentiated day 18 population. The movement of *Oct4* to the edge of the CT was also accompanied by the decondensation of the surrounding region in differentiated cells (*figure* 5.6), as

previously shown for human cells (*figure* 3.8). Therefore, it is possible that *Oct4*'s position, away from its neighbouring genes and towards the edge of the CT, allows for the association with a transcriptionally silent region of the nucleus such as centromeres. The association of genes with centromeric heterochromatin is thought to promote gene silencing (Brown et al., 1997, 1999; Su et al., 2004). However, here I have shown that neither *Oct4* nor *Nanog* relocated to centromeric heterochromatin when silenced (*figure* 5.7), a result also described for the neuronal gene *Mash1* in ES cells (Williams et al., 2006).

Accompanying the spatial reorganisation of the genome are changes in global levels of histone modifications such as decreased H3-K9ac, H3-K4me$_2$ and increased H3-K9me$_2$ (*figure* 5.8). By immunofluorescence, I have shown that the markers of gene expression (H3-K9ac and H3-K4me$_2$) are not present at centromeric heterochromatin or the nuclear periphery in differentiated cells (*figure* 5.9 and 5.10). This result has been reported previously for H3-K9ac in human fibroblasts and fibrosarcoma cells (Gilchrist et al., 2004) and another marker of hyperacetylated chromatin, H4-K8ac in human fibroblasts and mouse myoblasts (Sadoni et al., 1999). H3-K9me$_2$ however, increases across the nucleus during differentiation, including at the nuclear periphery (*figure* 5.10C). A similar result was observed between quiescent and cycling lymphocytes, were H3-K9me$_2$ increases as the cells come out of quiescence, suggesting that histone hypomethylation is a useful indicator of epigenetic plasticity (Baxter et al., 2004). However, as lymphocytes come out of quiescence their level of H3-K4me$_2$ also increased, unlike during differentiation. I would suggest that hypomethylation of H3-K9me$_2$ is a useful indicator of plasticity but not H3-K4me$_2$ as high levels of this histone modification are also present in mES cells.

Gene expression during oligodendrocyte development has previously been shown to accompany progressive chromatin modifications at gene promoters (Kondo and Raff, 2004; Song and Ghosh, 2004). In mES cells both H3-K4me$_2$ and H3-K9ac modifications were present on the *Oct4* promoter, however in the day 18 population both of these

modifications had been lost from the region (*figure* 5.11). H3-K4me$_2$ was also detected on the first exon of *Olig2* in mES cells, before the gene was expressed, whereas H3-K9ac is only present in the differentiated cells where the gene is expressed. Similarly, Williams et al., (2006) showed that H3-K27me$_3$ was present at the *Mash1* locus prior to differentiation, although they see H3-K9ac of this gene in undifferentiated mES cell. This could reflect differences in the expression patterns of *Mash1* and *Olig2*, or the homology of the starting population, as Williams et al., (2006) did not treat the cells with hygromycin before beginning their differentiation.

I found an increased association of centromeric heterochromatin with the nuclear periphery during differentiation (*figure* 5.13D). During the differentiation of mES cells centromeres clustered forming chromocentres. Following two days of culture as hanging drops without LIF there was a significant clustering of centromeric heterochromatin, analysed by both 3D FISH with a mouse minor satellite and by counting DAPI foci (*figure* 5.14). The clustering continued progressively throughout the differentiation until on day 18 there was a 37% percent decrease in the number of minor satellite clusters and 41% decrease in the number of major satellite clusters detectable by FISH (*table* 5.4). This result was confirmed by telomere FISH, which showed that 50% of the telomeres also clustered as expected by day 18 (*figure* 5.15).

Using mutant ES cells, I showed that this is independent of H3-K9me$_3$ at pericentric heterochromatin, catalysed by Suv39h. When Suv39h$^{-/-}$ cells were differentiated towards an ectodermal lineage, the centromeres clustered at the same rate as during the OS25 differentiation (*figure* 5.18; *table* 5.4). The heterochromatin protein HP1 is also lost from heterochromatin in Suv39h$^{-/-}$ cells (Lachner et al., 2001), which also suggests that this protein is not necessary for centromere clustering. Brero et al., (2005) recently suggested that MeCP2 along with other MBD proteins was involved in centromere clustering during differentiation, although here I have shown that centromeres cluster during the differentiation of mES lacking MeCP2 (*figure* 5.20; *table* 5.4).

Cell Type	% Decrease in number of signals		Time Point (Day)
	Minor Satellite	DAPI foci	
OS25	37	41	18
Suv39h$^{-/-}$	38	49	8
CGR8	23	32	8
MeCP2	32	23	18
WT41	32	21	18
Dnmt3$^{-/-}$	36	26	20
J1	35	16	20

Table 5.4 The percentage decrease in centromeric signals during differentiation of mutant and wild type mES cells. The number of signals counted on day 0 divided by the number counted at the end time point of differentiation, expressed as a percentage.

I also analysed centromere clustering in cells with a reduced level of *de novo* methylation. Similar to previous results *Oct4* did not switch off completely during the differentiation of Dnmt3$^{-/-}$ cells (Jackson et al., 2004) although due their rapid proliferation it did not switch off in the wild type cells either. However, centromeres still clustered during differentiation of the Dnmt3$^{-/-}$ cells as for the other cell types (*table* 5.4; *figure* 5.22). Perhaps the clustering in Dnmt3$^{-/-}$ cells is due to a redundancy in Dnmt3 and one of the other methyl transferases is responsible for centromere clustering in this population of cells, therefore the cells where centromeres do not cluster would die off during differentiation. Some mutant lines clustered less than the OS25 cells, although this was due to spontaneous differentiation in the starting population and the increased cell densities from culturing without the drug selection. I conclude that DNA methylation does not induce clustering. This opposes the hypothesis put forward by Brero et al., (2005), however they were using a myogenic differentiation, whereas I have used an ectodermal differentiation, therefore this affect could be cell type specific. Perhaps more importantly, they formed this hypothesis based on the over expression of MeCP2, whereas here I have used MeCP2 null cells. This would suggest that increasing

the level of MeCP2 within the nucleus can induce clustering, but as I have shown it is not necessary for chromocentre formation during differentiation.

To my knowledge, this is one of the first reports that Dnmt3$^{-/-}$ can differentiate into ectoderm *in vitro*. Most factors shown to influence glia are present in what is essential an astrogliogenic JAK-STAT pathway leading to *GFAP* expression (Nakashima et al., 1999; Song and Ghosh, 2004; Sun et al., 2001; He et al., 2005). The demethylation of a CpG site within the binding element of the STAT transcriptional activator, is required for binding of STAT3 to the *GFAP* promoter and expression of *GFAP* (Teter et al., 1994; Takizawa et al., 2001). Evidence from Dnmt1$^{-/-}$ cells, which display precocious astroglial differentiation *in vivo*, shows that the JAK-STAT pathway needs to be inhibited by DNA methylation to form neurons (Fan et al., 2005). In Dnmt3$^{-/-}$ cells, LIF signalling through the STAT3 pathway is normal (Jackson et al., 2004). Therefore, as some astrocytes do not express either *Dnmt3a* or *Dnmt3b* (Feng et al., 2005), it is not surprising that when pushed towards an ectodermal pathway the Dnmt3$^{-/-}$ cells would follow astroglial lineages, due to STAT3 acting via an unmethylated *GFAP* promoter.

Chapter 6: Discussion

Chapter 6

Discussion

At the beginning of my PhD, I set out to investigate whether there are cytologically distinctive features of nuclear organisation in ES cells, and to determine how these might change during differentiation. Initially I identified the spatial distribution of CTs, centromeres and genes within the hES cell nucleus (chapter 3), however at that time, protocols for the *in vitro* differentiation of these cells were not well developed. Therefore, to study changes in nuclear organisation that accompany the differentiation of ES cells towards a specific lineage, I switched to analysing mES cells, which have more established differentiation protocols (chapter 4). This facilitated, not only the study of nuclear architecture during differentiation, but also enabled questions relating to the role of chromatin silencing factors in neural development to be addressed (chapter 5). To date, this thesis is the only global comparison of mouse and hES cell nuclear organisation, and provides direct evidence for the spatial rearrangement of the genome throughout differentiation. Recently however, there has been increasing interest in epigenetic features that might contribute to the pluripotency of stem cells, and I will try to set my findings within this context.

6.1 Human ES cells have a distinctive nuclear organisation

In chapter 3, I demonstrated that the classic radial distribution of CTs found in differentiated cells is already established in hES cells. Since undifferentiated ES cells do

not express lamins A/C this suggests that the anchoring of gene-poor chromosomes to the nuclear periphery is independent of this nuclear lamin, as has been previously found for emerin (Boyle et al., 2001; Meaburn et al., 2005). The 12p CT, which contains genes important for ES cell function, occupies a more central position in the hES cell nucleus than in a LCL. Interestingly, Kuroda et al., (2004a) have also described a change in the position of chromosome 12 during adipocyte differentiation, in this case the change was not statistically significant, however they compared a terminally differentiated cell to an already committed progenitor, not a pluripotent stem cell. This suggests that relocation of the 12p CT might be characteristic of differentiation towards many lineages. However, whether this change in position is a consequence of higher levels of chromosome 12 gene expression in hES cells, or is functionally related to pluripotency remains to be determined. It has been suggested that HSA12p is transcriptionally advantageous to hES cells, due to the recurrent gain of chromosome 12, including iso12p, in these cells (Draper et al., 2004). To date, no significant change in the number of genes expressed on chromosome 12 between hES and differentiated cells has been reported. In contrast, hEC cells show a four-fold increase in the number of genes highly expressed on chromosome 12, when compared to hES cells (Sperger et al., 2003). Therefore, it would be interesting to compare the location of the 12p CT in hES and hEC cells with their differentiated counterparts, to determine whether maintaining a higher level of gene expression on chromosome 12 would affect the movement of this CT during EC cell differentiation, following the repression of the pluripotent genes.

It is unlikely that 12p is the only CT to change position during differentiation. Whatever this CT displaces by moving towards the periphery, may move into the space vacated by it in the centre of the nucleus. I have also shown that centromeres can relocate from the nuclear interior to the periphery during development, which agrees with the distribution previously shown for differentiated cells (reviewed in Gilchrest et al., 2004). It is still not known what determines the nuclear distribution of centromeres. Levels of histone acetylation have been reported to alter their position in both mouse and human cells (Taddei et al., 2001), which in the mouse, only occurs at satellite repeats upon

differentiation of ES cells (Keohane et al., 1996). This would be consistent with my data; however, other important changes to the hES cell nucleus, such as the association of lamin A/C with the nuclear periphery (Constantinescu et al., 2006), might also influence this relocation.

I have shown that in hES cells the gene-dense 11p15.5 region loops out of its CT whereas 11p13 is active from within the CT, as previously shown for differentiated cells (Mahy et al., 2002b). In accordance with this, a recent study by Brown et al., (2006) has shown that the β-*globin* gene (11p15.4) is predominantly located within the 11p CT in both non-expressing hES cells and expressing erythroid cells. Together these results suggest that some regions of the genome occupy a set position relative to their CT regardless of cell type/ transcriptional status, which is likely to be influenced by the surrounding genomic environment. In contrast, other genomic regions that contain domains of co-ordinately regulated genes e.g. Hox, MHC, EDC (Chambeyron and Bickmore, 2004; Volpi et al., 2000 and Williams et al., 2002), relocate to positions outside of their CTs coincident with their expression.

I have shown that *NANOG*, an important transcription factor for the maintenance of pluripotency, moves with its CT away from the nuclear centre during differentiation, whereas no change in radial nuclear position of 6p or *OCT4* was detected between hES cells and differentiated cells. However, compared with LCLs, *OCT4* is located significantly closer to, or just beyond the CT edge in hES cells. The chromatin structure surrounding *OCT4* has not been studied in hES cells but, in mouse, increased DNA methylation, H3-K9 methylation and histone deacetylation of the *Oct4* promoter are seen in differentiated cells compared with mES cells (Hattori et al., 2004; Feldman et al., 2006). The data I have presented would be consistent with a similar remodelling at the *OCT4* locus in hES cells, and might contribute to its transcriptional regulation.

6.2 Nuclear reorganisation during the differentiation of mouse ES cells

The differentiation of mES cells into ectodermal lineages has been achievable for the last ten years. However, one of the biggest problems facing the stem cell field is that of obtaining a pure population of differentiated cells. No differentiation protocol to date, has obtained a single lineage from an ES cell without the use of selection, and even with selection, the population is constrained by marker genes which are unlikely to be expressed by a single cell type. Therefore, using the OS25 cells described previously (Billon et al., 2002); in chapter 4, I differentiated mES cells into a restricted population of *Oct4* negative, *Sox2* positive cells. This resulted in a mixed population of neuronal and glial precursor cells, which I maintained in their progenitor state by adding bFGF (Li et al., 1998; Okabe et al., 1996). The balance between cell density and concentration of bFGF is key to this differentiation, as low levels of bFGF are known to increase neuronal differentiation, while higher levels expand glial progenitors (Dono et al., 1998; Qian et al., 1997). In addition, bFGF also regulates the expression of epithelial growth factor receptor (EGFR), which correlates with the appearance of astrogliogenic progenitors (Lillien and Raphael, 2000). In comparison to protocols that use either OS25 cells or their parental cell line, which has only *Sox2* under selection, a similar percentage of cells were expressing *Sox1* or *Nestin* at the end of the differentiation (Li et al., 1998; Billon et al., 2002; Perry et al., 2004). However, the absence of EGF in my culture media restricted the ability of these cells to proliferate and as markers of more terminal differentiation repressed *Sox2*, the cells died and the population size was greatly reduced. This differentiation would be improved by the addition of EGF alongside bFGF, to allow for the expansion of these self-renewing neural precursors (Conti et al., 2005).

In chapter 5, I compared the nuclear organisation of mES cells with cells differentiated towards an ectodermal lineage, using the protocol described in the previous chapter. I have shown that in mES cells the distribution of CTs has some similarity to chromosome size, whereas in the differentiated day 18 cell population CTs were arranged according

to gene density. Therefore, the distribution of CTs in mouse changes during differentiation of ES cells towards ectodermal lineages. This result led me to analyse the radial position of specific gene loci on these chromosomes, which was of particular interest since several genes have been reported to relocate away from the nuclear periphery when expressed (Zink et al., 2004; Williams et al., 2006). Out of the four genes analysed, none associate with the nuclear periphery when repressed (*table* 6.1). The two genes analysed that become expressed during the differentiation, *Nestin* and *Olig2*, both moved to a more central location in the nucleus. However, *Oct4* and *Nanog*, which were repressed during the differentiation also moved away from the nuclear periphery. The relocalisation of these pluripotent genes during differentiation reflects the movement of their respective CTs towards the nuclear centre. I therefore concluded that although expression of some neural genes is accompanied by relocation away from the nuclear periphery, the repression of the pluripotent genes *Oct4* and *Nanog* occurs by a mechanism independent of this.

I also located each of these genes relative to their CTs. Unlike in hES cells, where *NANOG* remained in the interior of its CT and the whole CT move, in mES cell, *Nanog* was found significantly closer to the edge of its CT when compared to the differentiated day 18 cells. In contrast *Oct4*, moved significantly nearer the CT edge when repressed in differentiated mouse cells, than in mES cells. I think that this is likely to be due to the activation of the surrounding MHC class I genes, which are not active in mES cells (Tian et al., 1997) and the expression of the class III genes, as I have shown a decondensation of the chromatin fibre between *Oct4* and *H2-Q1* during differentiation. Similarly, *Nestin* also located outside of its CT in a proportion of cells when not expressed, which is probably due to the surrounding genomic environment. The distribution of *Olig2* however, was found to change significantly during the differentiation, although the majority of loci were still located within the CT, there was a 9% increase in loci found >0.2μm outside of its CT. This likely reflects the ~15% increase of *Olig2* expressing cells within the population

Gene	Cell type	Gene expression	Replication timing	Radial gene position	Radial CT position	Position of gene relative to CT
Oct4	hES cells	Yes	-	Towards centre	Towards centre	Outside
	Human LCL	No	-	Towards centre	Towards centre	Edge
	mES cells	Yes	Early	Equidistant	Equidistant	Inside
	Mouse differentiated cells	No	Early	Towards centre	Towards centre	Edge
Nanog	hES cells	Yes	-	Central	Central	Inside
	Human LCL	No	-	Towards periphery	Equidistant	Inside
	mES cells	Yes	Early	Towards periphery	Towards periphery	Edge
	Mouse differentiated cells	No	Middle-late	Towards periphery	Equidistant	Inside
Nestin	mES cells	No	-	Equidistant	Towards periphery	Edge
	Mouse differentiated cells	Yes	-	Towards centre	Towards centre	Edge
Olig2	mES cells	No	Middle-early	Towards periphery	Equidistant	Inside
	Mouse differentiated cells	Yes	Early	Towards centre	Towards periphery	Movement towards outside

Table 6.1 The position of four loci in pluripotent and differentiated cells. The radial position of the four genes and their respective CTs, and the position of these genes relative to their CTs analysed in mES and differentiated cells in chapter 5, alongside results for two of the genes analysed in hES cells and LCL in chapter 3. Human cell lines are highlighted in green. Replication timings are taken from Perry et al., (2004).

It is interesting that both *Oct4* and *Nanog* show different patterns of nuclear organisation between mouse and hES cells, whereas the differentiated cell types analysed from both

species show the same spatial arrangement for these genes. This probably reflects the similarity in expression of their surrounding genomic regions, between mouse neural precursors and human lymphoblasts. Recent a study of α and β-globin genes in mouse and hES cells illustrated the importance of this underlying chromosomal context in cross-species comparisons (Brown et al., 2006). In the human genome, α-globin is within a very gene dense region of open chromatin on HSA16 (102 genes within 2Mb) and predominantly locates outside of its CT, whereas in the mouse genome this gene is situated in a relatively gene-poor region (21 genes within 2Mb) and is frequently located within the CT irrespective of transcriptional status. It has also been suggested that some genes are located to centromeric heterochromatin when silenced (Brown et al., 1997; Skok et al., 2001), however this was not seen for either *Oct4* or *Nanog*.

6.3 Epigenetic modifications and ES cell differentiation

I have shown that there is a global increase in H3-K9me$_2$, whereas levels of both H3-K9ac and H3-K4me$_2$ decrease following the differentiation of mES cells. This is confirmed by other analyses published during the course of my PhD (Lee et al., 2004; Hsieh et al., 2004). However, in the latter stage of this project, I began work using ChIP to identify these modifications at specific gene loci. Preliminary results show that both H3-K4me$_2$ and H3-K9ac are present at the promoter region of *Oct4*, where the gene is expressed in mES cells but not in the differentiated cell population. This is confirmed by previous studies, which show the *Oct4* region to be hyperacetylated in mES cells (Hattori et al., 2004; Kimura et al., 2004). However, both of these modifications were also present at the *Olig2* promoter in mES cells, well in advance of gene expression. Another histone modification, H3-K27, which is thought to prevent early gene expression (Bernstein et al., 2006a; Boyer et al., 2006) has also been reported at the *Olig2* locus in mES cells (Azuara et al., 2006). This combination of epigenetic markers prior to expression was also reported for the neuronal gene *Mash1*, in mES cells (Williams et al., 2006). It is interesting to note that this change in histone modifications

has been shown to accompany a change in the replication timing of some genes during differentiation (Perry et al., 2004; Azuara et al., 2006). In the case of *Mash1, Olig2* and *Nanog* this coincides with their relocation within the nucleus (Williams et al., 2006; and this thesis) whereas *Oct4*, which is early replicating throughout the differentiation, does not change its position within the nucleus (*table* 6.1).

6.4 Progressive centromere clustering during differentiation

In chapter 5, I have shown that unlike hES cells, centromeres were distributed throughout the *z*-plane of both mES cells and their differentiated counterparts, although in agreement with Mayer et al., (2005) significantly more centromeres were located at the nuclear periphery in differentiated cells. This would be consistent with the general movement of CTs toward the centre of the nucleus. It was also very apparent during this differentiation that centromeres were progressively clustering to forms chromocentres, shown previously in neuronal cells (Manuelidis, 1984) and during myogenesis (Brero et al., 2005; Terranova et al., 2005). A recent study reported that only major satellite is involved in this clustering, whereas minor satellite is located at the periphery of the clusters and forms individual entities (Guenatri et al., 2004). However, my data would suggest that both major and minor satellite sequences cluster during differentiation.

To investigate epigenetic mechanisms that might be responsible for the nuclear reorganisation and clustering of centromeric heterochromatin, I analysed this clustering during the differentiation of mES cells with null mutations for Suv39h, MeCP2 and Dnmt3a/3b. In the $Suv39^{-/-}$ cells both the differentiation and the centromere clustering occurred as normal, therefore H3-K9me_3 at major and minor satellites is not required for centromere clustering, which was later confirmed by Brero et al., (2005). However, whereas Brero et al., (2005) have reported that over-expression of MeCP2 can induce clustering in the absence of differentiation in myoblasts. Therefore, they suggested that DNA methylation and MeCP2 are both needed to promote chromocentre clustering.

However, using knock-out ES cells I have shown that neither DNA methylation nor MeCP2 is necessary for the clustering of centromeric heterochromatin during differentiation. This is particularly interesting because mutation in Dnmt3b causes an aberrant chromatin structure at pericentric heterochromatin (Xu et al., 1999). Therefore, over expression of MBPs might cause excess clustering in interphase nuclei (Brero et al., 2005), but DNA methylation is not necessary for their formation during differentiation.

6.5 Future directions

The finding that CT 12p was located in a different position in the hES cell nucleus when compared to a LCL, poses an interesting question, do large regions of the genome that are involved in stem cell function all change position during differentiation, or is this result specific to chromosome 12p? The most enriched region of 'stem cell' genes is on HSA 17, which is the other chromosome to be gained by hES cells in culture (Ramalho-Santos et al., 2002; Draper et al., 2004). However, being one of the most gene-dense chromosomes, HSA 17 is situated towards the nuclear centre in differentiated cells (Boyle et al., 2001). Therefore, it is unlikely that this CT would change position during differentiation, although it would be interesting to follow the clusters of genes involved in 'stemness' on chromosome 17, to see if they are rearranged within the nucleus. It is suggested that CTs themselves have a 'polar' organisation, whereby gene-rich regions are in the centre of the nucleus and gene-poor regions and centromeres are located towards the nuclear periphery (Ferguson and Ward, 1992; Amrichová et al., 2003). This arrangement is not fully established in hES cells, as I have shown that centromeres are located within the centre of the nucleus. Therefore, it would be interesting to follow the early differentiation of hES cells to find out when this reorganisation occurs, and how it relates to the association of proteins such as Lamin A/C at the nuclear periphery. Similarly, I have shown that the radial organisation of CTs is already present in hES cells, so it would be interesting to look at cells prior to the mid-blastocyst stage and find out when this arrangement is first apparent, and how the genome becomes organised

following fertilization i.e. what comes first, transcription or organisation? In the mouse a recent paper has reported that the organisation of chromocentres is completed at the blastocyst stage, corresponding with the onset of differentiation (Martin et al., 2006). It would be interesting to see if this organisation occurs on a comparative time scale in human development, as I have shown that hES cells have yet to establish this spatial distribution of centromeres.

It is possible that the distribution of centromeres in hES cells is related to their rapid cell cycle time. This would be addressed by repeating the analysis on cells isolated at different times during the cell cycle, and might provide further understanding of their spatial arrangement. Another question to be addressed is where are these genes relocating? Studies have shown the specific genes locate to PML bodies (Shiels et al., 2001; Wang et al., 2004b) SC-35 nuclear speckles (Brown et al., 2006) and transcription factories (Osborne et al., 2004) when active, and centromeric heterochromatin when repressed (Brown et al., 1997), although currently the factors which determines whether or not a gene leaves its CT to associate with one of these regions are still unclear. Over the next few years, as more regions are identified that locate to nuclear organelles and the epigenome is progressively mapped, markers that identify these genomic regions should become more apparent. It would also be useful to control the movement of genes within the nucleus. Currently this is not possible on a single gene basis, but as Tsuji-Takayama et al., (2004) have shown that demethylating the genome with 5-azacytidine switches pluripotent genes back on, it would be intriguing to see if re-expression of *Oct4* cause the gene to relocate back outside of its CT in human cells.

Recently, the idea that genes are maintained in an open state in ES cells, has been supported by the discovery of H3-K27 within lineage specific genes, which prevents their expression via polycomb mediated repression (Bernstein et al., 2006a; Boyer et al., 2006). However, confirmation of this theory would be provided by a combined sucrose sedimentation / genomic microarray approach, as used by Gilbert et al., (2004) to demonstrate the distribution of open and closed chromatin across the human genome in a

LCL. Polycomb proteins are also located at pericentromeric heterochromatin (Saurin et al., 1998). This is especially relevant in Suv39h$^{-/-}$ mice, whereby loss of pericentric H3-K9me$_3$ is compensated by H3-K27me$_3$ and H3-K9me suggesting cross talk between constitutive and facultative heterochromatin to rescue the repressed state (Peters et al., 2003). Therefore, these proteins might be responsible for the clustering of centromeres during differentiation.

The nuclear reprogramming capacity of oocytes was first demonstrated in mammals nearly ten years ago (Wilmut et al., 1997). Since then nuclear transfer has been shown to generate mice from post-mitotic cells, such as neurons, demonstrating that even terminally differentiated cell retain the potential for pluripotency (Eggan et al., 2004). Recently, hES cells were shown to be capable of nuclear reprogramming in somatic cell fusion (Cowan et al., 2005). However, with the announcement this year from the Yamanaka Lab in Kyoto, that a combination of only Oct4 and three other transcription factors can reprogram an adult fibroblast back into an ES cell (Zwaka personal communication) the stem cell field is looking for better ways to define these cells. Surface markers and gene expression profiles will not be enough to predict the behaviour of ES cells *in vivo*. Therefore, a comprehensive epigenetic map of pluripotent stem cells is needed if we are ever going to follow a direct lineage.

References

Abeyta M.J., Clark A.T., Rodriguez R.T., Bodnar M.S. et al., (2004) Unique gene expression signatures of independently-derived human embryonic stem cell lines. *Hum. Mol. Genet.* **13**(6):601-608.

Abranches R., Beven A.F., Aragon-Alcaide L and Shaw P.J. (1998) Transcription sites are not correlated with chromosome territories in wheat nuclei. *J. Cell Biol.* **143**:5-12.

Acampora D. and Simeone A. (1999) Understanding the roles of Otx1 and Otx2 in the control of brain morphogenesis. *Trends Neurosci.* **22**:116-122.

Akhmanova A., Verkerk T., Langeveld A., Grosveld F., et al., (2000) Characterisation of transcriptionally active and inactive chromatin domains in neurons. *J Cell Sci.* **113**:4463-4474.

Aladjem M.I., Spike B.T., Rodewald L.W., Hope T.J. et al., (1998) ES cells do not activate p53-dependent stress responses and undergo p53-independent apoptosis in response to DNA damage. *Curr. Biol.* **8**(3):145-155.

Alcobia I., Dilão R. and Parreira L. (2000) Spatial associations of centromeres in the nuclei of hematopoietic cells: evidence for cell-type-specific organization patterns. *Blood* **95**(5):1608-1615.

Alcobia I., Quina A.S., Neves H., Clode N., et al., (2003) The spatial organisation of centromeric heterochromatin during normal lymphopoiesis: evidence for ontogenically determined spatial patterns. *Exp. Cell Res.* **290**:358:369.

Amir R.E., Van Den Veyver I.B., Wan M., Tran C.Q. et al., (1999) Rett syndrome is caused by mutations in X-linked MECP2, encoding methyl-CpG-binding protein 2. *Nat. Genet.* **23**:185-188.

Amit M., Carpenter M.K., Inokuma M.S., Chiu C.P. et al., (2000) Clonally derived human embryonic stem cell lines maintain pluripotency and proliferative potential for prolonged periods of culture. *Dev Biol.* **227**(2):271-278.

Amrichová J., Lukášová E., Kozubek S. and Kozubek M. (2003) Nuclear and territorial topography of chromosome telomeres in human lymphocytes. *Exp. Cell Res.* **289**:11-29.

Andrulis E.D., Neiman A.M., Zappulla D.C. and Sternglanz R. (1998) Perinuclear localization of chromatin facilitates transcriptional silencing. *Nature* **394**:592-595.

Arney K.L. and Fisher A.G. (2004) Epigenetic aspects of differentiation. *J Cell Sci.* **117**:4355-4363.

Assady S., Maor G., Amit M., Itskovitz-Eldor J., (2001) Insulin Production by Human Embryonic Stem Cells. *Diabetes* **50**:1691-1697.

Avilion A.A., Nicolis S.K., Pevny L.H., Perez L. et al., (2003) Multipotent cell lineages in early mouse development depend on SOX2 function. *Genes Dev.* **17**:126-140.

Azuara V., Perry P., Sauer S., Spivakov M., et al., (2006) Chromatin signatures of pluripotent cell lines. *Nat. Cell Biol.* **8**(5):532-538.

Bain G., Kitchens D., Yao M., Huettner J.E., et al., (1995) Embryonic stem cells express neuronal properties in vitro. *Dev. Biol.* **168**:342-357.

Bain G., Ray W.J., Yao M. and Gottlieb D.I. (1996) Retinoic acid promotes neural and represses mesodermal gene expression in mouse embryonic stem cells in culture. *Biochem. Biophys. Res. Commun.* **223**(3):691-694.

Bannister A.J., Zegerman P., Partridge J.F., Miska E.A., et al., (2001) Selective recognition of methylated lysine 9 on histone H3 by the HP1 chromo domain. *Nature* **410**(6824):120-124.

Bantignies F., Grimaud C., Lavrov S., Gabut M., et al., (2003) Inheritance of Polycomb-dependent chromosomal interactions in Drosophila. *Gen. Dev.* **17**:2406-2420.

Barres B.A., Lazar M.A. and Raff M.C., (1994) A novel role for thyroid hormone, glucocorticoids and retinoic acid in timing oligodendrocyte development. *Development* **120**:1097-1108.

Bártová E., Kozubek S., Jirsová P., Kozubek M., et al., (2002) Nuclear structure and gene activity in human differentiated cells. *J Structural Biol.* **139**:76-89.

Baxter J., Sauer S., Peters A., John R., et al., (2004) Histone hypomethylation is an indicator of epigenetic plasticity in quiescent lymphocytes. *EMBO J.* **23**(22)4462-4472.

Beaujean N., Hartshorne G., Cavilla J., Taylor J. et al., (2004) Non-conservation of mammalian preimplantation methylation dynamics. *Curr. Biol.* **14**:R266-R267.

Beddington R.S.P. and Robertson E.J., (1989) An assessment of the developmental potential of embryonic stem cells in the midgestation mouse embryo. *Development* **105**:733-737.

Beil M., Dürschmied D., Paschke S., Schreiner B., et al., (2002) Spatial distribution patterns of interphase centromeres during retinoic acid-induced differentiation of promyelocytic leukemia cells. *Cytometry* **47**:217-225.

Ben-Shushan E., Sharir H., Pikarsky E. and Bergman Y. (1995) A dynamic balance between ARP-1/COUP-TFII, EAR-3/COUP-TFI, and retinoic acid receptor: retinoid X receptor heterodimers regulates Oct-3/4 expression in embryonal carcinoma cells. *Mol. Cell. Biol.* **15**(2):1034-1048.

Bernstein B.E., Kamal M., Lindblad-Toh K., Bekiranov S., et al., (2005) Genomic maps and comparative analysis of histone modifications in human and mouse. *Cell* **120**:169-181.

Bernstein B.E., Mikkelsen T.S., Xie X., Kamal M., et al., (2006a) A bivalent chromatin structure marks key developmental genes in embryonic stem cells. *Cell* **125**:315-326.

Bernstein E., Duncan E.M., Masui O., Gil J., et al., (2006b) Mouse polycomb proteins bind differentially to methylated histone H3 and RNA and are enriched in facultative heterochromatin. *Mol. Cell. Biol.* **26**(7):2560-2569.

Bestor T., Laudano A., Mattaliano R. and Ingram V. (1988) Cloning and sequencing of a cDNA encoding DNA methyltransferase of mouse cells. The carboxyl-terminal domain of the mammalian enzymes is related to bacterial restriction methyltransferases. *J Mol. Biol.* **203**(4):971-83.

Bickmore W.A., Mahy N.L. and Chambeyron S. (2004) Do higher-order chromatin structure and nuclear reorganization play a role in regulating Hox gene expression during development? *Cold Spring Harb. Symp. Quant. Biol.* **69**:251-257.

Billon N., Jolicoeur C., Ying Q.L., Smith A., et al., (2002) Normal timing of oligodendrocyte development from genetically engineered, lineage-selectable mouse ES cells. *J Cell Sci.* **115**(18):3657-3665.

Boiani M. and Schöler H.R. (2005) Regulatory networks in embryo-derived pluripotent stem cells. *Nat. Rev. Mol. Cell. Biol.* **6**(11):872-884.

Boisvert F.M., Hendzel M.J. and Bazett-Jones D.P. (2000) Promyelocytic leukemia (PML) nuclear bodies are protein structures that do not accumulate RNA. *J. Cell Biol.* **148**:283-292.

Bolzer A., Kreth G., Solovei I., Koehler D., et al., (2005) Three-dimensional maps of all chromosomes in human male fibroblast nuclei and prometaphase rosettes. *PLOS Biol.* **3**:5.

Bourc'his D., Xu G.L., Lin C.S., Bollman B. et al., (2001) Dnmt3L and the establishment of maternal genomic imprints. *Science* **294**:2536-2539.

Boyer L.A., Lee T.I., Cole M.F., Johnstone S.E. et al., (2005) Core transcriptional regulatory circuitry in human embryonic stem cells. *Cell* **122**:1-10.

Boyer L.A., Plath K., Zeitlinger J., Brambrink T., et al., (2006) Polycomb complexes repress developmental regulators in murine embryonic stem cells. *Nature* **441**(7091):349-353.

Boyes J. and Bird A. (1991) DNA methylation inhibits transcription indirectly via a methyl-CpG binding protein. *Cell* **64**:1123-1134.

Boyle S., Gilchrist S., Bridger J.M., Mahy N.L., (2001) The spatial organization of human chromosomes within the nuclei of normal and emerin-mutant cells. *Hum. Mol. Genet.* **10**(3):211-219

Bracken A.P., Dietrich N., Pasini D., Hansen K.H., et al., (2006) Genome-wide mapping of Polycomb target genes unravels their roles in cell fate transitions. *Genes Dev.* **20**(9):1123-1136.

Bradley A., Evans M.J., Kaufman M.H. and Robertson E., (1984) Formation of germ-line chimeras from embryo-derived teratocarcinoma cell lines. *Nature* **309**:255-256.

Branco M.R. and Pombo A. (2006) Intermingling of chromosome territories in interphase suggests role in translocations and transcription-dependent associations. *PLOS Biol.* **4**(5):0780-0788.

Brandenberger R., Wei H., Zhang S., Lei S. et al., (2004) Transcriptome characterization elucidates signalling networks that control human ES cell growth and differentiation. *Nat. Biotechnol.* **22**(6):707-716.

Brero A., Easwaran H.P., Nowak D., Grunewald I., et al., (2005) Methyl CpG-binding proteins induce large-scale chromatin reorganization during terminal differentiation. *J. Cell Biol.* **169**(5):733-743.

Bridger J.M. and Bickmore W.A. (1998) Putting the genome on the map. *TIG.* **14**(10):403-409.

Bridger J.M., Boyle S., Kill I.R. and Bickmore W.A. (2000) Re-modelling of nuclear architecture in quiescent and senescent human fibroblasts. *Current Biology* **10**:149-152.

Brinster R.L., (1974) The effect of cells transferred into the mouse blastocyst on subsequent development. *J. Exp. Med.* **140**:1049-1056.

Brown J.M., Leach J., Reittie J.E., Atzberger A., et al., (2006) Coregulated human globin genes are frequently in spatial proximity when active. *J. Cell Biol.* **172**(2):177-187.

Brown K.E., Baxter J., Graf D., Merkenschlager M., et al., (1999) Dynamic repositioning of genes in the nucleus of lymphocytes preparing for cell division. *Mol. Cell* **3**:207-217.

Brown K.E., Guest S.S., Smale S.T., Hahm K., et al., (1997) Association of transcriptionally silent genes with Ikaros complexes at centromeric heterochromatin. *Cell* **91**:845-854.

Brustle O., Jones K.N., Learish R.D., Karram K., et al., (1999) Embryonic stem cell-derived glial precursors: A source of myelinating transplants. *Science* **285**:754-756.

Bylund M., Andersson E., Novitch B.G. and Muhr J. (2003) Vertebrate neurogenesis is counteracted by Sox1-3 activity. *Nat. Neurosci.* **6**(11):1162-1168.

Caballero I.M. and Hendrich B. (2005) MeCP2 in neurons: closing in on the causes of Rett syndrome. *Hum. Mol. Genet.* **14**(1):R19-R26.

Cao R., Wang L., Wang H., Xia L., et al., (2002) Role of histone H3 lysine 27 methylation in Polycomb-group silencing. *Science* **298**(5595):1039-1043.

Caron H., van Schaik B., van der Mee M., Baas F., et al., (2001) The human transcriptome map: clustering of highly expressed genes in chromosome domains. *Science* **291**:1289-1292.

Carpenter M.K., Rosler E.S., Fisk G.J., Brandenberger R., et al., (2004) Properties of four human embryonic stem cell lines maintained in a feeder-free culture system. *Dev. Dynamics* **229**:243-258.

Carvalho C., Pereira H.M., Ferreira J., Pina C., et al., (2001) Chromosomal G-dark bands determine the spatial organization of centromeric heterochromatin in the nucleus *Mol. Biol. Cell* **12**:3563-3572.

Casolari J.M., Brown C.R., Komili S., West J., et al., (2004) Genome-wide localization of the nuclear transport machinery couples transcriptional status and nuclear organization. *Cell* **117**(4):427-439.

Catena R., Tiveron C., Ronchi A., Porta S. et al., (2004) Conserved POU Binding DNA Sites in the Sox2 Upstream Enhancer Regulate Gene Expression in Embryonic and Neural Stem Cells. *J Biol. Chem.* **279**(40):41846-41857.

Cerda M.C., Berrios S., Fernandez-Donoso R., Garagna S., et al., (1999) Organisation of complex nuclear domains in somatic mouse cells. *Biol. Cell* **91**:55-65.

Chaly N. and Munro S.B. (1996) Centromeres reposition to the nuclear periphery during L6E9 myogenesis *in vitro*. *Exp. Cell Res.* **223**(2):274-278.

Chambers I. and Smith A. (2004) Self-renewal of teratocarcinoma and embryonic stem cells. *Oncogene* **23**:7150-7160.

Chambers I., Colby D., Robertson M., Nichols J. et al., (2003) Function expression cloning of Nanog, a pluripotency sustaining factor in embryonic stem cells. *Cell* **133**:643-655.

Chambeyron S. and Bickmore W.A. (2004) Chromatin decondensation and nuclear reorganization of the HoxB locus upon induction of transcription. *Gen. Dev.* **18**:1119-1130.

Chambeyron S., Da Silva N.R., Lawson K.A. and Bickmore W.A., (2005) Nuclear re-organisation of the *Hoxb* complex during mouse embryonic development. *Development* **132**:2215-2223.

Chawengsaksophak K., James R., Hammond V.E., Kontgen F. et al., (1997) Homeosis and intestinal tumours in Cdx2 mutant mice. *Nature* **386**(6620):84-87.

Chen D., Ma H., Hong H., Koh SS., et al., (1999) Regulation of transcription by a protein methyltransferase. *Science* **284**(5423):2174-2177.

Chen R., Akbarian S., Tudor M. and Jaenisch R. et al., (2001) Deficiency of methyl-CpG binding protein-2 in CNS neurons results in a Rett-like phenotype in mice. *Nat. Genet.* **27**:327-331.

Chen T., Ueda Y., Dodge J.E., Wang Z., et al., (2003a) Establishment and maintenance of genomic methylation patterns in mouse embryonic stem cells by Dnmt3a and Dnmt3b. *Mol. Cell. Biol.* **23**(16)5594-5605.

Chen T.R., Hay R.J. and Macy M.L. (1983) Intercellular karyotypic similarity in near-diploid cell lines of human tumor origins. *Cancer Genet. Cytogenet.* **10**:351-362.

Chen W.G., Chang Q., Lin Y., Meissner A. et al., (2003b) Derepression of BDNF transcription involves calcium-dependent phosphorylation of MeCP2. *Science* **302**:885-889.

Ching R.W., Dellaire G., Eskiw C.H. and Bazett-Jones D.P. (2005) PML bodies: a meeting place for genomic loci? *J. Cell Sci.* **118**:847-854.

Chiquoine A.D. (1954) Distribution of alkaline phosphomonoesterase in the central nervous system of the mouse embryo. *J. Comp. Neurol.* **100**(2):415-439.

Chubb J.R., Boyle S., Perry P. and Bickmore W.A. (2002) Chromatin motion is constrained by association with nuclear compartments in human cells. *Curr. Biol.* **12**(6):439-445.

Clark A.T., Rodriguez R.T., Bodnar M.S., Abeyta M.J. et al., (2004). Human STELLAR, NANOG, and GDF3 genes are expressed in pluripotent cells and map to chromosome 12p13, a hotspot for teratocarcinoma. *Stem Cells* **22**:169-179.

Cmarko D., Verschure P.J., Otte A.P., van Driel R., et al., (2003) Polycomb group gene silencing proteins are concentrated in the perichromatin compartment of the mammalian nucleus. *J. Cell Sci.* **116**:335-343.

Cohen D.R., Matarazzo V., Palmer A.M., Tu Y., et al., (2003) Expression of MeCP2 in olfactory receptor neurons is developmentally regulated and occurs before synaptogenesis. *Mol. Cell Neurosci.* **22**(4):417-429.

Constantinescu D., Gray H.L., Sammak P.J., Schatten G.P., et al., (2006) Lamin A/C expression is a marker of mouse and human embryonic stem cell differentiation. *Stem Cells* **24**(1):177-185.

Conti L., Pollard S.M., Gorba T., Reitano E., et al., (2005) Niche-independent symmetrical self-renewal of a mammalian tissue stem cell. *PLOS Biol.* **3**(9):1594-1606.

Cook P.R., (2002) Predicting three-dimensional genome structure from transcriptional activity. *Nat Genet.* **32**(3):347-352.

Cowan C.A., Atienza J., Melton D.A., and Eggan K. (2005) Nuclear reprogramming of somatic cells after fusion with human embryonic stem cells. *Science* **309**(5739):1369-1373.

Cowan C.A., Klimanskaya I., McMahon J., Atienza J. et al., (2004) Derivation of Embryonic Stem-Cell Lines from Human Blastocysts. *N. Engl. J. Med.* **350**(13)1353-1356.

Craig J.M. and Bickmore W.A. (1994) The distribution of CpG islands in mammalian chromosomes. *Nat. Genet.* **7**:376-382.

Crawford G.F., Holt I.E., Mullikin J.C., Tai D., et al., (2004) Identifying gene regulatory elements by genome-wide recovery of DNase hypersensitive sites. *Proc. Natl. Acad. Sci. USA* **101**(4):992-997.

Cremer M., Küpper K., Wagler B., Wizelman L., et al., (2003) Inheritance of gene-density related higher order chromatin arrangements in normal and tumor cell nuclei. *J. Cell Biol.* **162**(5):809-820.

Cremer M., von Hase J., Volm T., Brero A., et al., (2001) Non-random radial higher-order chromatin arrangements in nuclei of diploid human cells. *Chromosome Res.* **9**(7):541-567.

Cremer T. and Cremer C. (2001) Chromosome territories, nuclear architecture and gene regulation in mammalian cells. *Nat. Rev. Genet.* **2**:292-301.

Cremer T., Cremer C., Baumann H., Luedtke E.K., et al., (1982) Rabl's model of the interphase chromosome arrangement tested in Chinese hamster cells by premature chromosome condensation and laser-UV-microbeam experiments. *Hum. Genet.* **60**(1):46-56.

Croft J., Bridger J.M., Boyle S., Perry P., (1999) Differences in the localization and morphology of chromosomes in the human nucleus *J. Cell Biol.* **145**(6):1119-1131.

Csink A.K. and Henikoff S. (1996) Genetic modification of heterochromatic association and nuclear organization in Drosophila. *Nature* **381**:529-531.

Cuthbert G.L., Daujat S., Snowden A.W., Erdjument-Bromage H., et al., (2004) Histone deamination antagonizes arginine methylation. *Cell* **118**:545-553.

Dahlstrand J., Zimmerman L.B., McKay R.D.G. and Lendahl U. (1992) Characterization of the human nestin gene reveals a close evolutionary relationship to neurofilaments. *J. Cell Sci.* **103**:589-597.

Dean W., Santos F., Stojkovic M., Zakhartchenko V., et al., (2001) Conservation of methylation reprogramming in mammalian development: Aberrant reprogramming in cloned embryos. *Proc. Natl. Acad. Sci. USA* **98**:13734-13738.

Dellaire G. and Bazett-Jones D.P. (2004) PML nuclear bodies: dynamic sensors of DNA damage and cellular stress. *BioEssays* **26**:963-977.

Dernburg A.F., Broman K.W., Fung J.C., Marshall W.F., et al., (1996) Perturbation of nuclear architecture by long-distance chromosome interactions. Cell 85:745-759.

Dietzel S.K., Schiebel K., Little G., Edelmann P., et al., (1999) The 3D positioning of ANT2 and ANT3 genes within female X chromosome territories correlates with gene activity. *Exp. Cell Res.* **252**:363-375.

Doetschman T.C., Eistetter H., Katz M., Schmidt W. et al., (1985) The in vitro development of blastocyst-derived embryonic stem cell lines: formation of visceral yolk sac, blood islands and myocardium. *J. Embryol. Exp. Morphol.* **87**:27-45.

Dono R., Texido G., Dussel R., Ehmke H., et al., (1998) Impaired cerebral cortex development and blood pressure regulation in FGF-2-deficient mice. *EMBO J.* **17**(15):4213-4225.

Donovan P.J., Stott D., Cairns L.A., Heasman J., et al., (1986) Migratory and postmigratory mouse primordial germ cells behave differently in culture. *Cell* **44**:831-838.

Draper J.S., Pigott C., Thomson J.A. and Andrews P.W. (2002) Surface antigens of human embryonic stem cells: change upon differentiation in culture. *J. Anat.* **200**:249-258.

Draper J.S., Smith K., Gokhale P., Moore H.D., et al., (2004) Recurrent gain of chromosomes 17q and 12 in cultured human embryonic stem cells. *Nat. Biotech.* **22**(1)53-54.

Drukker M., Katz G., Urbach A., Schuldiner M., et al., (2002) Characterization of the expression of MHC proteins in human embryonic stem cells. *Proc. Natl. Acad. Sci. USA* **99**(15):9864-9869.

Earnshaw W.C. and Rothfield N. (1985) Identification of a family of human centromere proteins using autoimmune sera from patients with scleroderma. *Chromosoma* **91**(3-4):313-321.

Eggan K, Baldwin K., Tackett M., Osborne J., et al., (2004) Mice cloned from olfactory sensory neurons. *Nature* **428**(6978):44-49.

Ehrlich M., Gama-Sosa M.A., Huang L.H., Midgett R.M. et al., (1982) Amount and distribution of 5-methylcytosine in human DNA from different types of tissues of cells. *Nucleic Acids Res.* **10**(8):2709-2721.

Ericson J., Rashbass P., Schedl A., Brenner-Morton S., et al., (1997) Pax6 controls progenitor cell identity and neuronal fate in response to graded Shh signalling. *Cell* **90**:169-180.

Esteller M. and Herman J.G. (2002) Cancer as an epigenetic disease: DNA methylation and chromatin alterations in human tumours. *J. Pathol.* **196**:1-7.

Evans M.J. and Kaufman M., (1981) Establishment in culture of pluripotential cells from mouse embryos. *Nature* **292**:154-156.

Evans M.J. and Kaufman M., (1983) Pluripotential cells grown directly from normal mouse embryos. *Cancer Surv.* **2**:185-208.

Evans M.J., (1972) The isolation and properties of a clonal tissue culture strain of pluripotent mouse teratoma cells. *J. Embryol. Exp. Morphol.* **28**:163-176.

Fan G., Beard C., Chen R.Z., Csankovszki G. et al., (2001) DNA hypomethylation perturbs the function and survival of CNS neurons in postnatal animals. *J. Neurosci.* **21**(3):788-797.

Fan G., Martinowich K., Chin M.H., He F. et al., (2005) DNA methylation controls the timing of astrogliogenesis through regulation of JAK-STAT signalling. *Development* **132**:3345-3356.

Feldman N., Gerson A., Fang J., Li E. et al., (2006) G9a-mediated irreversible epigenetic inactivation of Oct-3/4 during early embryogenesis. *Nat. Cell Biol.* **8**(2)188-194.

Felsenfeld G. and Groudine M. (2003) Controlling the double helix. *Nature* **421**:448-453.

Feng J., Chang H., Li E. and Fan G. (2005) Dynamic expression of de novo DNA methyltransferase Dnmt3a and Dnmt3b in the central nervous system. *J. Neurosci. Res.* **79**:734-746.

Feng Q. and Zhang Y. (2001) The MeCP2 complex represses transcription through preferential binding, remodelling, and deacetylating methylated nucleosomes. *Genes Dev.* **15**(7):827-832.

Ferguson M. and Ward D. (1992) Cell cycle dependent chromosomal movement in pre-mitotic human T-lymphocyte nuclei. *Chromosoma* **101**:557-565.

Ferreira J., Paolella G., Ramos C. and Lamond A.I. (1997) Spatial organization of large-scale chromatin domains in the nucleus: A magnified view of single chromosome territories. *J. Cell Biol.* **139**(7):1597-1610.

Ferri A.L., Cavallaro M., Braida D., Di Cristofano A., et al., (2004) Sox2 deficiency causes neurodegeneration and impaired neurogenesis in the adult mouse brain. *Development* **131**(15):3805-3819.

Fischle W., Wang Y. and Allis D. (2003) Histone and chromatin cross-talk. *Curr. Opin. Cell Biol.* **15**:172-183.

Fisher A.G. and Merkenschlager M. (2002) Gene silencing, cell fate and nuclear organisation. *Curr. Opin. Genet. Dev.* **12**(2):193-197.

Fox N., Damjanov I., Martinez-Hernandez A., Knowles B.B., et al., (1981) Immunohistochemical localization of the early embryonic antigen (SSEA-1) in postimplantation mouse embryos and fetal and adult tissues. *Dev. Biol.* **83**(2):391-398.

Fraichard A., Chassande O., Bilbaut G., Dehay C., et al., (1995) In vitro differentiation of embryonic stem cells into glial cells and functional neurons. *J. Cell Sci.* **108**:3181-3188.

Francastel C., Walters M.C., Groudine M. and Martin D.I.K. (1999) A functional enhancer suppresses silencing of a transgene and prevents its localization close to centromeric heterochromatin. *Cell* **99**:259-269.

Fujikura J., Yamato E., Yonemura S., Hosoda K. et al., (2002) Differentiation of embryonic stem cells is induced by GATA factors. *Gene Dev.* **16**:784-789.

Fujita N., Watanabe S., Ichimura T., Tsuruzoe S. et al., (2003) Methyl-CpG binding domain 1 (MBD1) interacts with the Suv39h1-HP1 heterochromatic complex for DNA methylation-based transcriptional repression. *J. Biol. Chem.* **278**(26):24132-24138.

Fujiwara Y., Komiya T., Kawabata H., Sato M., et al., (1994) Isolation of a DEAD-family protein gene that encodes a murine homolog of Drosophila vasa and its specific expression in germ cell lineage. *Proc. Natl. Acad. Sci. USA* **91**(25):12258-12262.

Fuks F., Burgers W.A., Godin N., Kasai M. et al., (2001) Dnmt3a binds deacetylases and is recruited by a sequence specific repressor to silence transcription. *EMBO J.* **20**(10):2536-2544.

Fuks F., Hurd P.J., Deplus R. and Kouzarides T. (2003b) The DNA methyltransferases associate with HP1 and the SUV39H1 histone methyltransferase. *Nuc. Acids Res.* **31**(9):2305-2312.

Fuks F., Hurd P.J., Wolf D., Nan X. et al., (2003a) The methyl-CpG-binding protein MeCP2 links DNA methylation to histone methylation. *J Biol. Chem.* **278**(6):4035-4040.

Fulka H., Mrazek M., Tepla O. and Fulka Jr J. (2004) DNA methylation pattern in human zygotes and developing embryos. *Reproduction* **128**:703-708.

Gabay L., Lowell S., Rubin L.L. and Anderson D.J. (2003) Deregulation of dorsoventral patterning by FGF confers trilineage differentiation capacity on CNS stem cells in vitro. *Neuron* **40**:485-499.

Gasser S.M. (2002) Visualizing chromatin dynamics in interphase nuclei. *Science* **296**(5572):1412-1416.

Gazave E., Gautier P., Gilchrist S. and Bickmore W.A. et al., (2005) Does radial nuclear organisation influence DNA damage? *Chromo. Res.* **13**:377-388.

Gidekel S. and Bergman Y. (2002) A unique developmental pattern of Oct-3/4 DNA methylation is controlled by a cis-demodification element. *J. Biol. Chem.* **277**(37)34521-34530.

Gilbert N., Boyle S., Fiegler H., Woodfine K., et al., (2004) Chromatin architecture of the human genome: gene-rich domains are enriched in open chromatin fibers. *Cell* **118**:555-566.

Gilbert N., Boyle S., Sutherland H., de La Heras J., (2003) Formation of facultative heterochromatin in the absence of HP1 *EMBO.* **22**:5540-5550.

Gilchrist S., Gilbert N., Perry P. and Bickmore W.A. (2004) Nuclear organization of centromeric domains is not perturbed by inhibition of histone deacetylase. *Chromosome Res.* **12**:505-516.

Ginis I., Luo Y., Miura T., Thies S. et al., (2004) Differences between human and mouse embryonic stem cells. *Dev. Biol.* **269**:360-380

Goldmit M., Ji Y., Skok J., Roldan E., et al., (2005) Epigenetic ontogeny of the Igk locus during B cell development. *Nat. Immun.* **6**(2)198-203.

Gowher H., Leismann O. and Jeltsch A. (2000) DNA of *Drosophila melanogaster* contains 5-methylcytosine. *EMBO J.* **19**:6918-6923.

Gritti A., Cova L., Parati E.A., Galli R., et al., (1995) Basic fibroblast growth factor supports the proliferation of epidermal growth factor-generated neuronal precursor cells of the adult mouse CNS. *Neurosci. Lett.* **185**(3):151-154.

Gu P., LeMenuet D., Chung A.C.K., Mancini M., et al., (2005) Orphan nuclear receptor GCNF is required for the repression of pluripotency genes during retinoic acid-induced embryonic stem cell differentiation. *Mol. Cell. Biol.* **25**(19):8507-8519.

Guan X.Y., Zhang H., Bittner M., Jiang Y., (1996) Chromosome arm painting probes. *Nat. Genet.* **12**:10-11.

Guenatri M., Bailly D., Maison C. and Almouzni G. (2004) Mouse centric and pericentric satellite repeats form distinct functional heterochromatin. *J. Cell Biol.* **166**(4):493-505.

Guy J., Hendrich B., Holmes M., Martin J.E. et al., (2001) A mouse MeCP2-null mutation causes neurological symptoms that mimic Rett syndrome. *Nat. Genet.* **27**:322-326.

Haaf T. and Schmid M. (1991) Chromosome topology in mammalian interphase nuclei. *Exp. Cell Res.* **192**(2):325-332.

Haaf T., Steinlein C. and Schmid M. (1990) Nucleolar transcriptional activity in mouse Sertoli cells is dependent on centromere arrangement. *Exp. Cell Res.* **191**(1):157-160.

Habermann F.A., Cremer M., Walter J., Kreth G., et al., (2001) Arrangement of macro- and microchromosomes in chicken cells. *Chromosome Res.* **9**:569-584.

Hall I.M., Shankaranarayana G.D., Noma K., Ayoub N., et al., (2002) Establishment and maintenance of a heterochromatin domain. *Science* **297**(5590):2215-2218.

Hata K., Okano M., Lei H. and Li E. (2002) Dnmt3L cooperates with the Dnmt3 family of *de novo* DNA methyltransferases to establish maternal imprints in mice. *Development* **129**:1983-1993.

Hattori N., Nishino K., Ko Y., Hattori N. et al., (2004) Epigenetic control of mouse *Oct-4* gene expression in embryonic stem cells and trophoblast stem cells. *J. Biol. Chem.* **279**(17)17063-17069.

Hay D.C., Sutherland L., Clark J. and Burdon T., (2004) Oct-4 knockdown induces similar patterns of endoderm and trophoblast differentiation markers in human and mouse embryonic stem cells. *Stem Cells* **22**:225-235.

He F., Ge W., Martinowich K., Becker-Catania S. et al., (2005) A positive autoregulatory loop of Jak-STAT signalling controls the onset of astrogliogenesis. *Nat. Neurosci.* **8**(5):616-25.

Heard E., Rougeulle C., Arnaud D., Avner P., et al., (2001) Methylation of histone H3 at Lys-9 is an early mark on the X chromosome during X inactivation. *Cell* **107**:727-738.

Henderson J.K., Draper J.S., Baillie H.S., Fishel S., et al., (2002) Preimplantation human embryos and embryonic stem cells show comparable expression of stage-specific embryonic antigens. *Stem Cells* **20**:329-337.

Hendrich B. and Bird A. (1998) Identification and characterization of a family of mammalian methyl-CpG binding proteins. *Mol. Cell. Biol.* **18**(11):6538-6547.

Hendrich B., Guy J., Ramsahoye B., Wilson V.A. et al., (2001) Closely related proteins MBD2 and MBD3 play distinctive but interacting roles in mouse development. *Genes Dev.* **15**:710-723.

Hoffman L.M., Hall L., Batten J.L., Young H. et al., (2005) X-inactivation status varies in human embryonic stem cell lines. *Stem Cells* **23**(10):1468-78.

Hogan B., Beddington R., Constantini F. and Lacy E. (1994) Manipulating the mouse embryo: A laboratory manual. New York: Cold Spring Harbor Lab. Press.

Höpfl G., Gassmann M. and Desbaillet I. (2004) Differentiating embryonic stem cells into embryonic bodies. *Meth. Mol. Biol.* **254**:79-98.

Horike S.I., Cai S., Miyano M., Cheng J.F. et al., (2005) Loss of silent-chromatin looping and impaired imprinting of DLX5 in Rett syndrome. *Nat. Genet.* **37**(1):31-40.

Hsieh J. and Gage F.H., (2005) Chromatin remodeling in neural development and plasticity. *Curr. Opin. Cell Biol.* **17**:664-671.

Hsieh J., Nakashima K., Kuwabara T., Mejia E., et al., (2004) Histone deacetylase inhibition-mediated neuronal differentiation of multipotent adult neural progenitor cells. *Proc. Natl. Acad. Sci. USA* **101**(47):16659-16664.

Hsu T.C. (1975) A possible function of constitutive heterochromatin: the bodyguard hypothesis. *Genetics* **79**:137-150.

Hsu T.C., Cooper J.E., Mace M.L. Jr. and Brinkley B.R. (1971) Arrangement of centromeres in mouse cells. *Chromosoma.* **34**(1):73-87.

Hurst L.D., Pal C. and Lercher M.J. (2004) The evolutionary dynamics of eukaryotic gene order. *Nat. Rev. Genet.* **5**:299-310.

Hyslop L., Stojkovic M., Armstrong L., Walter T. et al., (2005) Downregulation of NANOG induces differentiation of human embryonic stem cells to extraembryonic lineages. *Stem Cells* **23**(8):1035-1043.

Iborra F.J., (2002) The path that RNA takes from the nucleus to the cytoplasm: a trip with some surprises. *Histochem. Cell Biol.* **118**:95-103.

Ivanova N.B., Dimos J.T., Schaniel C., Hackney J.A. et al., (2002) A stem cell molecular signature. *Science*. **298**:601-604

Iwama A, Oguro H, Negishi M, Kato Y, et al., (2004) Enhanced self-renewal of hematopoietic stem cells mediated by the polycomb gene product Bmi-1. *Immunity.* **21**(6):843-51.

Jackson J.P., Lindroth A.M., Cao X. and Jacobsen S.E. (2002) Control of CpNpG DNA methylation by the KRYPTONITE histone H3 methyltransferase. *Nature* **416**(6880):556-60.

Jackson M., Krassowska A., Gilbert N., Chevassut T., et al., (2004) Severe global DNA hypermethylation blocks differentiation and induces histone hyperacetylation in embryonic stem cells. *Mol. Cell. Biol.* **24**(20):8862-8871.

Jaenisch R. (1997) DNA methylation and imprinting: why bother? *Trends Genet.* **13**:323-329.

Jenuwein T. and Allis C.D. (2001) Translating the histone code. *Science* **293**:1074-1080.

Jones P.A. and Baylin S.B. (2002) The fundamental role of epigenetic events in cancer. *Nat. Rev. Genet.* **3**:415-428.

Jones P.A., Wolkowicz M.J., Rideout W.M.3rd. Gonzales F.A. et al., (1990) *De novo* methylation of the MyoD1 CpG island during the establishment of immortal cell lines. *Proc. Natl. Acad. Sci. U S A.* **87**(16):6117-6121.

Jones P.L., Veenstra G.J., Wade P.A., Vermaak D., et al., (1998) Methylated DNA and MeCP2 recruit histone deacetylase to repress transcription. *Nat. Genet.* **19**(2):187-191.

Jung B.P., Jugloff D.G., Zhang G., Logan R., et al., (2003) The expression of methyl CpG binding factor MeCP2 correlates with cellular differentiation in the developing rat brain and in cultured cells. *J. Neurobiol.* **55**:86-96.

Kahan B.W. and Ephrussi B., (1970) Developmental potentialities of clonal in vitro cultures of mouse testicular teratoma. *J. Natl Cancer Inst.* **44**(5):1015–1036.

Kaji K., Caballero I.M., MacLeod R., Nichol J. et al., (2006) The NuRD component Mbd3 is required for pluripotency of embryonic stem cells. *Nat. Cell Biol.* **8**(3):285-292.

Kalantry S., Mills K.C., Yee D., Otte A.P., et al., (2006) The polycomb group protein Eed protects the inactive X-chromosome from differentiation-induced reactivation. *Nat. Cell Biol.* **8**(2):195-202.

Kamminga L.M., Bystrykh L.V., de Boer A., Houwer S., (2006) The Polycomb group gene Ezh2 prevents hematopoietic stem cell exhaustion. *Blood* **107**(5):2170-2179

Kaufman D.S., Hanson E.T., Lewis R.L., Auerbach R. et al., (2001) Hematopoietic colony-forming cells derived from human embryonic stem cells. *Proc. Natl. Acad. Sci. USA* **98**:10716-10721.

Kawai J., Hirose K., Fushiki S., Hirotsune S. et al., (1994) Comparison of DNA methylation patterns among mouse cell lines by restriction landmark genomic scanning. *Mol. Cell Biol.* **14**(11):7421-7427.

Kawasaki H., Mizuseki K., Nishikawa S., Kaneko S., et al., (2000) Induction of midbrain dopaminergic neurons from ES cells by stromal cell-derived inducing activity. *Neuron* **28**:31-40.

Keller G., Kennedy M., Papayannopoulou T., and Wiles M.V. (1993) Hematopoietic commitment during embryonic stem cell differentiation in culture. *Mol. Cell. Biol.* **13**(1):473-486

Keller G.M. (1995) In vitro differentiation of embryonic stem cells. *Curr. Opin. Cell Biol.* **7**(6):862-869.

Keohane A.M., O'Neill L.P., Belyaev N.D., Lavender J.S., et al., (1996) X-Inactivation and histone H4 acetylation in embryonic stem cells. *Dev. Biol.* **180**:618-630.

Kim S.H., McQueen P.G., Lichtman M.K., Shevach E.M., et al., (2004) Spatial genome organization during T-cell differentiation. *Cytogenet. Genome Res.* **105**:292-301.

Kim T.H., Barrera L.O., Zheng M., Qu C., et al., (2005) A high-resolution map of active promoters in the human genome. *Nature* **436**(7052):876-880.

Kimura H., Tada M., Nakatsuji N. and Tada T. (2004) Histone code modifications on pluripotential nuclei of reprogrammed somatic cells. *Mol. Cell. Biol.* **24**(13):5710-5720.

Kipling D., Wilson H.E., Mitchell A.R., Taylor B.A. and Cooke H.J. (1994) Mouse centromere mapping using oligonucleotide probes that detect variants of the minor satellite. *Chromosoma.* **103**(1):46-55.

Kleinsmith L.J. and Pierce G.B., (1964) Multipotentiality of single embryonal carcinoma cells. *Cancer Res.* **24**:1544-1552.

Klose R.J. and Bird A.P. (2006) Genomic DNA methylation: the mark and its mediators. *TIBS.* **31**(2):89-97.

Klose R.J., Sarraf S.A., Schmiedeberg L., McDermott S.M., et al., (2005) DNA binding selectivity of MeCP2 due to a requirement for A/T sequences adjacent to methyl-CpG. *Mol. Cell* **19**:667-678.

Klose R.J., Yamane K., Bae Y., Zhang D., et al., (2006) The transcriptional repressor JHDM3A demethylates trimethyl histone H3 lysine 9 and lysine 36. *Nature.* **442**(7100):312-316.

Kondo T. and Raff M. (2004) Chromatin remodeling and histone modification in the conversion of oligodendrocyte precursors to neural stem cells. *Genes Dev.* **18**:2963-2972.

Kosak S.T. and Groudine M. (2004) Form follows function: the genomic organization of cellular differentiation. *Gen. Dev.* **18**:1371-1384.

Kosak S.T., Skok J., Medina K.L., Riblet R., et al., (2002) Subnuclear compartmentalization of immunoglobulin loci during lymphocyte development. *Science* **296**:158-162.

Kourmouli N., Jeppesen P., Mahadevhaiah S., Burgoyne P., et al., (2004) Heterochromatin and tri-methylated lysine 20 of histone H4 in animals. *J. Cell Sci.* **117**:2491-2501.

Kuroda M., Tanabe H., Yoshida K., Oikawa K., et al., (2004a) Alteration of chromosome positioning during adipocyte differentiation. *J. Cell Sci.* **117**:5897-5903.

Kuroda T., Tada M., Kubota H., Kimura H. et al., (2004b) Octamer and Sox Elements Are Required for Transcriptional *cis* Regulation of *Nanog* Gene Expression. *Mol. Cell Biol.* **25**(6):2475-2485.

Kurz A., Lampel S., Nickolenko J.E., Bradl J., et al., (1996) Active and inactive genes localize preferentially in the periphery of chromosome territories. *J. Cell Biol.* **135**(5):1195-1205.

Kuzmichev A., Margueron R, Vaquero A, Preissner T.S., et al., (2002) Composition and histone substrates of polycomb repressive group complexes change during cellular differentiation. *Proc. Natl. Acad. Sci. USA.* **102**(6):1859-1864.

Lachner M., O'Carroll D., Rea S., Mechtler K., et al., (2001) Methylation of histone H3 lysine 9 creates a binding site for HP1 proteins. *Nature* **410**:116-120.

Lachner M., O'Sullivan R.J. and Jenuwein T. (2003) An epigenetic road map for histone lysine methylation. *J. Cell Sci.* **116**:2117-2124.

Lansdorp P.M., Verwoerd N.P., van de Rijke F.M., Dragowska V., et al., (1996) Heterogeneity in telomere length of human chromosomes. *Hum. Mol. Genet.* **5**(5):685-691.

Larsen F., Gundersen G., Lopez R. and Prydz H (1992) CpG islands as gene markers in the human genome. *Genomics* **13**(4):1095-107.

LaSalle J.M., Goldstine J., Balmer D. and Greco C.M. (2001) Quantitative localisation of heterogeneous methyl-CpG binding protein 2 (MeCP2) expression phenotypes in normal and Rett syndrome brain by laser scanning cytometry. *Hum. Mol. Genet.* **10**:1729-1740

Lee J., Hart S.R.L. and Skalnik D.G., (2004) Histone deacetylase activity is required for embryonic stem cell differentiation. *Genesis* **38**:32-38.

Lee S-H., Lumelsky N., Studer L., Auerbach J.M., et al., (2000) Efficient generation of midbrain neurons from mouse embryonic stem cells. *Nature Biotech.* **18**:675-679.

Lee T.I., Jenner R.G., Boyer L.A., Guenther M.G., et al., (2006) Control of developmental regulators by polycomb in human embryonic stem cells. *Cell* **125**:301-313.

Lehnertz B., Ueda Y., Derijck A.A.H.A., Braunschweig U. et al., (2003) Suv39h-mediated histone H3 lysine 9 methylation directs DNA methylation to major satellite repeats at pericentric heterochromatin. *Curr. Biol.* **13**:1192-1200.

Lei H., Oh S.P., Okano M., Jüttermann R. et al., (1996) De novo DNA cytosine methyltransferase activities in mouse embryonic stem cells. *Development* **122**:3195-3205.

Lendahl U., Zimmerman L.B. and McKay R.D. (1990) CNS stem cells express a new class of intermediate filament protein. *Cell* **60**(4):585-595.

Lercher M.J., Urrutia A.O. and Hurst L.D. (2002) Clustering of housekeeping genes provides a unified model of gene order in the human genome. *Nat. Genet.* **31**:180-183.

Levenstein M.E., Ludwig T.E., Xu R.H., Llanas R.A. et al., (2006) Basic FGF support of human embryonic stem cell self-renewal. *Stem Cells* **24**(3):568-574

Lewis J.D., Meehan R.R., Henzel W.J., Maurer-Fogy I. et al., (1992) Purification, sequence, and cellular localization of a novel chromosomal protein that binds to methylated DNA. *Cell* **69**(6):905-914.

Li E. (2002) Chromatin modification and epigenetic reprogramming in mammalian development. *Nat. Rev. Genet.* **3**:662-673.

Li E., Bestor T.H. and Jaenisch R. et al., (1992) Targeted mutation of the DNA methyltransferase gene results in embryonic lethality. *Cell* **69**:915-926.

Li M., Pevny L., Lovell-Badge R. and Smith A. (1998) Generation of purified neural precursors from embryonic stem cells by lineage selection. *Curr. Biol.* **8**:971-974.

Lillien H. and Raphael L. (2000) BMP and FGF regulate the development of EGF-responsive neural progenitor cells. *Development* **127**(22):4993-5005.

Litt M.D., Simpson M., Gaszner M., Allis C.D., et al., (2001) Correlation between histone lysine methylation and developmental changes at the chicken β-globin locus. *Science* **293**:2453-2455.

Liu S., Qu Y., Stewart T.J., Howard M.J., et al., (2000) Embryonic stem cells differentiate into oligodendrocytes and myelinate in culture and after spinal cord transplantation. *Proc. Natl. Acad. Sci. USA* **97**(11):6126-6131.

Loh Y.H., Wu Q., Chew J.L., Vega V.B., et al., (2006) The Oct4 and Nanog transcription network regulates pluripotency in mouse embryonic stem cells. *Nat. Genet.* **38**(4):431-440.

Lu Q.R., Sun T., Zhu Z., Ma N., et al., (2002) Common developmental requirement for Olig function indicates a motor neuron/oligodendrocyte connection. *Cell* **109**(1):75-86.

Ludwig T.E., Levenstein M.E., Jones J.M., Berggren W.T. et al., (2006) Derivation of human embryonic stem cells in defined conditions. *Nat. Biotechnol.* **24**(2):185-187

Luger K., Mader A.W., Richmond R.K., Sargent D.F. et al., (1997) Crystal structure of the nucleosome core particle at 2.8 A resolution. *Nature* **389**:251-260.

Lundgren M., Chow C., Sabbattini P., Georgiou A., et al., (2000) Transcription factor dosage affects changes in higher order chromatin structure associated with activation of a heterochromatic gene. *Cell* **103**:733-743.

Lunyak V.V., Burgess R., Prefontaine G.C., Nelson C., et al., (2002) Corepressor-dependent silencing of chromosomal regions encoding neuronal genes. *Science* **298**:1747-1752.

Lyko F., Ramsahoye B.H., and Jaenisch R. (2000) DNA methylation in *Drosophila melanogaster*. *Nature* **408**:538-540.

Mahy N.L., Perry P.E. and Bickmore W.A. (2002b) Gene density and transcription influence the localization of chromatin outside of chromosome territories detectable by FISH. *J. Cell Biol.* **159**:753-763.

Mahy N.L., Perry P.E., Gilchrist S., Baldock R.A., et al., (2002a) Spatial organization of active and inactive genes and noncoding DNA within chromosome territories *J. Cell Biol.* **157**(4):579-589.

Maison C., Bailly D., Peters A.H., Quivy J.P., et al., (2002) Higher-order structure in pericentric heterochromatin involves a distinct pattern of histone modification and an RNA component. *Nat. Genet.* **30**:329-334.

Manuelidis L. (1984) Different central nervous system cell types display distinct and nonrandom arrangements of satellite DNA sequences. *Proc Natl Acad Sci U S A.* **81**(10):3123-3127.

Manuelidis L. (1985) Indications of centromere movement during interphase and differentiation. *Ann N Y Acad Sci.* **450**:205-221.

Manuelidis L. (1990) A view of interphase chromosomes. *Science* **250**:1533-1540.

Marshall W.F., Dernburg A.F., Harmon B., Agard D.A., et al., (1996) Specific interactions of chromatin with the nuclear envelope: positional determination within the nucleus in Drosophila melanogaster. *Mol. Biol. Cell* **7**:825-842.

Martens J.H.A., Sullivan R.J.O., Braunschweig U., Opravil S., et al., (2005) The profile of repeat-associated histone lysine methylation states in the mouse epigenome. *EMBO* **24**:800-812.

Martin C., Beaujean N., Brochard V., Audouard C., et al., (2006) Genome restructuring in mouse embryos during reprogramming and early development. *Dev. Biol.* **292**:317-332.

Martin G.R. and Evans M.J., (1975) The formation of embryoid bodies in vitro by homogeneous embryonal carcinoma cell cultures derived from isolated single cells. In *Teratomas and Differentiation*, ed. MI Sherman, D Solter, New York: Academic 169-187.

Martin G.R., (1981) Isolation of a pluripotent cell line from early mouse embryos cultured in medium conditioned by teratocarcinoma stem cells. *Proc. Natl. Acad. Sci. USA* **78**:7634-7638.

Martinowich K., Hattori D., Wu H., Fouse S. et al., (2003) DNA methylation-related chromatin remodelling in activity-dependent *Bdnf* gene regulation. *Science* **302**:890-893.

Martou G. and De Boni U. (2000) Nuclear topology of murine, cerebellar Purkinje neurons: changes as a function of development. *Exp Cell Res.* **256**(1):131-139.

Matin M.M., Walsh J.R., Gokhale P.J., Draper J.S., et al., (2004) Specific knockdown of oct4 and β2-microglobulin expression by RNA interference in human embryonic stem cells and embryonic carcinoma cells. *Stem Cells* **22**:659-668.

Matsui Y., Zsebo K. and Hogan B.L.M., (1992) Derivation of pluripotential embryonic stem cells from murine primordial germ cells in culture. *Cell* **70**:841-847.

Maye P., Becker S., Kasameyer E., Byrd N., et al., (2000) Indian hedgehog signaling in extraembryonic endoderm and ectoderm differentiation in ES embryoid bodies. *Mech. Dev.* **94**:117-132.

Mayer R., Brero A., von Hase J., Schroeder T., et al., (2005) Common themes and cell type specific variations of higher order chromatin arrangements in the mouse. *BMC Cell Biol.* **6**:44

Meaburn K.J., Levy N., Toniolo D. and Bridger J.M. (2005) Chromosome positioning is largely unaffected in lymphoblastoid cell lines containing emerin or A-type lamin mutations. *Biochem. Soc. Trans.* **33**(6):1438-1440.

Melnick A. and Licht J.D. (1999) Deconstructing a disease: RARalpha, its fusion partners, and their roles in the pathogenesis of acute promyelocytic leukemia. *Blood.* **93**(10):3167-215.

Merkenschlager M., Amoils S., Roldan E., Rahemtulla A., et al., (2004) Centromeric repositioning of coreceptor loci predicts their stable silencing and the CD4/CD8 lineage choice. *J. Exp. Med.* **200**(11)1437-1444.

Meshorer E., Yellajoshula D., George E., Scambler P.J., et al., (2006) Hyperdynamic plasticity of chromatin proteins in pluripotent embryonic stem cells. *Dev. Cell* **10**:105-116.

Miao F. and Natarajan R. (2005) Mapping global histone methylation patterns in the coding regions of human genes. *Mol. Cell. Biol.* **25**(11)4650-4661.

Minami M., Inoue M., Wei S., Takeda K. et al., (1996) STAT3 activation is a critical step in gpl30-mediated terminal differentiation and growth arrest of a myeloid cell line. *Proc. Natl. Acad. Sci. USA* **93**:3963-3966,

Mintz B. and Illmensee K., (1975) Normal genetically mosaic mice produced from malignant teratocarcinoma cells. *Proc. Nat. Acad. Sci. USA* **72**(9):3585-3589.

Mitchell A.R., Gosden J.R. and Miller D.A. (1985) A cloned sequence, p82H, of the alphoid repeated DNA family found at the centromeres of all human chromosomes. *Chromosoma.* **92**(5):369-377.

Mitsui K., Tokuzawa Y., Itoh H., Segawa K. et al., (2003) The homeoprotein Nanog is required for maintenance of pluripotency in mouse epiblast and ES cells. *Cell* **113**:631-642.

Mizuguchi R., Sugimori M., Takebayashi H., Kosako H., et al., (2001) Combinatorial roles of Olig2 and neurogenin2 in the coordinated induction of pan-neuronal and subtype-specific properties of motoneurons. *Neuron* **31**:757-771.

Moen P.T. Jr., Johnson C.V., Byron M., Shopland L.S., (2004) Repositioning of muscle-specific genes relative to the periphery of SC-35 domains during skeletal myogenesis. *Mol. Biol. Cell* **15**(1):197-206.

Molenaar C., Wiesmeijer K., Verwoerd N.P., Khazen S., et al., (2003) Visualizing telomere dynamics in living mammalian cells using PNA probes. *EMBO.* **22**(24)6631-6641.

Moroi Y., Peebles C., Fritzler M.J., Steigerwald J., et al., (1980) Autoantibody to centromere (kinetochore) in scleroderma sera. *Proc. Natl. Acad. Sci. U S A.* **77**(3):1627-1631.

Mountford P., Zevnik B., Dowel A., Nichols J., et al., (1994) Dicistronic targeting constructs: Reporters and modifiers of mammalian gene expression. *Proc. Natl. Acad. Sci. USA* **91**:4303-4307.

Murrell A., Rakyan V.K. and Beck S (2005) From genome to epigenome. *Hum. Mol. Genet.* **14**(1):R3–R10.

Nagele R.G., Velasco A.Q., Anderson W.J., McMahon D.J., et al., (2000) Telomere association in interphase nuclei: possible role in maintenance of interphase chromosome topology. *J. Cell Sci.* **114**:377-388.

Nakashima K., Yanagisawa M., Arakawa M., Kimura N. et al., (1999) Synergistic signalling in fetal brain by STAT3-Smad1 complex bridged by p300. *Science* **284**:479-482.

Nan X., Campoy F.J. and Bird A. (1997) MeCP2 is a transcriptional repressor with abundant binding sites in genomic chromatin. *Cell* **88**(4):471-481.

Nan X., Ng H.H., Johnson C.A., Laherty C.D. et al., (1998) Transcriptional repression by the methyl-CpG-binding protein MeCP2 involves a histone deacetylase complex. *Nature* **393**(6683):386-389.

Ng H.H. and Bird A. (1999) DNA methylation and chromatin modification. *Curr. Opin. Genet. Dev.* **9**:158-163.

Ng H.H., Jeppesen P. and Bird A. (2000) Active repression of methylated genes by the chromosomal protein MBD1. *Mol. Cell Biol.* **20**(4):1394-1406.

Ng H.H., Zhang Y., Hendrich B., Johnson C.A. et al., (1999) MBD2 is a transcriptional repressor belonging to the MeCP1 histone deacetylase complex. *Nat Genet.* **23**(1):58-61.

Nichols J., Chambers I., Taga T. and Smith A.G., (2001) Physiological rationale for responsiveness of mouse epiblast and embryonic stem cells to gp130 cytokines. *Development* **128**:2333-2339.

Nichols J., Zevnik B., Anastassiadis K., Niwa H. et al., (1998) Formation of pluripotent stem cells in the mammalian embryo depends on the POU transcription factor Oct-4. *Cell* **95**:379-391.

Nielsen J.A, Hudson L.D. and Armstrong R.C. (2002) Nuclear organization in differentiating oligodendrocytes. *J. Cell Sci.* **115**:4071-4079.

Nielsen S.J., Schneider R., Bauer U.M., Bannister A.J., (2001) Rb targets histone H3 methylation and HP1 to promoters *Nature* **412**:561-565.

Nishikawa S.I., Nishikawa S., Hirashima M., Matsuyoshi N., et al., (1998) Progressive lineage analysis by cell sorting and culture identifies FLK1+VE-cadherin+cells at a diverging point of endothelial and hemopoietic lineages. *Development* **125**:1747-1757.

Niwa H., Burdon T., Chambers I. and Smith A.G., (1998) Self-renewal of pluripotent embryonic stem cells is mediated via activation of STAT3. *Genes Dev.* **12**:2048-2060.

Niwa H., Miyazaki J. and Smith A.G., (2000) Quantitative expression of Oct-3/4 defines differentiation, dedifferentiation or self-renewal of ES cells. *Nat. Genet.* **24**:372-376.

Niwa H., Toyooka Y., Shimosato D., Strumpf D. et al., (2005) Interaction between Oct3/4 and Cdx2 determines trophectoderm differentiation. *Cell* **123**(5):917-929.

Nobel M., Pröschel C. and Mayer-Pröschel M. (2004) Getting a GR(i)P on oligodendrocyte development. *Dev. Biol.* **265**:33-52.

Novitch B.G., Chen A.I. and Jessell T.M. (2001) Coordinate regulation of motor neuron subtype identity and pan-neuronal properties by the bHLH repressor Olig2. *Neuron* **31**:773-789.

Novitch B.G., Wichterle H., Jessell T.M. and Sockanathan S., (2003) A requirement for retinoic acid-mediated transcriptional activation in ventral neural patterning and motor neuron specification. *Neuron* **40**:81-85.

Ochs R.L. and Press R.I. (1992) Centromere autoantigens are associated with the nucleolus. *Exp. Cell Res.* **200**(2)339-350.

Ogawa H., Ishiguro K., Gaubatz S., Livingston D.M., et al., (2002) A complex with chromatin modifiers that occupies E2F- and Myc-responsive genes in G0 cells. *Science* **296**(5570):1132-1136.

Okabe S., Forsberg-Nilsson K., Spiro A.K., Segal M. et al., (1996) Development of neuronal precursor cells and functional postmitotic neurons from embryonic stem cells in vitro. *Mech. Dev.* **59**:89-102.

Okada Y., Shimazaki T., Sobue G., and Okano H., (2004) Retinoic-acid-concentration-dependent acquisition of neural cell identity during in vitro differentiation of mouse embryonic stem cells. *Dev. Biol.* **275**:124-142.

Okamoto K., Okazawa H., Okuda A., Sakai M. et al., (1990) A novel octamer binding transcription factor is differentially expressed in mouse embryonic cells. *Cell* **60**(3):461-472.

Okano M., Bell D.W., Haber D.A. and Li E. (1999) DNA methyltransferases Dnmt3a and Dnmt3b are essential for de novo methylation and mammalian development. *Cell* **99**:247-257.

Okano M., Xie S. and Li E. (1998) Cloning and characterization of a family of novel mammalian DNA (cytosine-5) methyltransferases. *Nat. Genet.* **19**:219-220.

Okumura-Nakanishi S., Saito M., Niwa H. and Ishikawa F., (2005) Oct-3/4 and Sox2 Regulate Oct-3/4 Gene in Embryonic Stem Cells. *J. Biol. Chem.* **280**(7):5307-5317.

O'Neill L.P. and Turner B.M. (1995) Histone H4 acetylation distinguishes coding regions of the human genome from heterochromatin in a differentiation-dependent but transcription-independent manner. *EMBO J.* **14**(16):3946-3957.

Orlando V. (2003) Polycomb, Epigenomes, and Control of Cell Identity. *Cell* **112**:599-606.

Osborne C.S., Chakalova L., Brown K.E., Carter D., et al., (2004) Active genes dynamically colocalise to shared sites of ongoing transcription. *Nat. Genet.* **36**(10)1065-1071.

Palmieri S.L., Peter W., Hess H. and Scholer H.R. et al., (1994) Oct-4 transcription factor is differentially expressed in the mouse embryo during establishment of the first two extraembryonic cell lineages involved in implantation. *Dev. Biol.* **166**(1):259-67.

Panning B. and Jaenisch R. (1996) DNA hypomethylation can activate Xist expression and silence X-linked genes. *Genes Dev.* **10**(16):1991-2002.

Parada L.A., McQueen P.G. and Misteli T. (2004) Tissue-specific spatial organization of genomes. *Genome Biol.* **5**:R44.

Parreira L., Telhada M., Ramos C., Hernandez R., et al., (1997) The spatial distribution if human immunoglobulin genes within the nucleus: evidence for gene topography independent of cell type and transcriptional activity. *Hum. Genet.* **100**:588-594.

Pera M.F. and Trounson A.O., (2004) Human embryonic stem cells: prospects for development. *Development* **131**:5515-5525.

Pera M.F., Andrade J., Houssami S., Reubinoff B. et al., (2004) Regulation of human embryonic stem cell differentiation by BMP-2 and its antagonist noggin. *J. Cell. Sci.* **117**: 1269-1280.

Pera M.F., Reubinoff B., Trounson A. et al., (2000) Human embryonic stem cells. *J. Cell Sci.* **113**:5-10.

Perry P., Sauer S., Billon N., Richardson W.D., et al., (2004) A dynamic switch in the replication timing of key regulator genes in embryonic stem cells upon neuronal induction. *Cell Cycle* **3**(12)1645-1650.

Pesce M. and Scholar H.R. (2000) Oct-4: control of totipotency and germline determination. *Mol. Reprod. Dev.* **55**(4):452-457.

Peters A.H.F.M., Kubicek S., Mechtler K., O'Sullivan R.J., et al., (2003) Partitioning and plasticity of repressive histone methylation states in mammalian chromatin. *Mol. Cell* **12**:1577-1589.

Peters A.H.F.M., O'Carroll D., Scherthan H., Mechtler K., et al., (2001) Loss of the Suv39h histone methyltransferases impairs mammalian heterochromatin and genome stability. *Cell* **107**:323-337.

Pevny L.H., Sockanathan S., Placzek M. and Lovell-Badge R. (1998) A role for SOX1 in neural determination. *Development* **125**:1967-1978.

Phair R.D., Scaffidi P., Elbi C., Vecerová J., et al., (2004) Global nature of dynamic protein-chromatin interactions in vivo: Three dimensional genome scanning and dynamic interaction networks of chromatin proteins. *Mol. Cell. Biol.* **24**(14):6393-6402.

Plath K., Fang J., Mlynarczyk-Evans S.K., Cao R., et al., (2003) Role of histone H3 lysine 27 methylation in X inactivation. *Science* **300**:131-135.

Pombo A., Cuello P., Schul W., Yoon J-B., et al., (1998) Regional and temporal specialization in the nucleus: a transcriptionally-active nuclear domain rich in PTF, Oct1 and PIKA antigens associates with specific chromosomes early in the cell cycle. *EMBO J.* **17**(6):1768-1778.

Qian X., Davis A.A., Goderie S.K. and Temple S. (1997) FGF2 concentration regulates the generation of neurons and glia from multipotent cortical stem cells. *Neuron.* **18**(1):81-93.

Raff M.C., Lillien L.E., Richardson W.D., Burne J.E., et al., (1988) Platelet-derived growth factor from astrocytes drives the clock that times oligodendrocyte development in culture. *Nature* **333**:562-565.

Ragoczy T., Telling A., Sawado T., Groudine M., et al., (2003) A genetic analysis of chromosome territory looping: diverse roles for distal regulatory elements. *Chromosome Res.* **11**:513-525.

Rajan P. and McKay R.D.G., (1998) Multiple routes to astrocyte differentiation in the CNS. *J. Neurosci.* **18**(10):3620-3629.

Ralston A. and Rossant J., (2005) Genetic regulation of stem cell origins in the mouse embryo. *Clin. Genet.* **68**:106-112

Ramalho-Santos M., Yoon S., Matsuzaki Y., Mulligan R.C., et al., (2002) "Stemness": Transcriptional profiling of embryonic and adult stem cells. *Science* **298**:597-600

Rastan S. and Robertson E., (1985) X chromosome deletions in embryo-derived (EK) cell lines associated with the lack of X chromosome inactivation. *J. Embryol. Exp. Morphol.* **90**:379-388.

Rea S., Eisenhaber F., O'Carroll D., Strahl B., et al., (2000) Regulation of chromatin structure by site-specific histone H3 methyltransferase. *Nature* **406**:593-599.

Reeves S.A., Helman L.J., Allison A. and Israel M.A. (1989) Molecular cloning and primary structure of human glial fibrillary acidic protein. *Proc. Natl. Acad. Sci. U S A.* **86**(13):5178-5182.

Reim G. and Brand M. (2002) Spiel-ohne-grenzen/pou2 mediates regional competence to respond to Fgf8 during zebrafish early neural development. *Development* **129**(4):917-933.

Reubinoff B.E., Itsykson P., Turetsky T., Pera M.F. et al., (2001) Neural progenitors from human embryonic stem cells. *Nat. Biotechnol.* **19**:1134-1140.

Reubinoff B.E., Pera M.F., Fong C.Y., Trounson A. et al., (2000) Embryonic stem cell lines from human blastocysts: somatic differentiation in vitro. *Nat. Biotechnol.* **18**(4):399-404.

Rhee I., Bachman K.E., Park B.H., Jair K.W. et al., (2002) DNMT1 and DNMT3b cooperate to silence genes in human cancer cells. *Nature* **416**(6880):552-556.

Richards E.J. and Elgin S.C. (2002) Epigenetic codes for heterochromatin formation and silencing: rounding up the usual suspects. *Cell* **108**(4):489-500.

Richards M., Tan S-P., Tan J-H., Chen W-K. et al., (2004) The transcriptome profile of human embryonic stem cells as defined by SAGE. *Stem Cells* **22**:51-64.

Robertson K.D. and Wolffe A.P. (2000) DNA methylation in health and disease. *Nat. Rev. Genet.* **1**:11-19.

Rodda D.J., Chew J-L., Lim L-H., Loh Y-H., et al., (2005) Transcriptional regulation of Nanog by OCT4 and SOX2. *J. Biol. Chem.* **280**(26):24731-24737.

Roh T.Y., Cuddapah S. and Zhao K. (2005) Active chromatin domains are defined by acetylation islands revealed by genome-wide mapping. *Genes Dev.* **19**:542-552.

Roh T.Y., Ngau W.C., Cui K., Landsman D., et al., (2004) High-resolution genome-wide mapping of histone modifications. *Nat. Biotechnol.* **22**(8):1013-1016.

Rohwedel J., Guan K. and Wobus A.M. et al., (1999) Induction of cellular differentiation by retinoic acid in vitro. *Cells Tissues Organs* **165**(3-4):190-202.

Rohwedel J., Kleppisch T., Pich U., Guan K., et al., (1998) Formation of postsynaptic-like membranes during differentiation of embryonic stem cells *in vitro*. *Exp. Cell Res.* **239**:214-225.

Rolletschek A., Chang H., Guan K., Czyz J., et al., (2001) Differentiation of embryonic stem cell-derived dopaminergic neurons is enhanced by survival-promoting factors. *Mech. Dev.* **105**:93-104.

Rosner M.H., Vigano M.A., Ozato K., Timmons P.M. et al., (1990) A POU-domain transcription factor in early stem cells and germ cells of the mammalian embryo. *Nature* **345**(6277):686-692.

Rossant J. and McBurney M.W. (1982) The developmental potential of a euploid male teratocarcinoma cell line after blastocyst injection. *J. Embryol. Exp. Morphol.* **70**:99-112

Rowitch D.H. and McMahon A.P. (1995) Pax-2 expression in the murine neural plate precedes and encompasses the expression domains of Wnt-1 and En-1. *Mech. Dev.* **52**(1):3-8.

Rugg-Gunn P.J., Ferguson-Smith A.C. and Pederson R.A. (2005) Epigenetic status of human embryonic stem cells. *Nat. Genet.* **37**(6):585-587.

Sabbattini P., Lundgren M., Georgiou A., Chow C., et al., (2001) Binding of Ikaros to the lambda5 promoter silences transcription through a mechanism that does not require heterochromatin formation. *EMBO J.* **20**(11):2812-2822.

Sabo P.J., Humbert R., Hawrylycz M., Wallace J.C., et al., (2004) Genome-wide identification of DNaseI hypersensitive sites using active chromatin sequence libraries. *Proc. Natl. Acad. Sci. USA* **101**(13):4537-4542.

Sachs R.K., van den Engh G., Trask B., Yokota H., et al., (1995) A random-walk / giant-loop model for interphase chromosome. *Proc. Natl. Acad. Sci. USA.* **92**:2710-2714.

Sadoni N., Langer S., Fauth C., Bernardi G., et al., (1999) Nuclear organisation of mammalian genomes: Polar chromosome territories build up functionally distinct higher order compartments. *J. Cell Biol.* **146**(6):1211-1226.

Sarraf S.A. and Stancheva I. (2004) Methyl-CpG binding protein MBD1 couples histone H3 methylation at lysine 9 by SETDB1 to DNA replication and chromatin assembly. *Mol. Cell* **15**:595-605.

Sato N., Meijer J., Skaltsounis L., Greengard P. et al., (2004) Maintenance of pluripotency in human and mouse embryonic stem cells through activation of Wnt signalling by a pharmacological GSK-3-specific inhibitor. *Nature Med.* **10**(1):55-63.

Sato N., Sanjuan I.M., Heke M., Uchida M. et al., (2003) Molecular signature of human embryonic stem cells and its comparison with the mouse. *Dev. Biol.* **260**:404-413.

Saurin AJ, Shiels C, Williamson J, Satijn DP, et al., (1998) The human polycomb group complex associates with pericentromeric heterochromatin to form a novel nuclear domain. *J. Cell. Biol.* **142**(4):887-898.

Sauvagoet C.M. and Stiles C.D. (2002) Molecular mechanisms controlling cortical gliogenesis. *Curr. Opin. Neurobiol.* **12**:244-249.

Scharnhorst V., Kranenburg O., van der Eb A.J. and Jochemsen A.G. (1997) Differential regulation of the Wilms' tumor gene, WT1, during differentiation of embryonal carcinoma and embryonic stem cells. *Cell Growth Differ.* **8**(2):133-143.

Schöler H.R., Hatzopoulos A.K., Balling R., Suzuki N. et al., (1989) A family of octamer-specific proteins present during mouse embryogenesis: evidence for germline-specific expression of an Oct factor. *EMBO J.* **8**(9):2543-2550.

Schoorlemmer J., van Puijenbroek A., van der Eijnden M., Jonk L., et al., (1994) Characterisation of a negative retinoic acid response element in the murine Oct4 promoter. *Mol. Cell. Biol.* **14**(2):1122-1136.

Schotta G., Lachner M., Sarma K., Ebert A., et al., (2004) A silencing pathway to induce H3-K9 and H4-K20 trimethylation at constitutive heterochromatin. *Genes Dev.* **18**:1251-1262.

Schroth G.P., Yau P., Imai B.S., Gatewood J.M. et al., (1990) A NMR study of mobility in the histone octamer. *FEBS Lett.* **268**:117-120.

Schübeler D., Francastel C., Cimbora D.M., Reik A., et al., (2000) Nuclear localization and histone acetylation: a pathway for chromatin opening and transcriptional activation of the human beta-globin locus. *Genes Dev.* **14**(8):940-950.

Selander L. and Edlund H. (2002) Nestin is expressed in mesenchymal and not epithelial cells of the developing mouse pancreas. *Mech. Dev.* **113**(2):189-192.

Setoguchi T. and Kondo T. (2004) Nuclear export of OLIG2 in neural stem cells is essential for ciliary neurotrophic factor-induced astrocyte differentiation. *J. Cell Biol.* **166**(7):963-968.

Shahbazian M., Young J., Yuva-Paylor L., Spencer C. et al., (2002) Mice with truncated MeCP2 recapitulate many Rett syndrome features and display hyperacetylation of histone H3. *Neuron* **35**(2):243-254.

Shamblott M.J., Axelman J., Wang S., Bugg E.M. et al., (1998) Derivation of pluripotent stem cells from cultured human primordial germ cells. *Proc. Natl. Acad. Sci. USA* **95**:13726-13731.

Shelby R.D., Hahn K.M. and Sullivan K.F. (1996) Dynamic elastic behaviour of α-satellite DNA domains visualized in situ in living human cells. *J. Cell Biol.* **135**(3)545-557.

Shen S., Li J. and Casaccia-Bonnefil P. (2005) Histone modifications affect timing of oligodendrocyte progenitor differentiation in the developing rat brain. *J. Cell Biol.* **169**(4):577-589.

Shi Y., Lan F., Matson C., Mulligan P., et al., (2004) Histone demethylation mediated by the nuclear amine oxidase homolog LSD1. *Cell* **119**:941-953.

Shiels C., Islam S.A., Vatcheva R., Sasieni P., et al., (2001) PML bodies associate specifically with the MHC gene cluster in interphase nuclei. *J. Cell Sci.* **114**:3705-3716.

Shimozaki K., Nakashima K., Niwa H., and Taga T. (2003) Involvement of Oct3/4 in the enhancement of neuronal differentiation of ES cells in neurogenesis-inducing cultures. *Development.* **130**(11):2505-2512.

Shopland L.S., Johnson C.V., Byron M., McNeil J., et al., (2003) Clustering of multiple specific genes and gene-rich R-bands around SC-35 domains: evidence for local euchromatic neighborhoods. *J. Cell Biol.* **162**(6)981-990.

Silva J., Mak W., Zvetkova I., Appanah R., et al., (2003) Establishment of histone h3 methylation on the inactive X chromosome requires transient recruitment of Eed-Enx1 polycomb group complexes. *Dev. Cell.* **4**(4):481-495.

Simeone A. (1998) Otx1 and Otx2 in the development and evolution of the mammalian brain. *EMBO J.* **17**(23):6790-6798.

Skalníková M. Kozubek S., Lukášová E., Bártová E., et al., (2000) Spatial arrangement of genes, centromeres and chromosomes in human blood cell nuclei and its changes during the cell cycle, differentiation and after irradiation *Chromosome Res.* **8**(6):487-499.

Skok J.A., Brown K.E., Azuara V., Caparros M-L., et al., (2001) Nonequivalent nuclear location of immunoglobulin alleles in B lymphocytes. *Nat. Immun.* **2**(9):848-854.

Smith A.G., (2001) Embryo-derived stem cells: of mice and men. *Annu. Rev. Cell Dev. Biol.* **17**:435-462.

Smith A.G., Heath J.K., Donaldson D.D., Wong G.G. et al., (1988) Inhibition of pluripotential embryonic stem cell differentiation by purified polypeptides. *Nature* **336**(6200):688-690.

Solter D. and Knowles B.B. (1978) Monoclonal antibody defining a stage-specific mouse embryonic antigen (SSEA-1). *Proc. Natl. Acad. Sci. U S A.* **75**(11):5565-5569.

Song M.R. and Ghosh A. (2004) FGF-2-induced chromatin remodelling regulates CNTF-mediated gene expression and astrocyte differentiation. *Nat. Neurosci.* **7**:229-235.

Spector D.L. (2001) Nuclear domains. *J. Cell Sci.* **114**(16):2891-2893.

Spector D.L., (2003) The dynamics of chromosome organization and gene regulation. *Annu. Rev. Biochem.* **72**:573-608.

Sperger J.M., Chen X, Draper J.S., Antosiewicz J.E., et al., (2003) Gene expression patterns in human embryonic stem cells and human pluripotent germ cell tumors. *Proc* Natl Acad Sci U S A. **100**(23):13350-13355.

Spilianakis C.G., Lalioti M.D., Town T., Lee G.R., et al., (2005) Interchromosomal associations between alternatively expressed loci. *Nature* **435**:637-645.

Stadler S., Schnapp V., Mayer R., Stein S., et al., (2004) The architecture of chicken chromosome territories changes during differentiation. *BMC Cell Biol.* **5**:44.

Stallcup M.R. (2001) Role of protein methylation in chromatin remodeling and transcriptional regulation. *Oncogene* **20**(24):3014-3020.

Stoykova A. and Gruss P. (1994) Roles of Pax-genes in developing and adult brain as suggested by expression patterns. *J. Neurosci.* **14**:1395-1412.

Strahl B.D. and Allis D.C. (2000) The language of covalent histone modifications. *Nature* **403**:41-45.

Strübing C., Ahnert-Hilger G., Shan J., Wiedenmann B., et al., (1995) Differentiation of pluripotent embryonic stem cells into the neuronal lineage in vitro gives rise to mature inhibitory and excitatory neurons. *Mech. Dev.* **53**:275-287.

Strumpf D., Mao C-A., Yamanaka Y., Ralston A, et al., (2005) Cdx2 is required for correct cell fate specification and differentiation of trophectoderm in the mouse blastocyst. *Development* **132**:2093-2102.

Stuurman N, de Graaf A, Floore A, Josso A, et al., (1992) A monoclonal antibody recognizing nuclear matrix-associated nuclear bodies. *J. Cell Sci.* **101**(4):773-784.

Su R-C., Brown K.E., Saaber S., Fisher A.G., et al., (2004) Dynamic assembly of silent chromatin during thymocyte maturation. *Nat. Genet.* **36**(5):502-506.

Sun H.B., Shen J. and Yokota H. (2000) Size-dependent positioning of human chromosomes in interphase nuclei. *Biophysical J.* **79**:184-190.

Sun Y., Nadal-Vicens M., Misono S., Lin M. et al., (2001) Neurogenin promotes neurogenesis and inhibits glial differentiation by independent mechanisms. *Cell* **104**:365-376.

Szentirmay M.N. and Sawadogo M. (2000) Spatial organization of RNA polymerase II transcription in the nucleus. *Nuc. Acids Res.* **28**(10):2019-2025.

Szostecki C., Guldner H.H., Netter H.J. and Will H. (1990) Isolation and characterization of cDNA encoding a human nuclear antigen predominantly recognized by autoantibodies from patients with primary biliary cirrhosis. *J. Immunol.* **145**:4338-4347.

Szutorisz H and Dillon N. (2005) The epigenetic basis for embryonic stem cell pluripotency. *BioEssays* **27**:1286-1293.

Szutorisz H., Canzonetta C., Georgiou A., Chow C-M., et al., (2005) Formation of an active tissue-specific chromatin domain initiated by epigenetic marking at the embryonic stem cell stage. *Mol. Cell. Biol.* **25**(5):1804-1820.

Tachibana M., Sugimoto K., Fukushima T. and Shinkai Y. (2001) Set domain-containing protein, G9a, is a novel lysine-preferring mammalian histone methyltransferase with hyperactivity and specific selectivity to lysines 9 and 27 of histone H3. *J. Biol. Chem.* **276**(27):25309-25317.

Taddei A., Maison C., Roche D. and Almouzni G. (2001) Reversible disruption of pericentric heterochromatin and centromere function by inhibiting deacetylases. *Nat. Cell Biol.* **3**:114-120.

Tajbakhsh J.H., Luz H., Bornfleth H., Lampel S., et al., (2000) Spatial distribution of GC- and AT-rich DNA sequences within human chromosome territories. *Exp. Cell Res.* **255**:229-237.

Takayama K., Inoue T., Ijiri Y., Otani T., et al., (2004) Demethylating agent, 5-azacytidine, reverses differentiation of embryonic stem cells. *Biochem. Biophy. Res. Com.* **323**:86-90.

Takizawa T., Nakashima K., Namihira M., Ochiai W. et al., (2001) DNA methylation is a critical cell-intrinsic determinant of astrocyte differentiation in the fetal brain. *Dev. Cell* **1**:749-758.

Tamaru H. and Selker E.U. (2001) A histone H3 methyltransferase controls DNA methylation in Neurospora crassa. *Nature* **414**(6861):277-283.

Tanabe H., Muller S., Neusser M., von Hase J., et al., (2002) Evolutionary conservation of chromosome territory arrangements in cell nuclei from higher primates *Proc. Natl. Acad. Sci. USA.* **99**(7):4424-4429.

Tanaka TS, Kunath T, Kimber WL, Jaradat SA, et al., (2002) Gene expression profiling of embryo-derived stem cells reveals candidate genes associated with pluripotency and lineage specificity. *Genome Res.* **12**(12):1921-1928.

Tate P., Skarnes W. and Bird A. (1996) The methyl-CpG protein MeCP2 is essential for embryonic development in the mouse *Nat. Genet.* **12**:205-208.

Terranova R., Sauer S., Merkenschlager M. and Fisher A.G. (2005) The reorganisation of constitutive heterochromatin in differentiating muscle requires HDAC activity. *Exp. Cell Res.* **310**:344-356.

Tesar P.J., (2005) Derivation of germ-line-competent embryonic stem cell lines from preblastocyst mouse embryos. *Proc. Natl. Acad. Sci. USA* **102**(23):8239-8244.

Teter B., Osterburg H.H., Anderson C.P. and Finch C.E. (1994) Methylation of the rat glial fibrillary acidic protein gene shows tissue-specific domains. *J. Neurosci. Res.* **39**(6):680-693.

Thomas J.O. (1999) Histone H1: location and role. *Curr. Opin. Cell Biol.* **11**:312-317.

Thomson J.A., Itskovitz-Eldor J., Shapiro S.S., Waknitz M.A. et al., (1998) Embryonic stem cells lines derived from human blastocysts. *Science* **282**:1145-1147.

Tian L., Catt J.W., O'Neill C. and King N.C. (1997) Expression of immunoglobulin superfamily cell adhesion molecules on murine embryonic stem cells. *Biol. Reprod.* **57**:561-568.

Tsuji-Takayama K., Inoue T., Ijiri Y., Otani T., et al., (2004) Demethylating agent, 5-azacytidine, reverses differentiation of embryonic stem cells. *Biochem. Biophy. Res. Commun.* **323**:86-90.

Tsukada Y., Fang J., Erdjument-Bromage H., Warren M.E., et al., (2006) Histone demethylation by a family of JmjC domain-containing proteins. *Nature* **439**(7078):811-816.

Tudor M., Akbarian S., Chen R.Z. and Jaenisch R. et al., (2002) Transcriptional profiling of a mouse model for Rett syndrome reveals subtle transcriptional changes in the brain. *Proc. Natl. Acad. Sci. U S A.* **99**(24):15536-15541.

Turnpenny L., Brickwood S., Spalluto C.M., Piper K. et al., (2003) Derivation of human embryonic germ cells: an alternative source of pluripotent stem cells. *Stem Cells* **21**:598-609.

Vakoc C.R., Mandat S.A., Olenchock B.A. and Blobel G.A. (2005) Histone H3 lysine 9 methylation and HP1γ are associated with transcription elongation through mammalian chromatin. *Mol. Cell* **19**:381-391.

Valk-Lingbeek M.E., Bruggeman S.W.M. and van Lohuizen M. (2004) Stem cells and cancer: the polycomb connection. *Cell* **118**:409-418.

Vallier L., Alexander M. and Pedersen R.A. et al., (2005) Activin/Nodal and FGF pathways cooperate to maintain pluripotency of human embryonic stem cells. *J. Cell Sci.* **118**(19):4495-1509.

van der Weyden L., Adams D.J. and Bradley A., (2002) Tools for targeted manipulation of the mouse genome. *Physiol. Genomics* **11**:133-164

van Driel R., Fransz P.F. and Verschure P.J. (2003) The eukaryotic genome: a system regulated at different hierarchical levels. *J. Cell Sci.* **116**:4067-4075.

van Steensel B., Smogorzewska A. and de Lange T. (1998) TRF2 Protects human telomeres from end-to-end fusions. *Cell* **92**:401-413.

Verheijen R., Kuijpers H.J., Schlingemann R.O., Boehmer A.L., et al., (1989) Ki-67 detects a nuclear matrix-associated proliferation related antigen. I. Intracellular localization during interphase. *J. Cell Sci.* **92**(1):123-130.

Verschure P.J., van der Kraan I., Enserink J.M., Mone M.J., et al., (2002) Large-scale chromatin organization and localization of proteins involved in gene expression in human cells. *J. Histochem. Cytochem.* **50**:1303-1312.

Verschure P.J., van der Kraan I., Manders E.M. and van Driel R. (1999) Spatial relationship between transcription sites and chromosome territories. *J. Cell Biol.* **147**:13-24.

Versteeg R, van Schaik B.D., van Batenburg M.F., Roos M., et al., (2003) The human transcriptome map reveals extremes in gene density, intron length, GC content, and repeat pattern for domains of highly and weakly expressed genes. *Genome Res.* **13**(9):1998-2004.

Visser A.E., Eils R., Jauch A., Little G., et al., (1998) Spatial distribution of early and late replicating chromatin in interphase chromosome territories. *Exp. Cell Res.* **243**:398-407.

Visser A.E., Jaunin F., Fakan S. and Aten J.A. (2000) High resolution analysis of interphase chromosome domains. *J. Cell Sci.* **113**:2585-2593.

Volpe T.A., Kidner C., Hall I.M., Teng G., et al., (2002) Regulation of heterochromatic silencing and histone H3 lysine-9 methylation by RNAi. *Science* **297**:1833-1837.

Volpi E.V., Chevret E., Jones T., Vatcheva R., et al., (2000) Large-scale chromatin organization of the major histocompatibility complex and other regions of human chromosome 6 and its response to interferon in interphase nuclei. *J. Cell Sci.* **113**:1565-1576.

Vourc'h C., Taruscio D., Boyle A.L. and Ward D.C. (1993) Cell cycle-dependent distribution of telomere, centromere, and chromosome-specific subsatellite domain in the interphase nucleus of mouse lymphocytes. *Exp. Cell Res.* **205**:142-151.

Wang H., Cao R., Xia L., Erdjument-Bromage H., et al., (2001a) Purification and functional characterization of a histone H3-lysine 4-specific methyltransferase. *Mol. Cell* **8**:1207-1217.

Wang H., Huang Z.Q., Xia L., Feng Q., et al., (2001b) Methylation of histone H4 at arginine 3 facilitating transcriptional activation by nuclear hormone receptor. *Science* **293**:853-857.

Wang J., Shields C., Sasieni P., Wu P.J., et al., (2004b) Promyelocytic leukemia nuclear bodies associate with transcriptionally active genomic regions. *J. Cell Biol.* **164**(4):515-526.

Wang Y., Wysocka J., Sayegh J., Lee Y., et al., (2004a) Human PAD4 regulates histone arginine methylation levels via demethylation. *Science* **306**:279-283.

Watt and Molloy, (1988) Cytosine methylation prevents binding to DNA of a HeLa cell transcription factor required for optimal expression of the adenovirus major late promoter. *Genes Dev.* **2**(9):1136-43.

Wei C.L., Miura T., Robson P., Lim S. et al., (2005) Transcriptome Profiling of Human and Mouse ESCs Identifies Divergent Paths Required to Maintain the Stem Cell State. *Stem Cells*; **25**:166-185

Weierich C., Brero A., Stein S., von Hase J., et al., (2003) Three-dimensional arrangement of centromeres and telomeres in nuclei of human and murine lymphocytes. *Chromosome Res.* **11**:485-502.

Weil M.R., Widlak P., Minna J.D. and Garner H.R. (2004) Global survey of chromatin accessibility using DNA microarrays. *Genome Res.* **14**:1374-1381.

Weimer R., Haaf T., Kruger J., Poot M., et al., (1992) Characterization of centromere arrangements and test for random distribution in G_0, G_1, S, G_2, G_1, and early S' phase in human lymphocytes. *Hum. Genet.* **88**:673-682.

Whetstine J.R., Nottke A., Lan F., Huarte M., et al., (2006) Reversal of histone lysine trimethylation by the JMJD2 family of histone demethylases. *Cell.* **125**(3):467-481.

Wiblin A.E., Cui W., Clark A.J. and Bickmore W.A. (2005) Distinctive nuclear organisation of centromeres and regions involved in pluripotency in human embryonic stem cells. *J. Cell Sci.* **118**:3861-3868.

Wichterle H., Lieberam I., Porter J.A. and Jessell T. (2002) Directed differentiation of embryonic stem cells into motor neurons. *Cell* **110**:385-397.

Williams R.L., Hilton D.J., Pease S., Willson T.A. et al., (1988) Myeloid leukaemia inhibitory factor maintains the developmental potential of embryonic stem cells. *Nature* **336**(6200):684-687

Williams R.R.E., Broad S., Sheer D. and Ragoussis J. (2002) Subchromosomal positioning of the epidermal differentiation complex (EDC) in keratinocyte and lymphoblast interphase nuclei. *Exp. Cell Res.* **272**:163-175.

Williams R.R.E., Azuara V., Perry P., Sauer S., et al., (2006) Neural induction promotes large-scale chromatin reorganisation of the *Mash1* locus. *J. Cell Sci.* **119**:132-140.

Wilmut I., Schnieke A.E., McWhir J., Kind A.J., et al., (1997) Viable offspring derived from fetal and adult mammalian cells. *Nature* **385**(6619):810-813.

Wobus A.M. (2001) Potential of embryonic stem cells. *Mol. Aspects Med.* **22**(3):149-164.

Wood H.B. and Episkopou V. (1999) Comparative expression of the mouse *Sox1*, *Sox2* and *Sox3* genes from pre-gastrulation to early somite stages. *Mech. Dev.* **86**:197-201.

Xian H.Q., Werth K. and Gottlieb D.I. (2005) Promoter analysis in ES cell-derived neural cells. *Biochem. Biophys. Res. Commun.* **327**(1):155-162.

Xian H-Q., McNichols E., St. Clair A. and Gottlieb D.I. (2003) A subset of ES-cell-derived neural cells marked by gene targeting. *Stem Cells* **21**:41-49.

Xu C., Inokuma M.S., Denham J., Golds K., et al., (2001) Feeder-free growth of undifferentiated human embryonic stem cells. *Nat. Biotech.* **19**:971-974.

Xu G.L., Bestor T.H., Bourc'his D., Hsieh C.L. et al., (1999) Chromosome instability and immunodeficiency syndrome caused by mutations in a DNA methyltransferase gene. *Nature* **402**(6758):187-191.

Xu R-H., Chen X., Li D.S., Li R. et al., (2002) BMP4 initiates human embryonic stem cell differentiation to trophoblast. *Nat. Biotechnol.* **20**:1261-1264.

Xu R-H., Peck R.M., Li D.S., Feng X. et al., (2005a) Basic FGF and suppression of BMP signalling sustain undifferentiated proliferation of human ES cells. *Nat. Meth.* **2**(3)185-190.

Xu Y., Zhang J.J., Grifo J.A. and Krey L.C. (2005b) DNA methylation patterns in human tripronucleate zygotes. *Mol. Hum. Reprod.* **11**(3):167-171.

Yamane K., Toumazou C., Tsukada Y., Erdjument-Bromage H., et al., (2006) JHDM2A, a JmjC-containing H3K9 demethylase, facilitates transcription activation by androgen receptor. *Cell* **125**(3):483-495.

Yang L., Xia L., Wu D.Y., Wang H., et al., (2002) Molecular cloning of ESET, a novel histone H3-specific methyltransferase that interacts with ERG transcription factor. *Oncogene* **21**:148–152.

Ying Q-L. and Smith A.G. (2003) Defined conditions for neuronal commitment and differentiation. *Meth. Enzymol.* **365**:327-341.

Ying Q-L., Nichols J., Chambers I., and Smith A. (2003) BMP induction of Id proteins suppresses differentiation and sustains embryonic stem cell self-renewal in collaboration with STAT3. *Cell* **115**:281-292.

Yoder J.A., Soman N.S., Verdine G.L. and Bestor T.H. (1997) DNA (cytosine-5)-methyltransferases in mouse cells and tissues. Studies with a mechanism-based probe. *J. Mol. Biol.* **270**(3):385-395.

Yoshida K., Chambers I., Nichols J., Smith A. et al., (1994) Maintenance of the pluripotential phenotype of embryonic stem cells through direct activation of gp130 signalling pathways. *Mech. Dev.* **45**:163-171.

Zaehres H., Lensch M.W., Daheron L., Stewart S.A. et al., (2005) High-efficiency RNA interference in human embryonic stem cells. *Stem Cells* **23**:299-305.

Zalenskaya I.A. and Zalensky A.O. (2002) Telomeres in mammalian male germline cells. *Int. Rev. Cytology.* **218**:37-67.

Zhang C.L., McKinsey T.A.. and Olson E.N. (2002) Association of class II histone deacetylases with heterochromatin protein 1: Potential role for histone methylation in control of muscle differentiation. *Mol. Cell. Biol.* **22**(20)7302-7312.

Zhang Y. and Reinberg D. (2001) Transcription regulation by histone methylation: interplay between different covalent modifications of the core histone tails. *Genes Dev.* **15**(18):2343-2360.

Zhang Y., Ng H.H., Erdjument-Bromage H., Tempst P. et al., (1999) Analysis of the NuRD subunits reveals a histone deacetylase core complex and a connection with DNA methylation. *Genes Dev.* **13**:1924-1935.

Zhao X., Ueba T., Christie B.R., Barkho B. et al., (2003) Mice lacking methyl-CpG binding protein 1 have deficits in adult neurogenesis and hippocampal function. *Proc. Natl. Acad. Sci. USA* **100**(11):6777-6782.

Zink D., Amaral M.D., Englmann A., Lang S., (2004) Transcription-dependent spatial arrangements of CFTR and adjacent genes in human cell nuclei. *J Cell Biol.* **166**(6)815-825.

Zuccotti M., Garagna S., Merico V., Monti M., et al., (2005) Chromatin organisation and nuclear architecture in growing mouse oocytes. *Mol. Cell. Endocrinology* **234**:11-17.

Zwaka T.P. and Thomson J.A., (2005) A germ cell origin of embryonic stem cells? *Development* **132**:227-233.

Appendix 1

Distinctive nuclear organisation of centromeres and regions involved in pluripotency in human embryonic stem cells

Distinctive nuclear organisation of centromeres and regions involved in pluripotency in human embryonic stem cells

Anne E. Wiblin[1], Wei Cui[2], A. John Clark[2] and Wendy A. Bickmore[1,*]

[1]MRC Human Genetics Unit, Crewe Road, Edinburgh, EH4 2XU, UK
[2]Roslin Institute, Roslin BioCentre, Midlothian, EH25 9PS, UK
*Author for correspondence (e-mail: w.bickmore@hgu.mrc.ac.uk)

Accepted 13 May 2005
Journal of Cell Science 118, 3861-3868 Published by The Company of Biologists 2005
doi:10.1242/jcs.02500

Summary

Nuclear organisation is thought to be important in regulating gene expression. Here we investigate whether human embryonic stem cells (hES) have a particular nuclear organisation, which could be important for maintaining their pluripotent state. We found that whereas the nuclei of hES cells have a general gene-density-related radial organisation of chromosomes, as is seen in differentiated cells, there are also distinctive localisations for chromosome regions and gene loci with a role in pluripotency. Chromosome 12p, a region of the human genome that contains clustered pluripotency genes including *NANOG*, has a more central nuclear localisation in ES cells than in differentiated cells. On chromosome 6p we find no overall change in nuclear chromosome position, but instead we detect a relocalisation of the *OCT4* locus, to a position outside its chromosome territory. There is also a smaller proportion of centromeres located close to the nuclear periphery in hES cells compared to differentiated cells. We conclude that hES cell nuclei have a distinct nuclear architecture, especially at loci involved in maintaining pluripotency. Understanding this level of hES cell biology provides a framework within which other large-scale chromatin changes that may accompany differentiation can be considered.

Key words: Centromere, Chromosome territory, Embryonic stem cell, *NANOG*, Nucleus, *OCT4*

Introduction

The human genome is spatially organised within the nuclei of differentiated cells. There is a radial arrangement of chromosome territories (CTs): gene-rich chromosomes such as chromosome 19 (HSA19) concentrate in the centre of the nucleus and more gene-poor chromosomes (e.g. chromosome 18) localise toward the nuclear periphery (Croft et al., 1999; Boyle et al., 2001; Cremer et al., 2001; Cremer et al., 2003). Centromeres are also generally found at the nuclear periphery, or around nucleoli (Carvalho et al., 2001; Weierich et al., 2003; Gilchrist et al., 2004), whereas telomeres are mainly found in the nuclear interior (Weierich et al., 2003). Gene clusters, and individual chromosomal domains also have distinctive localisations within respect to their CTs (Volpi et al., 2000; Williams et al., 2002; Mahy et al., 2002a).

In model organisms it is clear that nuclear organisation can regulate gene expression (Spector, 2003). Data are consistent with nuclear organisation also being a determinant of gene expression for the human genome. Therefore, there may be differences in the nuclear organisation of different cell types. Indeed, in some human cell types (amniocytes and fibroblasts) with flat/ellipsoid-shaped nuclei, HSA18 can be found toward the nuclear centre rather than at the nuclear periphery, as is typical in cells with more spherical nuclei (lymphocytes, keratinocytes, colon and cervix epithelial cells) (Cremer et al., 2001; Cremer et al., 2003). In the mouse, differences in the spatial and radial distribution of chromosomes have been documented in different tissues of the animal (Parada et al., 2004) as well as during the differentiation of T cells (Kim et al., 2004). However, to date no significant change in radial position of a human chromosome within the nucleus has been documented during differentiation, although there may be changes in chromosome associations (Kuroda et al., 2004).

Within CTs themselves, the position of gene clusters is altered in different differentiated human cell types (Volpi et al., 2000; Williams et al., 2002). This aspect of nuclear organisation has not been studied in human stem cells, but in the mouse, movement of specific genes out of CTs has been seen upon the differentiation of ES cells (Chambeyron and Bickmore, 2004). Human centromeres are localised close to either the nuclear periphery or the nucleolus (Carvalho et al., 2001; Weierich et al., 2003). However, changes of centromere distribution in relation to cell cycle, physiological or differentiation state have been reported (reviewed by Gilchrist et al., 2004). In addition, lineage-specific centromere associations into chromocentres have been reported during lymphoid and myeloid differentiation, with an overall increase in centromere clustering towards later stages of differentiation (Beil et al., 2002; Alcobia et al., 2003).

If nuclear organisation regulates gene expression, then it may have a key role in restricting it, as cells become more committed to a differentiation pathway. Therefore it is

important to determine how the genome is organised in the nucleus of pluripotent cells, and particularly in stem cells (Fisher and Merkenschlager, 2002). The organisation of human chromosomes and centromeres has been studied in haemopoietic progenitor cells (Cremer et al., 2003) and in $CD34^+$ stem cells from umbilical cord blood (Alcobia et al., 2003). However, there have been no studies of nuclear organisation in hES cells.

Human ES cells have been derived from the inner cell mass of blastocysts, and as well as being able to self-renew, they have the ability to differentiate into all three embryonic germ layers when injected into severe combined immunodeficient mice (Thomson et al., 1998). It is anticipated that hES cells will be an important tool for understanding early human development, with the hope that they may also have therapeutic potential. Although they share many features with mouse ES (mES) cells, including the expression of common genes important for pluripotency, there are also key differences between mES and hES cells (Pera and Trounson, 2004; Ginis et al., 2004). Moreover, there are fundamental differences in the organisation of chromosomes between the human and mouse genomes. Therefore, mES cells cannot serve as a suitable model for studying the nuclear organisation of human stem cells and an investigation of hES cell nuclei is required.

Here we compared the nuclear organisation of differentiated human cells with hES cells. We show that hES cells have a radial organisation of chromosomes in the nucleus that relates to gene density and that is typical of many differentiated cell types. However, we find differences in the localisation of chromosomes and gene loci with known roles in pluripotency. We also describe differences in centromere position in hES cell nuclei.

Materials and Methods

Human ES cell culture and analysis

Human ES cell lines H1 (46XY), H7 and H9 (46XX) (Thomson et al., 1998) were grown as previously described, with minor modification (Xu et al., 2001). Briefly, the cells were cultured on Matrigel-coated culture dishes with mouse embryonic fibroblast conditioned medium supplemented with 8 ng/ml basic fibroblast growth factor. Cells were routinely split 1:3 with collagenase. H7 cells were passage (p)55. H1 cells were used at p42-65 and H9 cells were at p39-55.

The cells were analysed by flow cytometry for the hES cell surface antigens SSEA4 and Tra-1-60 using a FACScan (BD Biosciences). Briefly, hES cells were harvested by trypsin/EDTA and washed with phosphate-buffered saline (PBS). After treatment with 10% goat serum to block non-specific binding, the cells were incubated with monoclonal antibodies against SSEA4 (1:5, DSHB, IA) or Tra-1-60 (1:12, Chemicon) on ice for 30 minutes. The cells were then treated with goat anti-mouse IgG3-FITC or goat anti-mouse IgM-PE (both at 1:100, Southern Biotechnologies). Finally, 10^4 cells were acquired for each sample and analysed with CELLQUEST software.

Human (46XY) 1HD primary fibroblasts and FATO LCLs (46XY) were grown as described previously (Croft et al., 1999).

Fluorescence in situ hybridisation

Chromosome paints were labelled with biotin-16-dUTP by nick translation or by PCR amplification (Croft et al., 1999) or obtained commercially (Cambio). BACs were labelled by nick translation with digoxigenin-11-dUTP. 200 ng paint and 70 ng BAC were used per slide, with 6 μg human Cot1 DNA (GIBCO BRL) as competitor.

For 2D analysis, cells were swollen in 75 mM KCl before fixation in 3:1 methanol:acetic acid. Hybridisation was as described previously (Croft et al., 1999) but with the denaturing time reduced to 1.15 minutes for hES cells. For 3D analysis, hES cells were trypsinised and washed twice in PBS before permeabilisation in CSK buffer (100 mM NaCl, 300 mM sucrose, 3 mM $MgCl_2$, 10 mM PIPES, pH 6.8, 0.5% Triton X-100) for 5 minutes on ice. After washing in PBS, cells were fixed with 4% paraformaldehyde/PBS for 10 minutes, washed again in PBS and cytospun onto slides at 11 ***g*** (Shandon, Cytospin3) for 5 minutes. Slides were then subjected to freeze-thaw in 20% glycerol/PBS and FISH was carried out as described previously (Croft et al., 1999). To check the preservation of nuclear structure after cytospinning, we compared the nuclear organisation of centromeres in primary fibroblasts grown on slides to that of primary fibroblasts cytospun onto slides.

After hybridisation, biotinylated probes were detected using fluorochrome-conjugated avidin (FITC or Texas Red) (Vector Laboratories) followed by biotinylated anti-avidin (Vector Laboratories) and a final layer of fluorochrome-conjugated avidin. Digoxigenin-labelled probes were detected with sequential layers of FITC-conjugated antidigoxigenin (BCL) and FITC-conjugated anti-sheep antibody (Vector Laboratories). Slides were counterstained with 0.5 μg/ml DAPI. Telomere FISH was carried out using a telomere PNA FISH Kit (DAKO).

Immunofluorescence

Centromeres were detected by immunofluorescence using either a CENP-C antibody (gift of W. Earnshaw, Wellcome Trust Centre for Cell Biology, University of Edinburgh, UK) and FITC-conjugated anti-rabbit secondary antibody, or CREST serum and a Texas Red anti-human secondary antibody. PML bodies were detected using 5S10 monoclonal antibody and Texas Red anti-mouse secondary antibody. Nucleoli were detected using a Ki67 antibody and FITC-conjugated anti-rabbit secondary antibody. All secondary antibodies were supplied by Jackson ImmunoResearch Laboratories.

Image capture and image analysis

2D slides were examined using a Zeiss Axioplan fluorescence microscope fitted with a triple band-pass filter (Chroma #83000). Grey-scale images were captured with a cooled CCD camera (Princeton Instruments Pentamax) and analysed using custom IPLab scripts. For 3D analysis, a focus motor was used to collect images at 0.25μm intervals in the *z*-plane using a Xillig CCD camera. 3D image stacks were analysed using IPLab and deconvolved using Hazebuster (Vaytek).

The radial distribution of CTs was determined in 2D specimens by an erosion script, as previously described (Croft et al., 1999). The radial distribution of specific gene loci was assessed manually across the five erosion shells from the edge (shell 1) to the centre (shell 5) of the nucleus. These distributions were normalised to the proportion of the total DAPI signal present in each shell. 3D chromosome position was determined as previously described (Bridger et al., 2000).

Analysis of probe position relative to the surface of CTs, and interphase separation (*d*) were as previously described (Mahy et al., 2002a; Mahy et al., 2002b; Chambeyron and Bickmore, 2004). Differences in the nuclear position of CTs and gene loci were tested for statistical significance using a Mann-Whitney U test in Minitab 13. This is a nonparametric test of the hypothesis that two groups come from the same distribution, without assuming that the data are normally distributed.

3D analysis of centromeres and telomeres in the *z*-plane was performed using a custom IPLab script. Briefly, the script defines the outline of the DAPI nucleus in each frame of the *z*-stack, calculates the highest level of intensity for each fluorescent spot and locates which frame the spot is positioned in.

Results

HSA18 and 19 have a radial distribution in the nuclei of human ES cells

The radial distribution of CTs in the nucleus, related to their gene density, was first described for HSA18 and 19 (Croft et al., 1999). These chromosomes are of approximately the same size (76 and 63 Mb, respectively) but HSA18 is very gene-poor, harbouring an estimated 449 genes, whereas HSA19 is very gene-rich with 1528 genes (http://www.ensembl.org/Homo_sapiens/). HSA18 is found towards the nuclear periphery in a variety of differentiated cells and HSA19 is in the centre of the nucleus (Croft et al., 1999; Cremer et al., 2003). This radial distribution is conserved amongst primates (Tanabe et al., 2002) and it is also applicable to other human chromosomes (Cremer et al., 2001; Boyle et al., 2001).

We investigated the radial position of HSA18 and HSA19 in the nuclei of H1 (XY) and H9 (XX) hES cells. The cells were cultured on Matrigel and the expression of cell-surface antigens SSEA-4 and Tra-1-60 cells was analysed by flow cytometry. Of the H1 cells, 70% were SSEA-4 positive and 55% were positive for Tra-I-60, indicating that most of the cells in the culture were undifferentiated (Draper et al., 2002; Carpenter et al., 2004). Chromosome position was first established using fluorescence in situ hybridisation (FISH) with chromosome paints for HSA18 and 19 in 2D preparations (Fig. 1A). Although this flattens nuclear morphology, it does not alter the measured radial distribution of chromosomes (Croft et al., 1999), and it allows for rapid and automated analysis of large numbers of nuclei. The radial position of each CT was established from the distribution of hybridisation signal, relative to that of total DNA, in five erosion shells (Croft et al., 1999; Boyle et al., 2001). In both cell lines, HSA19 has a more central nuclear location than HSA18 ($P \leq 0.001$), and data for H1 cells is shown in Fig. 1B. This was confirmed by 3D analysis of H1 cells (Fig. 1C). HSA18 is significantly closer to the nuclear periphery than HSA19 in the x and y-axes ($P \leq 0.001$), though differences through the z-axis were not significant ($P=0.68$).

An altered nuclear distribution of 12p in human ES cells

The data in Fig. 1 suggest that CTs in hES cell nuclei have a gene-density-related radial organisation similar to that seen in many differentiated human cell types. (Cremer et al., 2001; Cremer et al., 2003). To determine whether there might be changes in the nuclear distribution of specific CTs in hES cells, we examined the radial position of the CTs that carry genes with a known role in maintaining the undifferentiated state. *OCT4 (POU5F1)* is located within a cluster of non-class I genes embedded within the MHC class I region on HSA6p21.33. *OCT4* expression is essential to maintain the undifferentiated phenotype of hES cells (Matin et al., 2004). *NANOG* (12p13.31) expression is also required to maintain the undifferentiated state of hES cells (Zaehres et al., 2005). We hybridised chromosome paints for 6p and 12p, together with BACs for *OCT4* and *NANOG*, to nuclei from hES cells and lymphoblastoid cells (LCLs) (Fig. 2A). The radial position of the CTs was established using the same erosion analysis as used in Fig. 1. We have previously reported that human chromosomes 6 and 12 have nuclear distributions in LCLs and fibroblasts that are intermediate between those of HSA18 and HSA19, i.e. they are located neither at the nuclear periphery, nor in the nuclear centre (Boyle et al., 2001). This was confirmed here for 6p and 12p in LCLs (Fig. 2B). There was no significant difference in the radial position of 6p between LCLs and hES cells. However, 12p was located significantly closer to the nuclear centre (shell 5) in hES cells compared to LCLs ($P=0.04$) (Fig. 2B).

Nuclear organisation of pluripotency genes in ES and differentiated cells

If CT radial position differs between ES cells and differentiated cell types, then it might be expected that the radial position of specific gene loci on these chromosomes follow that of their host chromosome. Consistent with this, *NANOG* (12p), but not *OCT4* (6p) was located closer to the nuclear centre in hES compared with LCLs (Fig. 2C).

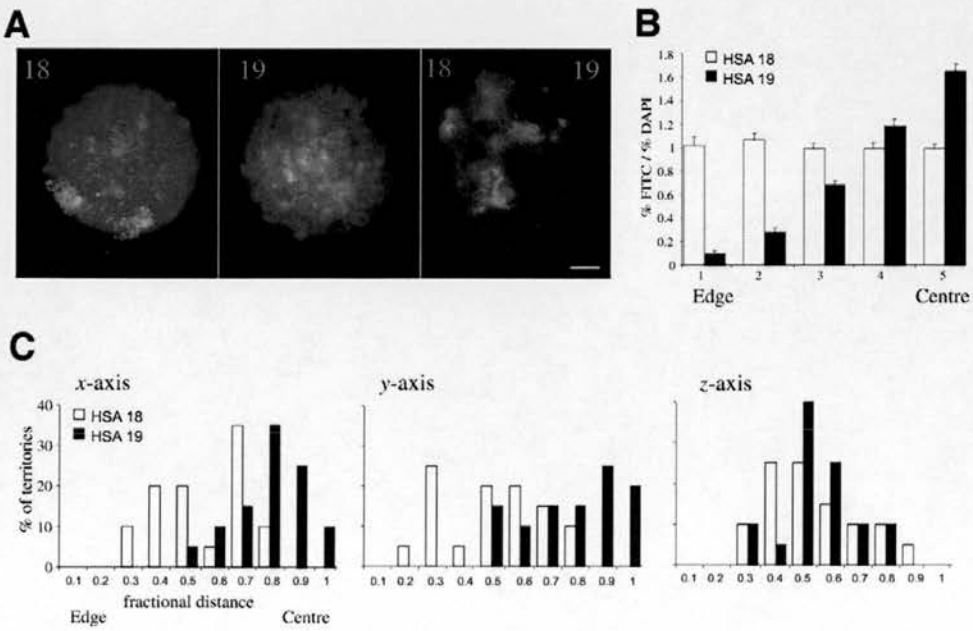

Fig. 1. The radial distribution of HSA18 and 19 in hES cells. (A) hES cell nuclei, counterstained with DAPI (blue) and hybridised with chromosome paints for HSA18 or 19. (B) Distribution of HSA18 and 19 hybridisation signals within the nucleus of H1 ES cells analysed by erosion of 2D images into five concentric shells from the edge (1) to the centre (5) of the nucleus. The mean (±s.e.m.) proportion of hybridisation signal, normalised to the amount of DAPI signal, is shown for each shell ($n=50$). (C) Analysis of HSA18 and 19 hybridisation signals within 3D-preserved hES cell nuclei. Graphs are the distributions of the centres of the HSA18 and 19 territories, along the fractional radius of each nucleus, along the x, y and z-axes ($n=20$). Bar, 5 μm.

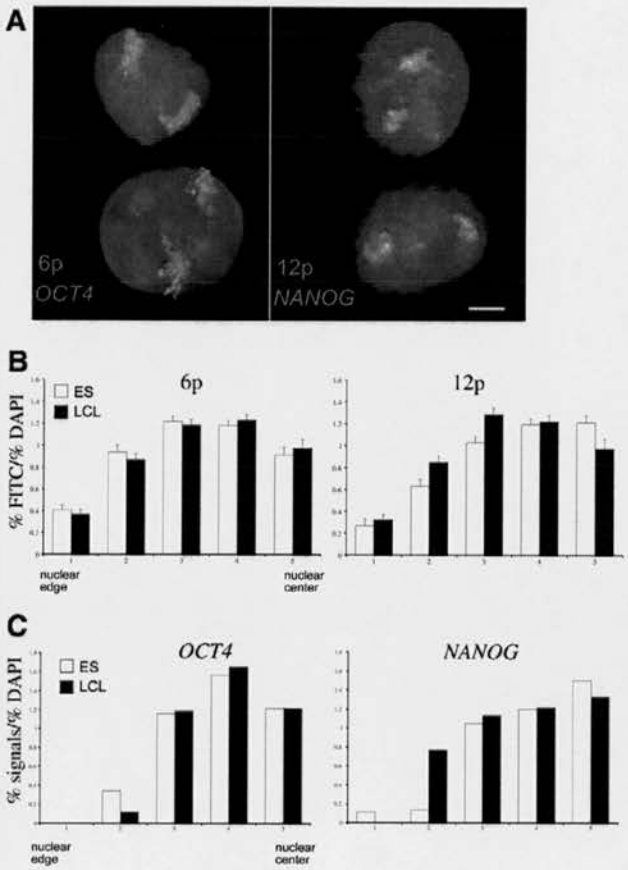

Fig. 2. Radial distribution of 6p, 12p, *OCT4* and *NANOG* in ES cells. (A) Interphase hybridisation of BAC probes containing *OCT4* or *NANOG* (red), and chromosome paints for either 6p or 12p (green), within the nuclei of human ES cells counterstained with DAPI (blue). (B) Distribution of HSA6p and 12p hybridisation signals within the nucleus of ES cells, by erosion of 2D images into 5 concentric shells from the edge (1) to the centre (5) of the nucleus. The mean (±s.e.m.) proportion of hybridisation signal, normalised to the amount of DAPI signal, is shown for each shell (n=50). C) Distribution of hybridisation signals from *OCT4* or *NANOG*-containing BACs within the nucleus of ES cells, by erosion of 2D images into five concentric shells from the edge (1) to the centre (5) of the nucleus. The proportion of hybridisation signals, normalised to the amount of DAPI signal, is shown for each shell (n=50). Bar, 5 μm.

As well as having a radial organisation within the nucleus, CTs also have a distinctive architecture themselves. In differentiated cells, gene-rich domains and regions of coordinately regulated gene expression, loop out from CTs (Volpi et al., 2000; Mahy et al., 2002a). One of the gene-rich domains of the human genome that we have previously shown to loop out from its CT in LCLs is the distal part of 11p15.5 (Mahy et al., 2002a). We found that loci from 11p15.5 (positions 0.25-2.1 Mb, NCBI build 35, http://www.ensembl.org/Homo_sapiens) are also located outside the 11p territory in hES cell nuclei, even though this region of the genome does not contain any genes with a known role in maintaining pluripotency (Table 1). In contrast, *RCN*, which is expressed in both LCLs (Mahy et al., 2002b) and hES cells (Ramalho-Santos et al., 2002), but which is located in a low gene-density region at 11p13 (32Mb), remains inside the CT (Table 1). Therefore, CT architecture is well developed in hES cells, and is organised in a similar manner to differentiated cells, with regions of generally high gene density located out side of CTs.

To determine whether a specific CT architecture could be detected at pluripotency genes expressed in ES cells, we analysed the intra-CT position of *NANOG* and *OCT4*. We measured the distances between hybridisation signals for BACs for the specific loci, and the visible edge of the hybridisation signal for the corresponding CT (Mahy et al., 2002). We found that *NANOG* is located well within the 12p CT in both LCL and ES cells (Table 1, Fig. 3A).

However, the intra-CT behaviour of *NANOG* contrasts with that of *OCT4*, which is a non-class I gene, embedded within the MHC Class I region (Fig. 3A). Classical class I region genes are expressed constitutively in human LCLs and fibroblasts. Unlike mES cells, hES cells also express class I genes (Tian et al., 1997; Drukker et al., 2002; Draper et al., 2002; Carpenter et al., 2004). The Class I and Class III regions have been found outside CTs in LCLs (Volpi et al., 2000). We confirmed this using BACs that flank *OCT4* and that contain either another non-class I gene (*FLOT1*), or the most centromeric genes of the class I region (*MICB*). We found that these regions were located, on average, outside the 6p CT in hES cells (Table 1 and Fig. 3A). However, the mean position of the intervening *OCT4* locus differed between ES and LCL cells. On average, *OCT4* was just inside the CT in LCLs, but outside the CT in ES cells (Table 1 and Fig. 3A). This difference was small, but statistically significant (P=0.041). Analysing the distribution of distances revealed that this

Table 1. Intra-CT position of loci in hES cells and LCLs

Locus	Cytogenetic position	Genomic position (Mb)	Probe name	Position relative to CT edge	
				LCL (μm)	ES (μm)
IFITM3	11p15.5	0.2	D11S483	−1.4±0.3	−0.70±1.13
INS	11p15.5	2.1	cINS/IGF2	−0.6±0.2	−0.55±0.15
RCN	11p13	32	cH11148	0.6±0.2	0.26±0.04
NANOG	12p13.31	7.8	RP11-358I17	0.23±0.06	0.32±0.04
FLOT1	6p21.33	30.8	RP11-324F19	−0.07±0.07	−0.11±0.08
OCT4	6p21.33	31.2	RP11-1058J10	0.03±0.06	−0.15±0.09
MICB	6p21.33	31.6	RP11-184F16	−0.25±0.09	−0.31±0.16

The cytogenetic position and genome position (from NCBI build 35, http://www.ensembl.org/Homo_sapiens) of each locus is indicated, together with the name of the cosmid or BAC probe used in FISH. Mean (±s.e.m.) position, in μm, of specific loci relative to the edge of CTs in nuclei from hES cells and from LCLs. Negative values indicate positions outside the visible limits of the CT. LCL data for 11p15.5 loci is taken from Mahy et al., 2002a.

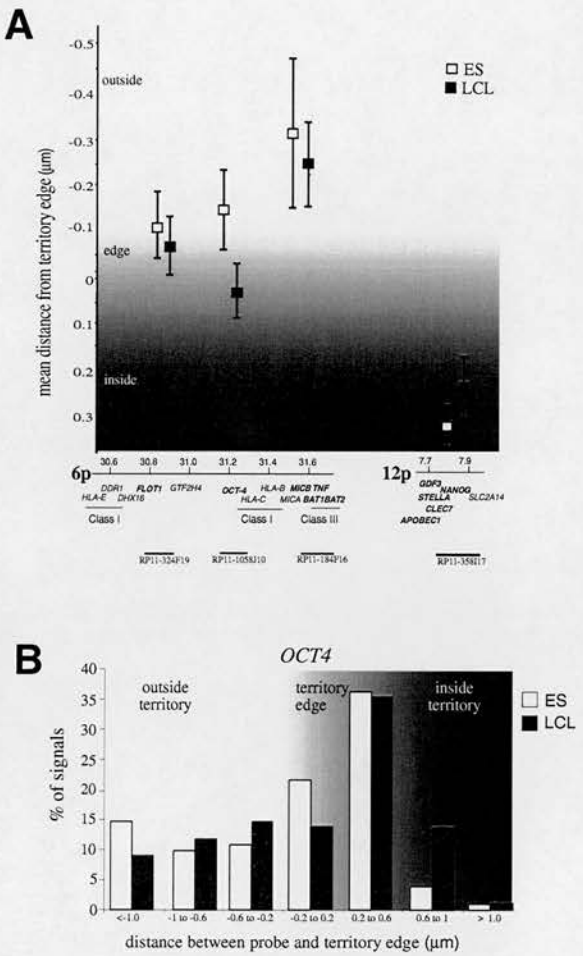

Fig. 3. Intrachromosome territory organisation of *NANOG* and *OCT4*. (A) Position (mean±s.e.m.) in μm, relative to the inside, edge or outside CTs, for loci including *NANOG* and *OCT4*, as well as loci flanking *OCT4*, in the nuclei of hES cells (□) and LCLs (■) (n=100). Negative values indicate localisation outside the CT. The map of the genomic regions around *OCT4* and *NANOG* (according to NCBI build 35) is shown below. Genes present in the BACs used are highlighted in bold. (B) Histogram of the distribution of FISH signals from a BAC containing *OCT4*, relative to the edge of the chromosome 6p CT, in nuclei from hES cells (open bars) and LCLs (filled bars). Negative distance indicates localisation outside the visible limits of the CT (n=100).

change in mean intra-CT position represented, not a change in the overall percentage of *OCT4* loci found well (>0.2 μm) outside the CT (36% for both LCLs and ES cells), but a reduction in the number of loci found deep within the CT (>0.6 μm), and a consequent increase in the *OCT4* loci positioned at the CT edge (Fig. 3B).

During the differentiation of mouse ES cells, the movement of loci relative to the surface of CTs is generally accompanied by cytologically detectable changes in chromatin condensation (Chambeyron and Bickmore, 2004). To investigate this further, we measured the interphase distance (d) between *OCT4* and the flanking BAC clones. In all cases, the distribution of d values conformed to that expected of a random-walk model of chromatin structure (s.d.=0.52-0.6; median/mean ~1.0) (Sachs et al., 1995; Chambeyron and Bickmore, 2004). There was no significant difference in the mean-squared interphase distance ($\langle d^2 \rangle$) between *OCT4* and *MICB* BACS (genomic distance, 350 kb) for hES cells and LCLs ($\langle d^2 \rangle$=0.5±0.06 and 0.41±0.04 μm^2 respectively, P=0.41). However, there was a significantly larger interphase separation between *OCT4* and *FLOT1* (genomic distance, 400 kb) in LCLs ($\langle d^2 \rangle$=0.33±0.04 μm^2) compared to hES cells (0.24±0.03 μm^2), P=0.04. In both LCLs and hES cells the large sizes of the d^2 values measured around *OCT4*, are consistent with the presence of a generally open chromatin fibre structure, rather than a compact one (Gilbert et al., 2004).

These data suggest that both the intra-CT architecture and the long-range chromatin configuration around the *OCT4* locus differ between hES cells and a differentiated cell type that does not express this marker of pluripotency.

Localisation and clustering of centromeres in human ES cells

We detected distinctive nuclear organisation of chromosome arms and specific gene loci in hES cells. To investigate other non-genic regions we compared the position and number of centromere clusters in hES cells with that in two diploid differentiated cell types: LCLs and primary fibroblasts. Centromeres were detected in paraformaldehyde-fixed cells using antibodies that recognise CENP-C or CREST serum. There were no significant differences in the extent of centromere clustering between hES cells and these two differentiated cell types. The average number of centromere signals scored per cell was 34, 36 and 38 for ES, LCL and proliferating fibroblasts, respectively (n=20). Centromere position was analysed with respect to the nuclear periphery, or to the nucleolus (detected with antibody that recognises pKi67) (Fig. 4A). A significantly lower proportion of centromeres was associated with the nuclear periphery of hES cells in comparison with LCLs (P<0.04) or fibroblasts (P<0.001) (Fig. 4B). Similar proportions of centromeres were associated with nucleoli in hES cells and fibroblasts (P>0.39). In hES cells a significantly higher proportion of centromeres were not associated with either the nuclear periphery or the nucleolus than either differentiated cell type (P<0.004). These differences were confirmed by examination of centromere distribution through the z-axis of nuclei (Fig. 4C). Centromeres have a normal distribution along the z-axis of ES cell nuclei, in contrast with a bimodal distribution towards the top and bottom surface of the nucleus of fibroblasts.

Telomeres are dispersed throughout the nucleoplasm of differentiated cells (Weierich et al., 2003). Most primary diploid somatic cells, including fibroblasts, do not have active telomerase activity, and so are subject to progressive telomere shortening. Germ cells and stem cells in contrast have active telomerase, and robust telomerase activity is detected in hES cells (Thomson et al., 1998). We found that telomeres had a near-normal distribution in the centre of the nucleus of both hES cells and LCLs, though this is skewed towards the bottom of the nucleus in fibroblasts (Fig. 4D).

Lastly, we also analysed the nuclear distribution of PML bodies. The function of these nuclear bodies remains unknown, though they have been implicated in transcriptional regulation, apoptosis, and DNA damage and stress sensing (Dellaire and

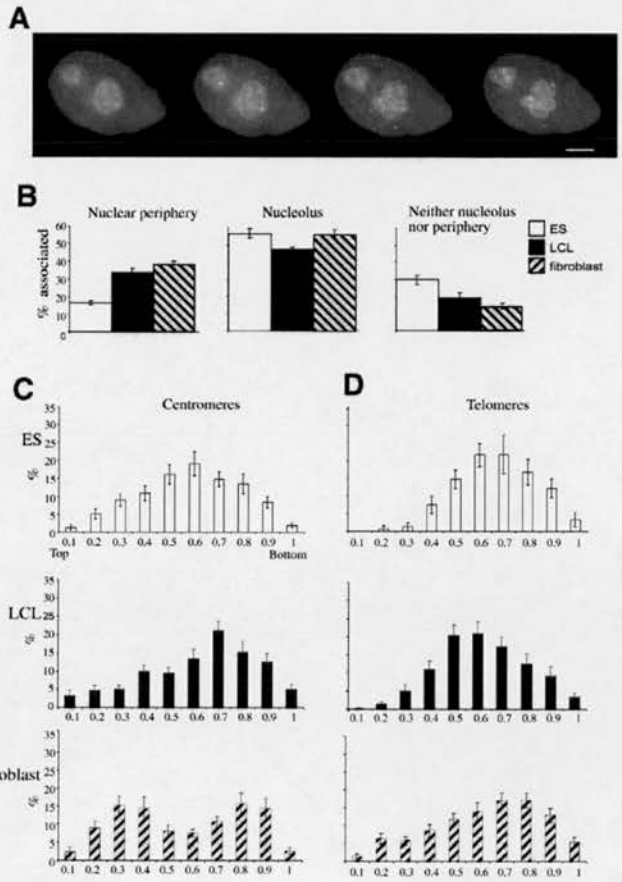

Fig. 4. Centromere and telomere localisation in hES cells. (A) Localisation of centromeres (CREST, red), and nucleoli (Ki67, green) in single image frames, taken at 0.75 μm intervals, through the *z*-axis of hES cell nuclei counterstained with DAPI (blue). Note the absence of centromeres from the nuclear periphery. (B) Mean (±s.e.m.) proportion of centromeres per cell that are associated with the nuclear periphery (left), the nucleolus (middle), or neither of these nuclear compartments (right), in H1 ES cells (open bars), LCLs (filled bars) and fibroblasts (hatched bars) (n=20). The mean (±s.e.m.) distribution of (C) centromeres and (D) telomeres through the *z*-plane from the top (0) to the bottom (1) of nuclei from ES, LCL and fibroblast cells (n=20). Bar, 5 μm.

Bazett-Jones, 2004). Their nuclear distribution has not been extensively studied, but many transcriptionally active genomic regions, including parts of the major histocompatibility complex (MHC) at 6p, are reported to be associated with them (Wang et al., 2004). The average number of PML bodies scored in hES cells (11), is lower than that seen in LCLs (15) or fibroblasts (27), but despite the differences in abundance of PML bodies between cell types, their intranuclear distribution towards the central mid-plane of the nucleus was the same in all three cell types (data not shown).

Discussion

The radial distribution of chromosome territories is present in hES cells

We found that a major organisational feature of human nuclei, the radial organisation of CTs, is already established in hES cells. Gene-poor chromosome 18 is located toward the nuclear periphery of ES cells, whereas gene-rich HSA19 is more internal (Fig. 1). HSA18 is seen towards the nuclear periphery of a variety of differentiated cell types including lymphocytes (Croft et al., 1999), keratinocytes, and leukaemic and cancer cell lines (Cremer et al., 2003). However, a peripheral localisation of HSA18 was not seen in the very flat nuclei of amniotic fluid cells and quiescent fibroblasts (Bridger et al., 2000; Cremer et al., 2001). The nuclei of H1 ES cells are quite spherical (average height:length ratio=1.02±0.1), more similar to the shape of lymphocyte nuclei (ratio=1.00±0.1), than to those of fibroblasts (ratio=0.25±0.4). A differential localisation of HSA18 and 19 was also reported for granulocyte-macrophage colony-forming cells (GM-CFCs) and it has been suggested that radial distribution is also present in the pluripotent haematopoietic progenitor cells (Cremer et al., 2003). As we show that this radial distribution is already present in hES cells, we think it highly likely that a similar nuclear organisation will be present in most, if not all, foetal and adult stem cells.

Chromosome 12p is located in the centre of the nucleus in ES cells

Differences in the radial distribution of mouse chromosomes have been documented in different tissues and during T-cell differentiation (Parada et al., 2004; Kim et al., 2004). However, to date no significant change in radial position of a human chromosome within the nucleus had been documented during differentiation, although there may be changes in chromosome associations (Kuroda et al., 2004).

Here we have detected a significantly more central nuclear localisation for the short arm of human chromosome 12 in ES cells. It is interesting to note that recurrent gains of chromosome 12, including iso12p, have been found in human ES cells (Draper et al., 2004). It has been suggested that increased dosage of genes on chromosome 12 (and therefore presumably increased gene expression levels) is advantageous to the propagation of undifferentiated ES cells. Although the functional significance of positioning in the nuclear centre of mammalian cells is unknown, the presence in this zone of the nucleus of the most gene-dense human chromosomes (Boyle et al., 2001) suggests that it may confer some transcriptional advantage. Chromosome 12p contains a cluster of genes whose expression is linked to the maintenance of pluripotency. *NANOG* expression is required to maintain ES cells in an undifferentiated state (Zaehres et al., 2005). It is located just proximal of two other genes, *STELLA* and *GDF3*, which are also expressed in ES cells and downregulated upon differentiation (Clark et al., 2004). A BAC that covers this gene cluster also shows a more central nuclear position in hES cells when compared with LCLs (Fig. 2C). Is it possible that it is the transcriptional activity of this gene cluster that is driving the nuclear localisation of 12p in hES cells?

Preferential association of inactive genes with the nuclear periphery has been reported in differentiated cells, compared with their position in expressing cell types (Zink et al., 2004). However, we detect no association of either *NANOG* or *OCT4* with the nuclear periphery in differentiated cells (Fig. 2C).

A relocalisation of *OCT4*, with respect to its chromosome territory, in hES cells

In contrast to the central nuclear localisation of 12p and *NANOG* in human ES cells, we detected no significant difference in the radial nuclear position of 6p or *OCT4* between ES and differentiated cells. Both gene and chromosome territory remain in an intermediate nuclear position (Fig. 2). However, we found that compared with LCLs, *OCT4* is located significantly closer to, or just beyond the CT edge in hES cells (Fig. 3). In both cell types, the flanking Class I and Class III MHC regions were located outside the 6p CT, consistent with other results (Volpi et al., 2000). The local chromatin structure of *OCT4* has not been studied in hES cells but, in the mouse, increased DNA methylation and histone deacetylation of the *Oct4* enhancer/promoter are seen in trophoblast cells compared with ES cells (Hattori et al., 2004). The data we have presented here would be consistent with a more long-range remodelling of chromatin architecture around *OCT4*, which might also contribute to its transcriptional regulation.

Therefore, for both of the best-studied genes involved in pluripotency, we find a distinctive nuclear organisation in human ES cells. In the case of *NANOG*, the whole chromosome arm is localised towards the nuclear centre, whereas for *OCT4* there is a more localised reorganisation that allows the gene to leave the confines of its chromosome territory.

Internal nuclear distribution of centromeres in hES cells

In most human cell types, the predominant reported distribution of centromeres is toward the nuclear periphery (reviewed by Gilchrist et al., 2004). In contrast, we have found that centromeres seem to be found mainly within the nuclear interior of hES cells (Fig. 4). Factors determining centromere position in the nucleus are not clear. Under some conditions, the levels of histone acetylation of centric heterochromatin can alter centromere position in human and mouse somatic cells (Taddei et al., 2001) and, in the mouse, histone hypoacetylation at satellite repeats only occurs upon the induction of differentiation of mES cells (Keohane et al., 1996). Histone modifications in hES cells have yet to be examined. Localisation of centromeres away from the nuclear periphery may also reflect the rapid cell cycles of hES cells. In turn the localisation of centromeres within the nucleus may influence mechanisms of gene silencing (Fisher and Merkenschlager, 2002). Most interestingly, changes in the nuclear distribution of centromeres have recently been correlated with the maturation and developmental competency of mouse oocytes (Zuccotti et al., 2005).

To our knowledge, this is the first study of nuclear organisation in human ES cells. We have found that hES cell nuclei have a distinct nuclear architecture, especially at loci involved in maintaining pluripotency. Understanding how this nuclear organisation is established and how it influences gene expression might subsequently allow a better understanding of pluripotency.

This work is dedicated to the memory of John Clark, who died 12th August 2004, and who is much missed. A.E.W. was funded by a stem cell studentship from the Medical Research Council, UK. W.A.B. is a Centennial fellow of the James S. McDonnell foundation. The work was supported in part by the EU FP6 Network of Excellence Epigenome (LSHG-CT-2004-503433). We thank W. Earnshaw (University of Edinburgh) for the gift of anti-CenpC antibody.

References

Alcobia, I., Quina, A. S., Neves, H., Clode, N. and Parreira, L. (2003). The spatial organization of centromeric heterochromatin during normal human lymphopoiesis: evidence for ontogenically determined spatial patterns. *Exp. Cell Res.* **290**, 358-369.

Beil, M., Durschmied, D., Paschke, S., Schreiner, B., Nolte, U., Bruel, A. and Irinopoulou, T. (2002). Spatial distribution patterns of interphase centromeres during retinoic acid-induced differentiation of promyelocytic leukemia cells. *Cytometry* **47**, 217-225.

Boyle, S., Gilchrist, S., Bridger, J. M., Mahy, N. L., Ellis, J. A. and Bickmore, W. A. (2001). The spatial organization of human chromosomes within the nuclei of normal and emerin-mutant cells. *Hum. Mol. Genet.* **10**, 211-219.

Bridger, J. M., Boyle, S., Kill, I. R. and Bickmore, W. A. (2000). Re-modelling of nuclear architecture in quiescent and senescent human fibroblasts. *Curr. Biol.* **10**, 149-152.

Carpenter, M. K., Rosler, E. S., Fisk, G. J., Brandenberger, R., Ares, X., Miura, T., Lucero, M. and Rao, M. S. (2004). Properties of four human embryonic stem cell lines maintained in a feeder-free culture system. *Dev. Dyn.* **229**, 243-258.

Carvalho, C., Pereira, H. M., Ferreira, J., Pina, C., Mendonca, D., Rosa, A. C. and Carmo-Fonseca, M. (2001). Chromosomal G-dark bands determine the spatial organization of centromeric heterochromatin in the nucleus. *Mol. Biol. Cell* **12**, 3563-3572.

Chambeyron, S. and Bickmore, W. A. (2004). Chromatin decondensation and nuclear reorganization of the HoxB locus upon induction of transcription. *Genes Dev.* **18**, 1119-1130.

Clark, A. T., Rodriguez, R. T., Bodnar, M. S., Abeyta, M. J., Cedars, M. I., Turek, P. J., Firpo, M. T. and Reijo Pera, R. A. (2004). Human STELLAR, NANOG, and GDF3 genes are expressed in pluripotent cells and map to chromosome 12p13, a hotspot for teratocarcinoma. *Stem Cells* **22**, 169-179.

Cremer, M., von Hase, J., Volm, T., Brero, A., Kreth, G., Walter, J., Fischer, C., Solovei, I., Cremer, C. and Cremer, T. (2001). Non-random radial higher-order chromatin arrangements in nuclei of diploid human cells. *Chromosome Res.* **9**, 541-567.

Cremer, M., Kupper, K., Wagler, B., Wizelman, L., von Hase, J., Weiland, Y., Kreja, L., Diebold, J., Speicher, M. R. and Cremer, T. (2003). Inheritance of gene density-related higher order chromatin arrangements in normal and tumor cell nuclei. *J. Cell Biol.* **162**, 809-820.

Croft, J. A., Bridger, J. M., Boyle, S., Perry, P., Teague, P. and Bickmore, W. A. (1999). Differences in the localization and morphology of chromosomes in the human nucleus. *J. Cell Biol.* **145**, 1119-1131.

Dellaire, G. and Bazett-Jones, D. P. (2004). PML nuclear bodies: dynamic sensors of DNA damage and cellular stress. *BioEssays,* **26**, 963-977.

Draper, J. S., Pigott, C., Thomson, J. A. and Andrews, P. W. (2002). Surface antigens of human embryonic stem cells: changes upon differentiation in culture. *J. Anat.* **200**, 249-258.

Draper, J. S., Smith, K., Gokhale, P., Moore, H. D., Maltby, E., Johnson, J., Meisner, L., Zwaka, T. P., Thomson, J. A. and Andrews, P. W. (2004). Recurrent gain of chromosomes 17q and 12 in cultured human embryonic stem cells. *Nat. Biotechnol.* **22**, 53-54.

Drukker, M., Katz, G., Urbach, A., Schuldiner, M., Markel, G., Itskovitz-Eldor, J., Reubinoff, B., Mandelboim, O. and Benvenisty, N. (2002). Characterization of the expression of MHC proteins in human embryonic stem cells. *Proc. Natl. Acad. Sci. USA* **99**, 9864-9869.

Fisher, A. G. and Merkenschlager, M. (2002). Gene silencing, cell fate and nuclear organisation. *Curr. Opin. Genet. Dev.* **12**, 193-197.

Gilbert, N., Boyle, S., Fiegler, H., Woodfine, K., Carter, N. P. and Bickmore, W. A. (2004). Chromatin architecture of the human genome: gene-rich domains are enriched in open chromatin fibers. *Cell* **118**, 555-566.

Gilchrist, S., Gilbert, N., Perry, P. and Bickmore, W. A. (2004). Nuclear organization of centromeric domains is not perturbed by inhibition of histone deacetylases. *Chromosome. Res.* **12**, 505-516.

Ginis, I., Luo, Y., Miura, T., Thies, S., Brandenberger, R., Gerecht-Nir, S., Amit, M., Hoke, A., Carpenter, M. K., Itskovitz-Eldor, J. et al. (2004). Differences between human and mouse embryonic stem cells. *Dev. Biol.* **269**, 360-380.

Hattori, N., Nishino, K., Ko, Y. G., Hattori, N., Ohgane, J., Tanaka, S. and Shiota, K. (2004). Epigenetic control of mouse Oct-4 gene expression in

embryonic stem cells and trophoblast stem cells. *J. Biol. Chem.* **279**, 17063-17069.

Keohane, A. M., O'Neill, L. P., Belyaev, N. D., Lavender, J. S. and Turner, B. M. (1996). X-Inactivation and histone H4 acetylation in embryonic stem cells. *Dev Biol.* **180**, 618-630.

Kim, S. H., McQueen, P. G., Lichtman, M. K., Shevach, E. M., Parada, L. A. and Misteli, T. (2004). Spatial genome organization during T-cell differentiation. *Cytogenet. Genome Res.* **105**, 292-301.

Kuroda, M., Tanabe, H., Yoshida, K., Oikawa, K., Saito, A., Kiyuna, T., Mizusawa, H. and Mukai, K. (2004). Alteration of chromosome positioning during adipocyte differentiation. *J. Cell Sci.* **117**, 5897-5903.

Mahy, N. L., Perry, P. E. and Bickmore, W. A. (2002a). Gene density and transcription influence the localization of chromatin outside of chromosome territories detectable by FISH. *J. Cell Biol.* **159**, 753-763.

Mahy, N. L., Perry, P. E., Gilchrist, S., Baldock, R. A. and Bickmore, W. A. (2002b). Spatial organization of active and inactive genes and noncoding DNA within chromosome territories. *J. Cell Biol.* **157**, 579-589.

Matin, M. M., Walsh, J. R., Gokhale, P. J., Draper, J. S., Bahrami, A. R., Morton, I., Moore, H. D. and Andrews, P. W. (2004). Specific knockdown of Oct4 and beta2-microglobulin expression by RNA interference in human embryonic stem cells and embryonic carcinoma cells. *Stem Cells* **22**, 659-668.

Parada, L. A., McQueen, P. G. and Misteli, T. (2004). Tissue-specific spatial organization of genomes. *Genome Biol.* **5**, R44.

Pera, M. F. and Trounson, A. O. (2004). Human embryonic stem cells: prospects for development. *Development* **131**, 5515-5525.

Ramalho-Santos, M., Yoon, S., Matsuzaki, Y., Mulligan, R. C. and Melton, D. A. (2002). "Stemness": transcriptional profiling of embryonic and adult stem cells. *Science* **298**, 597-600.

Sachs, R. K., van den Engh, G., Trask, B. and Hearst, J. E. (1995). A random-walk/giant-loop model for interphase chromosomes. *Proc. Natl. Acad. Sci. USA* **92**, 2710-2714.

Spector, D. L. (2003). The dynamics of chromosome organization and gene regulation. *Annu. Rev. Biochem.* **72**, 573-608.

Taddei, A., Maison, C., Roche, D. and Almouzni, G. (2001). Reversible disruption of pericentric heterochromatin and centromere function by inhibiting deacetylases. *Nat. Cell. Biol.* **3**, 114-120.

Tanabe, H., Muller, S., Neusser, M., von Hase, J., Calcagno, E., Cremer, M., Solovei, I., Cremer, C. and Cremer, T. (2002). Evolutionary conservation of chromosome territory arrangements in cell nuclei from higher primates. *Proc. Natl. Acad. Sci. USA* **99**, 4424-4429.

Thomson, J. A., Itskovitz-Eldor, J., Shapiro, S. S., Waknitz, M. A., Swiergiel, J. J., Marshall, V. S. and Jones, J. M. (1998). Embryonic stem cell lines derived from human blastocysts. *Science* **282**, 1145-1147.

Tian, L., Catt, J. W., O'Neill, C. and King, N. J. (1997). Expression of immunoglobulin superfamily cell adhesion molecules on murine embryonic stem cells. *Biol. Reprod.* **57**, 561-568.

Volpi, E. V., Chevret, E., Jones, T., Vatcheva, R., Williamson, J., Beck, S., Campbell, R. D., Goldsworthy, M., Powis, S. H., Ragoussis, J., Trowsdale, J. and Sheer, D. (2000). Large-scale chromatin organization of the major histocompatibility complex and other regions of human chromosome 6 and its response to interferon in interphase nuclei. *J. Cell Sci.* **113**, 1565-1576.

Wang, J., Shiels, C., Sasieni, P., Wu, P. J., Islam, S. A., Freemont, P. S. and Sheer, D. (2004). Promyelocytic leukemia nuclear bodies associate with transcriptionally active genomic regions. *J. Cell Biol.* **164**, 515-526.

Weierich, C., Brero, A., Stein, S., von Hase, J., Cremer, C., Cremer, T. and Solovei, I. (2003). Three-dimensional arrangements of centromeres and telomeres in nuclei of human and murine lymphocytes. *Chromosome Res.* **11**, 485-502.

Williams, R. R., Broad, S., Sheer, D. and Ragoussis, J. (2002). Subchromosomal positioning of the epidermal differentiation complex (EDC) in keratinocyte and lymphoblast interphase nuclei. *Exp. Cell Res.* **272**, 163-175.

Xu, C., Inokuma, M. S., Denham, J., Golds, K., Kundu, P., Gold, J. D. and Carpenter, M. K. (2001). Feeder-free growth of undifferentiated human embryonic stem cells. *Nat. Biotechnol.* **19**, 971-974.

Zaehres, H., Lensch, M. W., Daheron, L., Stewart, S. A., Itskovitz-Eldor, J. and Daley, G. Q. (2005). High-efficiency RNA interference in human embryonic stem cells. *Stem Cells* **23**, 299-305.

Zink, D., Amaral, M. D., Englmann, A., Lang, S., Clarke, L. A., Rudolph, C., Alt, F., Luther, K., Braz, C., Sadoni, N. et al. (2004). Transcription-dependent spatial arrangements of CFTR and adjacent genes in human cell nuclei. *J. Cell Biol.* **166**, 815-825.

Zuccotti, M., Garagna, S., Merico, V., Monti, M. and Redi, C. A. (2005). Chromatin organisation and nuclear architecture in growing mouse oocytes. *Mol. Cell. Endocrinol.* **234**, 11-17.